Submitochondrial organization of human mitochondrial aspartyl-tRNA synthetase and its implication in LBSL disease

Loukmane Karim

UNIVERSITÉ DE STRASBOURG

ÉCOLE DOCTORALE DES SCIENCES DE LA VIE ET DE LA SANTÉ

Architecture et Réactivité de l'ARN – UPR 9002 du CNRS

THÈSE

présentée par :

Loukmane KARIM

soutenue le : **04 Octobre 2016**

pour obtenir le grade de : **Docteur de l'université de Strasbourg**

Discipline/ Spécialité : Aspects moléculaires et cellulaires de la biologie

Organisation sous-mitochondriale de l'aspartyl-ARNt synthétase humaine et implication dans le syndrome LBSL

THÈSE dirigée par :

Dr. Marie SISSLER Directrice de Recherche au CNRS, IBMC, Université de Strasbourg

RAPPORTEURS :

Prof. Zofia CHRZANOWSKA-LIGHTOWLERS Professeur, Institut de Neuroscience, Université de Newcastle

Prof. Michael IBBA Professeur, Département de Microbiologie, Université de l'État d'Ohio

---

AUTRES MEMBRES DU JURY :

Dr. Agnès RÖTIG Directrice de Recherche à l'INSERM, Institut IMAGINE, Université Paris Descartes

Dr. Ivan TARASSOV Directeur de Recherche au CNRS, GMGM, Université de Strasbourg

Submitochondrial organization of human mitochondrial aspartyl-tRNA synthetase and its implication in LBSL disease

Table of contents

Abbreviations

A	Ampere
Å	Angstrom
aa	Amino acid
aaRS	Aminoacyl-tRNA synthetase
APP3	Aminopeptidase P
Asp	Aspartic acid (aspartate)
ATP	Adenosine triphosphate
BHK21	Baby hamster kidney cells
BN-PAGE	Blue native-polyacrylamide gel electrophoresis
CM	Cristae membrane
CNS	Central nervous system
CsA	Cyclosporin A
DLS	Dynamic light scattering
DNA	Deoxyribonucleic acid
DTT	Dithiothreitol
ER	Endoplasmic reticulum
GTP	Guanosine triphosphate
HEK293T	Human embryonic kidney cells
IBM	Inner boundary membrane
Icp55	Intermediate cleaving peptidase
IM	Inner membrane
IMP	Inner membrane peptidase
IMS	Intermembranes space
IPTG	Isopropyl β-D-1-thiogalactopyranoside
KCN	Potassium cyanide
kDa	kilo Dalton
KO	Knockout
LBSL	Leukoencephalopathy with brainstem and spinal cord involvement and lactate elevation
m/z	Mass/charge value
MDV	Mitochondrial derived vesicles
min	Minute
MIP	Mitochondrial processing peptidase (Oct1, ocatapeptidyl aminopeptidase)
mM	Millimolar
MPP	Mitochondrial processing peptidase
mPTP	Mitochondrial permeability transition pore
MRG	Mitochondrial RNA granules
MRI	Magnetic resonance imaging
MRS	Magnetic resonance spectroscopy
MSC	Multi-tRNA synthetases complex
mt	Mitochondrial
MTS	Mitochondrial targeting sequence (or signal)
MVA	Modified Vaccina Ankara
MW	Molecular weight
NGS	Next-generation sequencing
nm	Nanometer
OM	Outer membrane
PCR	Polymerase chain reaction
RNA	Ribonucleic acid
SDS-PAGE	Sodium dedocyl sulfate-polyacrylamide gel electrophoresis
TEM	Transmission electron microscopy
UV	Ultraviolet
µg	Microgram

List of figures

List of tables

INTRODUCTION

INTRODUCTION

Mitochondria are dynamic and multifunctional organelles with a huge variety in their number, shape, plasticity and function depending on the cell type (Kunz 2003). Morphologically, they are composed of inner and outer membranes. The inner membrane delimits the matrix, and is separated from the outer membrane by the intermembranes space. It is admitted that these organelles originated from an α-proteobacterium ancestor, which underwent an endosymbiosis with a host cell (Gray *et al.* 1999). The nature of this latter is, however, still a debated question (Archibald 2015, Martin *et al.* 2015). Several horizontal or lateral gene transfers (HGT or LGT) have occurred before, during and/or after the endosymbiosis (depending on the scenario) in addition to endosymbiotic gene transfer (EGT) from the endosymbiont to the host cell (Shutt and Gray 2006, Abhishek *et al.* 2011). After a long and complex evolutionary history strewn with genes loss and degeneracy, contemporary mitochondrial genomes (mt-DNA) ended up with diversity in size, shape (linear, circular or branched) and organization (e.g. presence or absence of introns). For instance, the size ranges from ~ 6 kbp (e.g. *Plasmodium falciparum*, Feagin 1992) to ~ 11 Mbp (e.g. *Silene conica*, Sloan *et al.* 2012). Human mt-DNA is about 16,569 bp coding for only 37 genes: 13 proteins, 22 transfer-RNAs (tRNAs) and 2 ribosomal RNAs (rRNAs). All these genes serve *in fine* to generate almost 95% of the cellular adenosine triphosphate (ATP) through oxidative phosphorylation (Figure 1). As compared to evolutionary-related species, mt-rRNAs seem to be phylogenetically conserved but are significantly reduced in size (Gutell *et al.* 2002, O'brien 2003), mt-mRNAs have inexistent or reduced untranslated regions (UTRs) (Temperley *et al.* 2010), and mt-tRNAs display reduced sizes with structural deviation (absence of some of conserved residues and long distance interactions) from the classical tRNA cloverleaf secondary structure (Helm *et al.* 2000).

As a consequence of gene loss and degeneracy, several mechanisms of adaptation have been adopted to maintain mitochondrial functions. The main thread of my introduction is the mitochondrial evolution and adaptations, where some aspects will be developed: 1) import and processing of nuclear encoded mitochondrial proteins; 2) crosstalk between the nuclear and mitochondrial genomes; 3) the general optimization of mitochondrial functions, with a focus on the role of the inner membrane as a platform; 4) structural and functional adaptation/peculiarities of mitochondrial aminoacyl-tRNA

synthetases (mt-aaRSs). In addition to mt-aaRSs, macromolecular organization, partnership, alternative functions of cytosolic aaRSs and their correlation to human diseases are presented; 5) and finally, a focus on one human mitochondrial disease correlated with the mt-aaRS model of the lab.

The hosting lab is working on human mitochondrial aminoacyl-tRNA synthetases (mt-aaRSs) and mt-tRNAs, which are key factors in mt-DNA gene expression, and studying their roles in health and disease. One of the major topics of the team is the functional and structural study of the human aspartyl-tRNA synthetase (mt-AspRS). Mutations on this latter have been specifically associated with a leukoencephalopathy named LBSL (Leukoencephalopathy with Brainstem and Spinal cord involvement and Lactate elevation) disease (Scheper *et al.* 2007). Most mutations do not impact the activity or the structure of mt-AspRS highlighting the lack of knowledge and raising many questions about the existence of macromolecular partners or regulators of mt-ApsRS, or a secondary unknown function. In order to fill the gaps and contribute to the understanding of LBSL etiology, my thesis work was focused on the study of the cellular properties of mt-AspRS.

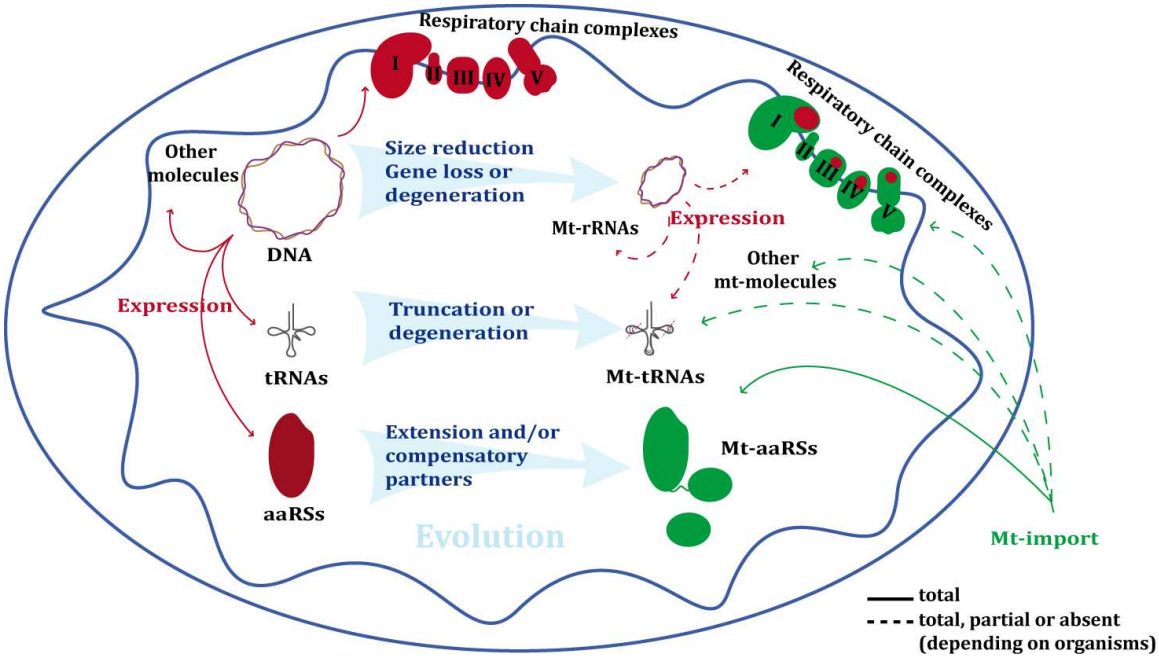

Figure 1: Evolutionary events occurred on the modern mitochondrial genome.

1. Import/processing of nuclear-encoded mitochondrial proteins

In human, except the 13 mitochondrially-encoded, all mt-proteins (~ 1,500) are encoded in the nucleus, translated on cytosolic ribosome, and targeted to mitochondria. The latter step is performed thanks to the mt membrane potential ($\Delta\Psi m$) and the Mitochondrial targeting signal (MTS). The MTS could be an N-terminal (cleavable or non-cleavable) amphipathic helix with positively charged, hydroxylated and hydrophobic amino acids (Vonheijne 1986), an internal sequence with negatively and positively charged residues (Diekert *et al.* 1999), or a C-terminal sequence resembling the tail-anchorage of mt-membrane proteins (Li *et al.* 2010). A combination of two MTSs can also occur in some proteins like the case of yeast Cytochrome c1 with internal and N-terminal MTSs (Arnold *et al.* 1998). The MTS allows targeting of the precursor protein to the surface of mitochondria where it is recognized by a receptor of the outer membrane translocase, and maybe cleaved by processing peptidases upon import.

1.1. Translocation machineries

The position of MTS on the protein sequence, as well as the topology of the protein, determines the type of translocation machinery used for the import, and consequently the final sub-mitochondrial localization of an mt-protein (as reviewed in Mokranjac and Neupert 2010, Schleiff and Becker 2011, Dudek *et al.* 2013, Wenz *et al.* 2015)(Figure 2).

Outer membrane (OM)

Proteins containing transmembrane β-barrel domains are inserted into the outer membrane with the Translocase of outer membrane (TOM) complex in addition to the Sorting and assembly machinery (SAM) complex. Mitochondrial import machinery (MIM) complex mediates the insertion of proteins with multiple transmembrane α-helices. However, single α-helical transmembrane proteins could be inserted directly into the outer membrane independently of any translocase machinery.

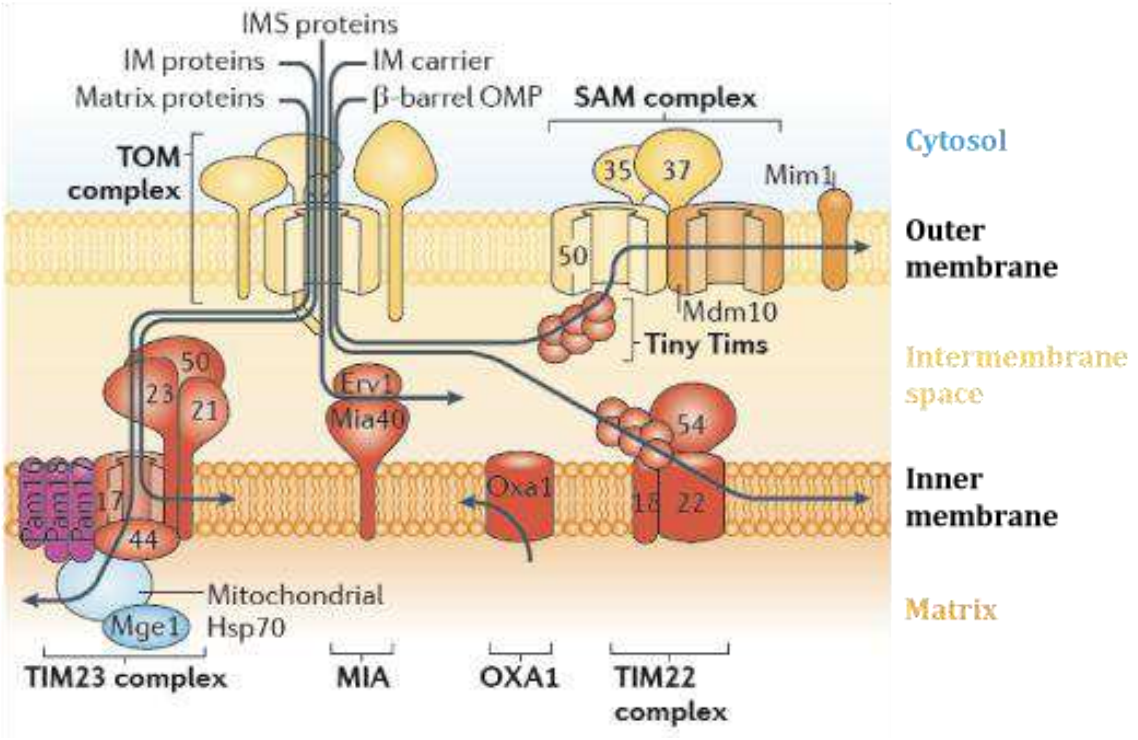

Figure 2: Mitochondrial translocation machineries (adapted from Schleiff and Becker 2011). Mitochondrial proteins are translated in the cytosol and imported into mitochondria through different machineries depending on the final sublocalization. IMS, intermembranes space. OMP, outer membrane protein. SAM, sorting and assembly machinery. MIM, mitochondrial import machinery. TOM, translocase of outer membrane. TIM, translocase of the inner membrane. OXA, oxidase assembly. MIA, mitochondrial IMS import and assembly.

Inner membrane (IM)

Inner membrane metabolite carrier precursors, constituted with only transmembrane helices, translocate across TOM complex before being inserted into the inner membrane with Translocase of inner membrane (TIM22) complex. Other transmembrane proteins can either be inserted into the IM by TIM23 complex, or cross through TIM23 complex to the matrix and then be inserted with the Oxidase assembly (OXA) complex. Of note, the principal function of this latter is the insertion of mitochondrially-translated proteins into the inner membrane.

Intermembranes space (IMS)

TOM complex allows translocation of precursors containing cysteine-rich motifs into the IMS. Then, mt Intermembranes space import and assembly (MIA) complex promotes disulfide-bridges formation and proper folding of the protein. Some proteins can also transit by the matrix (through TOM/TIM23) before being addressed to the IMS.

Matrix

All precursor proteins targeted to the matrix, either transiently (e.g. OXA-dependent insertion of IM proteins) or as a final destination, are translocating through TOM/TIM23 complexes. Most precursor proteins using TOM/TIM23 complexes translocate into the matrix in N- to C-terminal orientation, meaning that the N-terminal enters the matrix first, although it has been shown that the translocation can also occur in C- to N-terminal, and the orientation (N→C or C→N) is determined only by the position of MTS (Folsch *et al.* 1998). This observation has been confirmed with the unusual C-terminal MTS of a yeast mt helicase (Lee *et al.* 1999).

1.2. Peptidases implicated in MTS processing

Processing of the MTS is another important parameter determining the final destination of mt-proteins, and occurs either during or after translocation. Cleavage of the MTS concerns proteins of the IM, the IMS and the matrix. The central peptidase is the Mitochondrial processing peptidase (MPP), which acts either alone or in combination with other peptidases (as reviewed in Gakh *et al.* 2002, Schmidt *et al.* 2010, Mossmann *et al.* 2012, Teixeira and Glaser 2013)(Figure 3). Although processing peptidases/proteases are found in all eukaryotes, most of their studies have been conducted essentially in yeast (Quiros *et al.* 2015).

Mitochondrial processing peptidase (MPP) alone

No conserved cleavage site has been found for MPP. However, the presence of arginine residues seems to be an important criterion, and so far, three motifs have been detected in MPP substrates. Most of these latter (80%) have an R-2 or R-3 motif,

consisting in an arginine residue located upstream of the cleavage site (respectively, $R_{-2}x \Downarrow x_{+1}$ and $R_{-3}x(F/Y/L)_{-1} \Downarrow (A/S)_{+1}x$). However, it seems that only R-2 motif exists and that "R-3" more likely results from a double cleavage of both MPP (at R-2 motif) and Icp55 to remove a destabilizing amino acid (see Icp55) (Vogtle *et al.* 2009). All precursors displaying R-2 or R-3 motifs are exclusively matrix proteins after maturation. In plants, MPP has been shown to cleave MTSs containing no arginine residues (Zhang *et al.* 2001). Uncommonly, a cleavable MTS (with R-2 motif) has been found on the C-terminal of a yeast mt helicase, processed by MPP (Lee *et al.* 1999).

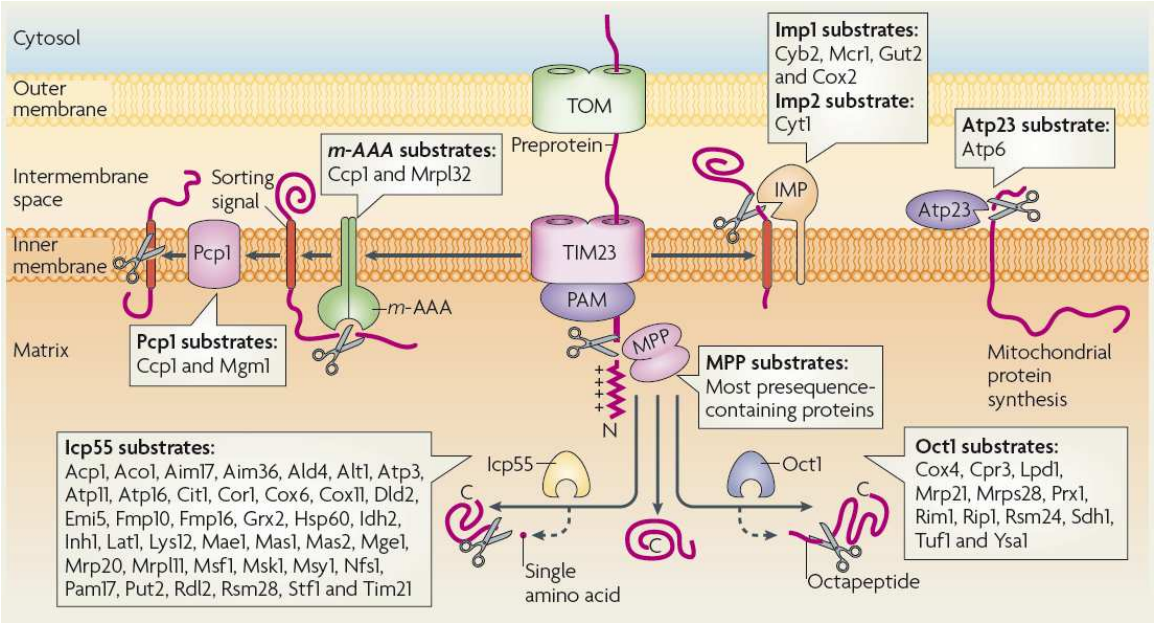

Figure 3: Mitochondrial processing peptidases and proteases (taken from Schmidt *et al.* 2010). Mitochondrial precursor proteins are processed to their mature form by different peptidases. Processing is important for the final sublocalization and the stability of mt-proteins. TOM, translocase of outer membrane. TIM, translocase of inner membrane. MPP, mitochondrial processing peptidase. IMP, inner membrane protease. Pcp1, processing of cytochrome c peroxidase. M-AAA, matrix ATPase associated with cellular activities. Oct1, octapeptidyl aminopeptidase (mitochondrial intermediate peptidase, MIP). Icp55, intermediate processing peptidase (homolog of aminopeptidase P, APP3/XPNPEP3).

MPP/ Mitochondrial intermediate peptidase (MIP)

Some MPP substrates have an R-10 motif, which is less common than R-2. The R-10 motif ($R_{-10}x \Downarrow (F/L/I)_{-8}xx(S/T/G)_{-5}xxxx_{-1} \Downarrow x_{+1}$) is cleaved sequentially by both MPP and MIP. This latter removes an octapeptide (8 residues) after a first cleavage by

MPP. Processing by MPP and MIP has been reported for many precursors targeted to the matrix or the inner membrane, and seems to be a mean of protein stabilization (Vogtle *et al.* 2011). MIP has been also shown to cleave rare K-10 and C-10 motifs (respectively, lysine and cysteine residues at position -10) in yeast (Vogtle *et al.* 2009, Vogtle *et al.* 2011), and to have more than one cleavage site on synthetic peptide (Marcondes *et al.* 2015). It has been hypothesized that mature proteins, which contained an arginine residue in position -18 of their precursor, could result from MPP/MIP/MIP triple cleavages (Vogtle *et al.* 2009).

MPP/Intermediate cleaving peptidase (Icp55/XPNPEP3)

Following MPP cleavage on substrates containing R-2 motif, some generated proteins can undergo additional maturation by Icp55, which removes one destabilizing residue (tyrosine, phenylalanine or leucine) in order to stabilize the protein (Vogtle *et al.* 2009). It has been shown that some precursors contain an arginine residue in position -11 of the cleavage site raising the possibility of a triple cleavage by MPP/Icp55/MIP (Vogtle *et al.* 2009). The controversy about R-2 and R-3 motifs (see above) came from Icp55, which has been discovered later. Indeed, it has been shown that MPP cleaves only R-2 motif ($R_{-2}x_{-1} \Downarrow (F/Y/L)_{+1}(A/S)_{+2}x$) followed by Icp55 removal of one residue ($(F/Y/L)_{-1} \Downarrow (A/S)_{+1}x$), leading to the R-3 motif ($R_{-3}x(F/Y/L)_{-1} \Downarrow (A/S)_{+1}x$) (Vogtle *et al.* 2009).

Yeast Icp55 is related to the human Aminopeptidase P family (APP), which includes a mitochondrial isoform (APP3 or XPNPEP3). However, XPNPEP3 (and APP family in general) is a proline-specific metalloaminopeptidase and removes one N-terminal residue upstream a proline (Ersahin *et al.* 2005, O'Toole *et al.* 2010).

MPP/Inner membrane protease (IMP)

In yeast, few protein precursors targeted to the IMS have a cleavable MTS at their N-terminus. Indeed, MPP removes the N-terminal MTS then the protein is inserted into the IM, and finally IMP cleaves the hydrophobic IMS-sorting signal (transmembrane) to liberate the mature protein into the IMS. In mammals, the proapoptotic protein Smac/DIABLO is the only substrate of IMP known so far, and is indeed processed after a first cleavage of MPP (Burri *et al.* 2005). IMP can also act alone in the processing of

yeast (but not human) Cox2, a mitochondrially-translated protein (Pratje *et al.* 1983). The N-terminal processing has been shown to be important for the stability and the function of Cox2 (Bonnefoy *et al.* 2001).

MPP/Rhomboid protease (Pcp1)

Yeast dynamin-related GTPase, Mgm1p, a protein involved in mt fusion and the formation of the cristae, is processed by MPP, inserted into the IM, and then further processed with Pcp1 (Teixeira and Glaser 2013), similarly to the MPP/IMP processing. However, OPA-1 (Optic atrophy 1), the mammalian homolog of Mgm1p is processed by MPP and OMA1 or YME1L (Guillery *et al.* 2008). Of note, IMP and PARL are inner membrane proteases and cleave their substrates near or in the transmembrane domain.

Matrix ATPase associated with cellular activities (m-AAA)/Pcp1

Despite its role in mt quality control, the yeast m-AAA participates in the processing of the cytochrome c peroxidase. After a first cleavage by m-AAA protease, Pcp1 cleaves and liberates the protein into the IMS (Esser *et al.* 2002). In yeast as well as in mammals, m-AAA can also act alone in processing the ribosomal protein MRPL32 (Bonn *et al.* 2011).

Maturation of mitochondrially-translated proteins

In addition to all proteases/peptidases presented above, which are dedicated to the processing of imported mt-proteins, few peptidases are involved in the maturation of mitochondrially-translated proteins. In yeast, this is the case of IMP in the processing of Cox2 (Pratje *et al.* 1983), ATP23 in the processing of Atp6 (Zeng *et al.* 2007) and METAP1D, a protease removing the initial methionine (Bradshaw *et al.* 1998). Although the three enzymes exist in human, only the activity of METAP1D has been detected (Serero *et al.* 2003).

Concluding remarks

Although proteases can act in combination generating intermediates before mature proteins, co-existence (co-presence) of the intermediate and mature forms has been observed only *in vitro* under certain conditions (Daum *et al.* 1982, Kalousek *et al.* 1988, Branda and Isaya 1995, Gordon *et al.* 1999, Vogtle *et al.* 2011). In addition, it has been demonstrated that the processing is a fast mechanism and that both intermediate and mature forms do not co-exist in mitochondria *in vivo* (Hartl *et al.* 1986). An exception is made for yeast Icp55, where substrates of this enzyme have been detected predominantly at their mature forms although intermediates have also been detected to a lesser extent (Vogtle *et al.* 2009). Recently, an additional case has been reported where MPP and MIP cleave the ribosomal protein MRPL12 (on R-10 motif) and generate two mature forms. Interestingly, they demonstrated that the long form is a constituent of the mitoribosome whereas the short one interacts with mt-RNA polymerase (mtRNAP or POLRMT)(Nouws *et al.* 2016).

Defining the mature form is important to express and study mt-proteins *in vitro* (e.g. production and purification of soluble recombinant protein from bacterial expression systems) and ultimately to understand their function in health and disease. Different programs exist to predict the presence of an N-terminal MTS and also potential cleavage sites (e.g. Small *et al.* 2004, Claros and Vincens 1996, Fukasawa *et al.* 2015). However, predicted MTS and mt-localization have to be experimentally validated. For example, predicted MTS of human mt-LeuRS was different from the experimentally defined one (Yao *et al.* 2003). In addition, lots of proteins are predicted not to be mitochondrial whereas experimentally they are either exclusively mitochondrial or dual localized to both mitochondria and other compartment.

2. Nuclear-mitochondrial genomes crosstalk

Mitochondrial proteome displays a mosaic of origins: from α-proteobacteria, non α-proteobacteria prokaryotes, eukaryotes and bacteriophages, in addition to proteins from ambiguous origin (Gray 2015). Thus, the import of mt-proteins is not as simple as "give back to mitochondria what belongs to mitochondria". As an adaptation, co-evolution of the nucleus with mitochondria has led to an efficient coordination and communication between their genomes so that mitochondria recover proteins (whatever are their origins) in order to fulfill all functions. The most concrete example is the orchestration of the respiratory chain complexes assembly of subunits from different evolutionary origins (e.g. Complex I, Gabaldon *et al.* 2005). Indeed, respiratory chain complexes consist of 83 subunits translated in the cytosol and 13 translated in mitochondria (HUGO Gene Nomenclature Committee), and their proportions and assembly must be tightly regulated. This regulation can be either at the transcriptional level where it has been shown that nuclear subunits of respiratory chain complexes and transcription factors acting in mitochondria are transcribed in the same factory (Dhar *et al.* 2013), or at the translational level, where some subunits translated in the cytosol have been reported to control the mt translation of some mitochondrial subunits (Couvillion *et al.* 2016). Nucleus-mitochondria communication is achieved using different mechanisms such as signaling (Butow and Avadhani 2004, Shadel and Horvath 2015) or dual localization of proteins (Yogev and Pines 2011). Possible mechanisms of the latter are further detailed in what's follow. Dual targeting (or dual localization) can be either constitutive so that to fulfill housekeeping functions at different cellular places, but also atypical or inducible localizations, in response to specific stimuli.

Constitutive dual targeting

99% of the human mitochondrial proteome is encoded by the nuclear genome. Some of those proteins are implicated in housekeeping functions that take place in several of the cellular compartments. Dual localization/targeting of proteins in both mitochondria and another cellular compartment (e.g. cytosol) can be achieved with different mechanisms implying translation duplicates, meaning two isoforms, which are

distinguished, at least, by the presence of the absence of an MTS: 2 different genes (e.g. human AspRSs, Bonnefond *et al.* 2005), 2 mRNAs from a single gene (e.g. human LysRSs, Tolkunova *et al.* 2000), and 2 proteins from a single mRNA (e.g. human GlyRSs, Mudge *et al.* 1998). A single protein can also be distributed between two or more compartments at different ratios if it has an ambiguous targeting or different targeting signals (e.g. *A. thaliana* LeuRS, Duchene *et al.* 2005). Dual localization is also used to qualify a same protein translocating from or into mitochondria. Here, only proteins (translated as the unique product) translocating from or into mitochondria as well as atypically dual localized proteins will be emphasized.

Atypical and spatiotemporal differential dual localization

Few studies have investigated the spatiotemporal mitochondrial targeting. For instance, it has been shown that Argininosuccinate synthase (AS), an enzyme involved in the urea cycle, is mitochondrial in the fetal and newborn liver but cytosol in adult liver of rat (Demarquoy *et al.* 1994). Glutamine synthase (GS) has been shown to possess an MTS, however, its mitochondrial localization is tissue-specific in chicken (Matthews *et al.* 2010). During spermatogenesis in hamster, Pyruvate dehydrogenase complex (PDC) has been found in spermatocytes mitochondria. In spermatozoa, however, additional localization of PDC in the acrosome has been detected (Mitra *et al.* 2005). In addition, mitochondrially-translated subunits of the Cytochrome c oxidase (complex IV of the respiratory chain) have been detected outside mitochondria. Cox I and II subunits have been retrieved in rat zymogen granules (pancreas) and in growth hormone granules (hypophysis) (Sadacharan *et al.* 2005), while Cox III has been detected in the cytoplasm of developing rat brain (Cannino *et al.* 2004).

In addition, several proteins are expressed and addressed to mitochondria under certain conditions. For instance ISG12b2 protein, which is induced during viral infection, by type I interferon (IFN), to regulate mitochondria-dependent apoptosis (Lu and Liao 2011).

Inducible protein translocation into mitochondria

The MTS of some proteins can be hidden and consequently their import to mitochondria inhibited. Upon metabolic changes or stress conditions, the MTS becomes accessible. For example, Cytochrome P450 (CYP1A1), which displays both endoplasmic reticulum (ER) and mitochondrial targeting signals, is normally addressed to the ER. When the ER signal (at the N-terminal of the protein) is cleaved by an endoprotease, the generated N-terminal contains the MTS and allows the import of the protein into mitochondria (Addya *et al.* 1997). Despite the translocation of p53 to the mitochondrial outer membrane to promote apoptosis, it is thought that a cleavage of a hidden MTS (similar mechanism to mt-Cytochrome P450) may drive the translocation of p53 into mitochondrial matrix to maintain the stability of mt-DNA (Lindenboim *et al.* 2011).

The MTS can also be hidden by an interaction with a partner that leads to the sequestration of the protein. This is the case for the yeast cytosolic glutamyl-tRNA synthetase (cERS), which in fermentative conditions interacts with Arcp1. It has been shown that when cells are switched to respiration, Arcp1 is down regulated and cERS is imported into mitochondria (Frechin *et al.* 2009).

Inducible protein translocation from mitochondria

Several mitochondrial proteins, after their import and processing, are "released" or "exported" from mitochondria to other subcellular compartments. For example, the heat shock protein 60 kDa (Hsp60), the mitochondrial glutamic-oxaloacetic-transaminase (GOT2) and the hydroxymethylglutaryl-CoA reductase (HMG-Co-A) (as reviewed in Soltys and Gupta 1999, Monaghan and Whitmarsh 2015). Pyruvate dehydrogenase complex (PDC) is retrieved outside mitochondria. It has been suggested that PDC, which is entrapped in Mitochondrial derived vesicles (MDVs), translocates to the lysosome likely to be degraded. PDC complex, in its active form, has also been detected in the nucleus (Sutendra *et al.* 2014). Intriguingly, nuclear PDC complex has been processed in mitochondria before translocation as witnesses the absence of subunits MTSs (reviewed in Ng and Tang 2014), raising questions about export from mitochondria and import to the nucleus of such a megadalton-sized complex.

The well-known examples of inducible translocation from mitochondria are apoptotic proteins, especially the Cytochrome c (Cyt c), which triggers caspase-dependent apoptosis. Release of Cyt c from mitochondria to the cytosol has been shown to occur by different ways: mt-Permeability transition pore (mPTP) opening (Yang and Cortopassi 1998), pro-apoptotic Bax/Bak oligomerization (Antonsson *et al.* 2000), anti-apoptotic Bcl-2 conformation change (Lei *et al.* 2006), and caspase-2/Bid pathway (Guo *et al.* 2002). It has been suggested that these different mechanisms might be mitochondrial responses to diverse apoptotic stimuli (Gogvadze *et al.* 2006). In addition, Cyt c has been shown to display a caspase-independent activity in the nucleus of mouse neurons undergoing necrosis (Zhao *et al.* 2010).

Since exported mt-proteins are retrieved in various cellular compartments, it has been proposed that mitochondria may have different export machineries (Soltys and Gupta 1999). Permeabilization of the outer membrane (Tait and Green 2010) and Mitochondrial derived vesicles (MDVs) (Neuspiel *et al.* 2008, Soubannier *et al.* 2012, Sugiura *et al.* 2014) can explain the release of some proteins, but for others, the mechanism remains ambiguous. An export pathway has been described for some IMS proteins intended to be degraded in the cytosol (Bragoszewski *et al.* 2015), but cannot explain the release of matrix proteins or the release of active proteins since it requires protein unfolding. Also, except the ABCB10 transporter, which exports peptides from the matrix to the IMS, no channel in known so far to export full-size proteins from the matrix (Herget and Tampe 2007).

Interestingly, proteins translocating from or into mitochondria may either perform the same function inside and outside mitochondria, or have a certain function inside mitochondria and a different function outside mitochondria (Monaghan and Whitmarsh 2015, Soltys and Gupta 1999).

In addition to the nucleus-mitochondria communication, it has been recently shown that cells can also communicate through whole mitochondria transfer. Indeed, in mammals (as reviewed in Berridge *et al.* 2016) as well as in plants (Gurdon *et al.* 2016), mitochondria and mt-DNA can move from one cell into neighbor cell in order e.g. to restore respiration defect or satisfy a bioenergetic need.

3. Optimization of mitochondrial functions: the inner membrane as a multifunctional Platform

In order to satisfy energetic and metabolic needs of the cell, mitochondria have evolved and adapted different mechanisms. For example, invagination of the inner membrane (IM) drastically enlarged its surface area as compared to the outer membrane (OM). This surface extension and the Mitochondrial contact site and cristae organizing system (MICOS) complex divide the IM into two subcompartments: the Inner boundary membrane (IBM) and Cristae membrane (CM). Respiratory chain complexes are assembled in supercomplexes essentially in the CM allowing the optimization of ATP production and release. The IBM is dedicated to translocation complexes and also for mt-DNA gene expression (van der Laan *et al.* 2016). Indeed, replication, transcription and translation are sequential and successive processes likely occurring close to the inner membrane (Jourdain *et al.* 2016)(Figure 4). Here, we review how these processes are clustered and anchored to the inner membrane.

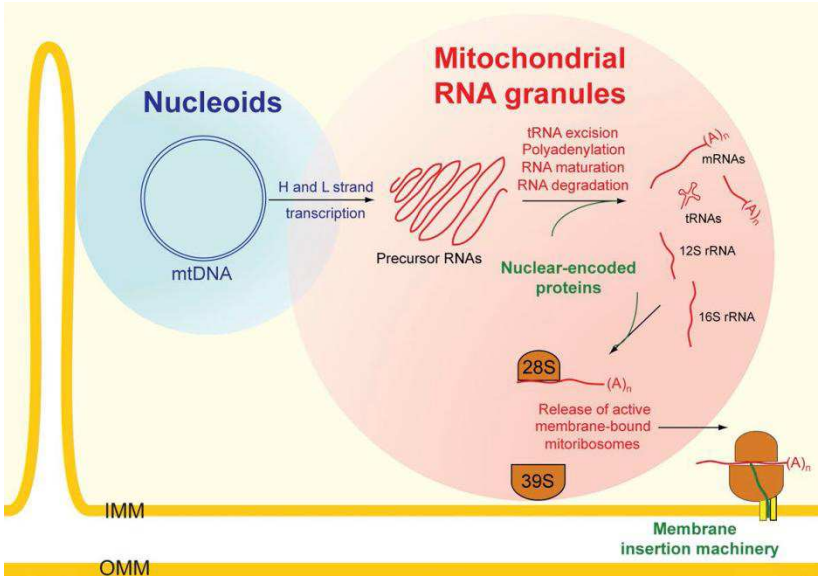

Figure 4: Interconnection of mt-DNA replication, transcription and translation (taken from Jourdain *et al.* 2016).

3.1. Replication/transcription

Human mt-genome is a circular double stranded DNA (Heavy and Light strands) present in cells at variable copy number and organized in structures named nucleoids. These latter are associated with the inner membrane and contain several mt-DNA molecules condensed and packaged thanks to DNA-interacting proteins (Gilkerson *et al.* 2013). Most of mt-DNA interacting proteins belong to the replication and transcription machineries such as the mitochondrial translation factor A (TFAM), single stranded DNA-binding protein (mtSSB) and helicase Twinkle (Wang and Bogenhagen 2006). Twinkle has been suggested as the platform of replication at the inner membrane. Although the mechanism is not well understood, it has been shown that Twinkle is tightly associated with cholesterol-rich structures of the inner membrane (Gerhold *et al.* 2015, Rajala *et al.* 2014). Other membrane-associated or integral proteins like the adenosine nucleotide translocator (ANT1) and Prohibitin have been co-purified with nucleoids in different species (Bogenhagen *et al.* 2003, He *et al.* 2012, Rajala *et al.* 2015). Replication and transcription of mt-DNA are tandem processes. Indeed, the mt-RNA polymerase (mtRNAP) synthesizes a short RNA using the light strand as template. In the absence of TEFM (mitochondrial transcription elongation factor), the short RNA has been shown to serve as a primer for the replication by the DNA polymerase gamma (Polγ), whereas in the presence of TEFM, mtRNAP continues the transcription (Agaronyan *et al.* 2015).

Mt-DNA is transcribed into three polycistronic RNAs, two from the heavy strand and one from the light strand. Processing of RNAs seems to occur in an RNA-rich domain named Mitochondrial RNA granules (MRGs) localized close to nucleoids (Antonicka *et al.* 2013, Jourdain *et al.* 2013). Several factors involved in the RNA processing, maturation and degradation are presents in these MRGs (Antonicka and Shoubridge 2015). Proximity of MRGs to the inner membrane and especially to the translocation machineries allows coordination during the mitoribosome assembly, between imported mt-ribosomal proteins and processed mt-rRNAs (Tu and Barrientos 2015). Interestingly, some mt aminoacyl-tRNA synthetases (mt-aaRSs), e.g. mt-AspRS, were co-purified or detected with nucleoids and/or RNA granules suggesting either a role

in replication/transcription or only a high clustering of mt-gene expression factors (Rajala *et al.* 2015, Antonicka and Shoubridge 2015).

3.2. Translation

From an evolutionary point of view, several factors involving in the replication/transcription of mt-DNA are from bacteriophage origin, acquired probably after infection of the α-proteobacterium ancestor at the early stage of endosymbiosis (Shutt and Gray 2006). Unlike replication and transcription, the mt translation machinery is likely bacterial-like (Koc *et al.* 2010, Kehrein *et al.* 2013). Mitoribosome is associated with the matrix side of the inner membrane (Liu and Spremulli 2000). Recently, it has been demonstrated that porcine mitoribosome is anchored into the inner membrane thanks to the mitochondrial ribosomal protein L45 (MRPL45) (Greber *et al.* 2014). The association of mitoribosome with the inner membrane, at least in mammals, is likely indispensable since the translation machinery synthesizes only highly hydrophobic inner membrane proteins (Ott and Herrmann 2010). Other mt translation factors are retrieved associated with the inner mitochondrial membrane e.g. bovine mitochondrial elongation factor Tu (EF-Tumt) (Suzuki *et al.* 2007). Mitochondrial transcription termination factor 3 (MTERF3) is a key coordinator between transcription and translation in mouse (Wredenberg *et al.* 2013). In addition to MTERF3, the ATPase ATAD3 and Prohibitin have been detected, in human cells, among major components of nucleoids and also as partners of mitoribosome, witnessing again of the association of mt-gene expression steps (He *et al.* 2012).

Substrates of the mitoribosome are mainly RNA molecules: mRNAs and aminoacylated-tRNAs. As mentioned above, mt-RNAs undergo processing and maturation in the RNA granule structures. Aminoacylation, which is an important step in the maturation of tRNAs, may occur in MRGs since several mt-aaRSs have been detected in these structures (Antonicka and Shoubridge 2015).

4. Mammalian aminoacyl-tRNA synthetases (aaRSs)

Aminoacyl-tRNA synthetases are housekeeping and ubiquitous enzymes, the primary function of which is to combine amino acids with tRNAs, and produce aminoacylated-tRNAs (aa-tRNAs). These latter are crucial molecules that convert the nucleotidic triplet code of mRNAs into the amino acid single code of proteins. Each aaRS recognizes one or more tRNAs thanks to a set of identity elements, present on both the primary and tertiary structures of the tRNA, and mostly conserved through all kingdoms. Although cytosolic and mt-aaRSs share the same primary function, several features differentiate them. In human, cytosolic and mitochondrial aaRSs are distinct, encoded by two sets of genes. The only exceptions concern LysRSs and GlyRSs (Bonnefond *et al.* 2005). Of note, no gene has been inferred to a mitochondrial glutaminyl-tRNA synthetase (GlnRS) to date, and it has been demonstrated that Gln-tRNA^{Gln} is produced indirectly by transamidation of Glu-tRNA^{Gln} by the GatCAB aminoacyl-tRNA amidotransferase. Glu-tRNA^{Gln} is synthesized by the non-discriminating mt-GluRS (Echevarria *et al.* 2014).

4.1. Mitochondrial aaRSs: structural and functional peculiarities

Mutation rate of mammalian mt-DNA is high, generating the peculiar situation where mt-RNAs are rather degenerated as compared to their bacterial ancestors and yet have to be recognized by nucleus-encoded partner proteins. Degeneracy of mt-tRNAs concerns their structure and function. Indeed, most of the 22 human mt-tRNAs have a biased nucleotide composition (less Gs), reduced D and/or T-loops, and are missing some of the canonical nucleotides required for long distance interaction and 3D folding (reviewed e.g. in Helm *et al.* 2000). These later lead to the thermodynamic instability of mt-tRNAs, as compared to cytosolic counterparts (Bhaskaran *et al.* 2014). It has also been shown that the set of tRNA identity elements is often restricted to few residues in human mitochondrial aminoayclation systems, while otherwise evolutionary conserved (e.g. Sohm *et al.* 2004, Bonnefond *et al.* 2005, Fender *et al.* 2006). Besides, nuclear-encoded mt-aaRSs were shown to evolve faster than cytosolic counterparts (Adrion *et al.* 2016), which may contribute to the mutual and adaptive recognition with “degenerated”

tRNAs. Here are exposed some structural and functional aspects of the adaptation, although sometimes it is difficult to separate both aspects.

Structural peculiarities

Few mt-aaRSs have been crystallized so far and allowed to gain deeper knowledge about their organization and mechanism of action (mt-SerRS, Chimnaronk *et al.* 2005; GlyRS, Xie *et al.* 2006; mt-TyrRS, Bonnefond *et al.* 2007; LysRS, Guo *et al.* 2008; mt-PheRS, Klipcan *et al.* 2012; mt-AspRS, Neuenfeldt *et al.* 2013). Mt-PheRS has large changes in the architecture leading to a particular oligomeric organization. Indeed, bacterial and cytosolic PheRSs are heterotetrameric, composed of two α subunits bearing the aminoacylation activity and two β subunits performing the editing activity. Mt-PheRS is, however, a chimera of α and β subunits and is a monomeric enzyme instead of the well-conserved heterotetrameric organization. Mt-SerRS illustrates another way of compensation. Mammals possess two mt-tRNA^{Ser} isoacceptors among which one is D-armless. Mt-SerRS has acquired additional N- and C-terminal extensions (compared to its bacterial homolog) and is able to recognize and aminoacylate both mt-tRNA^{Ser} isoacceptors (Chimnaronk *et al.* 2005). The resolution of mt-AspRS crystallographic structure and its comparison with the *E. coli* enzyme highlighted a common 3D architecture. However, functional differences in thermodynamics and biophysical properties, in stability and in substrate selectivity, were detected indicating a higher plasticity of the mt-enzyme (Neuenfeldt *et al.* 2013).

Functional peculiarities

As already mentioned above, mt-aaRSs have to recognize mt-tRNAs with reduced identity sets. It has been demonstrated for instance that the lost of a major (and primordial) identity element in mt-tRNA^{Asp} is accompanied by the replacement of a highly conserved catalytic residue in mt-AspRS (Fender *et al.* 2006). In addition, most mt-aaRSs have relaxed specificities and are able to aminoacyle tRNAs from different origins (cross-aminoacylation), and again mt-PheRS is a striking example. Mt-PheRS displays a high conformational plasticity (open and closed forms) to perform its activity, besides its ability to achieve conformational rearrangements allowing cross-

aminoacylation of bacterial and cytosolic $tRNA^{Phe}$ (Yadavalli *et al.* 2009, Kumazawa *et al.* 1989). Another example concerns AspRSs: while the human mt-AspRS has been shown to recognize and aminoacylate $tRNA^{Asp}$ from any species, bacterial AspRS cannot aminoacylate human mt-$tRNA^{Asp}$ due to the sequence and structural relaxation of the mt-tRNA (Fender *et al.* 2012). Finally, certain mt-aaRSs have lost their editing activity (e.g. Roy *et al.* 2005) and/or display low aminoacylation efficiency *in vitro* as compared to their cytosolic or bacterial homolog (as reviewed in Sissler *et al.* 2000).

Low aminoacylation efficiency and loss of editing in mitochondria may be due to the few number of proteins synthesized, and may also be signs of the organelle evolving toward its extinction (Khachane *et al.* 2007). This hypothesis could be reinforced by the recent discovery of a eukaryote organism having lost its acquired mitochondria (Karnkowska *et al.* 2016). The absence of editing is hypothesized to rely either on the accuracy and specificity of the mt-aaRS activity, or surveillance made by EF-Tu (Nagao and Suzuki 2007), or on quality control degradation of mistranslated proteins. However, since stress conditions, especially reactive oxygen species (ROS) enhance mistranslation in several systems (e.g. Netzer *et al.* 2009), and taking into account the bacterial origin of mitochondria, it cannot be excluded that mitochondrial mistranslation may be increased in stress conditions and might be a mean of adaptation to an environment prone to oxidative damages, as it has been shown for some bacteria (Javid *et al.* 2014, Fan *et al.* 2015, Bullwinkle and Ibba 2016).

Although no case has been reported so far, it has been suggested that protein partners may compensate the different peculiarities of mt-tRNAs and mt-aaRSs e.g. to increase the activity or for trans-editing, similarly to the case of mtEF-Tu where two isoforms have been detected in Enoplea, specific for D- and T-armless tRNAs (Ohtsuki and Watanabe 2007). Thus, investigation of mt-aaRSs partners may provide additional information about their function *in vivo*.

Altogether, the few studies conducted so far on mt-aaRSs state the high intricacy of the mitochondrial system, and the need for more investigations. In addition to solving intrinsic limitations of mt-aaRSs study (e.g. determination of the mature form for in vitro studies), it is important to benefit from the extensive work, which has been done on

cytosolic aaRSs essentially on their macromolecular organization, partnership, and their non-canonical functions.

4.2. Cytosolic aaRSs: macromolecular organization, partnership, alternative functions and human diseases

Macromolecular organization and partnership

In the cytosol, nine aaRSs are organized in a Multi-aminoacyl-tRNA synthetases complex (MSC) of 1.5 MDa (Mirande *et al.* 1982). This latter is composed of: two monomers of arginyl-tRNA synthetase (ArgRS); one monomer of each of glutaminyl-tRNA synthetase (GlnRS), leucyl-tRNA sythetase (LeuRS), isoleucyl-tRNA sythetase (IleRS) and methionyl-tRNA sythetase (MetRS); one dimer of each of aspartyl-tRNA sythetase (AspRS), lysyl-tRNA sythetase (LysRS) and glutamyl-prolyl-tRNA sythetase (GluProRS). In addition to these aaRSs, three scaffolding proteins (Aminoacyl-tRNA synthetases complex-interacting multifunctional proteins) AIMP1/p43, AIMP2/p38 and AIMP3/p18 play an important role in the assembly of MSC (Havrylenko and Mirande 2015). MSC has been demonstrated to interact with the elongation factor EF1α (Reed *et al.* 1994) and ribosomes (David *et al.* 2011). The sublocalization of MSC near the translation machinery is thought to be a means of tRNAs recycling (Stapulionis and Deutscher 1995).

Furthermore, valyl-tRNA synthetase (ValRS) interacts with the heavy form of the elongation factor 1 (EF-1H) and forms a stable complex of ~ 700 kDa (Bec *et al.* 1989). EF-1H interaction has been shown to enhance the aminoacylation activity of ValRS (Negrutskii *et al.* 1999).

In contrary to cytosolic aaRSs, no mt-aaRS has been detected in a complex so far.

Alternative functions

MSC is also considered as a functional depot or a platform where an aaRS performs its aminoacylation activity, and another (alternative) function when released from this platform (Ray *et al.* 2007). Indeed, it has been shown that several aaRSs from MSC can play non-canonical (alternative) functions unrelated to their canonical function,

and in a variety of pathways. Although the depot hypothesis is widely admitted, it cannot explain the case of free aaRSs having also alternative functions (see below).

Alternative functions are inducible (functional switch) and pass through either new networks of physical interactions or an enzymatic activity, generally preceded by translocation and/or post-translational modifications (PTMs). Although catalytic domains may be involved in alternative functions, most of these latter are performed by structural domains acquired during evolution. In addition, some alternative functions are performed by splice variants or paralogs rather than by the aaRS implicated in the aminoacylation activity (Guo and Schimmel 2013, Pang *et al.* 2014, Lo *et al.* 2014). In order to illustrate the diversity of alternative functions regulation, the example of LysRS (Motzik *et al.* 2013) and TrpRS (Mirando *et al.* 2014) are chosen.

LysRS is belonging to the MSC, able to translocate to different subcellular compartments. In mast cells and cardiomyocytes, LysRS dissociates from the MSC and translocates to the nucleus upon MAP kinase pathway-dependent phosphorylation. Once in the nucleus, LysRS synthesizes diadenosine tetraphosphate (Ap_4A) through its enzymatic activity by combining two ATP molecules. Ap_4A interacts with Hint-1 (Histidine triad nucleotide-binding protein 1), which consequently dissociates from Hint-1/MITF (Microphtalamia-associated transcription factor) complex. Then, freed MITF transcribes its target genes (Ofir-Birin *et al.* 2013). Full-length LysRS can be released to the extracellular environment to induce macrophage migration and TNFα secretion (Park *et al.* 2005). LysRS can also translocate to the plasma membrane upon phosphorylation (p38 MAPK-dependent) in cancer cells, where LysRS stabilizes Laminin receptor (67LR) and induce cell migration (Kim *et al.* 2012). In treated cancer cells (e.g. chemotherapy), LysRS, ERp57 (disulfide isomerase) and Calreticulin are hypothesized to translocate together to the plasma membrane in order to induce the immune response. However, the PTM allowing the release of LysRS from MSC in this condition has to be elucidated (Kepp *et al.* 2010). Finally, $tRNA^{Lys3}$ is packaged into HIV-1 virions in order to be used as a primer for reverse transcriptase. In additon to $tRNA^{Lys3}$, LysRS is also packaged into HIV-1 virions although its origin (cytosolic or mitochondrial) is a debated question (Halwani *et al.* 2004, Kobbi *et al.* 2011).

In contrary to LysRS, TrpRS is a free aaRS and does not belong to the MSC. This aaRS is produced either as a full-length protein or short version splice variant (mini-TrpRS). Upon stimulation with INFγ, expression of both full-length and mini-TrpRS is upregulated. Mini-TrpRS is released from the cell and interacts, using its catalytic domain, with VE-cadherin in order to inhibit angiogenesis. Full-length TrpRS is either released from the cell or translocated to the nucleus. When released outside the cell, TrpRS is cleaved and the C-terminal part (T2-TrpRS similar to the mini-TrpRS) plays the same function than mini-TrpRS (Tzima *et al.* 2005). When translocated to the nucleus, TrpRS interacts, *via* its WHEP domain (new acquired domain found in TrpRS, HisRS, GluProRS, GlyRS and MetRS), with both PARP-1 (Poly(ADP-ribose) polymerase 1) and DNA-PKcs (DNA-dependent protein kinase $_{\text{catalytic subunit}}$) in order to activate p53, which in turn inhibits cell proliferation (Sajish *et al.* 2012).

Correlation of cytosolic aaRSs with human diseases

Both canonical and alternative functions of cytosolic aaRSs are associated with human diseases including cancers, neurodegenerative and autoimmune disorders, in addition to predisposition to other diseases (reviewed e.g. in Park *et al.* 2008). Exploring aaRSs properties and functions has allowed understanding the etiology of several diseases. Also, investigations on pathology-related mutations have strongly suggested non-canonical function of some aaRSs since the impact has not been observed on the aminoacylation activities (Yao and Fox 2013). Intriguingly, mutations on some cytosolic aaRSs provoke in patients effects and symptoms similar to those provoked by some mt-aaRSs mutations e.g. leukoencephalopathies correlated with mutations in either cytosolic AspRS or mt-AspRS (Taft *et al.* 2013, Scheper *et al.* 2007, respectively). This striking observation raises the question about a possible metabolic connection between cytosolic and mitochondrial aaRSs that has not been discovered yet.

5. Mitochondrial diseases related to mt-aaRSs: a focus on LBSL

There is no consensus definition of the "human mitochondrial disease" and three definitions can be found: 1) it corresponds to a disorder caused only by mt-DNA mutation (World Health Organization); 2) it concerns only dysfunctions of the respiratory chain (e.g. DiMauro 2004); 3) it is the impairment of a mitochondrial function (e.g. Calvo and Mootha 2010). Considering all definitions, human mitochondrial disorders are either due to genetic dysfunctions or acquired (e.g. iatrogenic, Finsterer and Segall 2010, or environmental, Meyer *et al.* 2013). Due to the dual genetic origin of mitochondrial macromolecules, alterations can be found either in the mitochondrial genome (Hatakeyama and Goto 2016), or in the nuclear genome (Goldstein *et al.* 2013), or even, rarely, combination of both (mt-CYB/SDHB, Nesti *et al.* 2015). Due to the heterogeneity of clinical and genetic features of mitochondrial disorders, it is difficult to establish the diagnosis and the phenotype-genotype correlation. Interestingly, a diagnostic algorithm, based on Magnetic resonance imaging (MRI) and Magnetic resonance spectroscopy (MRS), has been developed to orient the genetic investigations of mitochondrial disease related to the respiratory chain deficiency (Devaux-Bricout *et al.* 2014). However, since the development of Next-generation sequencing (NGS), a set of mt-genes is systematically sequenced after the clinical and biochemical examinations of patients.

Alterations of the mt-DNA are of maternal inheritance and are responsible for several disorders e.g. encephalomyopathy, lactic acidosis, and stroke-like episodes (MELAS) and Leber hereditary optic neuropathy (LHON). Interestingly, some mt-tRNA mutations (associated with diseases) can be compensated by overexpression of their cognate mt-aaRS (e.g. Rorbach *et al.* 2008). Nuclear alterations are of mendelian inheritance and can affect a variety of mitochondrial functions. Altogether, the prevalence of mitochondrial diseases is high. For instance, mitochondrial diseases characterized by respiratory chain dysfunction (either from mt-DNA or nuclear DNA mutations) affect 1 in 5,000 live birth (Skladal *et al.* 2003).

Among diseases implying nuclear mutations (substitution, insertion and deletion

with or without frameshift), several are associated with mt-aaRSs, with a wide range of severity as well as tissue-specificity of phenotypic expression. Since 2007, when a leukoencephalopathy (see LBSL) has been correlated to mutations on mt-AspRS coding gene (*DARS2*) (Scheper *et al.* 2007), a variety of disorders, mostly neurodegenerative have been directly related to the 16 (out of 17) mt-aaRSs, in addition to GlyRS and LysRS, which have common genes with their cytosolic counterparts (reviewed in Konovalova and Tyynismaa 2013, Schwenzer *et al.* 2014) (Figure 5). The only exception concerns *WARS2* (coding for mt-TrpRS) for which no mutation has been detected so far, which may suggest that all mutations on TrpRS lead to embryo/fetus lethality. However, the expression of mt-TrpRS is modulated in breast cancer (Huang *et al.* 2013).

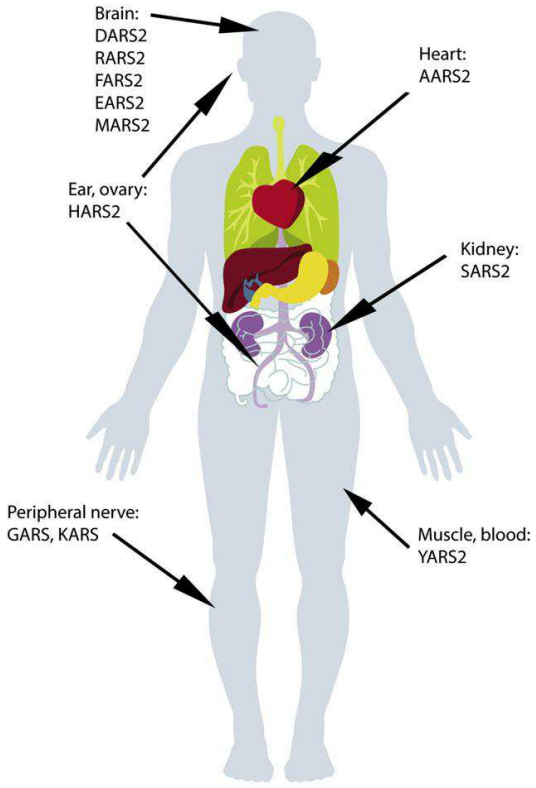

Figure 5: Tissue-specificity of mitochondrial disorders correlated with mitochondrial aminoacyl-tRNA synthetases (mt-aaRSs)(taken from Konovalova and Tyynismaa 2013).

The hosting lab is interested in human mitochondrial translation with a special focus on mt-tRNAs and mt-aaRSs. All these latter are associated with human diseases, but the link between mt-aaRSs mutations and the disease is often unknown. For example, to contribute in the deciphering of this link, a web server named **MiSynPat**, dedicated to

human mt-aaRSs diseases, is in the process of being finalized and published (in collaboration with L. Moulinier and O. Poch, LBGI, I-Cube, Strasbourg). It offers, for specialists and non-specialists, an analysis and follow-up tools: to retrieve literature and data related to each mt-aaRS (e.g. references, affected genes, related disorders, allelic compositions in patients); to locate the mutated amino acid on 3D representation (crystallographic structure or homology model) and/or generate a model of the mutant; and finally, to place the mutated position in multiple sequence alignments of aaRS sequences, ranging from bacteria up to human, to check the conservation.

Leukoencephalopathy with Brainstem and Spinal cord involvement and Lactate elevation (LBSL)

The most prominent case of mt-aaRSs genes associated with diseases concerns *DARS2*, for which mutations are specifically associated with a Leukoencephalopathy with Brainstem and Spinal cord involvement and Lactate elevation (LBSL), an autosomal recessive disease. LBSL disease is a slowly progressive white matter disorder affecting myelinated nerve fibers of the Central nervous system (CNS), with additional peripheral neuropathy in several patients. Although it was unclear whether mutations affect astrocytes, oligodendrocytes (which surround neurons and form the myelin sheath) or neurons, it was assumed that LBSL affects essentially these latter. Recently, two mice models have been established with inducible knockout (KO) of *DARS2* either in neurons or in oligodendrocytes. Besides a mild deficiency of the oxidative phosphorylation in corpus callosum (the part joining right and left hemispheres), no phenotype has been noticed for mt-AspRS KO in oligodendrocytes. However, when mt-AspRS was knocked-out in neurons, signs of neurodegeneration have been observed including defect in oxidative phosphorylation, atrophy of the cortex and hippocampus due to apoptosis, increased immune response and an abnormal behavior (Aradjanski *et al.* 2016).

LBSL patients suffer from motor skills generally legs are more affected, with impaired manual dexterity. They suffer also from ataxia and spasticity, in addition to epilepsy for some patients. Most of patients have normal intellectual capacity but can have problems of learning and/or speech articulation. Clinical severity varies from rapidly fatal disease when of infantile onset to slow and mild disease when of adult onset,

but the most common phenotype was characterized by childhood onset and slow neurological deterioration (reviewed in van Berge *et al.* 2014). So far, no correlation has been identified between the onset of LBSL and the type of mutations.

Diagnosis of LBSL leans on MRI and MRS, and genetic confirmation of *DARS2* mutation. White matter abnormalities observed by MRI are accompanied with lactate elevation. This latter is suggested to be associated with mitochondrial dysfunction; however, an LBSL-patient has been reported without lactate elevation (Sharma *et al.* 2011). Often a decrease in N-acetylaspartate (NAA) and an increase in myo-inositol are also detected in LBSL, which are respectively signs of gliosis (proliferation or hypertrophy of glial cells), and axonal damage or loss (van der Knaap *et al.* 2003).

Correlation of LBSL with *DARS2* mutations

LBSL has been correlated with mt-AspRS-coding gene, after a genome-wide linkage mapping analysis on 38 patients (from 30 different families) (Scheper *et al.* 2007). Nowadays, more than 60 different clinically relevant mutations have been identified (van Berge *et al.* 2014). Patients are mainly compound heterozygotes, and only few are homozygotes. Mutations are spread throughout the gene (including the 17 exons and the noncoding regions). Most of patients (almost 95%) display, on one allele, a mutation leading to a splicing defect, and on the other allele a deletion, nonsense or missense mutation, or another splicing defect (van Berge *et al.* 2014).

The splicing defect results from mutation in the intron 2, and leads to a frameshift (with premature stop codon) and skipping of the exon 3. The splicing defect of this latter is "leaky", meaning that a residual wild type (WT) mt-AspRS is still produced allowing patients survival. The general splicing in the neuronal cells has been shown to be less efficient than cells from other organs (van Berge *et al.* 2012, Roesser *et al.* 1993), it is thus hypothesized that the splicing defect of mt-AspRS may be enhanced in the brain leading to the tissue-specificity of LBSL (van Berge *et al.* 2012). A promising molecule (cantharidin) has been proved to correct the splicing defect and proposed as a therapy for LBSL, although more developments are needed because of the molecule toxicity (van Berge *et al.* 2014). However, it is unknown how patients survive and how the LBSL is tissue-specific for cases implying, not splicing defects, but other type of mutations e.g.

missense mutations.

In addition to few "in frame" deletions, five nonsense mutations leading to premature stop codon were reported. Deleted and truncated mt-AspRSs are most likely degraded. The most intriguing alterations are the 25 missense mutations. Indeed, it is difficult to predict the impact of a missense mutation, since it can affect the expression (transcription or translation), import, processing, folding and structure or the aminoacylation activity. Although yet unknown but expected, missense mutation might also affect an alternative function, a motif of interaction with a partner, or a site of regulation e.g. post-translational modification. Pioneered investigations on a subset of missense mutations highlighted that they do not systematically impair the canonical aminoacylation property of mt-aaRSs (Scheper *et al.* 2007, van Berge *et al.* 2013). Additional investigations contributed to further demonstrate the variability of impacts among mutations. *In cellulo* expression analysis on a set of nine mt-AspRS mutations revealed that 3 out of 9 mutants were affected in their protein expression. The same study investigated the targeting to mitochondria and dimerization of mutated mt-AspRS. Targeting of mutated mt-AspRSs was not affected at all, while the impact on dimerization was differential. Indeed, except one mutation drastically affecting the dimerization, most of mutations reduce this latter property of mt-AspRS (van Berge *et al.* 2013). One mt-AspRS mutant, which was *in vitro*-translated, has been assessed for its import *in organello*. It has been concluded that translocation of this mutant into mitochondria was impaired (Messmer *et al.* 2011).

Altogether, much more studies are necessary to understand the link between mt-AspRS mutations and the LBSL etiology. However, to do so we need first to learn more about the function of mt-AspRS in the cellular environment (e.g. partnership).

Objectives

In line with the team objectives, my work aimed at further understanding the link LBSL/mt-AspRS mutations. This work has been a virtuous circle that needs both studying of mt-AspRS cellular properties from a fundamental point of view to establish the link with LBSL, and exploring LBSL-related mutations, which may help and direct the investigations.

Cytosolic aaRSs have been extensively studied regarding their organization (free or belonging to the MSC) and their partnerships to perform the canonical aminoacylation activity as well as the alternative one. Alternative functions of mt-aaRS have been discovered in non-metazoan species (as reviewed in Annex 1, Huot *et al.* 2014). Alternative functions for metazoan (especially mammalian) mt-aaRSs are strongly suggested but no experimental evidence has been described so far. During writing of this manuscript, the first case of alternative function performed by a mammalian mt-aaRS was published. Indeed, rat mt-TrpRS has been reported to have a pro-angiogenic activity in contrary to its cytosolic counterpart, which is anti-angiogenic (Wang *et al.* 2016). This new activity may explain the association of mt-TrpRS with human breast cancer (an association, which is described in Huang *et al.* 2013). This discovery opens the door to the others. Furthermore, it has been suggested that mt-AspRS may have an alternative function since several mutations do not impact the enzymatic activity or the structure, and no general mechanism can explain the impact of all LBSL-causing mutations. However, in addition to a potential alternative function of mt-AspRS, absence of impact on the enzymatic activity *in vitro* may also be explained by alteration of a potential regulatory site of the aminoacylation e.g. a motif of interaction with a partner or a site of post-translational modification. Thus, in **Chapter 1**, we raise different interrogations about whether mt-AspRS has protein partners and whether it belongs to a complex. If any, whether partners are co-factors to the aminoacylation activity or to an unknown alternative function. We propose different approaches to answer these questions.

Replication of mt-DNA and expression (transcription and translation) of mt-genes are interconnected mechanisms, performed in defined and specialized structures at the inner membrane. Several factors involved in these different processes were co-purified with some mt-aaRSs, including mt-AspRS (Rajala *et al.* 2015, Antonicka and Shoubridge 2015). Whether mt-AspRS belongs to a specialized structure has to be demonstrated. Thus, **Chapter 2** is dedicated to characterize submitochondrial localization of mt-AspRS. Furthermore, processing and maturation steps may influence the submitochondrial localization, thus identification of mt-AspRS mature form would be valuable information. However, defining the mature form is not an easy task, since discrepancies have been observed after using prediction programs to define the MTS. Although the difference between the predicted MTS and the real one can differ only with few amino acids, it can drastically change enzyme features. This was observed with e.g. human mt-LeuRS (Yao *et al.* 2003). Along the same line, resolving the crystallographic structure and studying mt-AspRS were possible only after considering an MTS shorter than the predicted one (Neuenfeldt *et al.* 2013, Gaudry *et al.* 2012). However, we still do not know what is the exact mature form of mt-AspRS. In addition to the investigation of the submitochondrial localization of mt-AspRS, the objective of **Chapter 2** is also to identify the mature form of mt-AspRS after processing. Defining the mature form is important to express and study mt-proteins *in vitro* and ultimately to understand their function in health and disease.

Missense mutations can affect one of the multiple steps of mt-AspRS long journey, from its expression to its functional location. In addition to the canonical path, mutations may also impact a potential alternative function, or a functional switch of this latter (e.g. post-translational modification, interaction with a partner or a translocation). LBSL-mutations, studied so far, do not systematically impair the canonical aminoacylation (Scheper *et al.* 2007, van Berge *et al.* 2013). In addition to one mutant affecting mitochondrial translocation (Messmer *et al.* 2011), differential impacts have been observed for mt-AspRS expression and dimerization (van Berge *et al.* 2013). The objective of **Chapter 3** is to assess additional mt-AspRS properties including properties discovered during this work, using an *in cellulo* system. Results will be discussed in regards to the clinical context.

Integrating different approaches, my thesis work is contributing, from one hand, to the general understanding of mt-AspRS properties in its cellular environment, and to shed new light or at least to have a more precise overview of the link between mt-AspRS mutations and LBSL disease, from the other hand.

RESULTS & DISCUSSIONS

RESULTS & DISCUSSIONS

Chapter 1: Searching for biologically relevant protein partners of human mt-AspRS

1.1. Introduction

Several results and observations have led to consider the existence of potential protein partners interacting with mt-AspRS (and with mt-aaRSs in general):

A) Some of the cytosolic aaRSs have been detected in a complexed form (the MSC and ValRS/EF-1H), interacting with other aaRSs or with protein cofactors in order to perform their aminoacylation activities (Mirande *et al.* 1982, Bec *et al.* 1989). Some cytosolic aaRSs have also been shown to interact with proteins belonging to different pathways in order to play an alternative function (reviewed in Guo and Schimmel 2013, Pang *et al.* 2014).

B) The enzymatic activity of mt-AspRS *in vitro* is reduced in respect to its bacterial homolog, thus it has been suggested that the enzyme may need a partner to improve its activity *in vivo* (Neuenfeldt *et al.* 2013). This is the case for example of several aaRSs (including mammalian cytosolic ValRS), where their interaction with other aaRSs, or with cofactors stimulates their aminoacylation activity (as reviewed in Hausmann and Ibba 2008).

C) Several LBSL-causing mutations are affecting neither the structure nor the enzymatic activity (see Chapter 3), suggesting another causes for the disease. Two major hypotheses were put forward: these mutations could affect either an interaction of mt-AspRS with a partner regulating mt-AspRS activity (as mentioned in B), an alternative function or an interaction with a partner unrelated to aminoacylation activity (as mentioned in A).

So, these observations strongly suggest that mt-AspRS interacts with partners and/or belongs to a complex.

Former PhD students of the lab (Marie Messmer and Hagen Schwenzer) have tackled this question by using both immunoprecipitation experiments of the endogenous mt-AspRS, and pull down experiments with His-tagged recombinant mt-AspRS. The numerous experiments performed so far were however mostly non-reproducible, indicating that the partnership, if exists, would be either transient, dependent of some physiological conditions, or tissue specifiic. In the present chapter, other approaches are used to investigate whether mt-AspRS belongs to a stable or transient complex. In the latter case, cross-linkers are used to stabilize the potential transient complex. Alternatively, data mining was performed in order to extract information that would orient or help designing future experiments.

1.2. Experimental search of protein partners of mt-AspRS

1.2.1. Detection of human dimeric mt-AspRS within complexes, as a support of the existence of partners

1.2.1.1. Detection of different forms of mt-AspRS on 2D BN-PAGE/SDS-PAGE

The easiest way to detect a stable macromolecular complex is the native electrophoresis developed by Schägger and von Jagow, where complexes have been shown to keep their native and active forms (Schagger and von Jagow 1991). Migration and separation of proteins under native conditions rely either on their intrinsic charge (Colorless-Native polyacrylamide gel electrophoresis, CN-PAGE, Schagger *et al.* 1994) or on the charged G-250 dye (Blue-Native polyacrylamide gel electrophoresis, BN-PAGE, Schagger and von Jagow 1991). We applied a two dimensional BN-PAGE/SDS-PAGE electrophoresis (Schagger *et al.* 1994), which is commonly used for the study of respiratory chain complexes. Figure 35 (adapted from Eubel *et al.* 2005) explains/recalls the whole process.

Mitochondria from Human Embryonic Kidney cells (HEK293T) were purified, and mitochondrial proteins were solubilized using digitonin and separated on the native gel for the first dimension (Figure 6A). The presence of the Coomassie brilliant blue (G-250) makes major complexes visible without any additional staining. Respiratory chain complexes are thus visible, and were assigned thanks to works done in similar conditions (e.g. Wittig *et al.* 2006). The lane of gel, from high to low molecular weight, was cut out and placed horizontally on a standard denaturing 10% SDS-PAGE for the second dimension. After separation, proteins were transferred on PVDF membrane and blotted with anti-mt-AspRS antibody. On the western blot, three spots of mt-AspRS can be distinguished (Figure 6B). After calculation, the first spot displays an apparent MW of ~135 kDa, which likely corresponds to the dimeric form of mt-AspRS (Figure 6C). The 2^{nd} and 3^{rd} spots are slightly diffused and have apparent MW of ~ 225 and ~ 310 kDa, respectively. These spots do not correlate with theoretical oligomers of mt-AspRS, suggesting the existence of this enzyme in complexed forms.

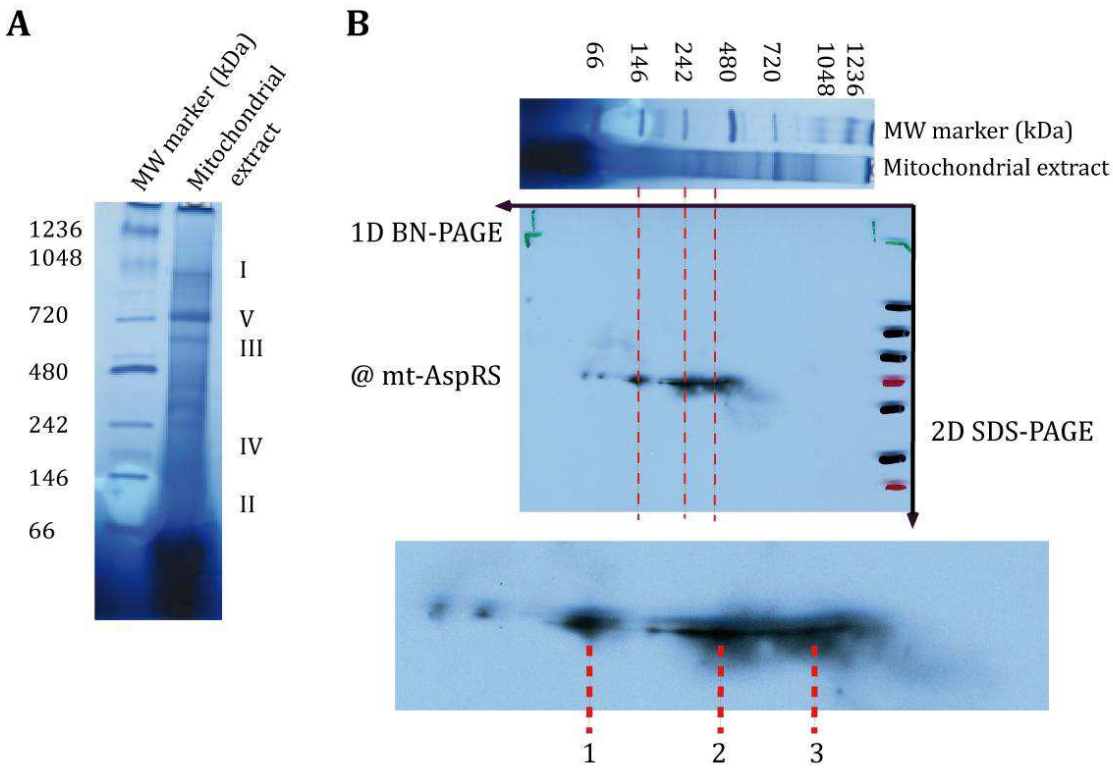

C

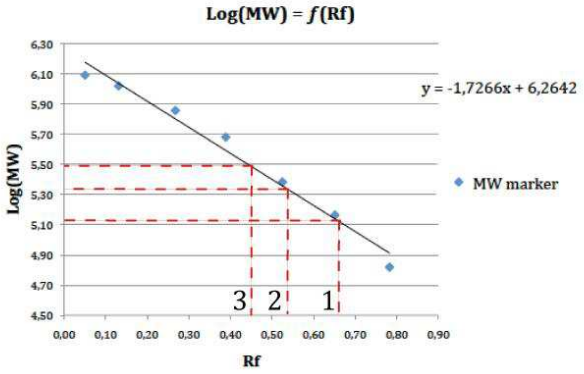

MW Marker	MW (Da)	log(MW)	Rf
	1236000	6,09	0,05
	1048000	6,02	0,13
	720000	5,86	0,27
	480000	5,68	0,39
	242000	5,38	0,53
	146000	5,16	0,65
	66000	4,82	0,78

Spot 1	133242,9	5,12	0,66
Spot 2	223409,7	5,35	0,53
Spot 3	307064,8	5,49	0,45

$$Rf = \frac{\text{Migration distance of the protein}}{\text{Migration distance of the dye front}}$$

Figure 6: BN-PAGE/SDS-PAGE 2D western blot on mitochondrial extract. A) Purified mitochondria from HEK293T cells were solubilized with digitonin prior to loading the mitochondrial extract on BN-PAGE. In these conditions, position of some of the respiratory chain complexes can be assigned. B) The lane of gel (from high to low molecular weight) was cut out and placed horizontally on denaturing gel (SDS-PAGE) followed by standard western blotting. Mt-AspRS was then immunodetected with anti-mt-AspRS on the PVDF membrane (zoom-in of the detected mt-AspRS). C) Mt-AspRS molecular weights were determined from the graph where log(MW Markers) is a function of the relative migration distance (Rf) of MW markers.

1.2.1.2. Detection of mt-AspRS in different bands after cross-linking of mitochondrial extract with glutaraldehyde

Glutaraldehyde (Figure 36A) is a bifunctional cross-linker bridging unspecifically almost any pairs of molecules close together at a distance of < 8 Å. It is used, for example, to determine the oligomerization state of proteins (Fadouloglou *et al.* 2008). The conditions of cross-linking used in our experiments were adapted and optimized from Freitag *et al.* 1997. Mitochondria were enriched from HEK293T cells. Proteins from mitochondrial extract were cross-linked, during 5 and 20 minutes, before being analyzed by western blot. After 5 min of cross-linking, three bands were detected using anti-mt-AspRS antibody (Figure 7A). The first band corresponds to the monomer of mt-AspRS as compared with the uncross-linked sample. The second band has an apparent MW likely corresponding to the dimer of mt-AspRS. The third band is located below the band 250 kDa of the MW ladder. After 20 min of cross-linking, 2 bands were detected (they correspond neither to the monomer nor to the dimer), in addition to the dimer detected with a very low intensity (Figure 7A). The first and the second band are located respectively below and above the band 250 kDa of the MW ladder. Disappearance of the monomer after 20 min of cross-linking means that the time was enough to covalently link all organized mt-AspRS (dimer and complexes). This result suggest that, in HEK293T cell, mt-AspRS is present as a dimer and belonging to 2 complexes and not present as a monomer, consistently with BN-PAGE experiment (section 1.2.1.1.).

Pure recombinant mt-AspRS was submitted to cross-linking experiment in order to verify that the bands observed above do not result from auto-crosslinking of the enzyme (Figure 7B). In addition to bands corresponding to the monomer and dimer of mt-AspRS, a smear is detected with some intense bands. Cross-linking of recombinant mt-AspRS displays a profile, which is different from the profile of endogenous mt-AspRS after cross-linking of mitochondrial extract (Figure 7A).

Although cross-linking experiment with glutaraldehyde is not so conclusive, detection of mt-AspRS in two different bands could suggest a correlation with what have been observed in BN-PAGE. In order to strengthen this approach, it would be interesting to perform the cross-linking on living cells prior to mitochondrial purification and western blot analysis.

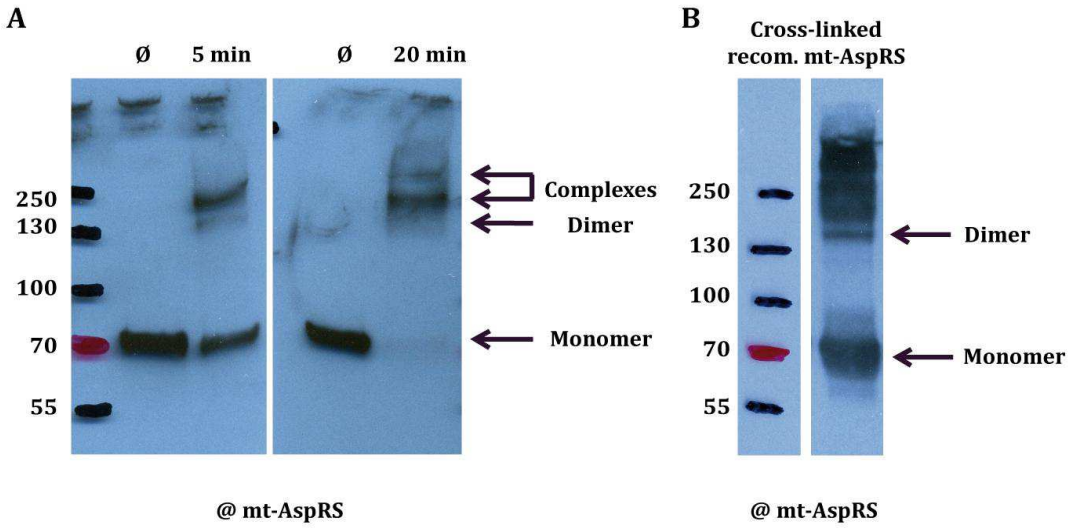

Figure 7: Cross-linking of mitochondrial extract, and recombinant mt-AspRS. A) Mitochondria were purified from HEK293T cells. Mitochondrial extract was subjected to cross-linking with glutaraldehyde prior to western blot analysis. B) Recombinant mt-AspRS was cross-linked with glutaraldehyde to assess the multimers formation.

Altogether, both BN-PAGE and cross-linking with glutaraldehyde approaches provide the first evidence that mt-AspRS likely belongs to two different complexes. These latter do not correspond to multimers of mt-AspRS, and their detection by BN-PAGE suggests a certain stability. Taking into account that a previous study, where different biophysical approaches were used *in vitro*, detected recombinant mt-AspRS only as a dimer (Gaudry *et al.* 2012, Sauter *et al.* 2015), we do not consider the monomeric but only the dimeric form of mt-AspRS to estimate the size of partners. Thus, our results suggest that dimeric mt-ApsRS interacts with at least macromolecules of ~ 85 and of 170 kDa. If we assume that the macromolecules interacting with dimeric mt-AspRS include one or two tRNAs, different sizes of the partners would be possible (Table 1).

Complex	Dimeric mt-AspRS	Number of tRNAs 25 kDa	Size of additional partner(s)
Complex 1 ~ 225 kDa	~ 140 kDa	0	85 kDa
		1	60 kDa
		2	35 kDa
Complex 2 ~ 310 kDa		0	170 kDa
		1	145 kDa
		2	120 kDa

Table 1: Prediction of mt-AspRS partner sizes. Based on the size of complexes detected by BN-PAGE and glutaraldehyde cross-linking, the size of the mt-AspRS partner is predicted (with or without tRNA molecules).

Although, mt-AspRS has a high affinity to its cognate tRNA with a K_d of ~ 250 nM (Neuenfeldt *et al.* 2013), it is unlikely that the tRNA still interacting with mt-AspRS. If this were the case, dimeric mt-AspRS would be detected at a molecular weight higher than 140 kDa. Because 85 kDa is a half of 170 kDa (in the case of no tRNA partner), one can speculate that the partner is composed of two monomers interacting with each mt-AspRS monomer.

1.2.2. Using cross-linking as a tool to identify mt-AspRS partners

As mentioned previously, a lot of effort was furnished to determine potential mt-AspRS partners by immunoprecipitation and pull-down experiments without any reproducible results. Now, we have a clear evidence of the belonging of mt-AspRS to a complex of higher molecular weight, suggesting the existence of cellular partners. Since cross-linking is stabilizing complexes that are too transient, we decided to keep using cross-linker while searching for mt-AspRS partners. However, immunoprecipitation experiments performed after glutaraldehyde cross-linking of mitochondrial extract, remained unsuccessful.

1.2.2.1. Fishing of mt-AspRS partners with sulfo-SBED cross-linker

We used another cross-linker having different properties suitable, in theory, to resolve our problem (Figure 36B). Sulfo-SBED is a multi-functional cross-linker, which allows tagging protein partners with biotin molecules upon UV exposure. Reduction by DTT releases His-tagged mt-AspRS from biotinylated protein partners. Theoretically, this biotin molecule will enable the detection of protein partners both by western blot using HRP-conjugated streptavidin, and also by mass spectrometry analysis. In addition, the biotin on partner proteins will allow their enrichment on streptavidin-conjugated beads (Figure 36C).

Recombinant His-tagged mt-AspRS was produced in *E. coli*, purified by affinity chromatography on a nickel column, and conjugated to the sulfo-SBED cross-linker. As a control experiment, sulfo-SBED-conjugated mt-AspRS was subjected to UV and reduced with DTT to investigate if the dimeric protein can "auto" cross-link, *via* either intra-molecular or inter-molecular bridges. Sulfo-SBED-conjugated mt-AspRS was detected by HRP-streptavidin during western blot analysis (band detected at a position corresponding to a protein of 70 kDa), which means that mt-AspRS is able to cross-link with itself. When the conjugated mt-AspRS is not cross-linked with UV, only a residual fraction of mt-AspRS is detected. This is likely due to the photosensitivity of sulfo-SBED moiety, as specified by the supplier. Unconjugated mt-AspRS was not detected with HRP-streptavidin, while detected with anti-mt-AspRS antibody, used as a control on the same PVDF membrane (Figure 8A).

Sulfo-SBED-conjugated mt-AspRS (at different concentrations; from 150 ng to 100 µg) was incubated with mitochondrial extracts, cross-linked with UV and analyzed by western blot (Figure 8B). Several and distinctive bands, which correspond to potential partners, were revealed by HRP-streptavidin in addition to a large band detected at 70 kDa corresponding to the auto-cross-linked mt-AspRS.

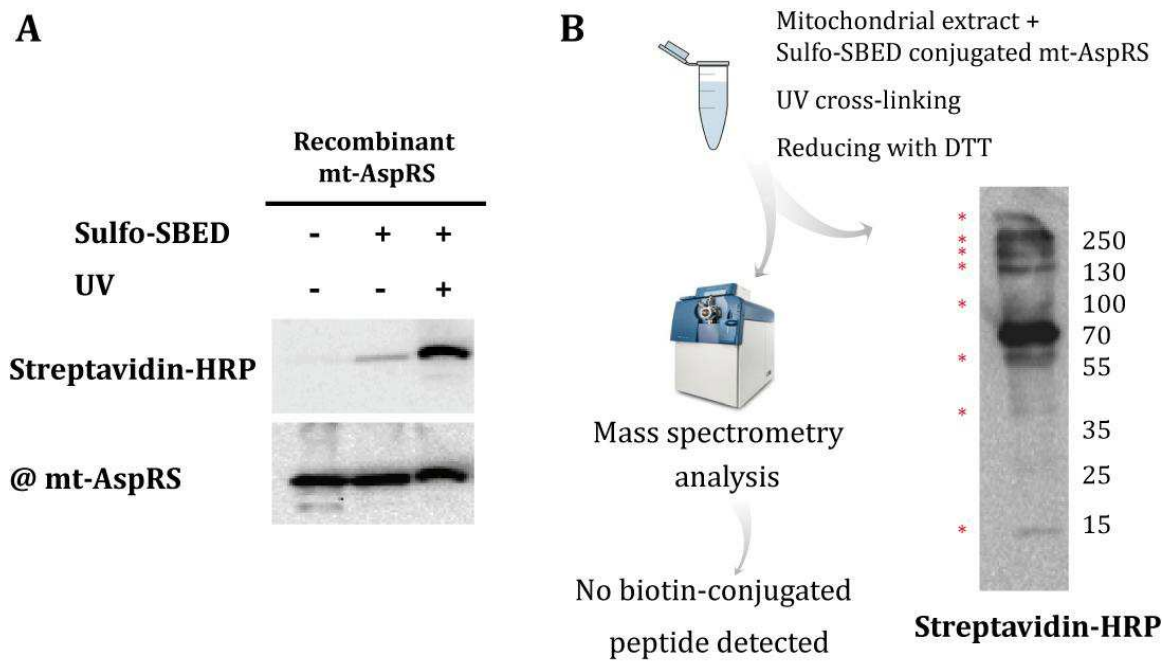

Figure 8: Cross-linking with Sulfo-SBED cross-linker. A) Recombinant mt-AspRS was used to evaluate the autocross-linking of the dimeric mt-AspRS after conjugation with Sulfo-SBED. B) Sulfo-SBED conjugated mt-AspRS was incubated with mitochondrial extract (from HEK293T cells) and cross-linked with UV. After reducing with DTT, proteins were analyzed by western blot and the biotin moiety of Sulfo-SBED detected with streptavidin-HRP.

In order to identify protein partners, mitochondrial extract was cross-linked with conjugated mt-AspRS and reduced with DTT. Biotinylated protein partners were enriched using streptavidin coupled to magnetic beads and analyzed by mass spectrometry (with or without prior SDS-PAGE separation). Several proteins were detected, but no biotinylated peptides. In other words, what was supposed to be the direct evidence of the interaction (the biotin on the partners) was not detected. In order to further define the problem, conjugated-mt-AspRS was cross-linked alone, reduced, and analyzed by mass spectrometry. Although, several peptides of mt-AspRS were detected, no biotinylated peptide was detected demonstrating clearly that the limitation was at the level of mass spectrometry detection.

Using sulfo-SBED cross-linker allowed the detection of protein partners of mt-AspRS on western blot, but failed to identify these partners by mass spectrometry.

1.2.2.2. Using of affinity purification to isolate cross-linked complexes

The mass spectrometer used was not able to detect the biotin moiety of sulfo-SBED. We thus decided to take advantage of this molecule and to exploit it as a mean of enrichment, using the biotin of sulfo-SBED in addition to the His-tag of mt-AspRS allowing the purification on Nickel column. Mitochondrial extract was cross-linked with sulfo-SBED conjugated mt-AspRS, and then subjected to affinity purification either on Nickel-agarose beads, streptavidin-magnetic beads, or both of them successively. The general strategy and the results we obtained are presented in figure 9.

Mass spectrometry analyses were performed after separation of proteins on SDS-PAGE in order to avoid the auto-cross-linked mt-AspRS (as observed in figure 8A). Venn diagrams display the number of identified proteins for each type of purification, and the number of common proteins between the three processes (Figure 9). Besides no common protein was detected, datasets were almost different for every duplicate (datasets differing by the identified proteins and their number). This indicates once more a lack of reproducibility. Despite we used purified mitochondria in our different experiments; lots of identified proteins were annotated as cytosolic proteins.

Although, mt-AspRS belongs to different complexes, we were unable to identify partners of mt-AspRS. Because each approach has its limitations, it would be necessary to combine different techniques to detect and validate the partner. One of the plausible hypotheses, which may explain why all approaches we used so far did not highlight a relevant candidate, is that the partners would be membrane proteins needing appropriate conditions. The other hypothesis is that mt-AspRS partner would be an RNA molecule rather than a protein. In that case, the techniques we used were incompatible and useless to identify the RNA partner.

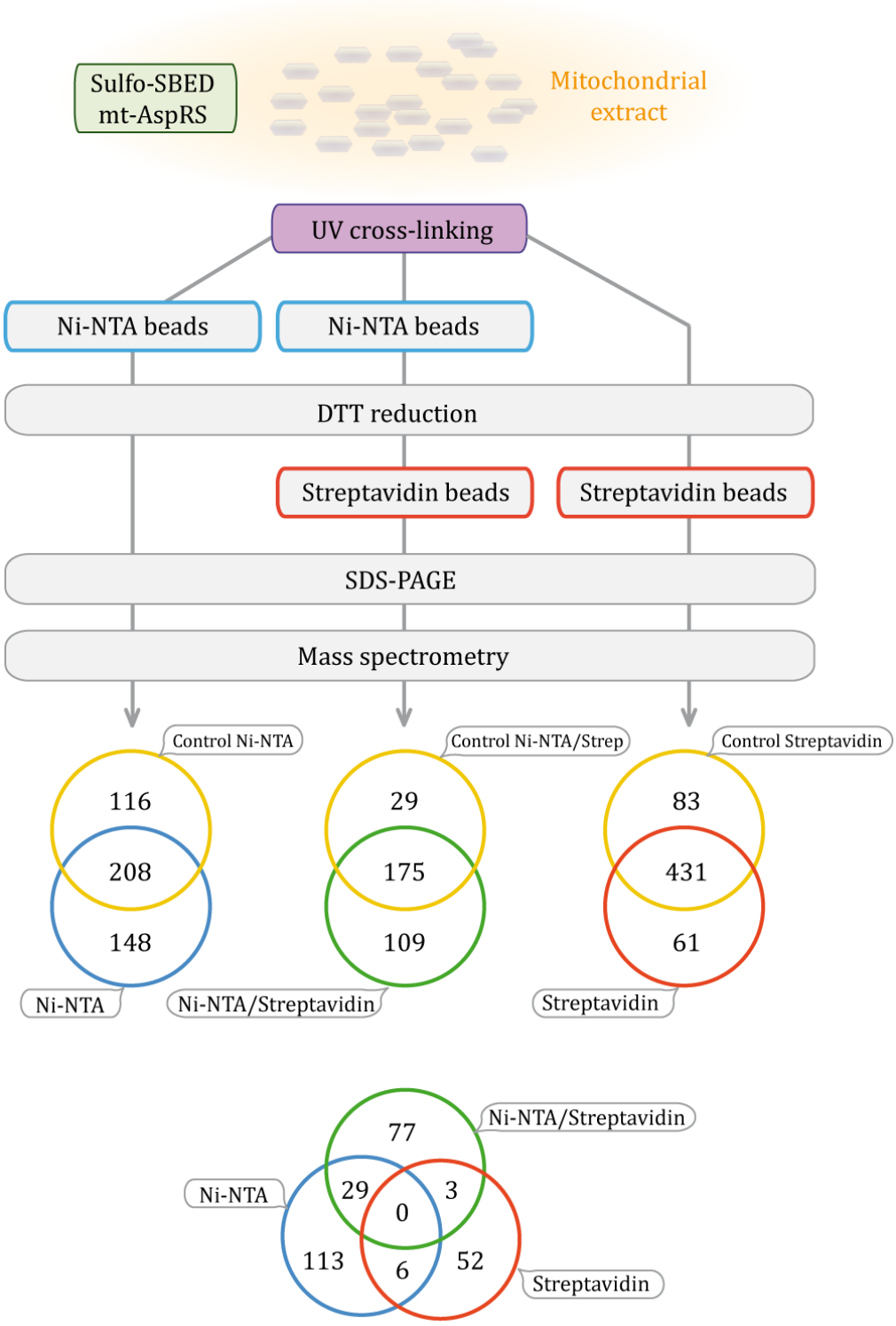

Figure 9: Strategies of fishing and mass spectrometry results. Recombinant mt-AspRS (displaying a His-tag) was conjugated with Sulfo-SBED cross-linker prior to incubation with mitochondrial extract (HEK293T cells) and UV cross-linking. Mt-AspRS partners were subjected to different processes of purification taking advantage from the presence of the biotin (transferred from Sulfo-SBED moiety to the partner) and the His-tag.

1.3. Data mining to help partners identification

Identifying mt-AspRS partners appears to be a difficult task. Although high throughput analyses and *in silico* prediction are not always fully reliable, they may provide additional information which would be of valuable help to define the orientation to take or the approach to use.

1.3.1. Partners of human mt-AspRS identified by experimental high throughput analyses

By using a variety of approaches (Affinity capture-MS, Two hybrid and Co-fractionation), different partners have been attributed to mt-AspRS (Table 2) and referenced in BioGRID[3.4] database (Emdal *et al.* 2015, Huttlin EL 2014, Huttlin *et al.* 2015, Giannone *et al.* 2010, Li *et al.* 2014, Li *et al.* 2015, Quevillon *et al.* 1999, Wan *et al.* 2015, Wang *et al.* 2011). All protein partners have been discovered once, except for lysyl-tRNA synthetase (KARS), which has been found twice using two different techniques. However, no report confirmed a functional interaction of mt-AspRS with one of these partners. Protein partners display also a wide range of cellular localization and only three proteins (or four, if we consider KARS which displays mitochondrial and cytosolic isoforms) are known to be localized in mitochondria: NARS2, MRPL12 and HSP60. Among mt-AspRS protein partners, two proteins possess an aminoacylation activity (KARS and NARS2), which might be good candidates for further investigation. Because mt-AspRS is directly implicated in LBSL disease (see Introduction section), High affinity nerve growth factor receptor (NTRK1), Dihydropyrimidinase-related protein 5 (DPYSL5) and Ephrin-type A receptor 8 (EPHA8) which are related to neuron growth and/or differentiation, are good candidates as well. However, these three proteins are, so far, annotated as being either cytosolic or plasma membrane proteins.

Interactor	Protein name	Cellular localization	Function	Method	Reference
NTRK1	High affinity nerve growth factor receptor	Plasma membrane	Involved in the development and the maturation of the central and peripheral nervous systems through regulation of proliferation, differentiation and survival of sympathetic and nervous neurons	Affinity Capture-MS	Emdal KB (2015)
TERF2	Telomeric repeat-binding factor 2	Nucleus	Binds the telomeric double-stranded 5'-TTAGGG-3' repeat and plays a central role in telomere maintenance and protection against end-to-end fusion of chromosomes	Affinity Capture-MS	Giannone RJ (2010)
GAPDHS	Glyceraldehyde-3-phosphate dehydrogenase, testis-specific	Cytosol/nucleus	May play an important role in regulating the switch between different pathways for energy production during spermiogenesis and in the spermatozoon	Affinity Capture-MS	Huttlin EL (2014/pre-pub)
HSPD1	60 kDa heat shock protein, mitochondrial	Mitochondria and cytosol	Implicated in mitochondrial protein import, correct folding and macromolecular assembly	Affinity Capture-MS	Huttlin EL (2014/pre-pub)
LAMP3	Lysosome-associated membrane glycoprotein 3	Lysosome	May play a role in dendritic cell function and in adaptive immunity	Affinity Capture-MS	Huttlin EL (2014/pre-pub)
MRPL12	39S ribosomal protein L12, mitochondrial	Mitochondria	Mitochondrial protein synthesis	Affinity Capture-MS	Huttlin EL (2014/pre-pub)
YBEY	Putative ribonuclease, putative metallopeptidase	Likely cytosol/nucleus	Likely RNA maturation	Affinity Capture-MS	Huttlin EL (2014/pre-pub)
ARHGEF26	Rho guanine nucleotide exchange factor 26	Likely plasma membrane	Activates RhoG GTPase by promoting the exchange of GDP by GTP. Required for the formation of membrane ruffles during macropinocytosis. Required for the formation of cup-like structures during trans-endothelial migration of leukocytes	Affinity Capture-MS	Huttlin EL (2015)
LOC554223	Histocompatibility antigen-related	ND	Likely immune response	Affinity Capture-MS	Huttlin EL (2015)
PLAUR	Urokinase plasminogen activator surface receptor	Extracellular	Acts as a receptor for urokinase plasminogen activator. Plays a role in localizing and promoting plasmin formation	Affinity Capture-MS	Huttlin EL (2015)
DCP2	m7GpppN-mRNA hydrolase	Cytosol/nucleus	Decapping metalloenzyme that catalyzes the cleavage of the cap structure on mRNAs	Affinity Capture-MS	Li S (2014)
FOXB1	Forkhead box protein B1	Nucleus	Transcription	Affinity Capture-MS	Li X (2015)
FOXH1	Forkhead box protein H1	Nucleus	Transcription	Affinity Capture-MS	Li X (2015)
FOXI2	Forkhead box protein I2	Nucleus	Transcription	Affinity Capture-MS	Li X (2015)
FOXL1	Forkhead box protein L1	Nucleus	Transcription	Affinity Capture-MS	Li X (2015)
FOXL2	Forkhead box protein L2	Nucleus	Transcription	Affinity Capture-MS	Li X (2015)
AIMP2	Aminoacyl tRNA synthase complex-interacting multifunctional protein 2	Cytosol	Required for assembly and stability of the aminoacyl-tRNA synthase complex. Mediates ubiquitination and degradation of FUBP1, and blocks MDM2-mediated ubiquitination and degradation of p53/TP53. Functions as a proapoptotic factor	Two-hybrid	Quevillon S (1999)
KARS	Lysine--tRNA ligase	Cytosol (+ extracellular)	Aminoacylation/Protein synthesis. Signaling molecule when secreted. Interacts with HIV-1 virus GAG protein	Two-hybrid	Quevillon S (1999)
FNTA	Protein farnesyltransferase /geranylgeranyltransferase type-1 subunit alpha	Cytosol	Contributes to the transfer of a farnesyl or geranylgeranyl moiety to a target cysteine	Co-fractionation	Wan C (2015)
KARS	Lysine--tRNA ligase	Cytosol (+ extracellular)	Aminoacylation/Translation. Signaling molecule when secreted. Interacts with HIV-1 virus GAG protein	Co-fractionation	Wan C (2015)
NARS2	Asparagine--tRNA ligase, mitochondrial	Mitochondria	Aminoacylation/Protein synthesis	Co-fractionation	Wan C (2015)
POR	NADPH--cytochrome P450 reductase	Endoplasmic reticulum membrane	Drug metabolism. Hormone synthesis	Co-fractionation	Wan C (2015)
RPA2	Replication protein A 32 kDa subunit	Nucleus	Replication	Co-fractionation	Wan C (2015)
DPYSL5	Dihydropyrimidinase-related protein 5	Cytosol	May have a function in neuronal differentiation and/or axon growth	Two-hybrid	Wang J (2011)
EPHA8	Ephrin type-A receptor 8	Plasma membrane	Implicated in axon guidance during embryonic development. Implicated, during adulthood, in different processes e.g. angiogenesis and stem cell differentiation	Two-hybrid	Wang J (2011)

Table 2: mt-AspRS partners detected by high throughput analyses (referenced in BioGRID[3,4])

1.3.2. Prediction of interacting partners based on short motifs present in mt-AspRS sequence

Protein-protein interaction is generally mediated by a physical contact between a domain and a short motif. Human mt-AspRS protein sequence was analyzed, using Minimotif Miner (MnM 3.0) program, to detect any functional short motif known to interact with a given protein (Balla *et al.* 2006). Table 3 shows all predicted partners based on the detected consensus sequences. Due to the high number of occurrence in the whole proteome of certain motifs, the presence of several motifs from the same family was necessary to consider a partner as a relevant one. From the Table 3, four major observations were made:

- Several consensus sequences (pale yellow) are predicted to interact with SH2 (Src Homology 2) or SH3 domains, which are generally present in signaling proteins
- Several consensus sequence (turquoise) are predicted to interact with FHA (forkhead-associated) domain present in different protein e.g. transcription factors
- Several consensus sequence (grey) are predicted to interact with protein adaptor from trafficking system e.g. AP complex implicated in the endocytosis
- Several consensus sequences (Orange) are predicted to interact with nuclear receptors

The first and second observations (pale yellow and turquoise) corroborate data of high throughput analyses. Indeed, some signaling proteins and 5 transcription factors members of Forkhead family have been detected as partners of mt-AspRS. Further investigations are needed to know whether results obtained by high throughput were false positives because of the interaction of these motifs of mt-AspRS with inappropriate partners, or in contrary, high throughput analyses confirmed the predicted interaction.

The third observation (grey) is vaguely correlated to data of high throughput analyses. AP complex mediates endocytosis upon external stimulation e.g. interaction of a receptor with its ligand. Among proteins referenced in BioGRID, two receptors are discovered as partners of mt-AspRS.

Motif Expression	Annotation	Occuring Positions	Comb. Filter Score	# In Proteome
Y[DY][DELY]V	This consensus motif binds the #1 SH2 domain of Lck; The Tyrosine at position 1 must be modified with a O4'-phospho-L-tyrosine	527	1.1	576
Yxx[IL]	This consensus motif binds the #2 SH2 domain of Syk; The Tyrosine at position 1 must be modified with a O4'-phospho-L-tyrosine	11, 30, 173	1.0	44849
Yxx[VILFWYM]	This consensus motif binds the SH2 domain of ZAP70; The Tyrosine at position 1 must be modified with a O4'-phospho-L-tyrosine	11, 30, 173, 258, 527	0.98	133560
TxxD	This consensus motif binds the #1 FHA domain of Rad53; The Threonine at position 1 must be modified with a O-phospho-L-threonine	279	0.97	42075
YxL	This consensus motif binds the #2 FHA domain of Rad53; The Tyrosine at position 1 must be modified with a O4'-phospho-L-tyrosine	185, 237, 527, 551	0.96	38809
TxxI	This consensus motif binds the FHA domain of Chk2; The Threonine at position 1 must be modified with a O-phospho-L-threonine	22, 138	0.95	38492
RxL	This consensus motif binds Cdk2	12, 31, 174, 495	0.95	188827
[RK]xL	This consensus motif binds Cdk2	12, 31, 105, 153, 174, 247, 377, 495, 562	0.89	206191
Txx[IL]	This consensus motif binds the #2 FHA domain of Rad53; The Threonine at position 1 must be modified with a O-phospho-L-threonine	22, 136, 145, 166, 212	0.92	122582
Y[ETM][NED][PVL]	This consensus motif binds the #1 SH2 domain of cAbl; The Tyrosine at position 1 must be modified with a O4'-phospho-L-tyrosine	516	0.91	2193
KK	This instance motif in matrix binds HO3	104, 153, 164, 520	0.87	70885
[FW]xxL[FWY]	This consensus motif binds Androgen receptor	26, 476	0.8	5411
ExxxxxxE	This consensus motif binds HIV tat	140, 225, 277, 491	0.76	97240
LxxLL	This consensus motif binds Oxysterol receptor LXR beta	553, 564	0.75	23958
YxxxxL[IVLFYW]	This consensus motif binds eIF4E	551	0.75	10884
[DE]xxxL[LI]	This consensus motif binds the Trunk domain of AP1,AP2,AP3 beta subunits	435, 458	0.75	27454
Lxxx[xxx[IL]	This consensus motif binds nuclear receptor	548	0.72	11865
[VILS]xYxx[LVIS]	This consensus motif binds the SH2 domain of SHP-1; The Tyrosine at position 3 must be modified with a O4'-phospho-L-tyrosine	28, 171	0.72	34412
RxxK	This consensus motif binds the SH3 domain of GADS	632	0.71	53665
PxxxRxxKP	This consensus motif binds the SH3 domain of STAM1	628	0.7	225
YxxL	This consensus motif binds AP complex and is trafficked by internalization	11, 30, 173	0.7	42342
MxxxL	This consensus motif binds AP2 mu2 subunit, clathrin terminal domain, PTB domain of Dab2 and is trafficked by internalization	183, 197, 251, 583	0.66	17276
Yxx[FSLMVWY]	This consensus motif binds AP1,AP2,AP3, AP4 mu subunits and is trafficked by endocytosis	11, 30, 173, 258, 527	0.66	133560
ExT	This consensus motif binds Slp2; The Threonine at position 3 must be modified with a O-phospho-L-threonine	65, 277	0.67	57290
K[KR]x[KR]	This consensus motif binds Importin alpha and is trafficked to Nucleus	520	0.65	21867
TxxxS	This consensus motif binds Slp1; The Serine at position 5 must be modified with a O-phospho-L-serine	291, 593	0.6	78113
[DE]D	This consensus motif binds AP2	435, 559	0.6	107029
PxxxD	This consensus motif binds platelet fibrinogen receptor	309, 507, 596	0.59	44535
EE	This instance motif in Nef binds Arf1	434, 491, 624	0.59	116074
YLDL	This instance motif in peptide binds the #1 SH2 domain of Blnk; The Tyrosine at position 1 in peptide must be modified with a O4'-phospho-L-tyrosine	175	0.58	258
Yxx[ILMP]	This consensus motif in peptide binds the #1 SH2 domain of Blnk; The Tyrosine at position 1 in peptide must be modified with a O4'-phospho-L-tyrosine	11, 30, 173, 237, 303, 516, 573	0.4	98980
[PSAT]x[QE]E	This consensus motif binds the TRAF domain of TRAF2	127, 432, 489, 622	0.38	47801
[RK]x[RK]	This consensus motif binds Sar1 and is trafficked by Endoplasmic Reticulum Export	142, 188, 196, 380, 454, 521	0.56	211560
Yxx[ILM]	This consensus motif binds the SH2 domain of Shc; The Tyrosine at position 1 must be modified with a O4'-phospho-L-tyrosine	11, 30, 173	0.55	74001
LLG	This instance motif in von Willebrand Factor binds Beta2-Integrin	451	0.54	12386
Rx[ADFQSTWY]x[ST]x[LMP]	This consensus motif binds the #1 14-3-3 domain of 14-3-3epsilon; The Serine at position 5 must be modified with a O-phospho-L-serine	75	0.52	8929
[HRK][ALSTV]x[ST]xx[DEFIPRS]	This consensus motif binds the #1 14-3-3 domain of 14-3-3epsilon; The Serine at position 2 must be modified with a O-phospho-L-serine	50	0.52	59731
FxP	This consensus motif binds the #1 EVH1(WH1) domain of N-WASP	476	0.48	24129
PxxxR	This consensus motif binds the #2 SH3 domain of Grb2	519, 605, 628	0.47	66274
PxxP	This consensus motif in SOS1 binds the SH3 domain of Grb2	132, 240	0.45	103587
[TS]xxxx[VI]	This consensus motif binds the SH2 domain of SH2D1A	36, 67, 136, 432, 477, 591	0.44	221955
Y[VIL][ED][VIL]	This consensus motif binds the #1 SH2 domain of PLCgamma1; The Tyrosine at position 1 must be modified with a O4'-phospho-L-tyrosine	175	0.43	2189
Y[LI]	This consensus motif binds the #1 SH2 domain of PLCgamma1; The Tyrosine at position 1 must be modified with a O4'-phospho-L-tyrosine	175, 200, 378, 551	0.41	67661

Most likely to be a true prediction (multifilter score > 0.91)
Likely to be a true prediction (multifilter score > 0.24 and < 0.91)

Table 3: Detection of potential functional short motif (physical interaction) on the full-length mt-AspRS, using Minimotif Miner 3.0.

For the fourth observation (orange), localization of nuclear receptor (NR)-interacting motifs on the 3D structure of mt-AspRS seems to be interesting (Figure 10). Three predicted motifs (plus one with a low score, which is not on Table 3) were close to each other and might form an interacting cluster with a nuclear receptor. Again, although some nuclear receptors exist in mitochondria (Lee *et al.* 2008), no experimental evidence has highlighted a relation with such proteins.

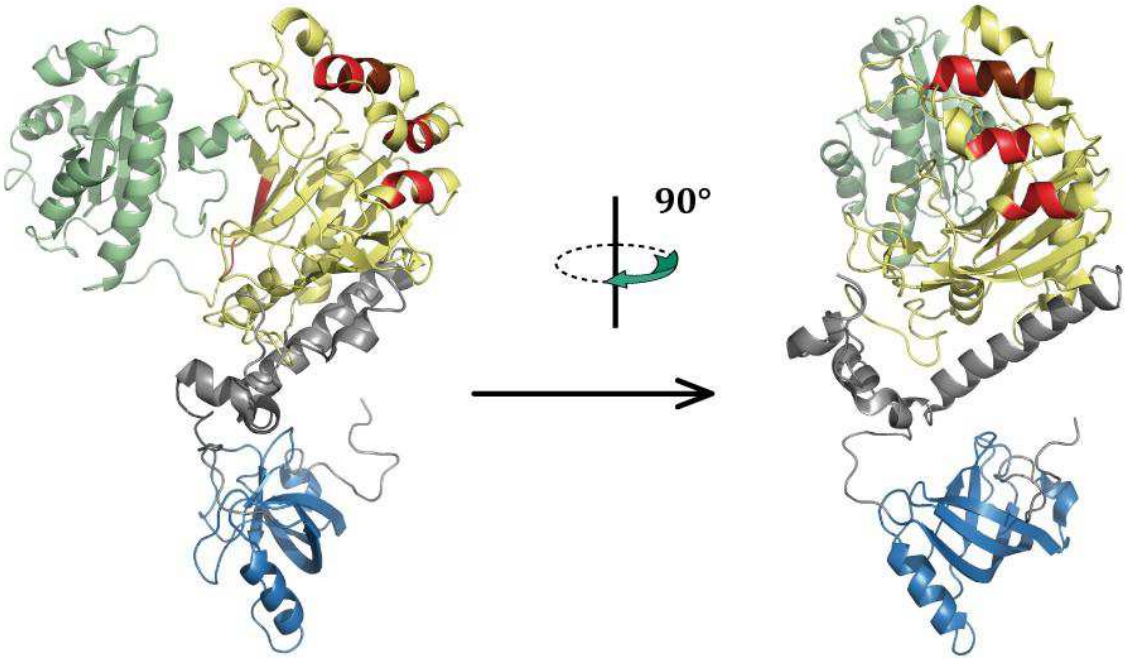

Figure 10: Conserved motifs are predicted in mt-AspRS sequence and are present in a cluster on its structure. 3D structure of mt-AspRS contains the catalytic domain (yellow), the anticodon-binding domain (blue), the hinge (grey) and the bacterial insertion domain (green). Four out of five predicted conserved motifs, interacting with nuclear receptors, are clustered at the external face of the catalytic pocket (two different views related by 90° rotation): 2 motifs in the 2nd helix (red and dark red), 1 in each of the 3rd and 4th helices (red).

1.4. Conclusions and Perspectives

Despite the effort furnished by two former PhD students using immunoprecipitation and pull-down experiments, no partner has been found. The aim of this chapter was to see whether human mt-AspRS has or not biologically relevant partners using other approaches.

Here, BN-PAGE and cross-linking approaches were used and showed that mt-AspRS exists in complexed forms, clearly different from the dimer form. Since we do not know the nature of partners, we propose digesting mitochondrial extract with an RNase before doing the same experiments. This would complement the result and discriminate between RNA and protein partners.

Immuoprecipitation combined with glutaraldehyde cross-linking failed to identify the partnership of mt-AspRS. As another approach, we used a multifunctional cross-linker (sulfo-SBED) theoretically able to reveal partners by western blot and by mass spectrometry. We were able to detect partners by western blot but unable to identify them by mass spectrometry. Then we used the properties of both sulfo-SBED and the His-tag present in mt-AspRS to perform "TAP-tag like" purification, but again we were unable to identify a relevant partner. We raised the hypothesis of a membrane protein partner for which the isolation and identification was not possible in our experimental conditions.

Data mining of high throughput and experimental data, as well as predicting interaction of mt-AspRS identified some interesting and valuable information about potential partners. However, they need additional experimental validation and/or further investigation. Lots of these potential partners are cytosolic proteins, which raises the question of how proteins annotated as cytosolic can interact with a protein annotated as mitochondrial. Are these proteins addressed to different compartments among which the mitochondrial localization has not been discovered yet? Or are they translocating from a compartment to another in certain conditions? In addition, we cannot exclude that they could be false-positives of high throughput analysis and insignificant prediction.

Although we were unable to identify the partner, our results about mt-AspRS complexes are promising. However, we are aware that this result is obtained in kidney cells (HEK293T) and cannot reflect what happens in neurons if we want to make a

correlation with the LBSL disease. In addition, studies on LBSL hypothesized a tissue-specific partner to explain the tissue-specificity of the disease, thus searching for a partner of mt-AspRS in neurons would be more relevant to understand the physiopathology of mt-AspRS as well as the etiology of LBSL.

Also, in this Chapter we only focused on protein partners of mt-AspRS, but this latter has been identified in the proteome of both mt-nucleoids (Rajala *et al.* 2015), and mt-RNA granules (Antonicka and Shoubridge 2015). In the future, it would be interesting to take into consideration especially RNA partners, by performing e.g. CLIP-Seq experiments, since mt-AspRS is known to interact with RNA.

Chapter 2: mt-AspRS displays multiple localizations

2.1. Introduction

Human mitochondrial DNA (mt-DNA) encodes for 13 membrane proteins, which are all subunits of the respiratory chain. The translation machinery synthesizing these subunits (mitoribosome) has been localized at the inner membrane (Liu and Spremulli 2000). Later on, it has been shown that nucleoids (containing mt-DNA) and mitoribosomes are associated to each other at the inner membrane (Bogenhagen *et al.* 2014, He *et al.* 2012), in addition to other factors implicated in the mt-transcription and translation (e.g. TFAM He *et al.* 2012 or mt-EF-Tu Suzuki *et al.* 2007, He *et al.* 2012). Although mt-IleRS has been co-purified with ATAD3 (a nucleoid component) and mt-AspRS has been identified in the proteome of both mt-nucleoids (Rajala *et al.* 2015) and mt-RNA granules (Antonicka and Shoubridge 2015), it is unclear if all mt-aaRSs are associated with this transcription/translation assembly. A former student, from the lab, has shown that mt-aaRSs do not all have the same sub-localization, some are both soluble (matrix) and membrane-associated, others are exclusively found in one of the two fractions. Also, it has been shown that the presence of a Mitochondrial targeting sequence (MTS), its position in the protein sequence as well as its mode of processing are important information for the sub-localization of a mitochondrial protein (Opalinska and Meisinger 2015). In this chapter, while summarizing what has been done on mt-AspRS in terms of maturation and sub-localization as well as the possible relationship between them, additional and complementary results are presented and discussed.

2.2. Different maturation products of human mt-AspRS after its import into mitochondria

The MTS is important for targeting and translocation, but its processing (removal) is also important for the folding and the function of some mt-proteins. Thus, determination of the mature form of any mt-protein is helpful and sometimes necessary for its characterization. However, discrepancy between reality and *in silico* predictions could be time and energy consuming. Here, we summarize results obtained by different approaches to determine MTS cleavage sites and the mature form of mt-AspRS.

2.2.1. *In vitro* mitochondrial import experiments revealed two products of mt-AspRS processing

Mitochondrial targeting sequence (MTS) of mt-AspRS is predicted *in silico* (Predotar, Small *et al.* 2004 and MitoProt, Claros and Vincens 1996) to be cleaved between residues Phe_{47} and Val_{48} (Bonnefond *et al.* 2005) or between residues Val_{48} and Val_{49} (Claros and Vincens 1996) (Figure 11). More recently, a new program MitoFate predicts mt-AspRS MTS to be cleaved between residue Ser_{32} and Leu_{33} (Fukasawa *et al.* 2015). However, Marie Messmer (a former PhD student) has performed *in vitro* import experiments and detected processed forms of mt-AspRS after its import into mitochondria (Messmer *et al.* 2011). Such pattern was similar to one obtained with e.g. the yeast mt Rieske Iron-sulfur protein, shown to be successively cleaved by the Mitochondrial processing peptidase (MPP) and the Mitochondrial intermediate peptidase (MIP) (Nett and Trumpower 1996). It has been reported afterwards that many mitochondrial protein precursors, targeted to the mitochondrial matrix or to the inner membrane, are processed in two sequential steps by both MPP and MIP. These precursors are characterized by a motif at the C-terminus of the leader peptide named R-10 with the following characteristic sequence: $R_{-10}x \Downarrow (F/L/I)_{-8}xx(S/T/G)_{-5}xxxx_{-1} \Downarrow x_{+1}$ (reviewed in Gakh *et al.* 2002 and Teixeira and Glaser 2013). By analyzing the MTS of mt-AspRS, she has found a sequence similar to an R-10 motif (**R**$_{-10}$S $\Downarrow$ **L**$_{-8}$LQ**S**$_{-5}$SQRR$_{-1}$

⇓ I_{+1}). Thus, the observed bands may correspond to MPP and MIP cleavages between residue Ser_{32} and Leu_{33}, and residues Arg_{40} and Ile_{41}, respectively. But, intermediate and mature forms have been detected (in import experiments) only after short time incubation of the precursor with mitochondria, or at low temperature, because the intermediate has a short half-life (Daum *et al.* 1982, Kalousek *et al.* 1988, Branda and Isaya 1995, Vogtle *et al.* 2011). So, it is unclear whether the detection of both intermediate and mature forms of mt-AspRS is biologically relevant, and whether their detection would be possible *in vivo*.

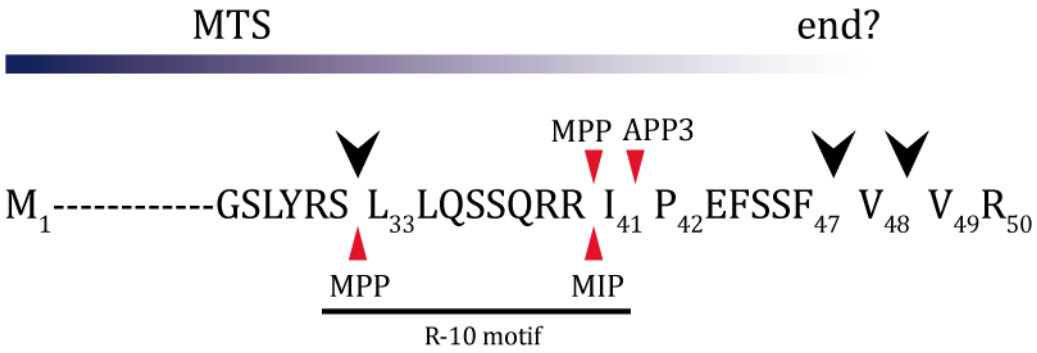

Figure 11: Mitochondrial targeting sequence (MTS) of mt-AspRS and cleavage sites. Cleavage sites of the MTS of mt-AspRS were predicted using different program (black arrows). Experimentally detected N-termini of mt-AspRS are indicated by red arrows. Processing peptidases likely leading to the detected forms are proposed. MPP, mitochondrial processing peptidase. MIP, mitochondrial intermediate peptidase. AAP3 (or XPNPEP3), aminopeptidase P. The R-10 motif is consecutively cleaved by both MPP and MIP.

2.2.2. Mass spectrometry analysis detected the Leu_{33} and Pro_{42} forms of mt-AspRS

Hagen Schwenzer (also a former PhD student) in collaboration with Lauriane Kuhn (Mass spectrometry platform/IBMC, Strasbourg) used another approach based on the calculation of all possible semi-tryptic peptides of the mt-AspRS N-terminus (from Nter-Met_1 to Phe_{47}). Theoretical masses of processed N-terminal peptides were then compared to the experimentally detected peptides by mass spectrometry after the analysis of immuoprecipitated mt-AspRS. Of note, trypsin cleaves proteins and generates peptides with C-terminal lysine (Lys) or arginine (Arg) residues. Eight semi-tryptic peptides were

detected, among which, the peptides starting at Leu_{33} and Pro_{42} were detected with the highest scores and the only validated (Table 4A). In addition, two peptides out of four were detected with high scores and may correspond either to tryptic or semi-tryptic sequences, meaning that they may correspond either to N-termini generated by the trypsin from a longer sequence, or to real N-termini, respectively (Table 4B). Additional analyses are needed to determine whether the two latter peptides are tryptic or semi-tryptic segments. This result, which is obtained with the endogenous mt-AspRS, is consistent with the previous result obtained after import of *in vitro*-translated mt-AspRS, concerning the detection of two maturation products of mt-AspRS.

A) Semi-tryptic peptides

Theoretical peptide sequence	Sequence name in the dedicated database	Sequence experimentally observed	m/z observed	Mascot Score
YFPSWLSQL YRGLSRPIRR TTQPIWGSLY RSLLQSSQRR IPEFSSFVVR	AA2	n.d.	n.d.	n.d.
FPSWLSQL YRGLSRPIRR TTQPIWGSLY RSLLQSSQRR IPEFSSFVVR	AA3	n.d.	n.d.	n.d.
PSWLSQL YRGLSRPIRR TTQPIWGSLY RSLLQSSQRR IPEFSSFVVR	AA4	n.d.	n.d.	n.d.
SWLSQL YRGLSRPIRR TTQPIWGSLY RSLLQSSQRR IPEFSSFVVR	AA5	SWLSQLYR	1093.5482 (547.7814=2+)	3
WLSQL YRGLSRPIRR TTQPIWGSLY RSLLQSSQRR IPEFSSFVVR	AA6	WLSQLYR	964.4956 (483.2551=2+)	2
LSQL YRGLSRPIRR TTQPIWGSLY RSLLQSSQRR IPEFSSFVVR	AA7	n.d.	n.d.	n.d.
SQL YRGLSRPIRR TTQPIWGSLY RSLLQSSQRR IPEFSSFVVR	AA8	SQLYRGLSR	1120.5786 (561.2966=2+)	8
QL YRGLSRPIRR TTQPIWGSLY RSLLQSSQRR IPEFSSFVVR	AA9	n.d.	n.d.	n.d.
L YRGLSRPIRR TTQPIWGSLY RSLLQSSQRR IPEFSSFVVR	AA10	n.d.	n.d.	n.d.
YRGLSRPIRR TTQPIWGSLY RSLLQSSQRR IPEFSSFVVR	AA11	n.d.	n.d.	n.d.
RGLSRPIRR TTQPIWGSLY RSLLQSSQRR IPEFSSFVVR	AA12	RGLSRPIR	953.6158 (477.8152=2+)	1
LSRPIRR TTQPIWGSLY RSLLQSSQRR IPEFSSFVVR	AA14	n.d.	n.d.	n.d.
SRPIRR TTQPIWGSLY RSLLQSSQRR IPEFSSFVVR	AA15	n.d.	n.d.	n.d.
RPIRR TTQPIWGSLY RSLLQSSQRR IPEFSSFVVR	AA16	n.d.	n.d.	n.d.
IRR TTQPIWGSLY RSLLQSSQRR IPEFSSFVVR	AA18	n.d.	n.d.	n.d.
RR TTQPIWGSLY RSLLQSSQRR IPEFSSFVVR	AA19	n.d.	n.d.	n.d.
TQPIWGSLY RSLLQSSQRR IPEFSSFVVR	AA22	n.d.	n.d.	n.d.
QPIWGSLY RSLLQSSQRR IPEFSSFVVR	AA23	n.d.	n.d.	n.d.
PIWGSLY RSLLQSSQRR IPEFSSFVVR	AA24	n.d.	n.d.	n.d.
IWGSLY RSLLQSSQRR IPEFSSFVVR	AA25	n.d.	n.d.	n.d.
WGSLY RSLLQSSQRR IPEFSSFVVR	AA26	WGSLYR	822.4238 (412.2192=2+)	6
GSLY RSLLQSSQRR IPEFSSFVVR	AA27	n.d.	n.d.	n.d.

SLY RSLLQSSQRR IPEFSSFVVR	AA28	n.d.	n.d.	n.d.
LY RSLLQSSQRR IPEFSSFVVR	AA29	n.d.	n.d.	n.d.
Y RSLLQSSQRR IPEFSSFVVR	AA30	n.d.	n.d.	n.d.
RSLLQSSQRR IPEFSSFVVR	AA31	RSLLQSSQRR	1229.67357 (410.8984=2+)	5
LLQSSQRR IPEFSSFVVR	AA33	LLQSSQR	830.4587 (416.2366=2+)	**38**
LQSSQRR IPEFSSFVVR	AA34	n.d.	n.d.	n.d.
QSSQRR IPEFSSFVVR	AA35	n.d.	n.d.	n.d.
SSQRR IPEFSSFVVR	AA36	n.d.	n.d.	n.d.
SQRR IPEFSSFVVR	AA37	n.d.	n.d.	n.d.
QRR IPEFSSFVVR	AA38	n.d.	n.d.	n.d.
RR IPEFSSFVVR	AA39	n.d.	n.d.	n.d.
PEFSSFVVR	AA42	PEFSSFVVR	1066.5447 (534.2785=2+)	**47**
EFSSFVVR	AA43	n.d.	n.d.	n.d.
FSSFVVR	AA44	n.d.	n.d.	n.d.
SSFVVR	AA45	n.d.	n.d.	n.d.
SFVVR	AA46	n.d.	n.d.	n.d.
FVVR	AA47	n.d.	n.d.	n.d.

B) Tryptic peptides

Theoretical peptide sequence	Sequence name in the dedicated database	Sequence experimentally observed	m/z observed	Mascot Score
MYFPSWLSQL YRGLSRPIRR TTQPIWGSLY RSLLQSSQRR IPEFSSFVVR	AA1-AA32	SLLQSSQRR	1073.5680 (537.7913=2+)	**3**
GLSRPIRR TTQPIWGSLY RSLLQSSQRR IPEFSSFVVR	AA13	GLSRPIR	839.5205 (420.7675=2+)	**7**
PIRR TTQPIWGSLY RSLLQSSQRR IPEFSSFVVR	AA17	n.d.	n.d.	n.d.
R TTQPIWGSLY RSLLQSSQRR IPEFSSFVVR	AA20	n.d.	n.d.	n.d.
TTQPIWGSLY RSLLQSSQRR IPEFSSFVVR	AA21	n.d.	n.d.	n.d.
SLLQSSQRR IPEFSSFVVR	AA32	n.d.	n.d.	n.d.
R IPEFSSFVVR	AA40	RIPEFSSFVVR	1335.7273 (446.2497=2+)	**39**
IPEFSSFVVR	AA41	IPEFSSFVVR	1179.6222 (590.8184=2+)	**53**

Table 4: Identification by mass spectrometry of the mt-AspRS N-terminal peptides. A theoretical database was created with all possible N-termini from Met 1 to Arg 50 (1-50, 2-50, 3-50 … 47-50). The Mascot algorithm was used to evaluate the most probable N-terminal peptide: the threshold to find a good hit was set to 31, corresponding to the individual identity score calculated by Mascot for p-value<0.05. For each detected peptide: the peptide sequence, the mass/charge (m/z) value, the charge state and the Mascot score are indicated (n.d., not detected). N-terminal peptides are divided into A) Semi-tryptic and B) tryptic peptides.

2.2.3. Labeling of free N-termini prior to mass spectrometry analysis revealed three processed forms of mt-AspRS

In collaboration with Christine Carapito (LSMBO/IPHC, Strasbourg), N-termini of all mt-aaRSs are being analyzed using a strategy recently developed (Vaca Jacome *et al.* 2015). Mitochondria were purified from BHK21 cells transfected with WT mt-AspRS construct, or from HEK293T cells. Free N-termini of mitochondrial proteins were then labeled with light and heavy trimethoxyphenyl phosphonium (TMPP) and analyzed by mass spectrometry (Figure 12A). In order to minimize false-positives, validation of the detected TMPP-peptides must meet some criteria as described in Figure 12B. This strategy identified and validated three TMPP-peptides on mt-AspRS. This result means that mt-AspRS displays three different free N-terminal residues Leu_{33}, Ile_{41} and Pro_{42}. Based on R-10 motif previously predicted, Leu_{33} and Ile_{41} forms are most likely generated by MPP and MIP, respectively. MIP probably generates the third form, as this peptidase has been shown to have more than one cleavage site *in vitro* (Marcondes *et al.* 2015). Aminopeptidase P family (APP), which includes a mitochondrial isoform (APP3 or XPNPEP3), cleaves one N-terminal residue upstream a proline (Ersahin *et al.* 2005, O'Toole *et al.* 2010). Thus, one can suppose that Pro_{42} form of mt-AspRS is generated by the mitochondrial XPNPEP3, however, in this case the Pro_{42} form of mt-AspRS would be generated after triple cleavages MPP, MIP and APP3. Alternatively, one can suppose that the MTS of mt-AspRS contains two MPP cleavage sites instead of an R-10 motif processed by MPP and MIP (as observed in Gordon *et al.* 1999). This hypothesis means that Leu_{33} and Ile_{41} forms would be generated by one MPP cleavage, and Pro_{42} form would be processed by both MPP and XPNPEP3 (Figure 11). What remains ambiguous is the fact we obtained the three forms simultaneously. Detection of both intermediate and mature forms has been reported for Icp55 (yeast homolog of human XPNPEP3 with a different cleavage specificity) cleavage (Vogtle *et al.* 2009), but no report has demonstrated this observation with human XPNPEP3. Recently, MPP and MIP have been demonstrated to cleave the ribosomal protein MRPL12 and generate two distinct mature forms. These latter have independent and different functions, respectively (Nouws *et al.* 2016).

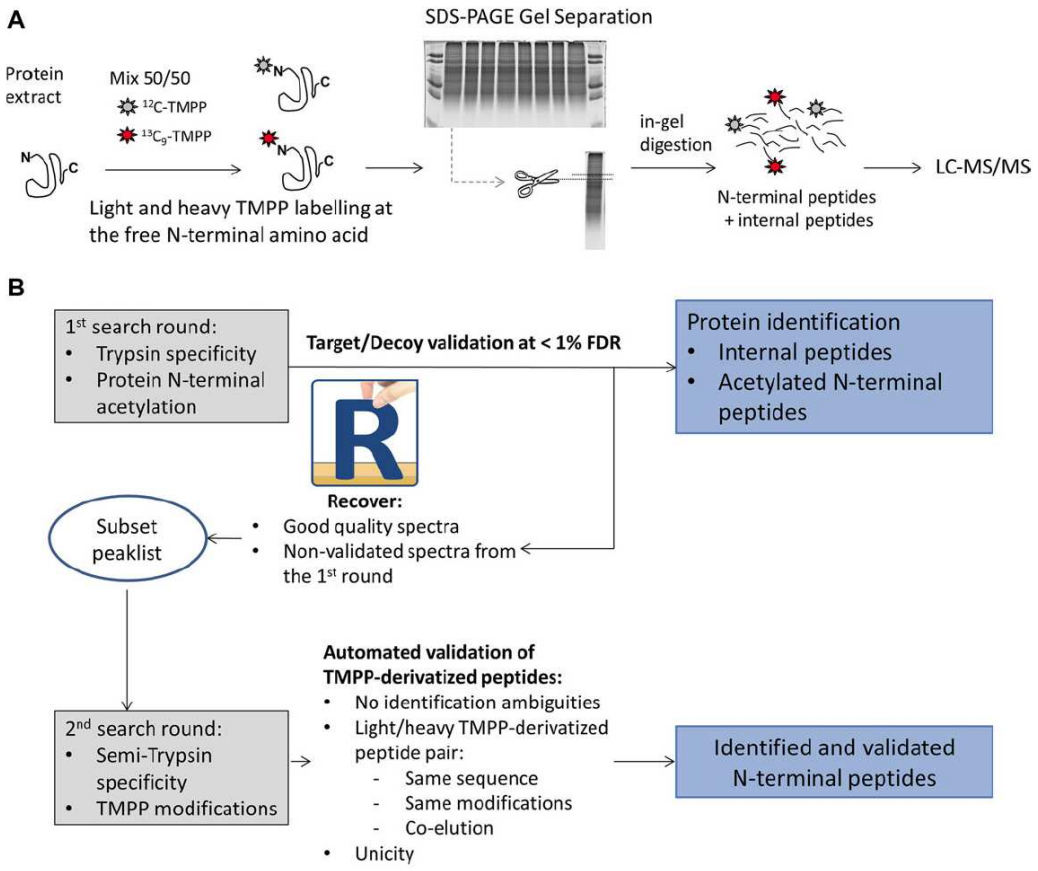

Figure 12: Labeling of N-terminal peptides with TMPP (taken from Vaca Jacome *et al.* 2015). A) Workflow of the N-terminal peptides labeling and analysis. B) Strategy of TMPP-peptides validation.

2.2.4. Combination of all experiments confirms the co-presence of three mature forms of mt-AspRS

Altogether, combination of all predictions and results strongly suggests the co-presence of three isoforms of mt-AspRS starting at Leu_{33}, Ile_{41} and Pro_{42} residues. However, it is unclear how these forms are generated. Two hypotheses can be raised and considered: 1) MTS of mt-AspRS contains two independent MPP and one XPNPEP3 cleavage sites; or 2) mt-AspRS MTS contains an R-10 motif processed with MPP and MIP, with an additional XPNPEP3 cleavage site. Branda and Isaya have observed, in yeast, the presence of R-10 motif in a subset of proteins belonging either to the respiratory chain complexes or to the mt-translation/mt-DNA maintenance (Branda and Isaya 1995). In addition, Vögtle and co-workers have demonstrated that yeast MIP and

Icp55 cleavages are means of protein stabilization (Vogtle *et al.* 2009, Vogtle *et al.* 2011). Except for Icp55 substrates, which have been detected predominantly at their mature forms in addition to intermediates forms to a lesser extent (Vogtle *et al.* 2009), no co-presence (co-existence) of the intermediate and mature forms has been observed *in vivo* (Hartl *et al.* 1986). Because MTS cleavage is a fast process, both forms have been detected only *in vitro* under certain conditions (Daum *et al.* 1982, Kalousek *et al.* 1988, Gordon *et al.* 1999). So far, only MRPL12 has been shown to display two mature forms (generated by MPP and MPP/MIP cleavages) playing distinct functions (Nouws *et al.* 2016). Thus, ours results in human cells raise questions about the biological relevance of the co-presence of three mt-AspRS forms: if some forms are intermediates and other matures, why the three forms are detected? Is there any correlation between the three forms and a potential multifunction of mt-AspRS? If the mt-AspRS contains an R-10 motif, does it correlate with its function and sub-localization?

2.3. Intra-mitochondrial localizations of the human mt-AspRS

As mentioned above, a former PhD student has started investigating the sub-mitochondrial localization of human mt-aaRSs, and has showed that these enzymes do not all have the same sub-localization, some are both soluble (matrix) and membrane-associated, others are exclusively found in one of the two fractions. Here, we focus only on the localization of mt-AspRS.

2.3.1. Dual localization of human mt-AspRS in different cell lines

Mitochondria from Human Embryonic Kidney cells (HEK293T) were purified and fractionated into soluble fraction (matrix and inter-membranes space) and membranes (inner and outer membranes) fraction (S and M in Figure 13). Purity of fractions was checked with antibodies raised against the Superoxide dismutase 2 (SOD2, Nair and McGuire 2005) and Prohibitin (He *et al.* 2012), which were used as markers for the soluble and membranes fractions, respectively. Markers proteins SOD2 and Prohibitin were detected in the soluble and membranes fractions, respectively (Figure 13). This means that fractions were pure and no cross-contamination was detected. Human mt-

AspRS was detected in both soluble and membranes fractions (Figure 13A). Same distributions were obtained with human fibroblasts and HeLa cells (Figure 13A). In parallel, Baby Hamster Kidney (BHK21) cells were transfected with a flag-tagged form of the human mt-AspRS prior to mitochondrial purification and fractionation. Expressed mt-AspRS was also detected in both soluble and membranes fractions using an anti-flag antibody, with pure fractions as demonstrated with controls (Figure 13B). With our fractionation protocol we cannot distinguish between matrix and IMS proteins in the soluble fraction, and between inner and outer membrane proteins in the membranes fraction, thus we suggest that mt-AspRS is in the matrix (soluble form) and interacting with the matrix side of the inner membrane (membrane-associated form) since mt-AspRS has been shown to be exclusively in the matrix side of human cells (Rhee *et al.* 2013). Of note, the western blot is not so resolving to distinguish between the three forms of mt-AspRS identified in section 2.2.

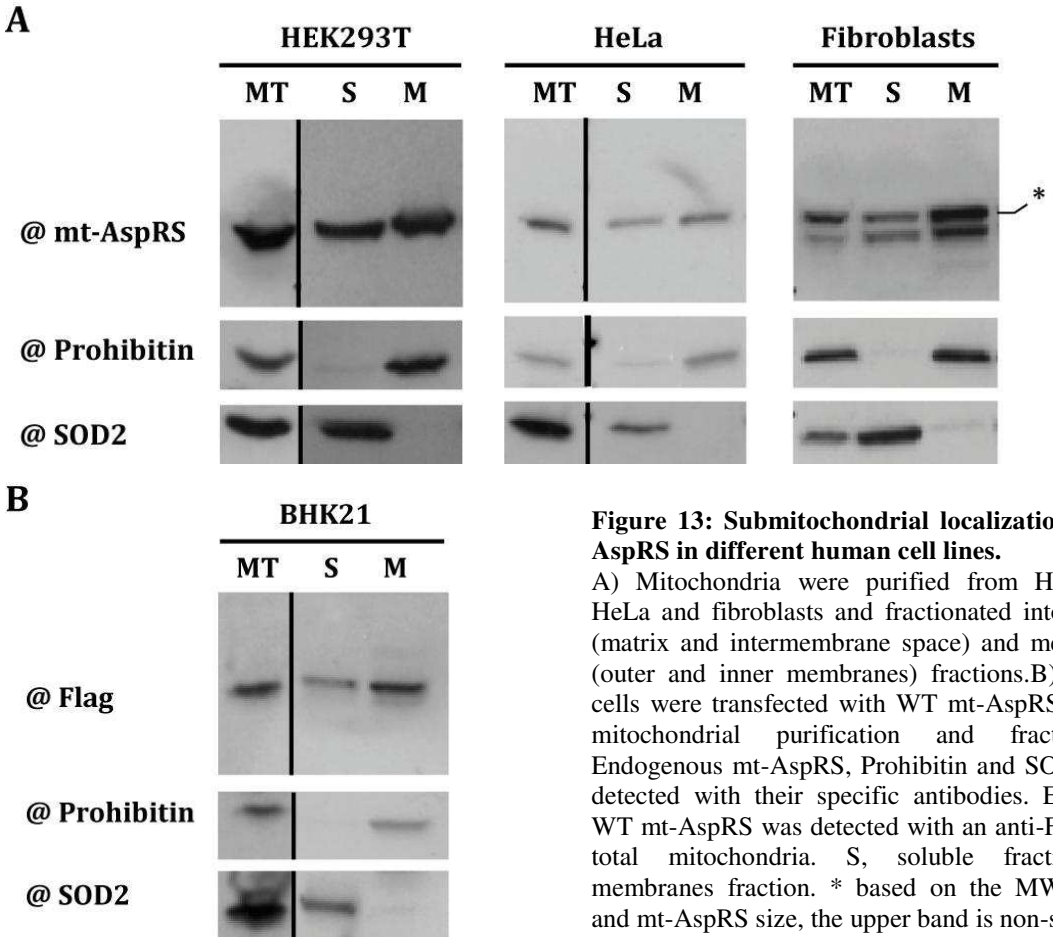

Figure 13: Submitochondrial localization of mt-AspRS in different human cell lines.
A) Mitochondria were purified from HEK293T, HeLa and fibroblasts and fractionated into soluble (matrix and intermembrane space) and membranes (outer and inner membranes) fractions.B) BHK21 cells were transfected with WT mt-AspRS prior to mitochondrial purification and fractionation. Endogenous mt-AspRS, Prohibitin and SOD2 were detected with their specific antibodies. Expressed WT mt-AspRS was detected with an anti-Flag. MT, total mitochondria. S, soluble fraction. M, membranes fraction. * based on the MW marker and mt-AspRS size, the upper band is non-specific.

Detection of mitochondrial proteins in both soluble and membrane fractions (dual localization) has been previously observed for e.g. some replication/transcription factors (Rajala *et al.* 2014). However, only few reports have established the link between dual localization and activity of the protein. For example, Isocitrate dehydrogenase from potato mitochondria has been shown to display distinct kinetic features depending on the soluble or membrane-associated localization, therefore the dual localization has been suggested as a mean of regulation of the enzyme (Tezuka and Laties 1983). We hypothesize that: 1) the dual localization may be also a mean of activity regulation and thus suggesting a dynamic repartition of mt-AspRS between soluble and membranes fractions depending on the cellular/mitochondrial demand; or 2) the dual localization may correspond to dual partnership e.g. a membrane protein partner with membrane-associated mt-AspRS and a soluble protein partner with soluble mt-AspRS, with different function for each partnership. Further investigations are needed to distinguish between the two hypotheses and also to see if there is a correlation between the dual localization of mt-AspRS and the mature products (isoforms) described in section 2.2.

2.3.2. Human mt-AspRS is a peripheral protein interacting with membrane most likely *via* electrostatic interactions

To help answering the questions raised above, we investigated how mt-AspRS is interacting with the inner membrane. As no transmembrane helix has been predicted with respect to the topology of mt-AspRS (it is not an integral protein), one of the most plausible hypotheses is that mt-AspRS may be a peripheral protein. To check that hypothesis, mitochondria from HEK293T cells were purified and fractionated. Mitochondrial membranes were then treated with sodium carbonate in order to release peripheral proteins and distinguish them from integral membrane proteins (TS and RM in Figure 14A) (as described in Mastrogiacomo *et al.* 1998, Delage *et al.* 2007, Kilbride *et al.* 2015). Western blots using antibodies against proteins of known sub-mitochondrial location were used to assess the quality of the fractionation process (Left box in Figure 14A). The Superoxide dismutase 2 (SOD2, Nair and McGuire 2005; Meyer *et al.* 2005) was used as a marker for matrix and soluble protein. Voltage-dependant anion selective channel protein 1 (VDAC1, Arnoult *et al.* 2009) and Prohibitin (He *et al.* 2012) were

shown to be integral proteins from the outer and the inner membranes, respectively. Mammalian mt ribosome (Liu and Spremulli 2000) as well as the Cytochrome c (Cyt c, Rytomaa and Kinnunen 1995), the Creatine kinase (CKMT1A, Schlattner and Wallimann 2000) and the heatshock protein 60 (Hsp60, Arnoult *et al.* 2009) were reported to be dual localized in the soluble and membranes fractions as peripheral proteins. Carbonate treatment released a fraction of membrane-bound mt-AspRS (TS fraction), but this latter is still detected in membranes fraction (RM) (Red box in Figure 14A). Protein markers of each mt compartment are discussed below.

Based on carbonate treatment result reproducibly obtained, we considered other hypotheses of mt-AspRS/inner membrane interaction. We tested the hypothesis of an anchorage *via* the mt-AspRS C-terminal extension, so we deleted this latter but the enzyme became insoluble. We also tested the possibility of an intermolecular disulfide bridge with an integral protein (Winger *et al.* 2007), S- or O-palmitoylation anchorage (Folmes *et al.* 2010, Kostiuk *et al.* 2008), or indirect interaction *via* mt-DNA or RNA (Rajala *et al.* 2014) (Figure 14B and C). Neither of the different treatments was able to release mt-AspRS from membranes, except for the treatment with 0.1 M of NaOH (but mt-AspRS was undetected in supernatant (Sp) fraction). This treatment did not release Prohibitin from membranes (Figure 14B).

While looking for an explanation to our result, we noticed that carbonate treatment could be performed alternatively. Indeed, instead of treating only mitochondrial membranes, whole mitochondria can be incubated (and sonicated) with sodium carbonate, and this approach seems to be more common than the first one (Rajala *et al.* 2014). Thus, we repeated the experiment of carbonate treatment on whole mitochondria prior to fractionation into soluble and membranes fractions (Right box in Figure 14A). This protocol released mt-AspRS, which was detected only in the soluble fraction (CS) similarly to other known peripheral proteins (Red box in Figure 14A). In agreement with the literature, SOD2 and VDAC1 were detected exclusively in the soluble and membranes fractions, respectively, with or without carbonate treatment. After carbonate treatment on mt membranes, Prohibitin was detected exclusively in the membranes fraction. However, upon carbonate treatment on whole mitochondria, a significant

amount was detected in the soluble fraction (CS). This contamination is probably due to the sensitivity of Prohibitin to carbonate extraction as it has been shown for some integral mt proteins (Kim *et al.* 2015). Cyt c, CKMT1A and the mitochondrial ribosomal protein 18 from the large subunit (MRPL18) were detected in both soluble and membranes fractions, and were recovered in the soluble fraction following carbonate extraction confirming their peripheral association with membranes. Hsp60 was also detected in the soluble and membranes fractions, however, after carbonate extraction Hsp60 was detected mostly in the soluble fraction with a slight contamination in the membranes fraction (CM), as observed by others (Engl *et al.* 2012). All these data assess for the quality of the fractionation process.

Similarly, we applied a treatment with KCl (250 and 500 mM) and were also able to release mt-AspRS from membranes (Figure 14D).

Despite the wrong path we took in the beginning to answer the question, we finally demonstrated that mt-AspRS is interacting with membranes most likely via electrostatic interactions.

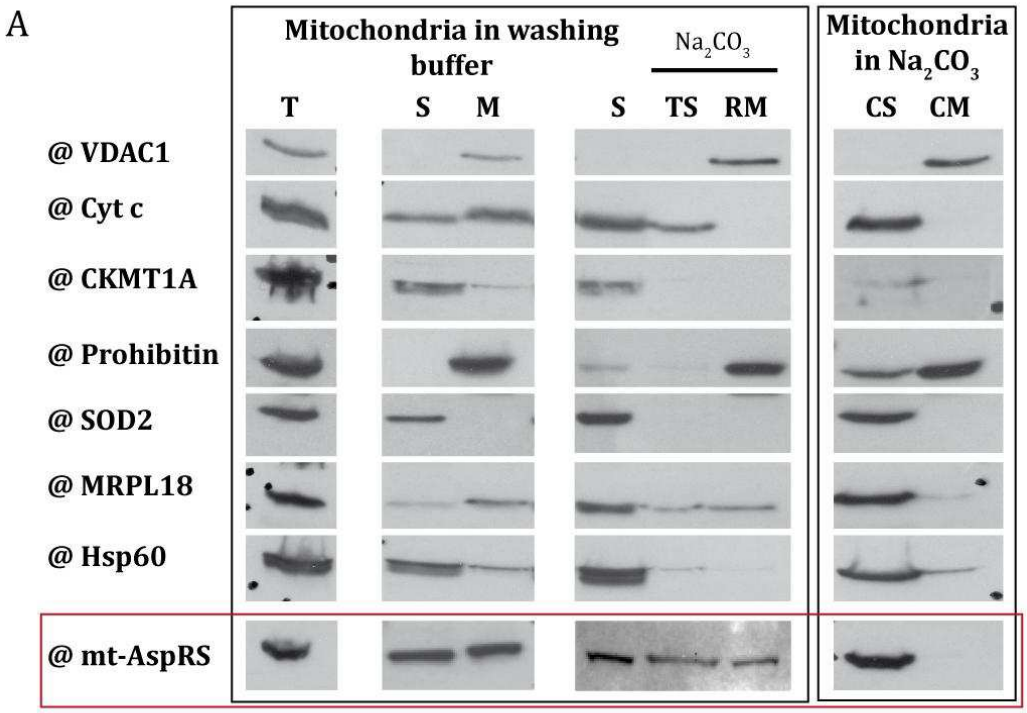

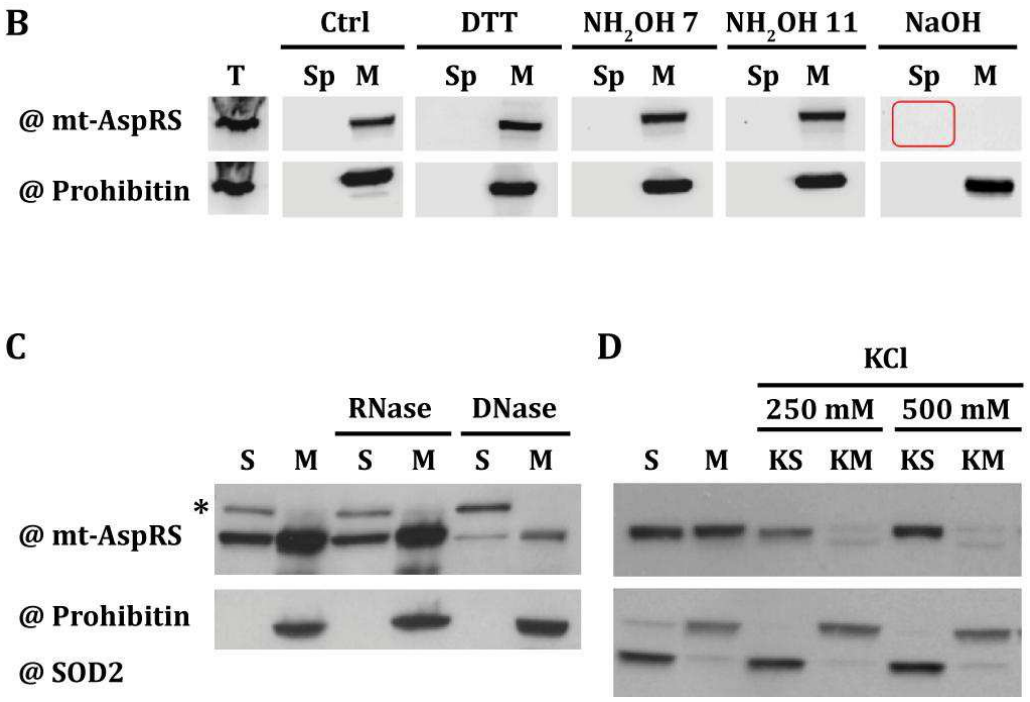

Figure 14: Interaction of mt-AspRS with the inner membrane. Mitochondria were purified from HEK293T cells. A) Carbonate (0.1 M Na_2CO_3) treatment was applied either on whole mitochondria (Left box) or on membranes fraction (Right box). T, total. S, soluble fraction. M, membranes fraction. TS, treatment-solubilized fraction. RM, residual membranes fraction. CS, carbonate soluble fraction. CM, carbonate membrane fraction. B) Treatment of membranes fraction (M) with: DTT (0.4 M), NH2OH (1M pH 7 and 11), NaOH (0.1 M). Sp, supernatant resulting after the treatment of the membrane fraction. C) Treatment of sonicated mitochondria with nucleases: RNase A (20 mg) or DNase I (10U). D) Treatment of whole mitochondria with 250 mM or 500 mM KCl. KS, KCl soluble fraction. KM, KCl membranes fraction. * based on the MW marker, the upper band is non-specific.

2.3.3. Interaction of mt-AspRS with membrane is maybe dynamic and reversible

In order to check whether the interaction of mt-AspRS with the inner membrane is dynamic, we searched for studies tackling the same question with other mitochondrial proteins. Waksman and Rendon (Waksman and Rendon 1971, Rendon and Waksman 1971, Rendon and Waksman 1973 and Waksman and Rendon 1974) have performed a series of studies on the dynamics of the interaction of certain mt proteins, essentially Aspartate aminotransferase (GOT2) and Malate dehydrogenase (MDH), with the inner membrane. They showed that extra-mitochondrial substances trigger specific and reversible release of these proteins from the inner mitochondrial membrane (Rendon and Waksman 1973). In addition, Williamson has showed in *E. coli* that leucyl-tRNA

synthetase was retrieved either soluble or membrane-associated depending on leucine concentration (Williamson 1993). We applied a similar approach and screened different chemicals at different concentrations (see the list and concentrations in the methods section) on mitochondria isolated from HEK293T cells. Distribution of mt-AspRS between soluble and membranes fractions was then assessed. In order to facilitate the analysis, only the membranes fractions were analyzed by western blot, and the intensity of mt-AspRS (membrane-associated form) was compared between treated and untreated mitochondria.

Among the numerous chemicals that were tested, only succinate and glutamate (50 and 10 mM, respectively) promoted a displacement of mt-AspRS from soluble to membrane-associated forms. This effect appeared, however, not to be mt-AspRS specific since the same observation was made to the matrix control SOD2 (treatment with 50 mM is presented in figure 15A).

Treatment of mitochondria with ATP at a concentration of 10 mM provoked a significant decrease in the intensity of mt-AspRS, but in both soluble and membranes fractions (Figure 15B). Western blot of Prohibitin is incomplete because only membranes fractions were analyzed during the screening (asterisk of Figure 15B). Since the treatment was performed on isolated mitochondria, mt-AspRS might be selectively degraded or released outside mitochondria.

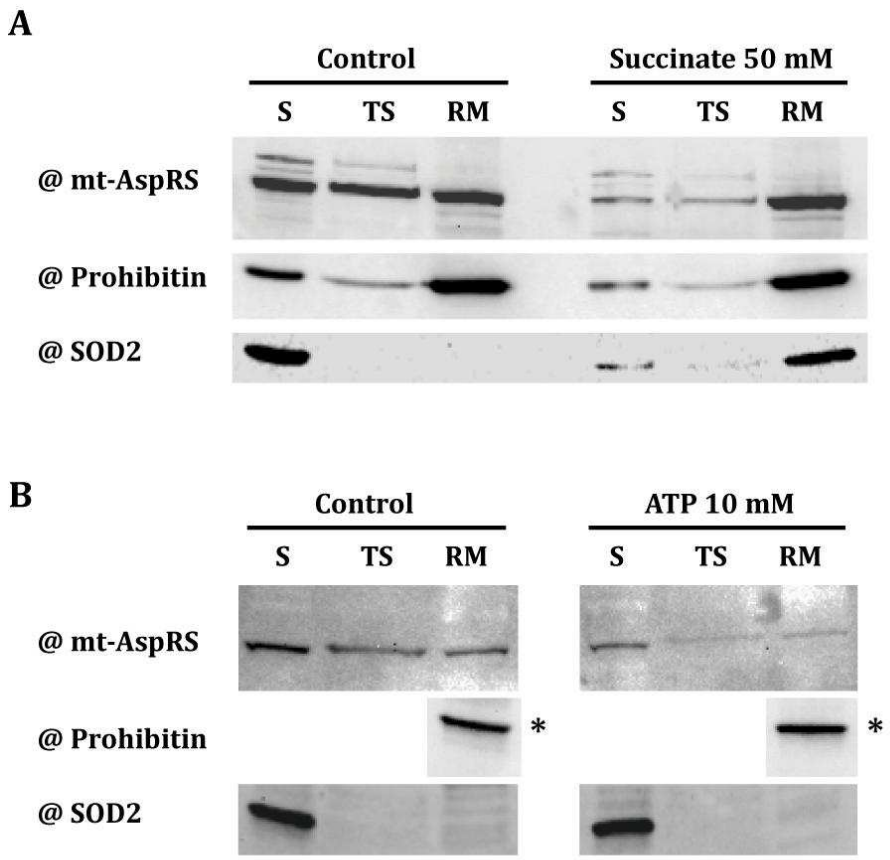

Figure 15: Some screened chemicals changed the dual localization of mt-AspRS. Mitochondria were purified from HEK293T cells and used for the screening of chemicals. Chemicals did not change the dual localization except for: A) treatment with 50 mM succinate (same profile was obtained with glutamate) and B) treatment with 10 mM ATP. S, TS and RM fractions were obtained following Protocol 2 fractionation. * Prohibitin was detected on membranes fractions. Of note, during chemicals screening, only membranes fractions were analyzed.

2.4. Extra-mitochondrial localization of mt-AspRS in certain stress conditions

In order to see whether mt-AspRS is selectively degraded or released outside mitochondria, the experiment was repeated and the extra-mitochondrial media were analyzed (EM in Figure 16A). As previously observed, the mt-AspRS is detected in both soluble and membranes fractions after fractionation of untreated mitochondria.

Mitochondria treated with either ATP or GTP (10 mM) displayed highly reduced intensities of mt-AspRS in soluble and membranes fractions, but significant intensities in the extra-mitochondrial media (EM). This observation is specific for mt-AspRS since neither SOD2 nor Prohibitin was detected in the EM, but remained in their respective fractions, whatever is the applied treatment (Figure 16B). These observations clearly showed the release of mt-AspRS outside mitochondria upon treatment with either ATP or GTP. Treatment with ADP (10 mM) released a fraction of mt-AspRS but less intense than what was observed for ATP or GTP.

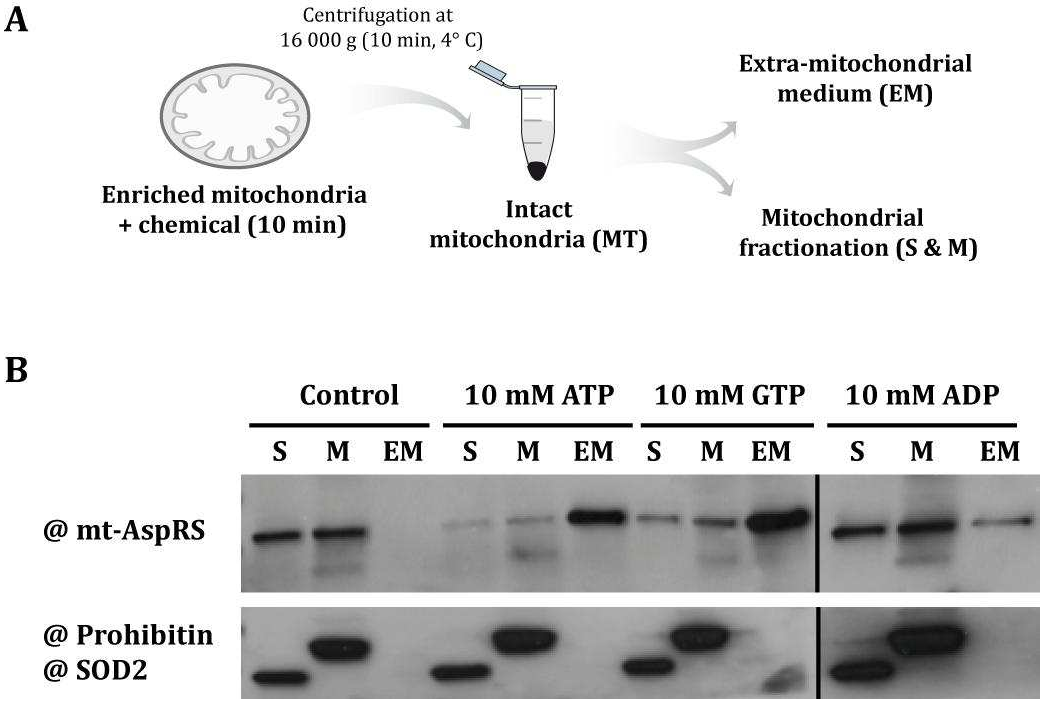

Figure 16: Analysis of the extra-mitochondrial medium (EM) after chemicals treatment. Mitochondria were purified from HEK293T cells and treated with different chemicals. A) Workflow of mitochondrial treatment and fractionation. B) Mitochondria untreated or treated with 10 mM of either ATP, GTP or ADP prior to fractionation were analyzed by western blot. S and M, soluble and membranes fractions.

2.4.1. mt-AspRS and Cytochrome c are released without affecting mitochondrial integrity

The same experiment was repeated with increasing concentration of ATP ranging from 0.1 to 50 mM (Figure 17). Again, mt-AspRS was detected in the extra-mitochondrial medium (EM) when mitochondria were treated with 10 mM or higher concentrations of ATP. The integrity of mitochondria during these treatments was verified (Figure 17). To do so, the presence of markers mitochondrial proteins on both mitochondria and extra-mitochondrial media was analyzed by western blot. Markers are VDAC1 for the outer membrane; Prohibitin for the inner membrane, CKMT1A and Cyt c for the intermembranes space; SOD2, Glud1 and Hsp60 for the matrix. VDAC1, Prohibitin and SOD2 were detected only in mitochondria and not in the EM. CKMT1A and Hsp60 were detected in mitochondria, and slightly in the EM whatever is the ATP concentration and even in its absence. Cytochrome c was released into the EM at 10 mM or higher concentration of ATP. This last observation is consistent with similar data obtained by Yang and Cortopassi. Indeed, they observed a specific release of Cyt c after treatment of isolated mitochondria with dATP (Yang and Cortopassi 1998). Altogether, our data confirm that mitochondria remained intact upon the range of applied ATP treatment.

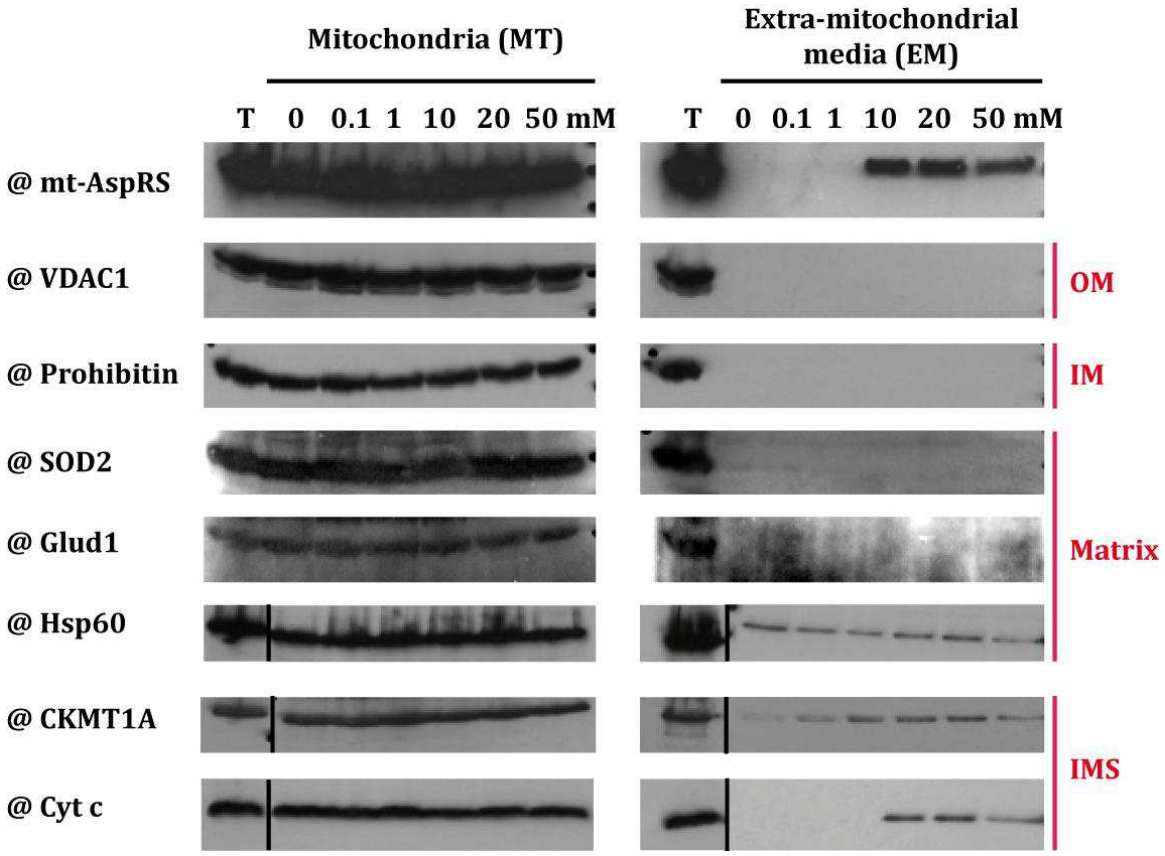

Figure 17: Verification of mitochondrial integrity upon ATP treatment. Mitochondria were purified from HEK293T cells and treated with different ATP concentrations, prior to fractionation into MT and EM fractions (see Figure 16A). Markers of each mitochondrial compartment were checked: VDAC1 for the outer membrane (OM), Prohibitin for the inner membrane (IM), CKMT1A and Cyt c for the intermembranes space (IMS), and for the matrix SOD2, Glud1 and Hsp60.

To refine the ATP concentration from which the release occurs, the experiment was repeated using ATP concentrations ranging from 1 mM to 10 mM (Figure 18A). Cyt c and mt-AspRS were released into the extra-mitochondrial medium around 4 and 6 mM of ATP, respectively. As ATP was shown to be an allosteric inhibitor of the complex IV (Cytochrome c Oxidase, COX) (Arnold and Kadenbach 1997), additional known inhibitors of the respiratory chain complexes were tested. None of them, however, provoked the release of mt-AspRS, except KCN, but at concentration higher than that used for complex IV inhibition (Figure 18B). After treatment with KCN, the integrity of

mitochondria was checked with the detection of SOD2. However, it has to be verified whether Cyt c is released into the EM after KCN treatment.

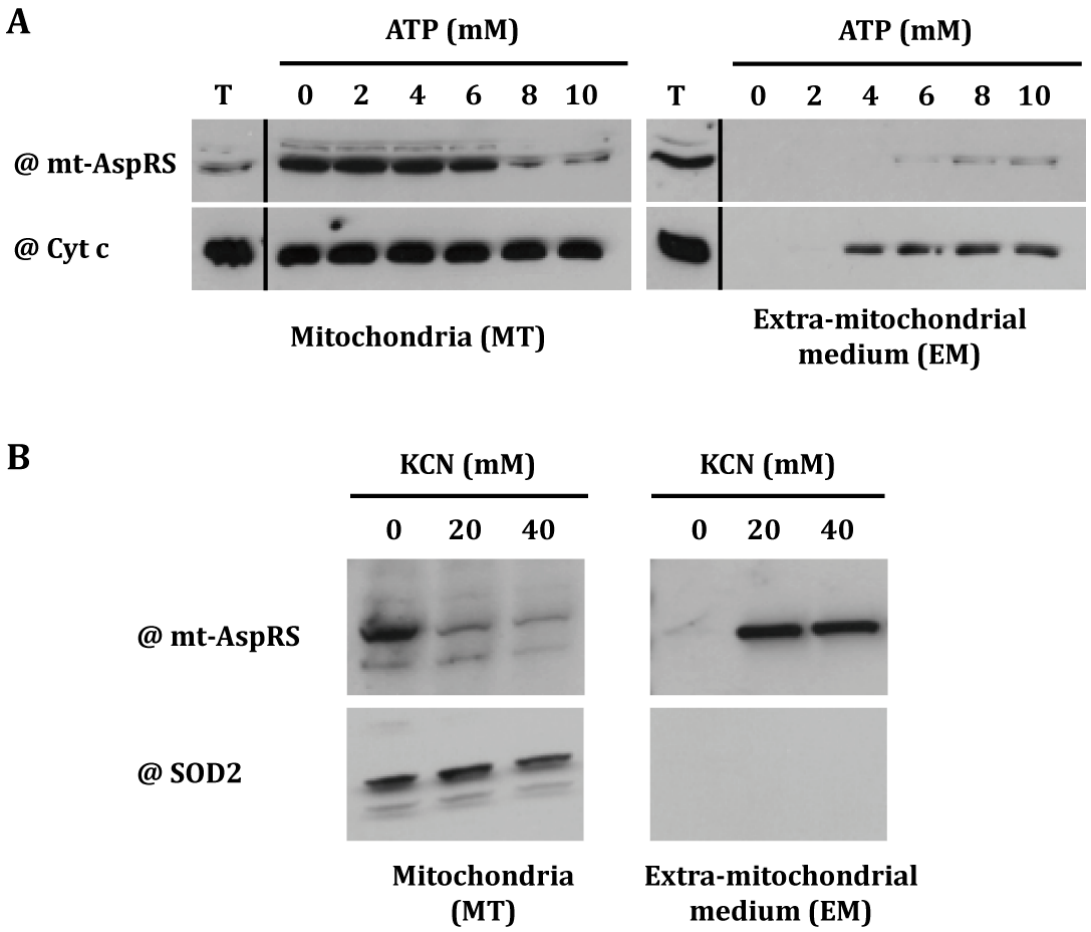

Figure 18: Analysis of the extra-mitochondrial medium (EM) after ATP and KCN treatments. Mitochondria purified from HEK293T cells were subjected to either A) ATP or B) KCN treatments.

Cyt c release, in both mt Permeability Transition Pore (mPTP) dependent (swelling) and mPTP-independent manner, is known to be a trigger of cell death (apoptosis or necrosis) process (as reviewed in Cosentino and Garcia-Saez 2014). However, whether mt-AspRS release is mPTP dependent or independent, and whether mt-AspRS is involved in cell death have to be established.

2.4.2. Release of mt-AspRS is not due to mitochondrial swelling, and is insensitive to Cyclosprin A

To check whether mt-AspRS release is caused by mitochondrial swelling, mitochondria were incubated either in a hypotonic buffer or a buffer containing 500 µM of Ca^{2+}, known to induce swelling (Halestrap *et al.* 2002), in comparison to ATP treatment. Mitochondria were also treated with Cyclosporin A (CsA) prior to treatment with ATP, hypotonic buffer or Ca^{2+}-containing buffer. CsA has been widely used to check the opening of mPTP and the swelling (Halestrap *et al.* 2002).

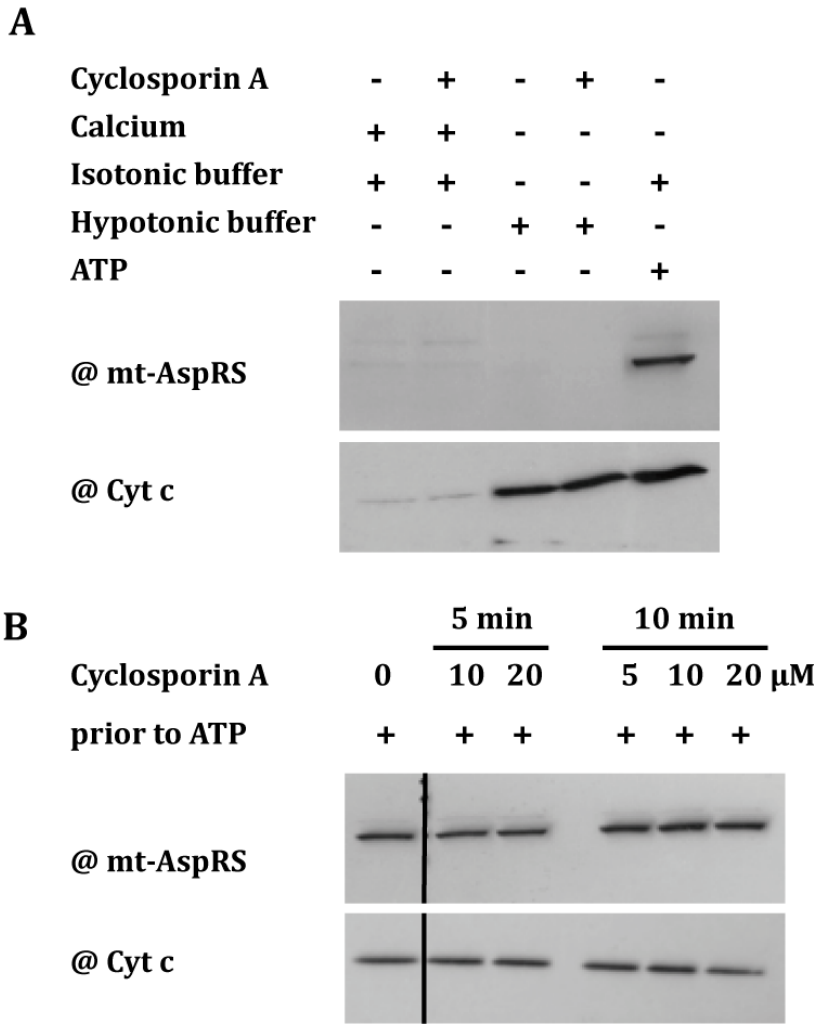

Figure 19: Verification of mitochondrial swelling, and sensitivity of mt-AspRS release to Cyclosporin A (CsA). Mitochondria were purified from HEK293T prior to: A) treatment with Ca^{2+} (500 µM) in an isotonic buffer, or incubation in a hypotonic buffer. Both treatments were performed with or without prior treatment with CsA (10 µM) for 2 min. B) Treatment of mitochondria with different concentrations of CsA and incubation times, prior to treatment with ATP (10 mM) for 10 min.

Cyt c was released into the EM after incubation of mitochondria in the hypotonic buffer. However, incubation of mitochondria with calcium provoked only a slight release of Cyt c. In contrary to this latter, neither of the two treatments was able to release mt-AspRS into the EM. As seen above, treatment of mitochondria with ATP released both Cyt c and mt-AspRS. Treatment with CsA did not inhibit the release of either Cyt c or mt-AspRS (Figure 19). Usage of CsA has to be optimized since the control condition (Ca^{2+}/CsA), where the CsA was expected to inhibit Cyt c release, was unsuccessful.

Altogether, our results show that mt-AspRS and Cyt c release after ATP treatment is not caused by mitochondrial swelling, suggesting a selective and specific release in our conditions, although we do not know whether this phenomenon is sensitive or not to CsA. Of note, release of Cyt c has been shown to occur by different ways: mPTP opening (Yang and Cortopassi 1998), pro-apoptotic Bax/Bak oligomerization (Antonsson *et al.* 2000), anti-apoptotic Bcl-2 conformation change (Lei *et al.* 2006), and caspase-2/Bid pathway (Guo *et al.* 2002). It has been suggested that these mechanisms may be different mitochondrial responses to various apoptotic stimuli (Gogvadze *et al.* 2006). In addition to Cyt c, other pro-apoptotic proteins such as Apoptosis inducing factor (AIF), endonuclease G (Endo G), can be released into the cytocol (reviewed in Saelens *et al.* 2004). However, all these proteins are resident of the intermembranes space (IMS). Some matrix proteins have been detected outside mitochondria (reviewed in Soltys and Gupta 1999, Ng and Tang 2014), but so far no release of matrix protein under stress conditions has been reported. This observation raises the questions of how mt-AspRS is specifically released, and what are the other released proteins if any.

Interestingly, leucyl-tRNA synthetase (LeuRS) and its tRNA from *E. coli* have been detected in the periplasmic space under stress condition, suggesting a non-canonical function of this aaRS (Zhao and Martinis 2015).

2.4.3. Analysis of the extra-mitochondrial medium (EM)

Extra-mitochondrial media (EM) of ATP-treated and untreated mitochondria were subjected to different analyses so that to complement the results and clarify following interrogations:

- As it has been shown in Chapter 1, mt-AspRS exists in dimeric and complexed forms; is mt-AspRS released into the EM as a dimer or in a complexed form?
- Since mitochondria can generate small mitochondrial-derived vesicles (MDVs) (as reviewed in Sugiura *et al.* 2014), is mt-AspRS free in the EM or entrapped into vesicles?
- Are mt-AspRS and Cytochrome c the only proteins released into the EM, or are there any others?

2.4.3.1. Dynamic Light Scattering (DLS)

Extra-mitochondrial media (EM) of ATP-treated and untreated mitochondria were analyzed by DLS and showed roughly homogeneous sized particles with a hydrodynamic diameter of 20 ± 5 nm in both samples. EM from ATP-treated mitochondria was three fold higher than the control EM in term of object number (Figure 20A). This result confirms the effect of ATP on the EM composition. Particles probably correspond to either lipid vesicles or protein complexes of about 700 to 1.10^3 kDa.

2.4.3.2. Electron microscopy

Extra-mitochondrial media (EM) of ATP-treated and untreated mitochondria were analyzed with Transmission electron microscopy (TEM) after a negative staining. The analysis revealed the presence of globular objects displaying heterogeneous sizes ranging from 6 to 13 nm, in ATP-treated EM. Control EM was completely empty (Figure 20B). The latter result is intriguing since particles of 20 nm were detected by DLS in the same sample (Figure 20A). Taking into account the dehydratation during TEM analysis, these objects could be small vesicles or protein complexes estimated at ~ 500 to 10^3 kDa of

molecular weights. For sake of comparison, mitochondrial ribosome is about 26 nm with a molecular weight of about 3.10^3 kDa (O'Brien 2003), and membrane vesicles of living organisms of all kingdoms are ranging from 10 to 300 nm of diameter depending on their lipid and protein compositions (Deatherage and Cookson 2012).

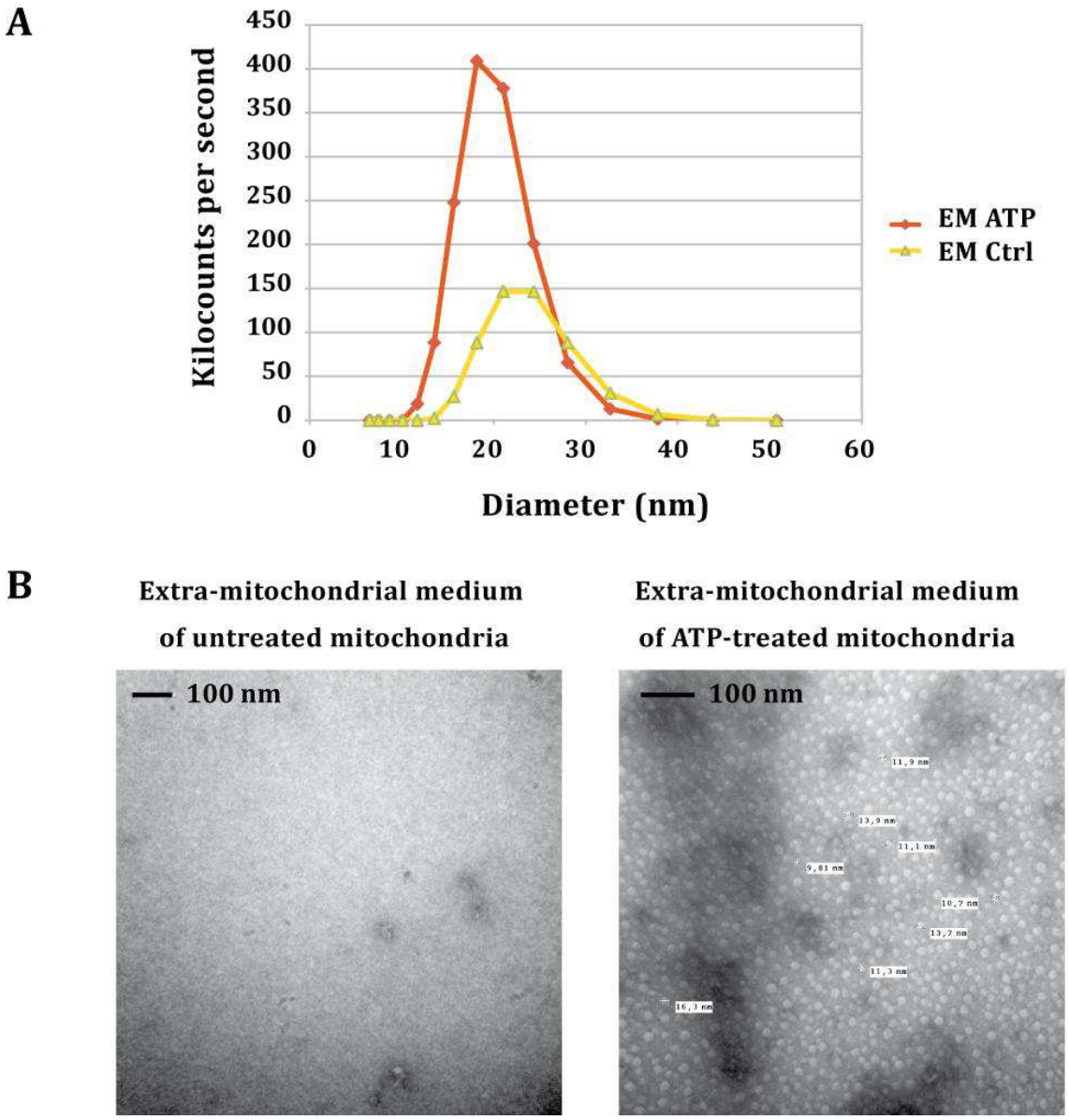

Figure 20: Analysis of the extra-mitochondrial medium (EM) with Dynamic light scattering (DLS) and Transmission electron microscopy (TEM). A) The EM was analyzed by DLS to measure the size of contained objects, and the diameter of these latter was plotted in the graph as function of the kilocounts per second. B) The EM was analyzed by negative staining with TEM.

Altogether, TEM and DLS results suggest the presence of objects in the EM corresponding to free protein complexes, or to lipid vesicles. Release from mitochondria has been demonstrated for several proteins, including Pyruvate dehydrogenase complex (PDC), a big complex of about 8.10^3 kDa (reviewed in Soltys and Gupta 1999, Ng and Tang 2014). Some of these proteins are released entrapped within Mitochondrial-derived Vesicles (MDVs) to target other organelles (Neuspiel *et al.* 2008, Soubannier *et al.* 2012, Sugiura *et al.* 2014). However, the size of these MDVs has been shown to measure between 70 and 100 nm, and do not correspond to the 20 nm observed in our experiments. Since we performed our experiments *in organello*, we cannot exclude that formation of MDVs *in vivo* requires factors that are absent *in organello*, which might explain the size difference. If the released mitochondrial proteins were free in the EM, this would suggest the existence of an export machinery. This hypothesis has been confirmed in certain conditions for intermembranes space (IMS) proteins, which are exported through Tom40 to be degraded in the cytosol by the proteasome (Bragoszewski *et al.* 2015). However, no such machinery has been described so far for the "export" of matrix proteins.

2.4.3.3. Mass spectrometry

Mass spectrometry analyses were performed on EM from ATP-treated and untreated mitochondria, in quadruplicate from independent experiments (4 EMs for each condition). Because of the large data obtained, we set a strong threshold to validate proteins. Indeed, these latter must be detected within the 4 experiments (quadruplicate) with 5 spectral counts in at least one experiment, and must be absent from the 4 controls. 143 proteins were exclusively detected in the EM of ATP-treated mitochondria, among which 13 are annotated as mitochondrial proteins (Table 5. The complete list is presented in Annex 5). More than 90% of detected proteins are annotated as cytosolic or nuclear. We think that ATP treatment might have provoked the dissociation of contaminant complexes as it has been shown for some complexes (Okorokov and Milner 1999, Huss and Wieczorek 2007, Adamek and Geeves 2014). In that case, ATP-liberated proteins would be then detected in the EM, while for control EM the contaminant complexes would be pelleted with mitochondria. In addition, due to the poor annotation of some proteins in databases, we cannot exclude that some of the so-called "contaminant" proteins (initially annotated exclusively cytosolic or nuclear proteins) could be mitochondrial proteins.

Except Cyt c, which is released in the apoptosis process (Yang *et al.* 1997, Kluck *et al.* 1997), no other pro-apoptotic proteins were detected (Saelens *et al.* 2004). However, some of the 13 released proteins (annotated as mitochondrial proteins) have been directly or indirectly related to apoptosis: SUVP3L1 (Szczesny *et al.* 2007), CKMT1A (Datler *et al.* 2014), PPIF or Cyclophilin D (Eliseev *et al.* 2009), PYCR1 (Ernst *et al.* 2002). This observation raise the question whether all the released proteins are implicated or not in the apoptosis. Of note, Cyclophilin D is the mitochondrial target of Cyclosporin A (Halestrap *et al.* 2002).

Our mass spectrometry analysis was focused only on protein detection, and it would be worth checking whether other mitochondrial macromolecules (especially RNA) are present in the EM, since some mt-tRNAs can be detected in the cytosol under stress conditions (Maniataki and Mourelatos 2005, Mei *et al.* 2010, Marnef *et al.* 2016).

						CTRL-1		CTRL-2		CTRL-3		CTRL-4		ATP-1		ATP-2		ATP-3		ATP-4	
ACCESSION Nb	Description	MW(kDa)	pI	Gene ID	Symbol	Score	#Spectres	Score	#Spectres	Score	#Spectres	Score	#Spectres	Score	#Spectres	Score	#Spectres	Score	#Spectres	Score	#Spectres
DHE3_HUMAN	Glutamate dehydrogenase 1, mitochondrial OS=Homo sapiens OX=GLUD1 PE=1 SV=2	61.4	8.3	2746	GLUD1									611.5	23	765.6	30	301.9	9	1016.9	41
SYDM_HUMAN	Aspartate--tRNA ligase, mitochondrial OS=Homo sapiens GN=DARS2 PE=1 SV=1	71.5	9.6	55157	DARS2									434.3	20	181.2	5	119.2	9	980.9	35
CYC_HUMAN	Cytochrome c OS=Homo sapiens GN=CYCS PE=1 SV=2	11.7	10.1	54205	CYCS									603.9	98	621.1	119	511.2	116	641.8	83
KCRS_HUMAN	Creatine kinase S-type, mitochondrial OS=Homo sapiens GN=CKMT1A PE=1 SV=1	47.9	9.6	1159	CKMT1B									1082.6	63	721.7	40	796.7	42	779.1	49
PYC01_HUMAN	Pyrroline-5-carboxylate reductase 1, mitochondrial OS=Homo sapiens GN=PYCR1 PE=1 SV=2	33.3	8.6	5831	PYCR1									343.6	14	174.9	6	406.6	12	459.6	17
TOM34_HUMAN	Mitochondrial import receptor subunit TOM34 OS=Homo sapiens GN=TOMM34 PE=1 SV=2	34.3	9.8	10953	TOMM34									361.9	16	280.5	11	435.6	16	395.4	15
DDX3_HUMAN	ATP-dependent RNA helicase DDX3X,L mitochondrial OS=Homo sapiens GN=DDX3X,L PE=1 SV=1	87.9	9.1	6830	DDX3X,L									165.8	9	102.0	3	139.9	6	351.3	11
DECR_HUMAN	2,4-dienoyl-CoA reductase, mitochondrial OS=Homo sapiens GN=DECR1 PE=1 SV=1	36.0	10.1	1666	DECR1									121.2	2	39.3	1	139.9	2	387.7	11
PPB_HUMAN	Peptidyl-prolyl cis-trans isomerase B, mitochondrial OS=Homo sapiens GN=PPIB PE=1 SV=1	22.6	10.4	10105	PPIB									413.3	17	276.5	13	305.6	9	242.0	9
SYVM_HUMAN	Tyrosine--tRNA ligase, mitochondrial OS=Homo sapiens GN=YARS2 PE=1 SV=2	54.2	9.7	51067	YARS2									226.9	6	152.9	3	165.6	2	315.2	9
THIL_HUMAN	Acetyl-CoA acetyltransferase, mitochondrial OS=Homo sapiens GN=ACAT1 PE=1 SV=1	45.2	9.6	38	ACAT1									302.9	17	197.6	7	243.9	6	285.4	8
TIM13_HUMAN	Mitochondrial import inner membrane translocase subunit Tim13 OS=Homo sapiens GN=TIMM13 PE=1 SV=1	18.5	9.7	26517	TIMM13									225.5	5	394.2	10	343.7	10	169.6	4
CAH17_HUMAN	Putative transferase CAH17, mitochondrial OS=Homo sapiens GN=CRAT PE=2 SV=3	38.1	10.8	108105	CRAT									177.2	5	180.0	5	144.0	5	139.6	5

Table 5: Mass spectrometry analysis of the extra-mitochondrial medium (EM) of four independent experiments.
Mitochondria were purified from HEK293T cells and treated (or not) with ATP 10 mM. EMs of the four experiments (ATP-1 to -4 and 4 Ctrl-1 to -4) were analyzed by mass spectrometry. To be validated, a protein must be: 1) absent from the four controls, and 2) detected with 5 spectral counts in at least one ATP experiment.

As observed previously by western blot (Figure 17, 18A and 19), mass spectrometry analysis detected both mt-AspRS and Cyt c with high scores. Intriguingly, CKMT1Awas exclusively detected in the EM of ATP-treated mitochondria by MS analysis, whereas it was detected in the EM of both conditions by western blot (Figure 17). Glud1, as well, was detected by mass spectrometry but not by western blot analysis, raising the question of whether the antibody we used for this protein was specific or not (Figure 17). Mt-TyrRS was detected in the EM after MS analysis, and slightly detected after western blot analysis (Figure 21). Taking into account MS scores and western blot intensities, mt-TyrRS was released to a lesser extent than mt-AspRS. Although some released proteins (annotated as mitochondrial) need further validation, our results confirm at least the release of mt-AspRS and Cyt c.

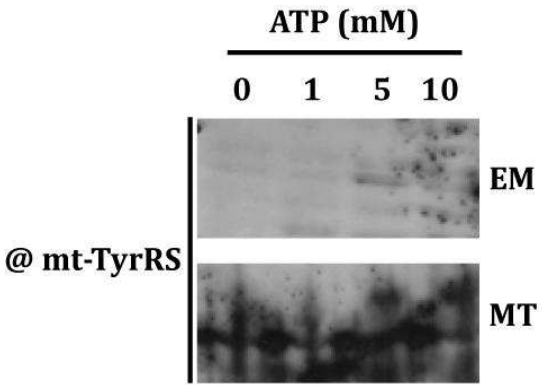

Figure 21: Detection of mt-TyrRS in the extra-mitochondrial medium (EM) of ATP-treated mitochondria. Mitochondria were purified from HEK293T cells and treated with different concentrations of ATP. After separation of the EM from mitochondria (MT), samples were analyzed by western blot to detect mt-TyrRS.

2.4.3.4. Cross-linking with glutaraldehyde

Extra-mitochondrial media (EM) of ATP-treated and untreated mitochondria were cross-linked (as performed in 1.3.1.2. of Chapter 1) prior to western blot analysis. Mt-AspRS was detected only in the EM of ATP-treated mitochondria at a high molecular weight, around 250 kDa (Figure 22). It seems that mt-AspRS is released in a small complex. The size of this latter is close to what was observed in Figure 7A (Chapter 1).

In Chapter 1, we speculated that dimeric mt-AspRS is maybe interacting with 2 monomers of unknown partner having a theoretical MW of 85 kDa. In the list of released proteins, only SUPV3L1 has a MW of 88 kDa (including an MTS of about 5 kDa, Szczesny *et al.* 2010), which makes this protein as a potential partner even though the starting point was pure speculation. In addition, SUPV3L1 and mt-AspRS have been recently co-immunoprecipitated with GRSF1, a protein involved in post-transcriptional mt-gene regulation (Antonicka and Shoubridge 2015, Antonicka *et al.* 2013).

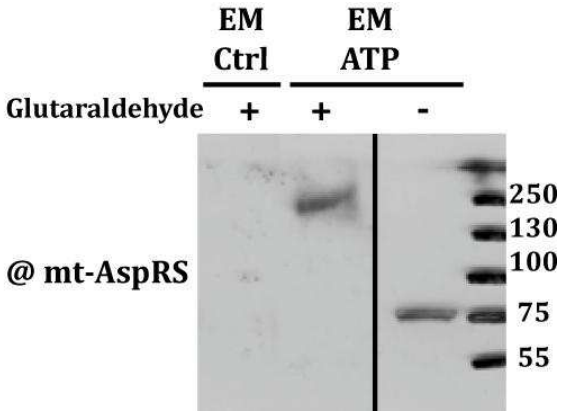

Figure 22: Glutaraldehyde cross-linking of the extra-mitochondrial medium (EM) of both treated and untreated mitochondria.

2.4.4. Preliminary results about the cellular destination of mt-AspRS after release from mitochondria

So far, mt-AspRS release was observed after ATP treatment *in organello* (with isolated mitochondria), so we decided to see if the same effect would be observed *in cellulo* (with whole cells). However, assuming that high ATP concentration may not provoke *in cellulo* the observed effect on mitochondria *in organello*, we treated cells with KCN (see section 2.4.1.), which has already been performed in other studies (Prabhakaran *et al.* 2002).

HEK293T cells were treated with KCN at 0.4 mM for 1h, and then fractionated by differential centrifugation into nuclear, mitochondrial, microsomal (endoplasmic reticulum and plasma membrane) and cytosolic enriched fractions. Mt-AspRS was

detected in nuclear and cytosolic fractions of both treated and untreated cells. In the control, however, mt-AspRS was detected in mitochondria but not in the microsomal fraction, while mt-AspRS was detected in the microsomal fraction and less importantly in the mitochondrial fraction, in treated cells (Figure 23). Detecting mt-AspRS in the microsomal fraction is consistent with the hypothesis we made after TEM and DLS analyses i.e. mt-AspRS is probably released within vesicles. But for the moment we cannot know whether mt-AspRS was detected in the released vesicles or in vesicles already targeted (and fusioned) to the ER or to plasma membrane.

Our protocol for cell fractionation into different fractions (nuclear, mitochondrial, microsomal and cytosolic fractions) was not so optimized (e.g. detection of mt-AspRS in nuclear and cytosolic fractions) and also for KCN concentration since this inhibitor can induce either apoptosis or necrosis depending on its concentration (Prabhakaran *et al.* 2002). However, although the fractionation was not clean and the experiment has to be reproduced with appropriate markers for each fraction, we have a preliminary encouraging result indicating that mt-AspRS is likely released within vesicles and likely relocated to another cellular compartment.

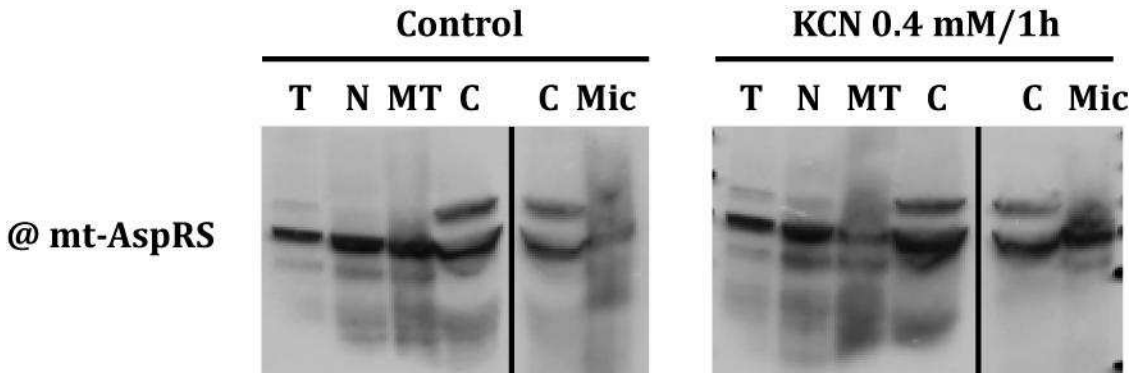

Figure 23: Cell fractionation of KCN-treated and untreated HEK293T cells. Cells were treated with KCN (0.4 mM) for 1h prior to fractionation by differential centrifugation to obtain fractions enriched in different organelles. T, total. N, nuclear fraction (400 g). MT, mitochondrial fraction (16 000 g). Mic, microsomal fraction (endoplasmic reticulum and plasma membrane vesicles). C, cytosol.

2.5. Conclusions and perspectives

Mitochondrial gene expression factories (transcription/translation) are at the inner membrane vicinity, but it has to be clarified whether it is a general rule for all factors/macromolecules. To contribute answering this question, the lab started investigating sub-mitochondrial localization of mt-aaRSs with a specific focus on mt-AspRS.

First of all, combination of different results dealing with processing and maturation of mt-AspRS showed that this latter has three mature forms in mitochondria. These mature forms are likely generated following different cleavages of mt-AspRS MTS: 1) the form Leu_{33} is most likely generated by a single cleavage of MPP (referred to as the first site); 2) the form Ile_{41} is generated either by the second and independent cleavage of MPP, or by a combination of MPP and MIP cleavages; 3) the third form Pro_{42} can be generated either by MPP/MIP/XPNPEP3 triple cleavages, or by XPNPEP3 after the second MPP cleavage. If we consider some forms as intermediates, the co-presence of the three forms is, however, uncommon since no intermediates have been detected with the ultimate mature protein, except for MRPL12 (Nouws *et al.* 2016). Interestingly, we observed in Chapter 1 (1.3.1.) that MRPL12 is among mt-AspRS partners, and has been detected by high throughput analysis (Table 2). If XPNPEP3 behaves like its yeast homolog Icp55 (Vogtle *et al.* 2009), co-presence of Ile_{41} and Pro_{42} forms would be explained. It has to be explored experimentally how the three forms of mt-AspRS are generated and whether their co-presence is biologically relevant.

Following mitochondrial fractionation into soluble and membranes fractions, mt-AspRS has been detected in both fractions. To answer how mt-AspRS is interacting with the inner membrane, we showed that this interaction is sensitive to carbonate and KCl treatments, and that mt-AspRS is a peripheral protein. To answer whether the dual localization of mt-AspRS is dynamic, we screened different chemicals on isolated mitochondria and followed the distribution of mt-AspRS between soluble and membranes fractions. Although, no chemical was able to change obviously the dual localization, it seems that this latter might be dynamic.

Unexpectedly, few chemicals provoked the release of mt-AspRS from intact mitochondria. Mt-AspRS was released together with few other proteins, among which the Cyt c. The release is not due to mitochondrial swelling and its sensitivity to Cyclosporin A treatment has to be tested again. Since Cyt c release is known to be a trigger of the apoptosis, our results suggest that mt-AspRS is probably playing a role in cell death or survival (pro- or anti-apoptotic). This hypothesis needs further investigations especially concerning: 1) the partner, which was interacting with mt-AspRS during its release, and which was detected after cross-linking experiment, 2) the new cellular localization of mt-AspRS after its release. These observations reinforce our willing to discover mt-AspRS partners (objective of Chapter 1).

Altogether, our results contribute to decipher additional properties of mt-AspRS, and give the first strong indication for an alternative function associated with the human mt-AspRS. Our results open the door to new investigations and new perspectives, particularly, in our understanding of the etiology of mt-AspRS associated disease (objective of Chapter 3).

Chapter 3: Impact of LBSL-associated mutations on human mt-AspRS properties

3.1. Introduction

Leukoencephalopathy with Brainstem and Spinal cord involvement, with Lactate elevation (LBSL) is associated with mutations of the human mitochondrial aspartyl-tRNA synthetase (mt-AspRS) sequence. The link between these mutations and the etiology of LBSL disease is still elusive, essentially due to the lack of fundamental knowledge about mt-AspRS. Our investigations on partnership and organization of mt-AspRS (Chapter 1 & 2) and their link with the expected alternative function may contribute to the understanding of the possible molecular relationship between mutations and LBSL phenotype. In turn, the study of pathology-related mutations may also contribute to discover new properties of the mt-AspRS. In this Chapter, we assess the impact of some representative LBSL-causing mutations on some *in cellulo* properties of the mt-AspRS such as its solubility, its dual localization, and its release from mitochondria. To reach this aim, we used a mammalian expression system to study the chosen mutations individually, as well as fibroblasts derived from heterozygous compound patient bearing the frequently reported splicing defect on one allele and a new unreported missense mutation on the other one.

3.2. Description of mutations and experimental procedure

Human mt-AspRS is composed of Anticodon (AC) binding domain, Catalytic domain interrupted by the Bacterial insertion domain, and the C-terminal extension (Figure 24A). LBSL-causing mutations are spread throughout the sequence of mt-AspRS, and most of them are associated in patients with a splicing defect of the exon 3. This splicing defect is qualified as leaky because residual WT mt-AspRS can be produced (~ 15%) allowing patient survival (van Berge *et al.* 2012). Our team has investigated some

mutations *in vitro*, *in cellulo* or *in organello* for their expression, dimerization, targeting to mitochondria (Messmer *et al.* 2011; van Berge *et al.* 2013). This work is in the continuity of what has been previously done, but using a new approach and exploring other mt-AspRS properties.

A

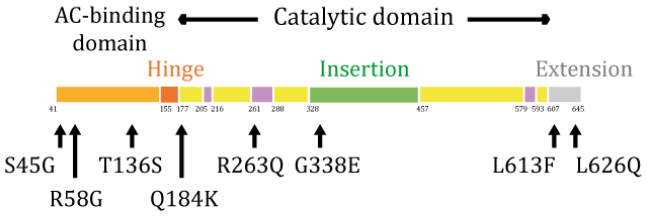

B

Patient	Allele 1	Allele 2	Ref.
1	R58G	T136S	van Berge et al., 2014
2	R76SfsX5	S45G	Scheper et al., 2007
3	R76SfsX5	Q184K	
4	R76SfsX5	R263Q	
5	L613F	L626Q	
6	R76SfsX5	G338E	Karim et al., In preparation

C

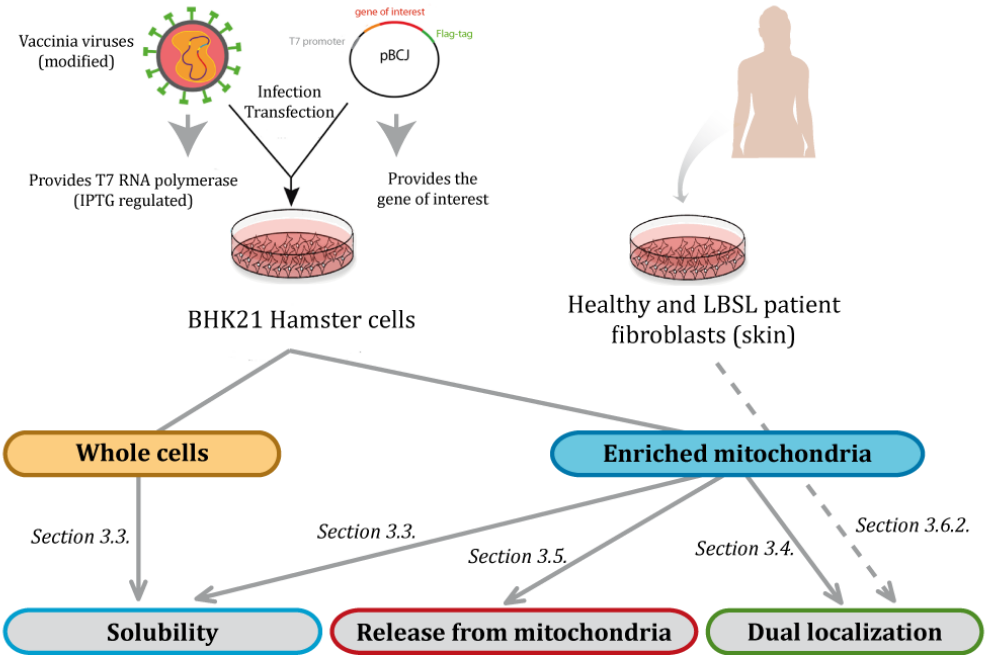

Figure 24: The chosen LBSL-causing mutations and the general strategy of their study. A) Seven reported and one unreported LBSL-related mutations are indicated on the structure of mt-AspRS: S45G, R58G and T136S are located in the anticodon-binding (AC) domain (orange); Q184K and R263Q are located in the catalytic domain (yellow); G338E is located in the bacterial insertion domain (green); L613F and L626Q are located in the C-terminal extension. B) The allelic composition of LBSL patients bearing the chosen mutations. C) The general strategy followed in this work with the section number, specific of each mt-AspRS property.

For our studies, representative mutations were chosen: S45G, R58G and T136S are located in AC-binding domain, Q184K and R263Q in the Catalytic domain, L613F and L626Q in the C-terminal extension. Some of these mutations are found in combination, and others are combined with splicing defect in patients (the allelic compositions are given in Figure 24B). Using BHK21/MVA expression system (Jester *et al.* 2011), the chosen mutations were studied individually for their solubility, dual localization, and their release from mitochondria (Figure 24C). Furthermore, except one mutation leading to a premature stop codon, no missense mutation in the Bacterial insertion domain has been reported so far. Here, we report newly discovered and unreported G338E mutation located near the Bacterial insertion domain. To study the dual localization of this mutant, we used both fibroblasts derived from LBSL patient, and BHK21 expression system. Due to technical issues, the impact of this mutation on the release of mt-AspRS from mitochondria was studied only in the expression system (Figure 24C).

3.3. Some LBSL-associated mutations impact the solubility of mt-AspRS *in cellulo*

WT and mutants of mt-AspRS were expressed and their solubility either in whole cells or in enriched mitochondria was estimated by western blot on three independent sets of experiments (Figure 25A). The aim of the present study is to analyze the impact of individual mutations on the solubility of mt-AspRSs, regardless of the impact on the expressions (already investigated in van Berge *et al.* 2013). To do so, we normalized the total amount of expressed protein (either WT or mutated) to a value of 100% and considered the relative distribution into either the soluble or the insoluble fractions. In general, the solubility determined after mitochondrial enrichment by differential centrifugation was slightly higher than the solubility of mt-AspRS in the whole cells. After quantification of mt-AspRS from soluble fractions and comparison to the WT (Figure 25B), mutants could be grouped in four classes ranging from slightly more soluble (L613F), very weakly impacted/non impacted (L626Q), moderately impacted (S45G, R58G, T136S, R263Q), to strongly impacted (Q184Q). The most significant decrease in solubility was observed for mutant Q184K (with p-values ≤ 0.01, upper panel of Figure 25B). Quantification of insoluble fractions showed a highest and statistically significant insolubility for Q184K mutant (lower panel of Figure 25B). Intriguingly, Q184K mutant has been produced in *E. coli* and has been shown to not impair the aminoacylation activity *in vitro* although the mutation is located in the catalytic site (van Berge *et al.* 2013). Thus, Q184K mutation likely affects the solubility *in fine* but could be due to refolding (after the import into mitochondria) as it has been reported with the human mt-PheRS (Banerjee *et al.* 2011; Elo *et al.* 2012). Mutations S45G and G338E are discussed in section 3.4. and 3.6., respectively.

Except for S45G and G338E mutants, this part of work belongs to a wider investigation of the impact of pathology-related mutations on the biophysical properties of the mt-AspRS (Annex 2, Sauter *et al.* 2015). This article showed that the studied mutations impact differentially the solubility and the stability, but not the architecture of mt-AspRS.

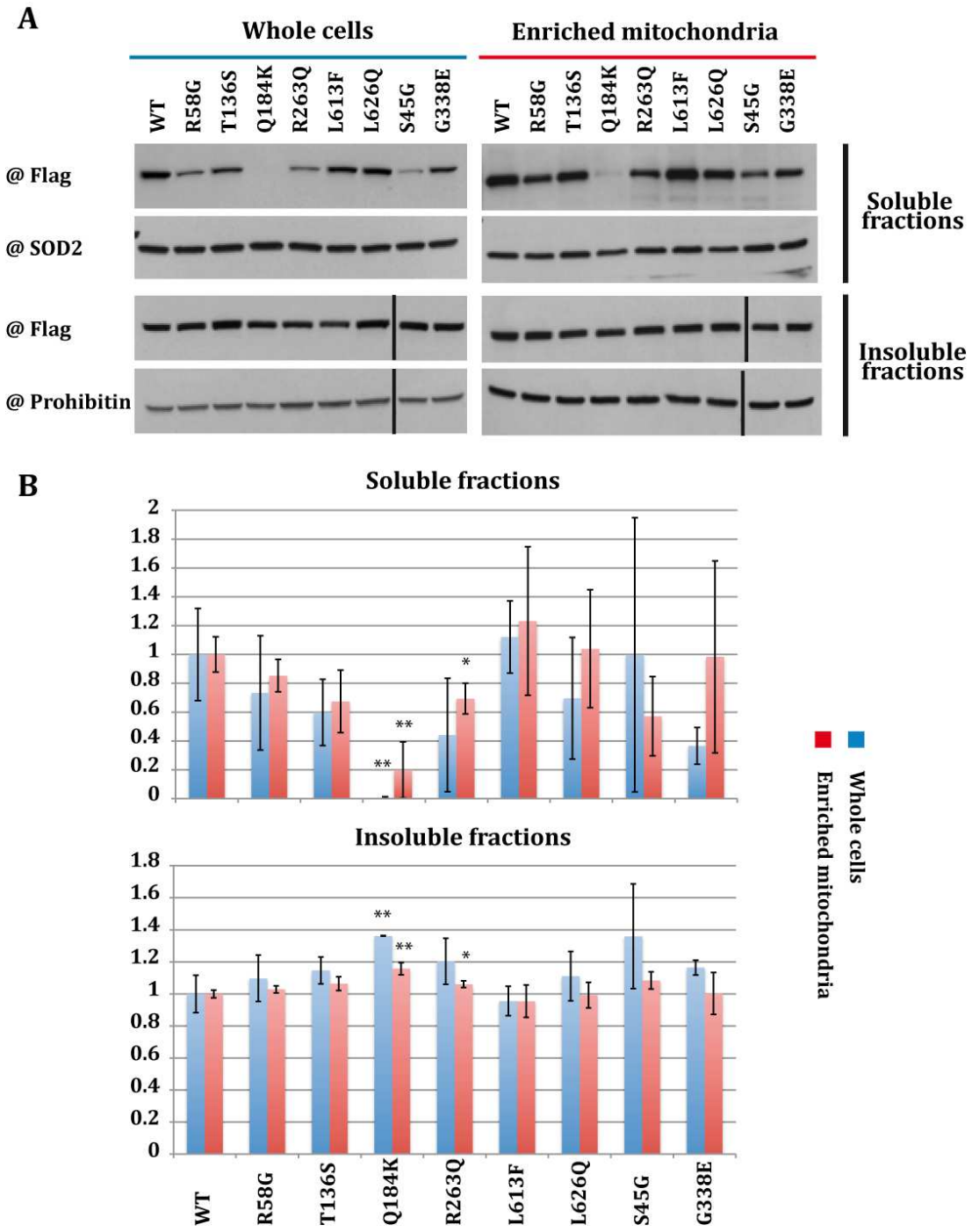

Figure 25: Solubility of WT and mutated mt-AspRSs *in cellulo*. A) Representative western blots of WT and mutant mt-AspRS (detected with anti-Flag antibodies) insoluble and insoluble fractions, within whole cells or enriched mitochondria. Detections of SOD2 and Prohibitin were performed as loading controls for the soluble and the insoluble fractions, respectively. Three sets of independent experiments for each condition (whole cells and enriched mitochondria) were analyzed. B) Relative abundance of mutant proteins as compared to WT mt-AspRS in soluble (top) and insoluble (bottom) fractions. Relative amounts of polypeptides were estimated and normalized according to the WT mt-AspRS, arbitrarily set to a value of 1 in both soluble and insoluble fractions. Errors bars illustrate the standard deviations calculated from the three sets of independent experiments. *$p < 0.05$ and **$p \leq 0.01$ based on Student's *t*-test.

3.4. Most of LBSL-associated mutations do not impact mt-AspRS dual localization

WT and mutants of mt-AspRS were expressed and their distribution between soluble (S), membranes (M) and residual (R) fractions was determined by western blot (Figure 26A). The experiment was repeated three times and the percentage of each fraction (in each experiment) was calculated, assuming that S + M + R = 100% of the total expressed protein. Histograms displaying relative amounts of mt-AspRS in the three fractions are shown in Figure 26B. A statistically significant (p-values < 0.05) reduction in the soluble IMS/matrix fraction was observed for Q184K and R263Q mutants. Even with variations, no significant effect was noticed in the membranes fractions of all mutants. The residual fraction of Q184K mutant was significantly increased compared to WT mt-AspRS (p-value < 0.05).

Q184K mutation affected the matrix localization of mt-AspRS, consistently with what has been observed in section 3.2.: the mutant Q184K showed the lowest solubility and the highest propensity to aggregate (Sauter *et al.* 2015). However, Q184K did not affect significantly the inner membrane localization of mt-AspRS. Therefore, it seems that the membrane localization of this mutant protects a fraction of the protein from aggregation. R263Q mutant showed variable results from one experiment to the other in terms of matrix localization. This variability has already been observed when investigating the solubility of this mutant *in cellulo* (Sauter *et al.* 2015). Again, the membrane localization of R263Q was not affected suggesting a sort of protection. It has been suggested that the survival of LBSL patient is probably due to the residual activity of WT mt-AspRS since the splicing defect associated with most mutations is leaky (van Berge *et al.* 2012) and because patients homozygous for the splicing defect have been reported (e.g. Miyake *et al.* 2011). Thus the membrane localization of mutated mt-AspRS could also contribute to the residual activity if this latter is not affected by the mutation, and if the membrane-associated form of mt-AspRS is active at this localization.

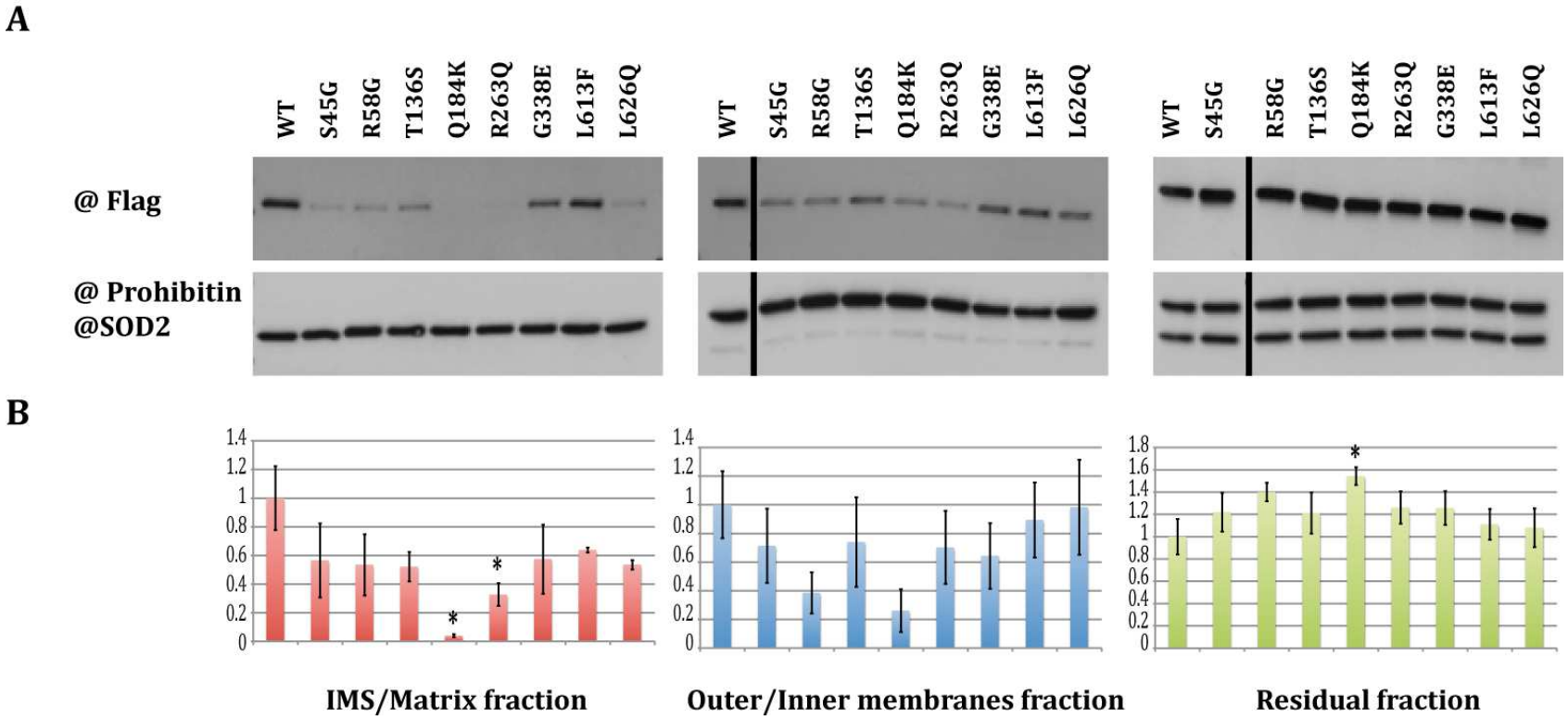

Figure 26: Impact of LBSL-causing mutations on the dual localization of mt-AspRSs *in cellulo*. BHK21 cells were transfected with different construction of mt-AspRS (WT and mutants). Mitochondria were purified and fractionated into soluble (containing matrix and intermembranes space proteins), membranes (containing outer and inner membrane proteins), and residual (containing unbroken mitochondria and possible aggregates) fractions. A) Representative western blots of WT and mutant mt-AspRS (detected with anti-Flag antibody). Detections of both SOD2 and Prohibitin were performed as loading controls for all fractions. Three sets of independent experiments were analyzed. B) Relative abundance of mutant proteins as compared to WT mt-AspRS in each fraction. Relative amounts of polypeptides were estimated and normalized according to the WT mt-AspRS, arbitrarily set to a value of 1. Errors bars illustrate the standard deviations calculated from the three sets of independent experiments. *$p < 0.05$ and **$p \leq 0.01$ based on Student's *t*-test.

The case of S45G mutant is puzzling. Indeed, patient bearing this mutation displays quite normal mitochondrial activity in lymphoblasts (Scheper *et al.* 2007). Another study on HEK293T cells, has showed impairment of the mutant import *in organello*, but with a normal processing and targeting *in vitro* and *in cellulo*, respectively (Messmer *et al.* 2011). Of note, the latter experiment has been performed with a truncated form of mt-AspRS, and mitochondria isolated from their cellular environment. Our *in cellulo* results showed that S45G mutant is soluble and dually localized in mitochondria similarly to the WT suggesting its normal import and processing. One of the hypotheses, which may explain all results, is that the location of S45G mutation near the processing site (see Chapter 2) could alter the efficiency of the import but not its total impairment. In consistence with that hypothesis, mutation in hungtingtin protein has been shown to impair and reduce mitochondrial import, in neurons but not other cells, and lead to neuronal death in Huntington disease (Yano *et al.* 2014). In addition, it has been demonstrated that targeting and import of a same protein can be different from one cell or tissue to another (Matthews *et al.* 2010).

3.5. Preliminary results on the impact of LBSL-associated mutations on extra-mitochondrial localization of mt-AspRS

In HEK293T, we showed that mt-AspRS is released from mitochondria into the extra-mitochondria medium (EM) upon treatment with 10 mM of ATP (section 2.4. of Chapter 2). This result was also obtained with BHK21 cells transfected with WT mt-AspRS (Figure 27A). Here, we test the effect of mutations on the release of mt-AspRS. To do so, BHK21 cells were transfected with different constructions (WT and eight LBSL-mutants) and mitochondria were purified 36h after transfection. Isolated mitochondria were treated with 10 mM ATP for 10 min then centrifuged to separate mitochondria from the extra-mitochondrial medium (EM). These latter were ultracentrifuged before western blot analysis. WT and all mt-AspRS mutants were released to the EM but not at the same extent (Figure 27B). This preliminary result indicates that the release is observed with the expressed mt-AspRS WT in BHK21 cells

similarly to the endogenous protein in HEK293T cells. It indicates also that mutations tested in this study presumably do not impact the property of being released outside mitochondria. The experiment, however, has to be repeated so that to be statistically relevant. Interestingly, Q184K mutant was released even though we showed that this mutant is mostly insoluble (section 3.2.) and that its matrix localization is highly affected by aggregation (section 3.3.). This result means that the released Q184K mutant is provided only by the membrane-associated form since we showed that membrane localization of Q184K mutant is not significantly affected (section 3.3.). This result is also consistent with our hypothesis (Chapter 2) that mt-AspRS may be released entrapped into vesicles.

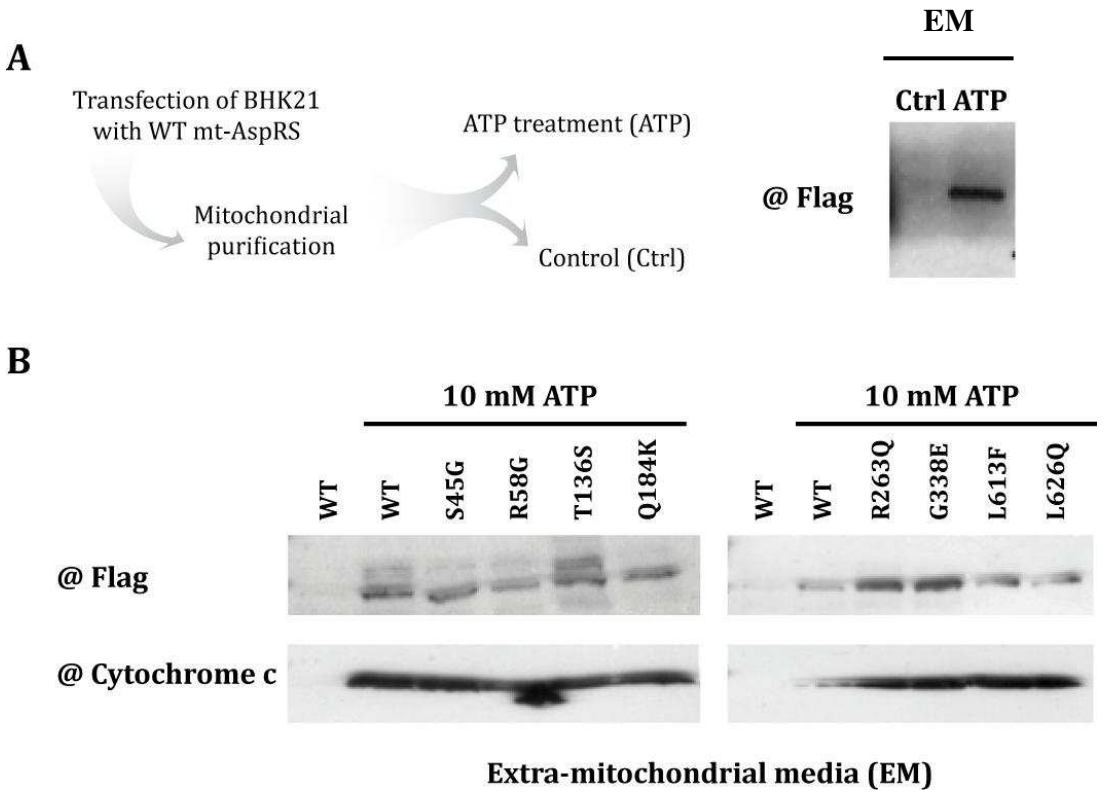

Figure 27: Release of WT and mutated mt-AspRSs from mitochondria. BHK21 cells were transfected with mt-AspRS DNA (WT or mutants). A) After transfection, purified mitochondria were treated with ATP (10 mM) for 10 min prior to separation of mitochondria from the extra-mitochondrial medium (EM). A same amount of mitochondria was untreated to serve as a control. B) Analysis of EM from the different mutant by western blot. For technical reasons, the experiment was split into two parts with separated controls.

Altogether, our preliminary results show that the studied mutations do not impact the release of mt-AspRS. To be conclusive and statistically relevant, the experiments have to be repeated.

3.6. LBSL patient bearing a new G338E mutation is reported

Our collaborators, from the institute IMAGINE (Paris), identified a patient with MRI pattern typical of the Leukoencephalopathy with brainstem and spinal cord involvement and lactate elevation (LBSL) disorder. PCR-based exome sequencing technique was further used to confirm mutation on *DARS2* gene and the LBSL diagnosis. The patient was found to be heterozygous compound, displaying an already reported c.228-20_21delTTinsC (p.R76SfsX5) mutation (Scheper *et al.* 2007) on the first allele, and a novel c.1013G>A (p.G338E) mutation on the second allele.

3.6.1. G338E mutation of mt-AspRS affects a mammal-conserved residue

Gly338 is located at the junction between the catalytic domain and the bacterial insertion domain of human mt-AspRS (Neuenfeldt *et al.* 2013), situated downstream of a sequence highly conserved in all bacterial-type AspRSs namely G_{329}TDKPDTR$_{336}$, (based on a multiple alignment made of 120 sequences of AspRS proteins from bacteria (encompassing all bacterial subgroups) and 60 sequences of mt-AspRS proteins from eukaryotes (with representatives of mammals, arthropods, fungi and protists) (Schwenzer *et al.* 2014). Interestingly, a glycine residue (G) at position corresponding to 338 in the human mt-AspRS is found to be 100% conserved in solely the sub-group of mammalian mt-AspRS, and not conserved in all other clusters of the alignment, emphasizing an importance of the glycine residue at this position in the restricted cluster of mammalian mt-AspRSs. More strikingly, a glutamate residue (E) is naturally found in corresponding position of *Schizosaccharomyces pombe* and *Aedes aegypti* mt-AspRSs, indicating that in those organisms, the substitution is not pathology-prone.

3.6.2. Mt-AspRS is weakly expressed in fibroblasts but dually localized

Mitochondria from fibroblasts, which are derived either from LBSL-diagnosed patient (p.R76SfsX5/p.G338E) or from a healthy control, were enriched and fractionated into soluble (S) and membranes (M) fractions. Of note, due to the slow growth of fibroblasts, and to the relatively low abundance of mt-AspRS mRNA in this type of cells (http://biogps.org; Ringwald *et al.* 2012), a huge number of fibroblasts was necessary for the experiments (20 fold of cells than for the same experiment using HEK293T cells). No difference of growth between healthy and LBSL-derived fibroblasts was noticed in high glucose medium. However, it is worth assessing the growth in e.g. galactose containing medium in order to force cells to respire and not rely essentially on glycolysis, which would be less important in the presence of galactose (Aguer *et al.* 2011).

In mitochondria from healthy fibroblasts, mt-AspRS was detected in both soluble and membranes fractions, similarly to the profile observed in HEK293T cells. In LBSL-derived fibroblasts, mt-AspRS was markedly less detected, but the profile of distribution, between soluble and membrane fractions, was similar to that found in healthy fibroblasts (Figure 28). Although, the expression of mt-AspRS in both fibroblasts was variable from one experiment to the other one and has to be reproduced, the impact of G338E mutation seems to be mild. In addition, it has to be elucidated whether the detected mt-AspRS in G338E-fibroblasts is the WT form (resulting from the leaky splicing defect), the mutated form, or a mixture of both. To answer this question and to assess the stability of both molecules, we propose to determine the ratio between WT and mutated forms either by RT-qPCR for mRNAs detection, or by mass spectrometry for proteins detection.

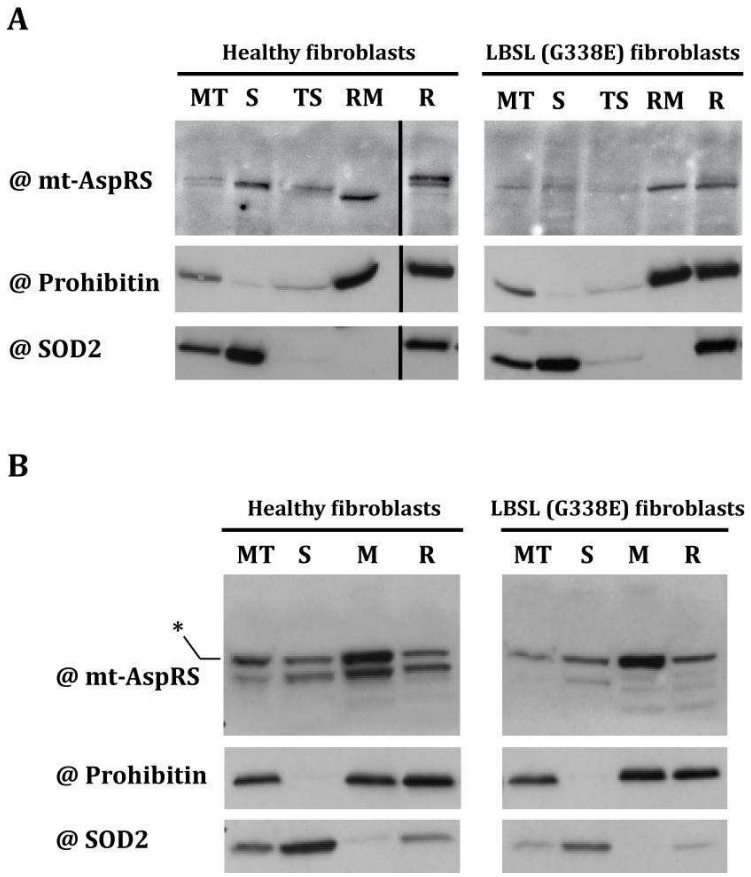

Figure 28: Dual localization of mt-AspRS in LBSL-fibroblasts. Mitochondria were purified from healthy and LBSL-fibroblasts and fractionated using: A) protocol 2 and B) Protocol 1 (see materials and methods section). All fractions were analyzed by western blot. MT, mitochondria. S, soluble. TS, carbonate treatment soluble. RM, residual membranes. M, membranes fraction. R, residual fraction containing unbroken mitochondria and possible aggregates. * based on the size of mt-AspRS, the upper band is non-specific.

In mammalian expression system (BHK21), solubility and dual localization of mt-AspRS were insignificantly impaired by the G338E mutation. Although aminoacylation of this mutant was not tested, it is likely that G338E mutation would not impact mt-AspRS activity because located far from the catalytic site and does not interfere with tRNA interaction. The absence of a strong or obvious impact of G338E mutation (at least on solubility and dual localization) reinforces our hypothesis on the existence of interacting partners or a moonlighting activity (or both) *in vivo*.

3.7. Conclusions and perspectives

LBSL disease has been specifically associated with mutations on mt-AspRS coding gene. The molecular link between mt-AspRS and the disease is, however, unclear. In this chapter, we assessed the impact of representative LBSL-causing mutations on cellular mt-AspRS properties, using mammalian expression system as well as fibroblasts derived from patient bearing unreported G338E mutation.

Leaning on previous studies (including those of the lab) and by combining biochemical and biophysical approaches, we demonstrated that mt-AspRS mutations do not affect a unique property of the enzyme, and each of them has an idiosyncratic impact. The impact of mutation on mt-AspRS solubility *in cellulo* was not significant, except for Q184K, which has a drastic impact on the solubility and a high propensity to aggregate (Annex 2, Sauter *et al.* 2015). This impact is probably due to refolding of mt-AspRS after its import into mitochondria.

We evaluated the impact of some LBSL-causing mutations on the multiple localizations of mt-AspRS (intra-mitochondrial dual localization and the release from mitochondria). The release of mt-AspRS was not affected by the mutations, neither was the dual localization. An exception was made for Q184K mutation, which affects the matrix localization of mt-AspRS consistently with our results on the solubility, but not the membrane localization. The membrane localization seems to protect a fraction of the mutant from aggregation and thus might contribute to the residual activity of mt-AspRS in the pathological context.

The usage of mammalian expression systems allowed studying mutations individually in contrary to fibroblast where both residual WT and mutated forms are assumed to co-exist. It had also the advantage of controlling the level of mt-AspRS expression. Furthermore, we were aware that the most limitation of this system is the use of viruses. Indeed, we do not know the impact of MVA virus infection on mitochondria, since some viruses can affect properties of this organelle (Ilkow *et al.* 2010, Khan *et al.* 2015). However, all our experiments were performed in comparison to WT mt-AspRS.

The expression of mt-AspRS in G338E-fibroblasts was less important than healthy fibroblasts. The dual localization of mt-AspRS, however, was similar for both types of fibroblasts. This experiment has to be reproduced despite limitations encountered with fibroblasts growth. Solubility and dual localization of the expressed G338E mutant, in BHK21 cells, are insignificantly affected. The major question we asked is whether the detected mt-AspRS is a WT, mutated form or both of them. RT-qPCR and mass spectrometry analyses should help answering that question.

Most of LBSL-causing mutations studied here do not drastically impact mt-AspRS properties. This result is consistent with the observation made after analysis of the impact of some mutations on the structure and the aminoacylation activity of mt-AspRS. Altogether these results are coherent with our strong hypothesis suggesting the existence of a non-canonical function of mt-AspRS although we need to provide the experimental evidence.

CONCLUSIONS & PERSPECTIVES

CONCLUSIONS & PERSPECTIVES

1. Objectives of the thesis

The general aim of the project is to contribute to the understanding of the link between mt-AspRS mutations and LBSL disease, by studying the properties of the mt-AspRS and by exploring LBSL-related mutations to direct the investigations. My PhD project contributed to this general aim through three objectives:

Chapter 1: to explore the organization of mt-AspRS in mitochondria, and whether this enzyme has or not protein partners.

Chapter 2: to identify the mature form of mt-AspRS and also to characterize the submitochondrial localization of this latter.

Chapter 3: to assess, *in cellulo*, the impact of some LBSL-causing mutations on properties of mt-AspRS not explored so far.

2. Summary of results from the three Chapters and general discussion

2.1. Newly discovered properties of mt-AspRS

Human mt-AspRS is processed into different mature forms

By different and complementary approaches, we demonstrated that mt-AspRS is processed into three mature forms upon its import. These mature forms start with Leu_{33}, Ile_{41} and Pro_{42} residues, respectively (this part of work is in the process to be published, see abstract in Annex 3). Our hypotheses are: 1) the form Leu_{33} is most likely generated by a single cleavage of MPP (referred to as the first site); 2) the form Ile_{41} is generated either by the second and independent cleavage of MPP, or by a combination of MPP and MIP cleavages; 3) the third form Pro_{42} can be generated either by MPP/MIP/XPNPEP3 triple cleavages, or by XPNPEP3 after the second MPP cleavage. Our hypotheses have to

be experimentally validated using recombinant peptidases or total mitochondrial extract for *in vitro* experiments with WT and mutated MTS e.g. substitution of the two arginine residues of the two MPP sites (R-2 motifs), followed by the same mass spectrometry approaches. Furthermore, what is intriguing in our results is the fact we detected simultaneously the three forms of mt-AspRS. If we assume that XPNPEP3 is similar to yeast Icp55, and that removal of one residue ($Ile_{41} \rightarrow Pro_{42}$) is only a mean of stabilization, we would have *in fine* predominantly the Leu_{33} and Pro_{42} forms. The co-presence of these forms may have a biological relevance, since a similar case has been reported with MPRL12. Indeed, MRPL12 displays two mature forms generated by "alternative processing" from the same precursor protein, and each mature form has its own partnership and its specific function (Nouws *et al.* 2016).

Human mt-AspRS is dually localized inside mitochondria, with soluble form and peripherally membrane-associated form

Western blot analyses were performed on purified and fractioned mitochondria, isolated from different cell lines. Anti-mt-AspRS specific antibody detected the protein in both soluble and membrane fractions. The purity of fractions was checked with appropriate markers and showed no cross-contamination. Due to its topology and the absence of predicted transmembrane domain, mt-AspRS is expected to be a soluble protein, so we explored how this protein is associated with membranes. We showed that mt-AspRS/membranes interaction is sodium carbonate- and potassium chloride-sensitive suggesting the occurrence of an electrostatic interaction with membranes or with integral protein(s). Since mt-AspRS has been reported as being a matrix protein (Rhee *et al.* 2013), we conclude that the membrane form of mt-AspRS is peripheral and interacting with the matrix side of the inner membrane (directly or indirectly). In addition, we explored whether the dual localization of mt-AspRS is dynamic and reversible by screening several chemicals on intact mitochondria. Our results were, at the time of writing of this manuscript, not so clear to allow conclusions about this question. Moreover, detection of three mature forms of mt-AspRS suggests a static dual localization, where one form (e.g. Leu_{33}) would interact with the inner membrane or with

an integral protein, and the others (e.g. Ile_{41}/Pro_{42}) remain soluble in the matrix, considering that Pro_{42} and Ile_{41} forms would behave similarly. In order to validate this hypothesis, we propose to analyze separately the soluble and membranes fractions and identify the mature N-termini of mt-AspRS, with the same approaches previously used.

Taking into account the mature forms of mt-AspRS, dual localization of mt-AspRS strongly suggests dual partnerships and/or dual functions, as it has been observed with MRPL12 (Nouws *et al.* 2016). Since mt-AspRS has been co-purified with Guanine-rich sequence binding factor 1 (GRSF1), a protein belonging to the RNA granules (MRG) and playing an important role in mt-RNA processing (Antonicka and Shoubridge 2015), one can hypothesize as a first avenue of research that membrane-associated form of mt-AspRS may be localized to or belong to the MRG.

Human mt-AspRS is belonging to different macromolecular complexes

We used BN-PAGE and glutaraldehyde cross-linking approaches and detected three species of mt-AspRS in HEK293T cells. One species corresponds very likely to the dimeric mt-AspRS (~ 140 kDa), while the second and third ones showed higher molecular weights (~ 225 and ~ 310 kDa) and may correspond to different complexes mt-AspRS belongs to. Despite several attempts, we were unable to identify the partner(s) by mass spectrometry analyses though. Interestingly, detection of three species of mt-AspRS, corresponding likely to a dimer and two complexes, may be correlated with the three forms of mature mt-AspRS. Relying on the case of MRPL12, one can hypothesize that each mature form of mt-AspRS has its own partnership. In addition, one can also speculate that the dimeric and complexed forms of mt-AspRS would be soluble and membrane associated, respectively.

Because we failed to detect mt-AspRS partners by mass spectrometry, one of the hypotheses is that the partners are membrane proteins. To overcome this problem, we suggest the use of soft detergents, which are compatible with mass spectrometry analyses (e.g. Saveliev *et al.* 2013). Another hypothesis to account for the lack of detection of mt-AspRS partners is that they would be RNA molecules. Consistently, since mt-AspRS has been found in MRG structures (Antonicka and Shoubridge 2015), it would be interesting

to take into consideration RNA partners. We propose to treat samples with RNase prior to BN-PAGE and cross-linking experiment to prove or disprove this hypothesis. Then we can perform e.g. CLIP-Seq experiments to identify the partners if any.

Furthermore, data mining of high throughput and experimental data, as well as predicting interaction of mt-AspRS identified interesting potential partners most of which are annotated as cytosolic proteins, although they need experimental validation before further investigations. These potential partners become more interesting since mt-AspRS can be released under certain conditions (see the section below).

Human mt-AspRS is released from mitochondria under stress conditions

During the screening of chemicals to see whether the dual localization of mt-AspRS is dynamic, few of these chemicals (e.g. 10 mM of ATP) provoked unexpectedly the release of mt-AspRS from mitochondria into the extra-mitochondrial medium. Mt-AspRS was released in a complexed form with a partner that we were, so far, unable to identify. Interestingly, the apparent molecular weight of the released complex is similar to one of the two mt-AspRS complexes detected by BN-PAGE and cross-linking, suggesting that it may be the same complex. In addition, mt-AspRS release occurs probably through vesicles smaller than mitochondrial derived vesicles (MDVs). Consistently, preliminary results on whole cell fractionation after KCN treatment showed the decrease of mt-AspRS signal in mitochondrial fraction and its increase in the microsomal (plasma membrane and ER) fraction, suggesting a release of mt-AspRS in vesicles. We have to confirm first this result with appropriate markers of different fraction, and then complete it with additional experiments. We propose to treat cells with KCN and detect mt-AspRS by immunofluorescence to follow the translocation of this latter. One can also speculate (hypothesize) that mt-AspRS might transit from mitochondria into the ER through Mitochondrial-associated membranes (MAMs). It would be difficult, however, to test this hypothesis.

Mt-AspRS is released together with few other proteins (annotated as mitochondrial), among which the Cyt c. The release is not due to mitochondrial swelling

and is insensitive to Cyclosporin A treatment. Since Cyt c release is known to be a trigger of the apoptosis process, our results suggest that mt-AspRS is probably playing a role in cell death or survival (pro- or anti-apoptotic). We propose either to transfect cells with DNA constructs of mt-AspRS lacking the MTS (Leu_{33} or Pro_{42} forms preceded by a methionine in that condition), or transfect cell with the recombinant proteins directly and check whether mt-AspRS of cytosolic location (since deprived of a MTS) promotes apoptosis. This experiment can also be combined with a pro-apoptotic treatment, to see whether mt-AspRS protects the cells from apoptosis. The result that will be obtained could allow knowing if mt-AspRS release is involved in apoptosis. However, we cannot exclude the implication of released mt-AspRS in other process than apoptosis.

Concluding remarks

As mentioned above, data mining pointed to several interesting cytosolic-annotated proteins as potential partners, but these latter were not so relevant since they are not in the same compartment (e.g. receptor at the plasma membrane) than mt-AspRS. Since we discovered that mt-AspRS could be released from mitochondria, these cytosolic partners become interesting. In addition to the search of mitochondrial partners, we propose to search also cytosolic ones by using other fractions than the mitochondrial extract. If ever we find a cytosolic partner, it would orient our investigation to the function of released mt-AspRS. The main limitation would be the cell type to be used since it cannot be excluded that the interaction (and also the alternative function) might be spatiotemporally regulated or induced only under certain conditions.

SUPV3L1, a mitochondrial RNA helicase and component of mt-RNA degradosome, and mt-AspRS have been co-purified with GRSF1 (Antonicka and Shoubridge 2015). In addition, SUPV3L1 is one of the 13 mitochondrial proteins released with mt-AspRS upon treatment of mitochondria with high concentration of ATP. This protein has been detected either as a monomer (Minczuk *et al.* 2002) or a dimer (Wang *et al.* 2009). Based on the BN-PAGE and cross-linking experiments, the predicted size of mt-AspRS partner (~ 225 and ~ 310 kDa) fits the size of SUPV3L1 88 kDa (including an MTS of about 5 kDa, Szczesny *et al.* 2010). One can speculate then that the first mt-

AspRS complex ~ 225 kDa would be formed by a dimer of mt-AspRS (140 kDa) and a monomer of SUPV3L1 (~ 83 kDa), and the second complex (~ 310 kDa) would be composed of a dimer of each mt-AspRS (140 kDa) and SUPV3L1 (~ 165 kDa) (heterotetramer). Although SUPV3L1 fits well our results, its implication has still to be experimentally validated. The easiest way to check this hypothesis is to test anti-SUPV3L1 antibody after BN-PAGE and cross-linking experiments, and to see whether the signal co-localize with that of anti-mt-AspRS antibody. The physical interaction can be checked *in vitro* with e.g. band-shift or Surface Plasmon Resonance (SPR) techniques.

2.2. Correlation of human mt-AspRS mutations with LBSL disease

LBSL disease has been specifically correlated with mutations in the mt-AspRS coding gene. The molecular link between mt-AspRS and the disease is, however, unclear. In **Chapter 1** and **2** we discovered new cellular properties of mt-AspRS. In **Chapter 3**, we tested, *in cellulo*, the impact of some LBSL-causing mutations on additional properties of mt-AspRS: solubility, dual localization and release from mitochondria. For that, we used the same set of LBSL-related mutations, which have already been investigated either for aminoacylation (Scheper *et al.* 2007, van Berge *et al.* 2013), expression and dimerization (van Berge *et al.* 2013), or import (Messmer *et al.* 2011) of mt-AspRS.

Studied LBSL-causing mutations do not impact the solubility of mt-AspRS

We assessed the impact of LBSL-causing mutations on the solubility of mt-AspRS. We demonstrated that the impact of these mutations was not statistically significant, except for Q184K that dramatically affects the solubility of mt-AspRS. This work was part of a global study combining different biochemical and biophysical approaches. In this study, it has been shown that the architecture of mutants was not affected. The thermal stability of these mutants was slightly affected witnessing a certain fragility as compared to the WT mt-AspRS, except for Q184K that, again, had a high

propensity to aggregate. This study showed that most of the investigated LBSL-causing mutations do not impact the structure (Annex 2, Sauter *et al.* 2015).

Among the studied LBSL-causing mutations, Q184K partially affects dual localization of mt-AspRS, but not its release from mitochondria

We evaluated also the impact of the same mutations on the dual localization of mt-AspRS as well as on the property of being released outside mitochondria. Except for Q184K, no significant impact has been noticed. Interestingly, Q184K mutation affects the matrix localization of mt-AspRS, consistently with our results on solubility, but not the membrane localization. The membrane localization seems to protect a fraction of the mutant from aggregation and thus might contribute to the residual activity of mt-AspRS in the pathological context, since Q184K mutation does not affect the activity of mt-AspRS (van Berge *et al.* 2013). In addition, our preliminary results showed that Q184K does not impact the release of mt-AspRS from mitochondria. This observation reinforces our hypothesis that mt-AspRS may be released in small vesicles. Detection of mt-AspRS by immunofluorescence (proposed above) would allow further investigations on this question.

Additional and concluding remarks

Furthermore, it has been shown that the S45G mutation impairs the import of mt-AspRS *in organello*, but with a normal processing and targeting *in vitro* and *in cellulo*, respectively (Messmer *et al.* 2011). However, *in organello* and *in vitro* experiments have been performed with a truncated form of mt-AspRS, and mitochondria isolated from their cellular environment. Our results showed that S45G mutant impacts neither the solubility and dual localization of mt-AspRS, nor its release from mitochondria suggesting a normal import and processing, at least in our conditions. In addition, our results about the mature forms of mt-AspRS show that S45G mutation is not in the targeting signal as it was though. One of the hypotheses, which may explain all results, is that the location of S45G mutation near the processing site could alter the efficiency but not completely impair the import of mt-AspRS, as it has been demonstrated for hungtingtin protein mutant in neurons (Yano *et al.* 2014).

Most of LBSL-causing mutations studied here, including the newly discovered G338E mutation, do not drastically impact mt-AspRS properties. Altogether these results put more emphasis on the need of exploring other properties of mt-AspRS to understand LBSL etiology. As a next step, we propose to assess the impact of mutations on the macromolecular organization of mt-AspRS (formation of complexes). Our results are also coherent with our strong hypothesis suggesting the existence of a non-canonical function of mt-AspRS although experimental evidence for this is required.

A combination of some results (multiple localizations of mt-AspRS and the impact of some LBSL-causing mutations on this mt-AspRS property) is in the way to be finalized and published (see abstract Annex 4).

2.3. What else about LBSL?

Importance of the infection history and the genetic background in LBSL phenotypic expression

LBSL is characterized by elevation of lactate (van der Knaap *et al.* 2003, Scheper *et al.* 2007), however, several patients have been reported to display a normal level of lactate (e.g. Petzold *et al.* 2006, Tzoulis *et al.* 2012). Lactate accumulation was considered as resulting from hypoxia or mitochondrial dysfunction (Hlatky *et al.* 2004, Verweij *et al.* 2000), but now increasing evidence suggests that accumulation of lactate is due to its non-utilization by damaged neurons. Thus, release of lactate by astrocytes to the extracellular environment after injuries is protective to neurons (Carpenter *et al.* 2015).

Labauge and co-workers reported the case of two sisters bearing exactly the same mt-AspRS mutations, but only one of them has developed very mild LBSL symptoms (Labauge *et al.* 2011). Tylki-Szymanska and co-workers presented the case of two brothers diagnosed with the LBSL but displaying differences in the progression of the disease. They have suggested that the case of the affected one may be aggravated with a previous varicella infection (Tylki-Szymanska *et al.* 2014). Recently, Köhler and co-

workers reported the case of a child who developed the LBSL with sever neurological deterioration, after a respiratory tract infection (Kohler *et al.* 2015). Altogether, these cases point to the importance of the infection history of patients. In other words, in some cases LBSL is not systematically developed, although the "patient" is bearing mutations (homozygous or heterozygous) on mt-AspRS. One can also hypothesize the importance of the genetic background e.g. association with another gene than *DARS2* or an aggravating factor. Consistently, an equivalent of the LBSL disease, with the same features, has been found in dog but not related to *DARS2*. The gene associated with this LBSL-like has not yet been identified (Hirschvogel *et al.* 2013).

In line with the previous point, it has been suggested that LBSL disease is underdiagnosed (Martikainen *et al.* 2013). Based on the severity of the impact of the mutations on mt-AspRS properties, one can class them in three groups:

- Lethal mutations, which drastically affect mt-AspRS properties and embryo development.
- Severe mutations, which lead to LBSL with early-onset and rapid progression.
- Mild mutations, needing a trigger to develop the LBSL (e.g. infection or trauma).

People of the last group would not be diagnosed unless they incur an infection or trauma that leads to LBSL development. This hypothesis could also explain some cases of adult onset of LBSL. In addition, if the trauma, and thus the LBSL onset, occurs in an old age, it would be correlated likely with senile neurodegeneration rather than with mt-AspRS mutations (underdiagnosis).

Furthermore, our results showed that mt-AspRS is released from mitochondria under stress conditions, probably to play an alternative function. One can try to explain the intriguing cases of LBSL where the disease is developed after a trauma, by speculating that: 1) the alternative function of mt-AspRS is induced under stress conditions (release from mitochondria and translocation to another cellular compartment); 2) the alternative function is anti-apoptotic (protective to neurons); 3) mutated mt-AspRS cannot perform this neuron-protective alternative function leading to neurons apoptosis. Again, this is a speculation that needs solid experimental validations.

Peculiarities of the brain and a potential mt-AspRS alternative function

Since LBSL disease is Central nervous system (CNS)-specific, it would be interesting to explore the mt-AspRS properties in the brain or at least in neural cells, especially neurons. For instance, we cannot exclude a spatiotemporally regulated alternative function. In addition, we do not know if mt-AspRS is addressed only to mitochondria in neurons, as it has been shown for Glutamine synthase (GS) of chicken the subcellular localization of which is different depending on the tissue, although with the same MTS (Matthews *et al.* 2010).

We have also to take into consideration the brain development and neuron structure. For example, mitochondria have been shown to be important during synaptogenesis (synapse formation). The number of mitochondria per neuron increases in addition to their localization in presynaptic terminals to supply energy demand (as reviewed in Mattson *et al.* 2008). Thus, concentrating mitochondria in presynapses increase the local ATP concentration (Rangaraju *et al.* 2014). This information is important since our results showed that mt-AspRS is released at high concentration of ATP. So, we cannot exclude that mt-AspRS release *in vivo* may occur in response to certain physiological conditions that are not related to apoptosis.

As mentioned in the introduction, whole transfer of mitochondria is used as crosstalk between cells, a mechanism that has also been observed between neurons and astrocytes. Mitochondria are transferred from neurons to astrocytes in order to be degraded (transmitophagy), and vice-versa to support neurons viability and protection in case of damage (Davis *et al.* 2014, Hayakawa *et al.* 2016). The extracellular mitochondrial transfer occurs through vesicles containing ATP and lipid droplet, in addition to mitochondria (Falchi *et al.* 2013). However, it is unclear whether “acceptor” cells use only whole mitochondria, or also individual mt-proteins. This communication between cells complicates the task of the researcher, since an mt-protein (and function) can be cell-specific, but its action may be on another cell type.

Several aaRSs are able to produce dinucleotide polyphosphates (reviewed in Tshori *et al.* 2014). This latter mediates one of the alternative functions of mammalian LysRS (Nechushtan *et al.* 2009). It cannot be excluded that mt-aaRSs (especially those

able to produce aminoacyl-adenylate without tRNA binding requirement) may generate the same metabolites. It is worth checking whether mt-AspRS produces secondary metabolites that might mediate its probable alternative function. This hypothesis can be tested by thin-layer or capillary chromatography or mass spectrometry after an *in vitro* assay.

Cytosolic AspRS, mt-AspRS, mt-GluRS and mt-AlaRS mutations correlate with leukoencephalopathies (respectively, Taft *et al.* 2013, Scheper *et al.* 2007, Steenweg *et al.* 2012, Dallabona *et al.* 2014). Except for mt-AlaRS, mentioned aaRSs are pointing toward a probable link with brain metabolism. The link might be the synthesis of N-acetylaspartate (NAA) and N-acetylaspartylglutamate (NAAG), two major neurotransmitters in the brain synthesized respectively in mitochondria and in the cytosol. Currently, preliminary investigation in the lab is exploring a potential link between mt-AspRS and Nat8L, the mt-enzyme synthesizing NAA.

3. Conclusion

Altogether, ours results showed new cellular properties of mt-AspRS with the first strong evidence of a potential alternative function. We tested the impact of some LBSL-causing mutation on some properties of mt-AspRS, and showed that roughly all mutations do not have a significant impact. This underscores the need for more studies about mt-aspRS properties, and again suggests a potential alternative function. We discussed our results and proposed different experiments either to validate or to explore new avenues. We also proposed a tentative explanation of the LBSL in connection to an alternative function of mt-AspRS. My PhD work can serve as a stepping-stone to other studies.

The new PhD student of the lab (Ligia Elena Gonzalez-Serrano) is studying the mt-arginyl-tRNA synthetase (mt-ArgRS), which is correlated with pontocerebellar hypoplasia (Edvardson *et al.* 2007). Recently, she detected mt-ArgRS only in the membranes fraction (after mitochondrial fractionation) behaving like an integral protein.

The different submitochondrial localization of mt-ArgRS, as compared to mt-AspRS, is promising for potential new discoveries.

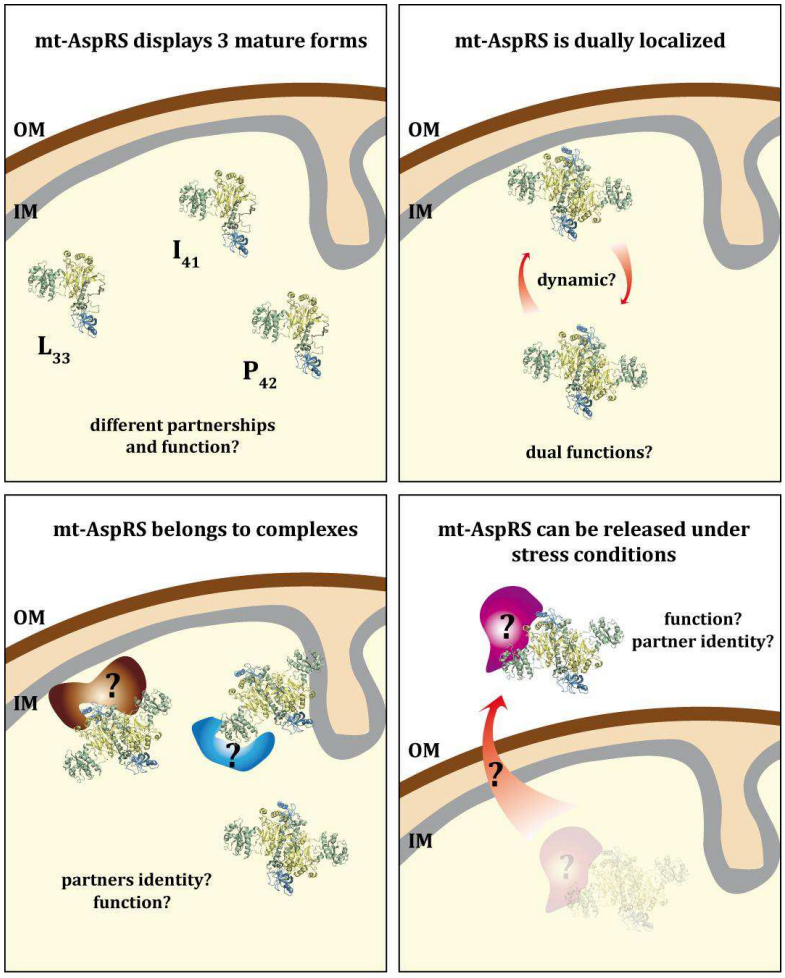

Figure 29:
Graphical conclusions.

MATERIALS & METHODS

MATERIALS & METHODS

1. Materials

1.1. Cells, biochemicals and chemicals

Human Embryonic Kidney cells 293T (HEK293T) were from Invitrogen. HeLa cells and Human Fibroblasts (from LBSL-patient and healthy control) were from the Imagine Institute (Paris). Baby Hamster Kidney cells strain 21 (BHK21) (ATCC # CRL-12072) and modified Vaccinia Ankara strain (MVA-EM24) were generous gifts from Robert Drillien (IGBMC, Strasbourg). *E. coli* One Shot® TOP 10 cells were purchased from Invitrogen™. These latter are chemically competent and genotypically characterized by: F- *mcrA* Δ(*mrr-hsd*RMS-*mcr*BC) Φ80*lac*ZΔM15 Δ *lac*X74 *rec*A1 *ara*D139 Δ(*araleu*)7697 *gal*U *gal*K *rps*L (StrR) *end*A1 *nup*G. Chemiluminescent detection kit was purchased from Pierce (Thermo Scientific). Mini-Protean® TGX Precast polyacrylamid gels, Trans-Blot Turbo system were from BioRad. Arrest™ protease inhibitor cocktail and polyethylenimine (PEI, linear 25 kDa) were purchased from GBiosciences and Polysciences, respectively. Tryptose Phosphate Broth (TPB) and sodium pyruvate were from Sigma. Trypsin, Penicillin/Streptomycin (Pen-Strep), Phosphate buffered Saline (PBS), Dulbecco's Modified Eagle's Medium (DMEM) and Glasgow's Minimum Essential Medium (GMEM) were purchased from Gibco. Fetal Calf Serum (FCS) was from Eurobio.

1.2. Sequences

Human mitochondrial aspartyl-tRNA synthetase (mt-AspRS) was studied in both *in cellulo* (*in vivo*) and *in vitro* experiments. The mt-AspRS sequence having the Uniprot accession number Q6PI48 (Entry name: SYDM_HUMAN) referred to as the endogenous protein (given in Figure 30). To generate a tagged mt-AspRS for an expression in mammalian cells, endogenous sequence was modified by adding Flag- (DYKDDDDK) and Strep- (WSHPQFEK) tag sequences at the C-terminus, in addition to some amino acids (MHPW and GS) added for cloning purpose. For the recombinant mt-AspRS, the N-terminus mitochondrial targeting sequence (MTS) was removed and a methionine (M) was added to allow the expression (start codon). The

recombinant mt-AspRS was tagged at the C-terminus with 6 consecutive histidines (H) after additional amino acids (VMYLE) added for cloning purpose (Gaudry *et al.* 2012).

Endogenous mt-AspRS:

MYFPSWLSQLYRGLSRPIRRTTQPIWGSLYRSLLQSSQRRIPEFSSFVVRTNTCGELRSSHL
GQEVTLCGWIQYRRQNTFLVLRDFDGLVQVIIPQDESAASVKKILCEAPVESVVQVSGTVI
SRPAGQENPKMPTGEIEIKVKTAELLNACKKLPFEIKNFVKKTEALRLQYRYLDLRSFQM
QYNLRLRSQMVMKMREYLCNLHGFVDIETPTLFKRTPGGAKEFLVPSREPGKFYSLPQSP
QQFKQLLMVGGLDRYFQVARCYRDEGSRPDRQPEFTQIDIEMSFVDQTGIQSLIEGLLQYS
WPNDKDPVVVPFPTMTFAEVLATYGTDKPDTRFGMKIIDISDVFRNTEIGFLQDALSKPH
GTVKAICIPEGAKYLKRKDIESIRNFAADHFNQEILPVFLNANRNWNSPVANFIMESQRLE
LIRLMETQEEDVVLLTAGEHNKACSLLGKLRLECADLLETRGVVLRDPTLFSFLWVVDFP
LFLPKEENPRELESAHHPFTAPHPSDIHLLYTEPKKARSQHYDLVLNGNEIGGGSIRIHNAE
LQRYILATLLKEDVKMLSHLLQALDYGAPPHGGIALGLDRLICLVTGSPSIRDVIAFPKSFR
GHDLMSNTPDSVPPEELKPYHIRVSKPTDSKAERAH

Expressed Flag-Strep tagged mt-AspRS:

MYFPSWLSQLYRGLSRPIRRTTQPIWGSLYRSLLQSSQRRIPEFSSFVVRTNTCGELRSSHL
GQEVTLCGWIQYRRQNTFLVLRDFDGLVQVIIPQDESAASVKKILCEAPVESVVQVSGTVI
SRPAGQENPKMPTGEIEIKVKTAELLNACKKLPFEIKNFVKKTEALRLQYRYLDLRSFQM
QYNLRLRSQMVMKMREYLCNLHGFVDIETPTLFKRTPGGAKEFLVPSREPGKFYSLPQSP
QQFKQLLMVGGLDRYFQVARCYRDEGSRPDRQPEFTQIDIEMSFVDQTGIQSLIEGLLQYS
WPNDKDPVVVPFPTMTFAEVLATYGTDKPDTRFGMKIIDISDVFRNTEIGFLQDALSKPH
GTVKAICIPEGAKYLKRKDIESIRNFAADHFNQEILPVFLNANRNWNSPVANFIMESQRLE
LIRLMETQEEDVVLLTAGEHNKACSLLGKLRLECADLLETRGVVLRDPTLFSFLWVVDFP
LFLPKEENPRELESAHHPFTAPHPSDIHLLYTEPKKARSQHYDLVLNGNEIGGGSIRIHNAE
LQRYILATLLKEDVKMLSHLLQALDYGAPPHGGIALGLDRLICLVTGSPSIRDVIAFPKSFR
GHDLMSNTPDSVPPEELKPYHIRVSKPTDSKAERAHMHPWDYKDDDDKGSWSHPQFEK

Recombinant mt-AspRS:

MIPEFSSFVVRTNTCGELRSSHLGQEVTLCGWIQYRRQNTFLVLRDFDGLVQVIIPQDESA
ASVKKILCEAPVESVVQVSGTVISRPAGQENPKMPTGEIEIKVKTAELLNACKKLPFEIKNF
VKKTEALRLQYRYLDLRSFQMQYNLRLRSQMVMKMREYLCNLHGFVDIETPTLFKRTPG
GAKEFLVPSREPGKFYSLPQSPQQFKQLLMVGGLDRYFQVARCYRDEGSRPDRQPEFTQI
DIEMSFVDQTGIQSLIEGLLQYSWPNDKDPVVVPFPTMTFAEVLATYGTDKPDTRFGMKII
DISDVFRNTEIGFLQDALSKPHGTVKAICIPEGAKYLKRKDIESIRNFAADHFNQEILPVFLN
ANRNWNSPVANFIMESQRLELIRLMETQEEDVVLLTAGEHNKACSLLGKLRLECADLLET
RGVVLRDPTLFSFLWVVDFPLFLPKEENPRELESAHHPFTAPHPSDIHLLYTEPKKARSQH
YDLVLNGNEIGGGSIRIHNAELQRYILATLLKEDVKMLSHLLQALDYGAPPHGGIALGLD
RLICLVTGSPSIRDVIAFPKSFRGHDLMSNTPDSVPPEELKPYHIRVSKPTDSKAERAHVMY
LEHHHHHH

Figure 30: Sequences of mt-AspRS either native (top), or obtained after expression in mammalian cells (middle), or in bacterial strain (bottom).

Tagged mt-AspRS (for mammalian cells expression) sequence was inserted in a plasmid (Figure 31) derived from described pBCJ739.14 (Jester *et al.* 2011).

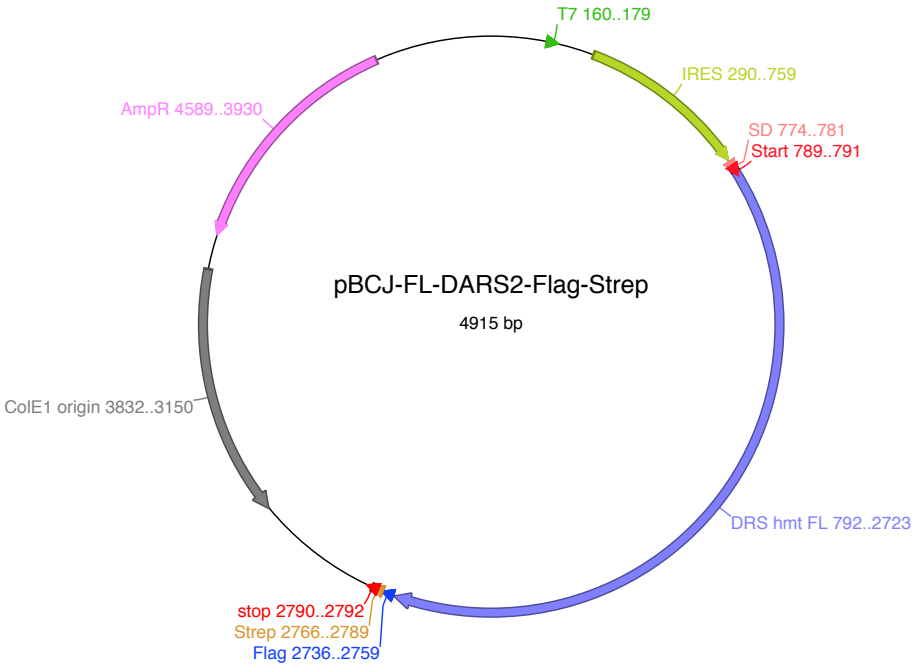

Figure 31: Plasmid map of the pBCJ-FL-DARS2-Flag-Strep (derived from Jester *et al.* 2011) transfected into mammalian cells and allowing for the expression of the human mt-AspRS. Abbreviation used: AmpR, gene of ampicillin resistance; ColE1, Origin of replication; SD, Shine-Dalgarno sequence; IRES, Internal Ribosome Entry Site; T7, T7 promoter; DRS hmt FL, Full length human mitochondrial aspartyl-tRNA synthetase.

1.3. Primers

Oligonucleotides were ordered from Sigma-Aldrich. They were resuspended in adequate volume of H_2O so that to reach a final concentration of 10 and 100 µM for usage and storage (at -20 C°) respectively.

Type	Sequence (5'-3')	Purpose (mt-AspRS)
F	CCAACACAGCTGGAGAGTTGC	Mutagenesis Cys 54 => Ala
R	GCAACTCTCCAGCTGTGTTGG	
F	GTCACCTTGAATGGATGGATTC	Mutagenesis Cys 69 => Asn
R	GAATCCATCCATTCAAGGTGAC	
Combined the primers above to construct the double mutant C54A/C69N		
F	CCAGAATTCGGTAGCTTTG	Mutagenesis Ser 45 => Gly
R	CAAAGCTACCGAATTCTGG	
F	GAGAGTTGGGTTCGTCTCAC	Mutagenesis Arg 58 => Gly
R	GTGAGACGAACCCAACTCTC	

F	CCAAAAATGCCAAGTGGTGAGATTG	Mutagenesis Tyr 136 => Ser
R	CAATCTCACCACTTGGCATTTTTGG	
F	CCAAATGAAGTATAACCTGC	Mutagenesis Gln 184 => Lys
R	GCAGGTTATACTTCATTTGG	
F	GGTTGCCCAATGTTATCGAG	Mutagenesis Arg 263 => Gln
R	CTCGATAACATTGGGCAACC	
F	CCTGACACTCGCTTTGAAATGAAGATTATAGATATCAG	Mutagenesis Gly 338 => Glu
R	CTGATATCTATAATCTTCATTTCAAAGCGAGTGTCAGG	
F	GGACATGACTTCATGAGCAATAC	Mutagenesis Leu 613 => Phe
R	GTATTGCTCATGAAGTCATGTCC	
F	CCTGAGGAACAGAAGCCCTATC	Mutagenesis Leu 626 => Gln
R	GATAGGGCTTCTGTTCCTCAGG	
F	CTTTGAAGAAGAAGGTTACCATATGTATTTCC	C-terminal deletion 631-645 aa
R	AAATATATGCATGATATGATAGGGCTTCAGTTC	

Table 6: Primer sequences used for directed mutagenesis and PCR-mediated deletion. F and R stand for forward and reverse primers, respectively.

1.4. Antibodies

Antibodies were diluted in Tris-Buffered Saline (TBS) containing 1% (w/v) of fat-free milk and 0.1% (v/v) of Tween 20, and used at concentrations either optimized in the laboratory or recommended by the supplier.

Protein		Antigen	Specificity	Clonality	Source	Dilution (WB)	Reference
Mitochondrial aspartyl-tRNA synthetase	Mt-AspRS	486-497 aa	Human	Polyclonal	Rabbit	1/40 000	IGBMC (Illkirch)
		Full length	Human	Polyclonal	Mouse	1/500	Abnova
Prohibitin	PHB	100-200 aa	Hu, Ms, Rt	Polyclonal	Rabbit	1/30 000	Abcam
Superoxide dismutase	SOD2	Full length	Hu, Ms, Hs	Polyclonal	Rabbit	1/10 000	
Voltage dependent anion-selective channel	VDAC1 (HRP)	150-250 aa	Hu, Ms, Rt	Polyclonal	Rabbit	1/7 500	
Cytochrome c	Cyt c	nd	Hu, Ms, Rt	Monoclonal	Rabbit	1/10 000	
Glutamate dehydrogenase 1	Glud1	64-366 aa	Human	Polyclonal	Rabbit	1/5 000	
Mitochondrial tyrosyl-tRNA synthetase	Mt-TyrRS	N-terminal?	Human	Polyclonal	Rabbit	1/5 000	
		C-terminal	Human	Polyclonal	Rabbit	1/5 000	Santa Cruz
Mitochondrial U-type creatine kinase	CKMT1A	41-417 aa	Hu, Ms	Polyclonal	Rabbit	1/10 000	ProteinTech

Heat shock protein 60	Hsp60	250-300 aa	Hu, Ms	Polyclonal	Rabbit	1/5 000	Bethyl Lab
Mitochondrial ribosomal protein L18	MRPL18	?	Human	?	Mouse	1/5 000	Gift from Dr Entelis
Anti-Flag primary antibody	Flag (HRP)	DYKDDDDK	-	Monoclonal	Mouse	1/2 000	Sigma-Aldrich
Anti-Rabbit secondary antibody	Rabbit (HRP)	-	Rabbit	Polyclonal	Goat	1/15 000	BioRad
Anti-Mouse secondary antibody	Mouse (HRP)	-	Mouse	Polyclonal	Sheep	1/10 000	GE Healthcare

Table 7: Used antibodies and their properties: name of the protein, antigen, specificity, clonality, host species, dilution used in western blot (WB) and the supplier. Abbreviations used: HRP, Horseradish peroxidase; Hu, human; Ms, mouse; Rt, rat; Hs, hamster.

2. LBSL patient features

Fibroblasts were isolated from healthy and LBSL-diagnosed patient (skin biopsy) after written informed consent and local National Ethic Committee approval.

LBSL patient is an heterozygous compound of DARS2 mutations, bearing c.228-20_21delTTinsC (p.R76SfsX5) mutation on the first allele from paternal origin and c.1013G>A (p.G338E) mutation on the second allele from maternal origin.

3. Methods

3.1. Cloning

3.1.1. PCR-mediated deletion of mt-AspRS C-terminal extension

3.1.1.1. Gene amplification

Forward primer was designed to anneal the 5' extremity of mt-AspRS sequence and the BstEII unique restriction site near the SD sequence of the pBCJ-FL-DARS2-Flag-Strep plasmid (Figure 31). Reverse primer was designed so that to remove the 3' of mt-AspRS sequence coding for 14 C-terminal amino acids (632-RVSKPTDSKAERAH-645) and to introduce NsiI unique restriction site. PCR reaction ingredients and program are indicated in Table 8. PCR mixture was prepared for 5 reactions (50 µl each) in order to perform the same reaction at 5 different temperatures of annealing (from 69 to 72 °C). For negative control, same PCR mixture was prepared without DNA. To assess the quality and to estimate the quantity, PCR products were loaded on agarose gel 1% (supplemented with 1/15000 (v/v) GelRed™ dye).

Ingredient	Volume
pBCJ-FL-DARS2-Flag-Strep plasmid (20 ng/µl)	5 µl
dNTP (5 mM)	2 µl
Forward primer (10 µM)	2.5 µl
Reverse primer (10 µM)	2.5 µl
H_2O	27.5 µl
Phusion HF buffer (x5)	10 µl
Phusion High Fidelity DNA Polymerase	0.5 µl (1U)

Step	Temp.	Time	
Initial denaturation	98 °C	30 sec	
Denaturation	98 °C	30 sec	30 cycles
Annealing	From 69 to 72 °C	30 sec	
Extension	72 °C	90 sec	
Final extension	72 °C	5 min	

Table 8: PCR reaction ingredients and program.

3.1.1.2. Enzymatic digestions

Five µl of PCR mixture (insert) and ~ 100 ng of pBCJ-FL-DARS2-Flag-Strep (vector) were, separately, double digested with 1 µl BstEII (Eco90l) and 1 µl NsiI (Mph1103l) in 12 µl of H_2O and 2 µl of Buffer R 10x (Enzymes and buffer from ThermoFisher). The reaction was performed during 2h at 37 °C after what insert and vector were separated on agarose gel 1% (1h at 100 V) then purified using NucleoSpin™ gel extraction kit (Macherey-Nagel) and their concentration were determined using NanoDrop™ spectrophotometer. Insert and vector were recovered at 8.5 and 4.5 ng/µl, respectively.

3.1.1.3. pBCJ-FL-DARS2-Flag-Strep dephosphorylation

Ten µl (45 ng) of the vector were supplemented with 1.2 µl of Buffer R 10x and 1 µl of FastAP (Alkaline Phosphatase) and incubated 10 min at 37 °C for dephosphorylation, and 5 min at 75 °C to inactivate the enzyme.

3.1.1.4. Ligation of the insert into dephosphorylated pBCJ-FL-DARS2-Flag-Strep

Insert (10 µl) was ligated into dephosphorylated vector (12 µl) in the presence of 1 µl of T4 DNA ligase and its appropriate buffer, in a final volume of 40 µl. The ligation was performed at 20 °C during 10 min. Ligation mixture was directly used for bacterial transformation.

3.1.2. Directed mutagenesis

Substitution of amino acids was performed according to reported LBSL-causing mutations observed in patients (S45G, R58G, T136S, Q184K, R263Q, G338E, L613F and L626Q); otherwise, the choice of substitution was done with respect to amino acids observed at the same position (different from the original one) in other organisms (C54A and C69N). Codons allowing the substitution with minimal changes in the template sequence (pBCJ-FL-DARS2-Flag-Strep) were favored. PCR reaction ingredients and program are indicated in Table 9. PCR mixture was prepared

for 5 reactions (50 µl each) in order to perform the same reaction at 3 different temperatures of annealing (gradient from 57 to 72 °C). For negative control, same PCR mixture was prepared without DNA. At the end of the reaction, 1 µl of DpnI (digesting exclusively methylated DNA) was added (overnight at 20 °C) to digest DNA template. PCR mixture was directly used for bacterial transformation.

Ingredient	Volume
pBCJ-FL-DARS2-Flag-Strep plasmid (20 ng/µl)	5 µl
dNTP (5 mM)	2 µl
Forward primer (10 µM)	2.5 µl
Reverse primer (10 µM)	2.5 µl
H_2O	32.5 µl
Pfu HF buffer (x10)	5 µl
Pfu High Fidelity DNA Polymerase	0.5 µl (1U)

Step	Temp.	Time	
Initial denaturation	95 °C	30 sec	
Denaturation	95 °C	30 sec	12 cycles
Annealing	From 57 to 72 °C	1 min	
Extension	68 °C	5 min	

Table 9: Reaction ingredients of mutagenesis PCR, and program.

3.1.3. Bacterial transformation

Chemically competent One Shot® TOP 10 cells were transformed with either 5 µl of ligation mixture or mutagenesis PCR mixture following the given protocol:

- Thaw on ice a vial of competent cells (50 µl)
- Add DNA to cells and incubate 30 min on ice
- Incubate cells 30 sec at 42 °C, and then 2 min on ice
- Add to the vial 250 µl of prewarmed SOC (Super Optimal Catobolite) medium and incubate 1h at 37 °C with shaking
- Spread 80 and 160 µl of the vial content on 2 different LB-agar plates (supplemented with 100 µg/ml of ampicillin)
- Invert and incubate the plates at 37 °C overnight

Colonies were picked and amplified in 5 ml of LB medium containing 100 µg/ml of ampicillin. After overnight incubation, cells were centrifuged and the plasmid DNA was extracted using a MiniPrep kit (Macherey-Nagel). The

concentration of DNA was determined using NanoDrop™ spectrophotometer. Plasmids were then sequenced by GATC Biotech Company.

3.1.4. Plasmid amplification and purification

For mammalian cells transfection, bacterial cells containing desired vectors were grown in 250 ml of LB medium containing 100 µg/ml of ampicillin, then plasmid DNA was purified using a MaxiPrep kit (Macherey-Nagel). The DNA was resuspended is sterile water and the concentration was determined using NanoDrop™ spectrophotometer.

3.2. Production of recombinant WT mt-AspRS in bacterial strain

The cDNA of mt-AspRS (lacking the 40 N-terminal amino acids and having a VMYLE sequence before the C-terminal 6-His tag) was previously cloned in bacterial strain RosettaTM2 (DE3) (Gaudry *et al.* 2012). The recombinant mt-AspRS was purified to homogeneity by affinity and size exclusion chromatography as reported (Gaudry *et al.* 2012, Neuenfeldt *et al.* 2013).

3.3. Mammalian expression systems

An engineered mammalian expression system composed of Modified Vaccinia virus Ankara (MVA) and Baby Hamster Kidney cells (BHK21) that leans on the controlled-expression of recombinant proteins has been developed in the lab and published (Jester *et al.* 2011). This expression system was used to express and analyze WT and mutated sequence of mt-AspRS.

3.3.1. BHK21 cell culture

BHK21 cells were cultured in GMEM supplemented with 10% FCS, 1% Pen-Strep and 5% TPB. At confluence, cells were washed with PBS and trypsinized

(0.25% Trysin-EDTA (1X), Gibco) for 2 min, and then 10 ml of medium containing FCS were added to stop the action of the trypsin. After that, cells were centrifuged at 400 g for 3 min at 20 °C. Cells were then resuspended in 10 ml of GMEM supplemented with 10% FCS, 1% Pen-Strep and 5% TPB, counted using LUNA^{TM} automated cell counter (logos biosystems), and seeded at 15.10^5 and 4.10^6 cells per plate of 60 and 150 cm^2, respectively. Cells were incubated at 37°C with 5% CO_2.

For cryopreservation, cells (~ 2.10^6 cells/ml) were supplemented with DMSO (final concentration of 10%) and frozen at – 80 °C using Mr. Frosty^{TM} Freezing Container (Nalgen®) for 1 day, then stored in liquid nitrogen.

3.3.2. Transfection of BHK21 cells

Transfection of BHK21 cells was performed as described in Sauter *et al.* 2015. Cells were washed with PBS and infected with modified vaccinia virus (MVA) expressing IPTG-inducible T7 polymerase. Infection was performed using 20 µl and 50 µl of MVA in 1 and 3 ml of unsupplemented GMEM per plate of 60 and 150 cm^2, respectively. Every 10 min, plates were tilted to avoid drying and to spread virus over cells. After 30 min of incubation with MVA, 14 ml of GMEM (supplemented with 10% FCS, 1% Pen-Strep and 5% TPB) were added to cells. This latter were then transfected with WT and mutants constructs under the dependence of T7 promoter (full-length mt-AspRS including its MTS, followed by the sequence coding for the Flag® tag DYKDDDDK) using polyethylenimine (PEI). Plasmid/PEI complexes were prepared extemporaneously in a ratio of 1:4.5 (w/w) and incubated for 15 min at 20°C prior transfection (5 and 15 µg of DNA per plate of 60 and 150 cm^2, respectively). Protein expression was induced by 1 mM IPTG. After 36h of transfection, cells were harvested for further study.

3.3.3. Modified Vaccinia virus Ankara (MVA) production

BHK21 cells were seeded at 4.10^6 cells/150 cm^2 plate. 24h later, cells were washed with PBS and then incubated at 20 °C with 3 ml of diluted MVA (1 ml of stock solution in 50 ml of FCS-free GMEM, MVA propagation and titration were performed as described previously Hebben *et al.* 2007). From time to time, plates

were tilted in order to spread the virus on cells and avoid drying. After 30 min of incubation, 14 ml of GMEM (supplemented with 10% FCS, 1% Pen-Strep and 5% TPB) were added. Cells were scraped 36h post-infection, washed with PBS, resuspended in 2 ml de FCS-free GMEM per plate. Cells were then lysed by freezing/thawing cycles to liberate virus. Finally, the solution is centrifuged to eliminate cell debris.

3.4. HEK293T cells and fibroblasts culture

HEK293T cells and fibroblasts were cultured in DMEM supplemented with 10% FCS and 1% Pen-Strep. At confluence, cells were washed with PBS (except for HEK293T cells, which are loosely adherent) and trypsinized (0.25% Trysin-EDTA (1X), Gibco) for 2 min, and then 10 ml of medium containing FCS were added to stop the action of the trypsin. Cells were seeded in new plates at dilution of 1/5 and 1/2 for HEK293T cells and fibroblasts, respectively (NB: fibroblasts do not support high dilution). Cells were incubated at 37°C with 5% CO_2. For fibroblasts, medium was changed once every 2 days.

For cryopreservation, cells (~ 2.10^6 cells/ml) were supplemented with DMSO (final concentration of 10%) and frozen at – 80 °C using Mr. Frosty™ Freezing Container (Nalgen®) for 1 day, then stored in liquid nitrogen.

3.5. Isolation and fractionation of mitochondria

Since the study concerned a mitochondrial protein, it was appropriate to use enriched mitochondria in the applied experiments for all cell lines.

3.5.1. Mitochondrial enrichment

3.5.1.1. Crude mitochondria

Cells were collected, washed with PBS and resuspended in an isotonic buffer (220 mM Mannitol, 70 mM Sucrose, 1 mM $MgCl_2$, 1 mM EDTA, 10 mM

HEPES/KOH pH 7.4) containing a protease inhibitor cocktail. Cells were then disrupted mechanically using 2 mm diameter ceramic beads in a FastPrep-24^{TM} 5G machine (MP biomedicals). Intact cells, nuclei and debris (pellet) were discarded after 10 min of centrifugation at 400 g (4°C). Supernatant was centrifuged 10 min at 12 000 g (4°C) to collect mitochondria.

3.5.1.2. Purified mitochondria

Cells were collected, washed with PBS and resuspended in 12 ml of an isotonic buffer (220 mM Mannitol, 70 mM Sucrose, 1 mM $MgCl_2$, 1 mM EDTA, 10 mM HEPES/KOH pH 7.4) containing a protease inhibitor cocktail. Cells were then disrupted mechanically using a blender (3 x 10 sec). Intact cells, nuclei and debris (pellet) were discarded after 10 min of centrifugation at 400 g (4°C). Supernatant was centrifuged 10 min at 12 000 g (4°C) to collect mitochondria. Mitochondria were resuspended in 500 µl of gradient buffer (600 mM Sucrose, 20 mM HEPES/KOH pH 7.4, 10 mM EDTA, 2% ethanol) and loaded on the Percoll/sucrose gradient. Percoll/sucrose gradient was prepared as followed:

- 2 ml of sucrose solution (1.8 M Sucrose, 20 mM HEPES/KOH pH 7.4, 10 mM EDTA, 2% ethanol) were loaded into a polycarbonate tube
- 6 ml of premixed Percoll (3 ml) and gradient buffer (3 ml) were carefully loaded on the sucrose solution

The gradient was centrifuged 30 min at 100 000 g (4 °C). After centrifugation, mitochondria appeared in a white layer in the upper 1/3rd of the gradient. Mitochondria were collected and washed once with gradient buffer, then washed 3 times with washing buffer (300 mM Mannitol, 10 mM K_2HPO_4/KH_2PO_4 pH 7.5, 1 mM EDTA). All steps are depicted in Figure 32.

Depending on the application, mitochondria were simply weighed or the total protein content was measured with a standard Bradford assay (Bradford 1976).

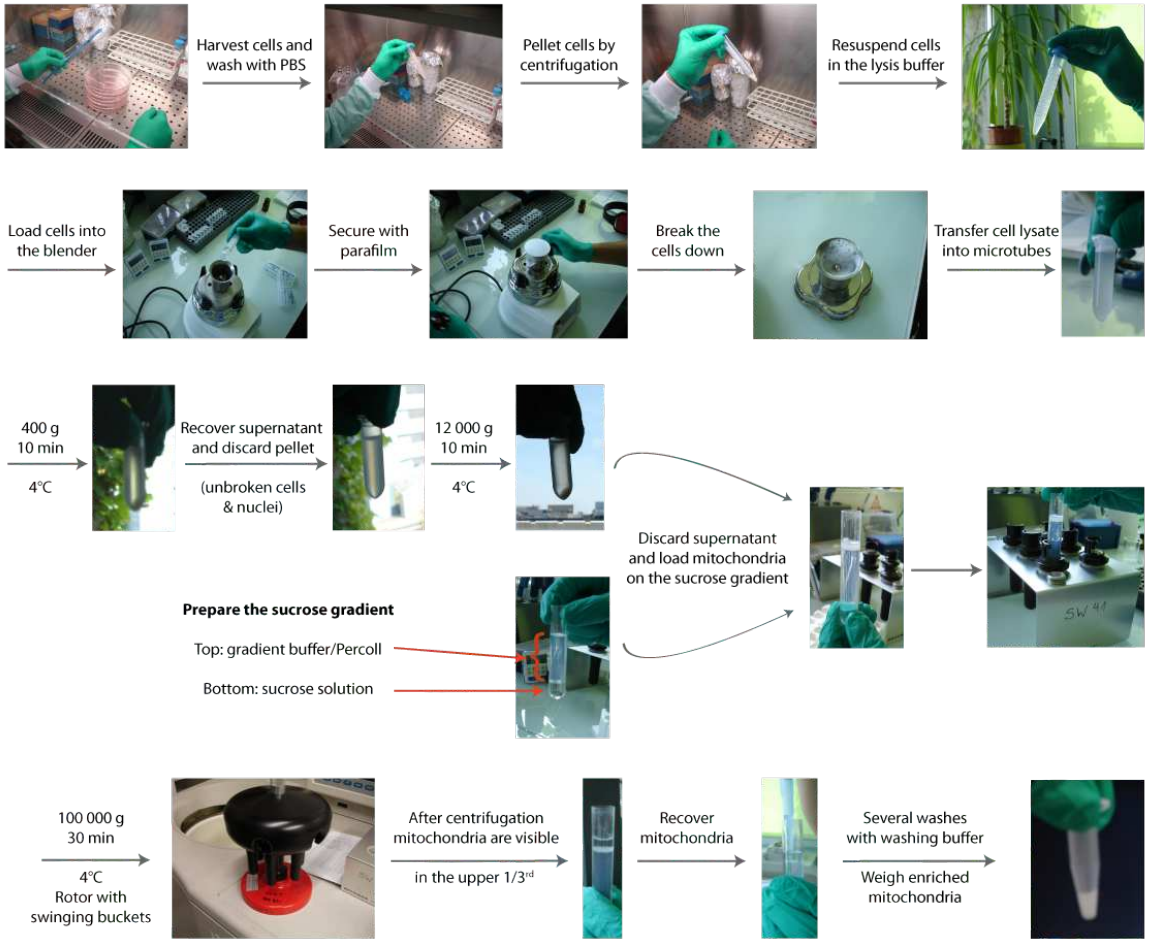

Figure 32: Mitochondrial purification by both differential centrifugation and sucrose gradient (from cell culture plate to mitochondrial pellet)

3.5.2. Protease protection assay and mitochondrial shaving

Mitochondria (~ 10 mg per condition) were incubated with different concentration of Proteinase K (0.5; 2; 5 and 10 µg) or Trypsin (5; 20 and 50 µg), at 20 °C or 4 °C, during 1 to 10 min. Protease activity was stopped with PMSF/AEBSF (2.5 mM each) and protease inhibitor cocktail for Proteinase K and Trypsin, respectively. Mitochondria were then pelleted by 10 min of centrifugation at 16 000 g (4 °C).

3.5.3. Mitochondrial fractionation

Flowcharts of experimental procedures to fractionate mitochondria (purified as described in section 3.5.1.2.) are given in Figure 33.

Protocol 1: Mitochondria were resuspended in 10 mM K_2HPO_4/KH_2PO_4 pH 7.5, 300 mM Mannitol, 1 mM EDTA, containing a protease inhibitor cocktail, and sonicated 6 x 10s on ice. Sonicated mitochondria were centrifuged during 10 min at 16 000 g (4°C). The resulted pellet (named residual fraction **R**) corresponds to unbroken mitochondria and aggregates, if any. The supernatant was further ultracentrifuged 30 min at 125 000 g (4°C) in order to separate soluble (**S**) from membranes (**M**) fractions.

Protocol 2: Same as "Protocol 1" but the membranes fraction was further treated with 100 mM Na_2CO_3 pH 11.5 for 30 min at 20 °C to recover peripheral membrane proteins. Treated membranes were then ultracentrifuged at 125 000 g during 30 min (4°C) to separate the proteins solubilized by the treatment ("treatment solubilized", **TS**) from those that remain in the membranes ("residual membranes", **RM**) (Delage *et al.* 2007).

Protocol 3: Same as "Protocol 1" but mitochondria were resuspended in 100 mM Na_2CO_3 pH 11.5 containing a protease inhibitor cocktail, prior to fractionation. In this protocol, soluble and membranes fractions are named "carbonate soluble" (**CS**) and "carbonate membrane" (**CM**), respectively (Fujiki *et al.* 1982). A variant of this protocol was applied using either 250 or 500 mM of KCl, leading to "KCl soluble" (**KS**) and "KCl membrane" (**KM**) fractions.

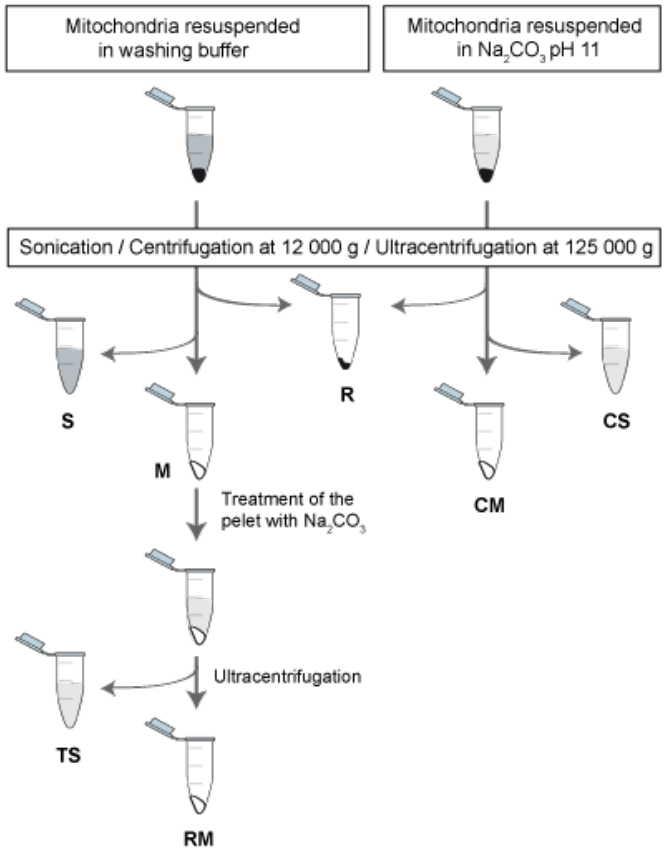

Figure 33: Mitochondrial fractionation protocols. Purified mitochondria were fractionated following different protocols, depending on the study requirement. S, soluble fraction. M, membranes fraction. R, residual fraction. TS, treatment solubilized fraction. RM, residual membranes fraction. CS, carbonate soluble fraction. CM, carbonate membranes fraction.

3.6. Cell fractionation

3.6.1. For the analysis of the soluble/insoluble state of mt-AspRS

WT and mutants constructs were generated by directed mutagenesis from pBCJ749.77 plasmid, derived from described pBCJ739.14 (Jester *et al.* 2011) with the sequence coding for the Flag® tag DYKDDDDK added downstream of the coding sequence of the full-length mt-AspRS including the mitochondrial sequence (MTS). Constructs were introduced in BHK21 using a protocol adapted from the transfection-infection approach (Jester *et al.* 2011), under conditions where protein expression is moderate. Cells were washed with PBS and infected with modified vaccinia virus expressing IPTG-inducible T7 polymerase, and subsequently transfected. For transfection, plasmid/PEI complexes were prepared extemporaneously, in a mass ratio

of 1:4.5 and incubated for 15 min at 20 °C. Protein expression was induced by 1 mM IPTG. 36 h post-transfection, ~5.10^6 cells were harvested, washed with PBS.

As described in Figure 34, whole cells and mitochondria (section 3.5.1.1.; crude mitochondria) were sonicated 6 times (6 A during ~ 10 s) on ice in 160 µl of 10 mM Tris-HCl pH 7.5 containing a protease inhibitor cocktail. The lysates were then ultracentrifuged 30 min at 125 000 g (4 °C) and the soluble fractions (supernatants) were separated from the insoluble fractions (pellets). An aliquot of each soluble fraction (16 µl) was withdrawn and added to 4 µl of Laemmli denaturing buffer, heated to 95 °C for 10 min and loaded on a 10% (m/v) polyacrylamide gel. Pellets were solubilized in 160 µl of 10 mM Tris-HCl pH 7.5 to which 40 µl Laemmli buffer was added before heating and 20 µl of this mixture was analyzed on a gel (section 3.9.).

Mt-AspRS in each sample distributed in either soluble or insoluble fraction, the total corresponding to 100%. The blots of these fractions were revealed simultaneously in the same bath to allow for strict comparison of protein amounts and determination of relative distribution in both fractions. In that way, the result was independent of expression. The loading controls, SOD2 or prohibitin respectively for soluble or insoluble fractions, were used to adjust the amount of mt-AspRS in every lane of a given blot. Resulting mt-AspRS intensities were converted to percentages of protein amount (WT or mutants) in soluble and insoluble fractions.

Mean values and standard deviations were derived from three independent experiments. Histograms were normalized with regard to WT mt-AspRS to compare the relative abundance of the mutated proteins in whole cell extracts and enriched mitochondria.

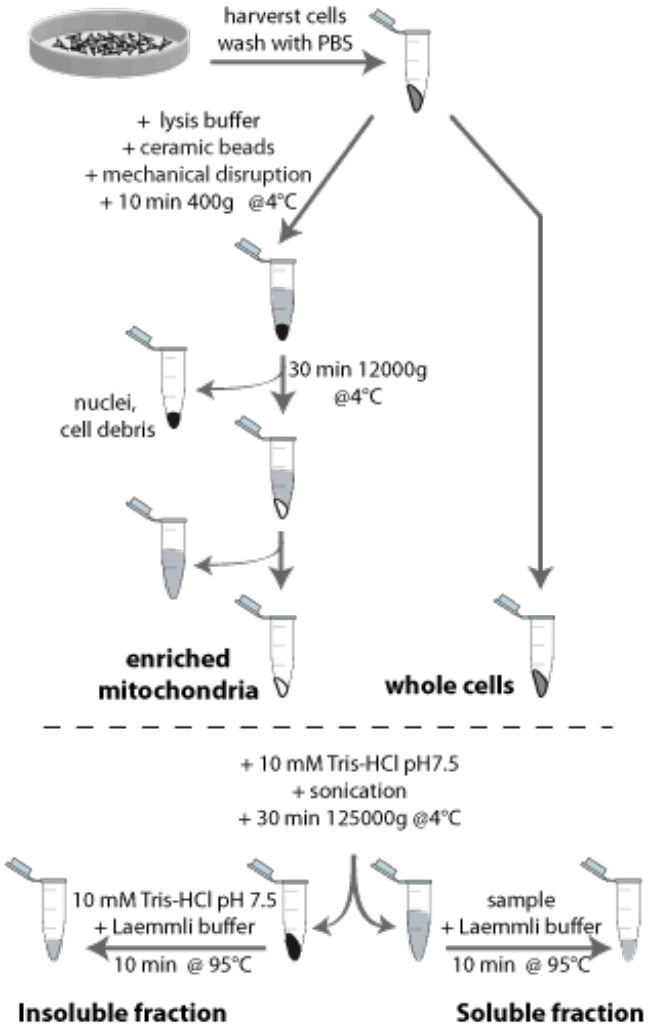

Figure 34: Workflow of the analysis of WT and mutated mt-AspRSs solubility (taken from Annex 2, Sauter *et al.* 2015).

3.6.2. For the determination of the cellular relocation of mt-AspRS after chemical treatment

HEK293T cells were treated or not with 0.4 mM of Potassium Cyanide (KCN) for 1h at 37 °C, prior to cell fractionation by differential centrifugation. Cells were harvested, washed with PBS and then mechanically disrupted with 2 mm diameter ceramic beads in a FastPrep-24^{TM} 5G machine (MP biomedicals) in an isotonic buffer (220 mM Mannitol, 70 mM Sucrose, 1 mM $MgCl_2$, 1 mM EDTA, 10 mM HEPES/KOH pH 7.4) containing a protease inhibitor cocktail. Cell lysates were

centrifuged for 3 min at 10 g (4°C) to discard debris and unbroken cells. Nuclei were recovered after 15 min of centrifugation at 400 g (4°C). Supernatants were centrifuged 15 min at 16 000 g (4°C) to collect, in theory, different organelles: mitochondria, Golgi, lysosomes and peroxisomes. The remaining supernatants were further ultracentrifuged at 125 000 g for 1h (4 °C) to separate cytosol from the microsomal fraction (plasma membrane and endoplasmic reticulum). Cytosolic fractions were concentrated to 150 µl, and all other fractions were resuspended in 150 µl of 10 mM K_2HPO_4/KH_2PO_4 pH 7.5, 300 mM Mannitol, 1 mM EDTA, containing a protease inhibitor cocktail, prior to a brief sonication (10s at 2A) on ice. After that, 30 µl of Laemmli buffer was added before heating and 20 µl of this mixture was analyzed on a gel (section 3.9.).

3.7. Treatment of isolated mitochondria

3.7.1. Chemical treatments

Enriched mitochondria (3.5.1.1.) (~ 30 mg per experiment) were incubated with different chemicals at different concentrations in 1 ml of 10 mM K_2HPO_4/KH_2PO_4 pH 7.5, 300 mM Mannitol, 1 mM EDTA and containing a protease inhibitor cocktail for 10 min at 20 °C. After treatment, mitochondria were centrifuged 10 min at 16 000 g (4 °C), then the supernatant (extra-mitochondrial medium or EM) was separated from mitochondrial pellet. This latter was kept intact or fractionated. Tested molecules: Succinate (1, 5, 10 and 50 mM), Glutamate (10 mM), Pyruvate (10 mM), Aspartate (5 and 10 mM), Leucine (5 mM), EDTA (20 mM), Tris-HCl (10 mM pH 7.4), MOPS-KOH (20 mM pH 7.4), Sodium acetate (30 mM pH 6), DTT (1, 2, 5, 10 and 20 mM), β-Me (20 mM), GSH (0.5, 1 and 5 mM), NADH (0.5, 1 and 5 mM), NADPH (0.5 mM), DPS (1 mM), Rotenone (10 and 20 µM), Malonate (5 and 10 mM), Antimycin (1 and 2 µM), Oligomycin (12.5 and 25 µM), KCN (0.4, 0.8, 10, 20, 40 and 100 mM), CCCP (10 and 100 µM), Chloramphenicol (100 µM), ATP (0.1, 1, 2, 4, 6, 8, 10, 20 and 50 mM), GTP (10 mM), ADP (10 mM), Ca^{2+} (0.1, 0.5 and 1 mM). When mitochondria were treated with Ca^{2+}, buffer was prepared without EDTA. Mitochondria were also treated for 10 min with a hypotonic buffer containing 120 mM KCl, 10 mM Tris-HCl pH 7.6 and 5 mM $KH2PO_4$ (with or without Ca^{2+}).

ATP treatment was further combined with the inhibition of the mt permeability transition pore (mPTP) by Cyclosporin A (Takeyama *et al.* 1993). To do so, mitochondria were incubated with Cyclosprin A (2, 10 or 20 µM) for 2, 5 or 10 min prior to the treatment with ATP (10 mM) for 10 min, in 1 ml of 10 mM K_2HPO_4/KH_2PO_4 pH 7.5, 300 mM Mannitol, 1 mM EDTA and containing a protease inhibitor cocktail. As control experiments, mitochondria were either untreated, or treated with DMSO (used to dissolve Cyclosporine A in a 1M stock solution), with Cyclosporin A (10 µM) alone, with ATP (10 mM) alone, respectively. Extra-mitochondrial media (EM) were ultracentrifuged 30 min at 125 000 g (4 °C), then concentrated in order to be analyzed by western blot (3.9), dynamic light scattering (3.7.2.), mass spectrometry (3.8.3.) or electron microscopy (3.7.3).

For mitochondrial membranes, treatments were adapted from Rajala *et al.* 2014. Enriched mitochondria (~ 30 mg per experiment) were resuspended in 100 mM Na_2CO_3 pH 11; 1M NH_2OH pH 7 or 11; 50 mM Tris-HCl pH 7.5 containing either 400 mM DTT, or 100 mM NaOH and incubated on ice for 30 min followed by 6 x 10s of sonication. For hydroxylamine (NH_2OH), treatments were also performed for 2h and 16h. For nuclease treatment, mitochondria were resuspended and sonicated (6 x 10s) in 50 mM Tris-HCl pH 7.5, 50 mM NaCl, 3mM $CaCl_2$, 2 mM $MgCl_2$. DNase I (10U) or RNase A (20 mg) were added to sonicated mitochondria and incubated at 37°C for 30 min under gentle agitation. After treatment, all samples were ultracentrifuged 30 min at 125 000 g (4°C) to separate soluble fraction (matrix and intermembranes space) from membranes fraction (outer and inner membranes).

3.7.2. Dynamic light scattering (DLS)

Extra-mitochondrial media (EM) of ATP-treated and untreated mitochondria were transferred into 2 µl or 20 µl quartz cells for parallel analyses at 20 °C with two light scattering instruments: Wyatt Technology NanostarTM and Malvern ZetasizerTM NanoS. Hydrodynamic diameters were corrected for solvent refractive index 1.338 and absolute viscosity 1.178 cP (mPa.s). Analyses were performed with Dr Bernard Lorber.

3.7.3. Transmission electron microscopy (TEM)

Extra-mitochondrial media (EM) of ATP-treated and untreated mitochondria were analyzed by negative staining with a 2% (m/v) (47 mM) aqueous uranyl acetate solution (solubility ~7.6% m/v or 179 mM in water at 20 °C, pH ~4.5). Nickel grids coated with a polyvinyl formal (Formvar®) film were covered with 2–20 µl of the EM samples. The excess was blotted after 2 min and 5 µl of uranyl acetate solution was added for staining. After 10 s the excess stain was blotted by contact with a piece of filter paper and the grid was air-dried for 5 min at 20 °C. Negatively stained air-dried samples were examined with transmission electron microscope: a Hitachi H-600 operated at 75 kV equipped with a Hamamatsu CCD Advantage HR camera. Analysis performed by Dr Mathieu Erhardt from "Plateforme RIO d'imagerie cellulaire Strasbourg-Esplanade".

3.8. Searching for mt-AspRS partners

3.8.1. Blue Native-PolyAcrylamide Gel Electrophoresis (BN-PAGE)

Mitochondria were purified from HEK293T cells (see 3.5.1.2. section; purified mitochondria). Mitochondria corresponding to 200 µg of protein content, as estimated using a standard Bradford assay (Bradford 1976), were centrifuged 10 min at 16 000 g (4 °C) to pellet mitochondria.

For the BN-PAGE, a kit from Invitrogen™ (NuPAGE™ Novex™) containing all buffers and precast gels (4-16%) was used. The principle of BN-PAGE is illustrated in Figure 35.

First dimension: 200 µg of mitochondrial proteins were mixed with 6 µl of NativePAGE Sample Buffer (4X), 8 µl of H_2O and 8 µl of Digitonin 10% (w/v) to have a final concentration of 50 mM BisTris pH 7.2, 6 N HCl, 50 mM NaCl, 10% w/v Glycerol, 0.001% Ponceau S and 4% Digitonin. Mitochondrial proteins were solubilized for 30 min at 20 °C, with gentle up-and-down every 5 min. The mixture was then ultracentrifuged 15 min at 125 000 g (4 °C). The supernatant was recovered and the pellet discarded. 2 µl of 5% G-250 Sample Additive were added to the supernatant and the mixture was loaded on a precast 4-16% native gel, and the

electrophoresis was performed at 4 °C according to the manufacturer's instructions: 30 min at 150 V with Dark Blue Anode Buffer, then 30 min at 150 V with Light Blue Anode Buffer. The voltage was then raised up to 250 V to allow migration reaching the button of the gel. Alternatively, this last step can be performed overnight at 40 V.

Second dimension: the lane, from high to low MW, was cut out and briefly denatured in 100 mM Tris-HCl pH 6.8 containing 4% SDS, 5% β-Me and 10% glycerol, using a microwave (~ 20 sec at 700 W, till the boiling). The lane was washed and placed on the top of the stacking gel of a 10% SDS-PAGE. After migration, the gel was electroblotted as described in western blot section (3.9.). To remove the G-250 blue dye, the PVDF membrane was briefly washed with distaining buffer (25% Acetic acid and 25% Ethanol).

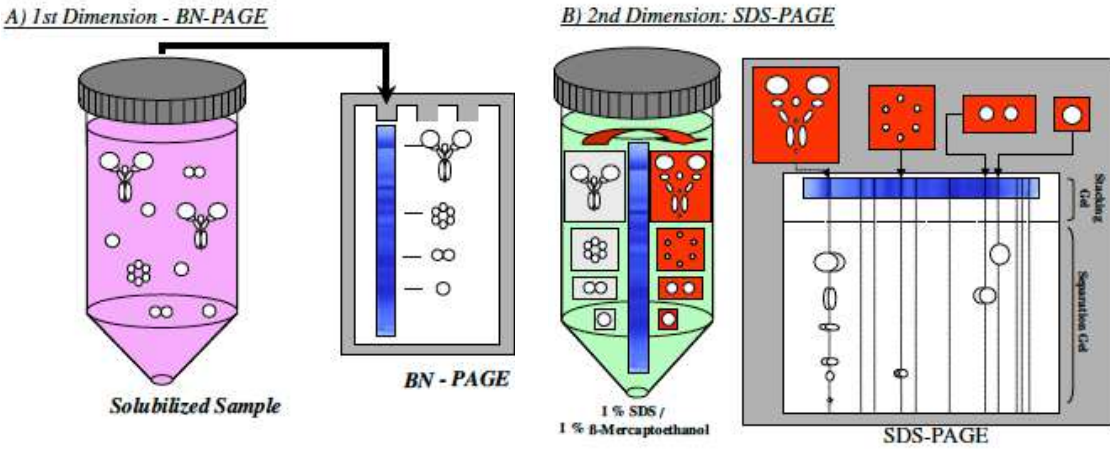

Figure 35: Principle of BN-PAGE/SDS-PAGE (adapted from Eubel *et al.* 2005). In the first dimension, protein complexes are separated in their native forms by BN-PAGE, after solubilization with gentle detergent (e.g. digitonin). The lane is cut out, denatured, and then subjected to a denaturing electrophoresis (standard SDS-PAGE). In the second dimension, denatured complexes are separated into individual proteins.

3.8.2. *In vitro* Crosslinking

3.8.2.1. Cross-linking with glutaraldehyde

Mitochondria, purified from HEK293T cells (see 3.5.1.2.), were resuspended in 10 mM Tris-HCl pH 7.5 containing a protease inhibitor cocktail, and sonicated 6 times (6 A during 10 s) on ice. Mitochondrial lysate was then centrifuged 10 min at 16 000 g (4 °C). The pellet was discarded, and the protein content of the supernatant

was measured with a standard Bradford assay (Bradford 1976). Mitochondrial proteins (100 µg per condition) were incubated with glutaraldehyde (Figure 36A) at a final concentration of 0.02% (stock solution at 25% (w/v), Sigma) for 2, 5, 10, 15 and 20 min in 1 ml of 10 mM Tris-HCl pH 7.5 under rotation at 20 °C. After incubation, the reaction of cross-linking was stopped by quenching with 100 µl of 1.5 M of Tris-HCl pH 8.8 (10 min at 20 °C, under rotation). Samples were concentrated up to a volume of 80 µl using Amicon®Ultra-0.5 centrifugal filters (10K, Millipore), and supplemented with 20 µl of Laemmli dissociating buffer, for SDS-PAGE and western blot analysis (section 3.9.).

3.8.2.2. Cross-linking with Sulfo-SBED

Cross-linking with Sulfo-SBED (Figure 36B) was performed using a Kit from Pierce (Sulfo-SBED Biotin Label Transfer Kit). The principle of this cross-linker is represented in Figure 36C. Purified recombinant mt-AspRS (1 mg in 50 mM K_2HPO_4/KH_2PO_4 pH 7.5 containing 150 mM KCl and 5% glycerol) was labeled with 3.5 fold excess of Sulfo-SBED (44 µg in DMSO) using the formula given by the supplier: Sulfo-SBED MW (880) x µg of mt-AspRS x 3.5 (fold excess) / mt-AspRS MW (70 000) = µg of Sulfo-SBED needed. Mt-AspRS/Sulfo-SBED mixture was incubated 2h at 4 °C (in the dark). Labeled mt-AspRS was then dialyzed overnight at 4 °C in its initial buffer (50 mM K_2HPO_4/KH_2PO_4 pH 7.5 containing 150 mM KCl and 5% glycerol). Different concentrations ranging from 150 ng to 100 µg of labeled mt-AspRS were incubated with 2 mg of mitochondrial proteins (prepared as described in 3.8.2.1. section) in a total volume of 120 µl, during 1h at 20 °C and under rotation. Cross-linking was performed on ice during 10 min using UV Cross-linker (Fisher Scientific 5 x 8 Watt) at a distance of 5 cm from lamps. Laemmli dissociating buffer (4 µl) was added to an aliquot of cross-linked samples (16 µl) for SDS-PAGE and western blot analysis (section 3.9.). Proteins cross-linked with mt-AspRS were purified by affinity purification (section 3.8.2.3.) and analyzed by mass spectrometry (3.8.3.).

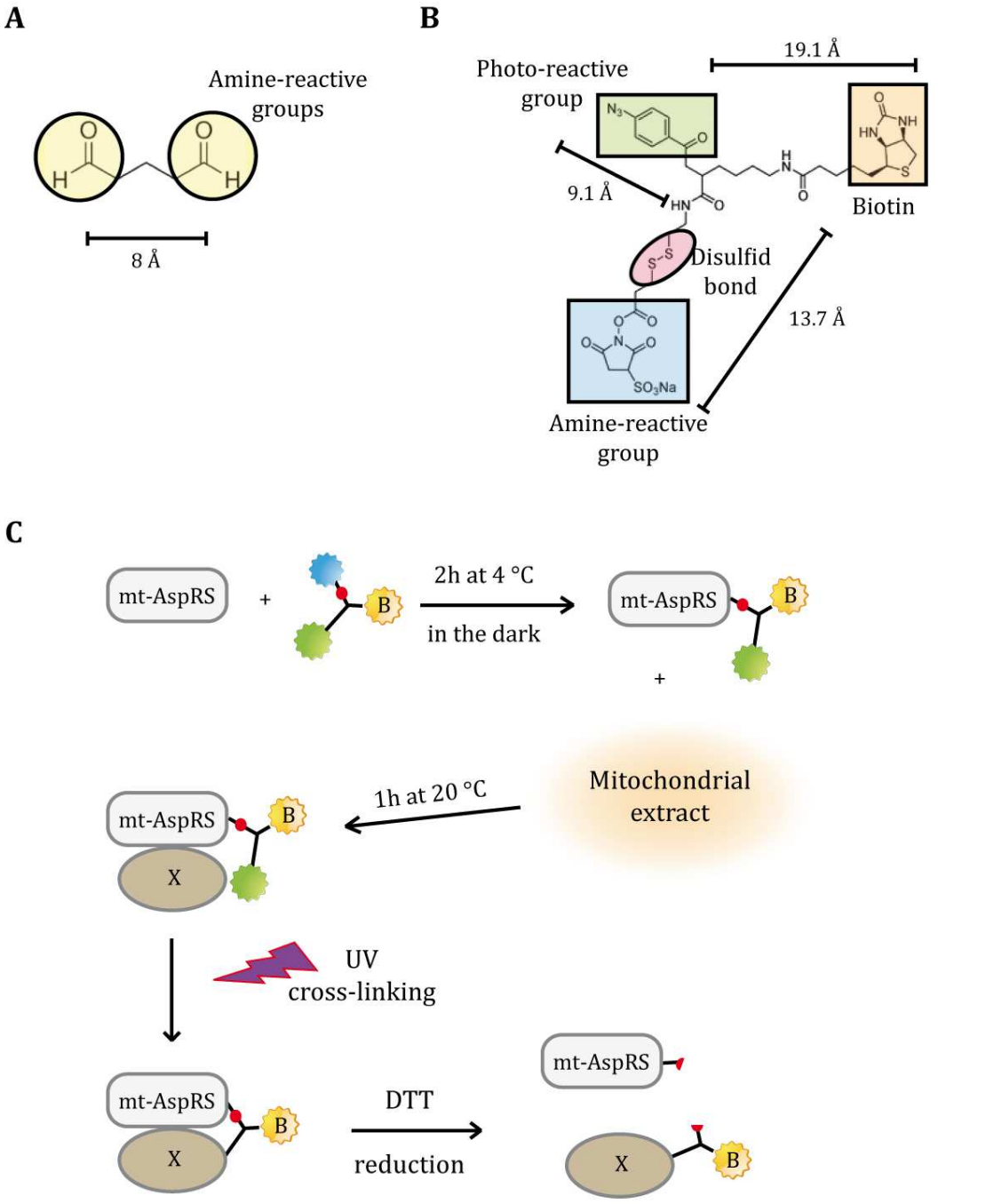

Figure 36: Cross-linking experiments. A) Glutaraldehyde molecule with its amine-reactive groups. B) Sulfo-SBED molecule composed of an amine-reactive group, a photo-reactive group, a disulfide bond, and a biotin moiety. C) Theoretical strategy of fishing with Sulfo-SBED cross-linker. The same color code is used for both B) and C).

3.8.2.3. Affinity purification

3.8.2.3.1. Proteins cross-linked with recombinant and Sulfo-SBED-labeled mt-AspRS

Mitochondrial extract cross-linked in the presence of recombinant mt-AspRS, which was labeled with Sulfo-SBED, was purified either on Nickel-agarose Ni-NTA (His SpinTrap™, GE Healthcare) or Streptavidin-magnetic beads (Dynabeads® MyOne™ streptavidin C1; Invitrogen™). A combination of both types of purification was also used.

Ni-NTA purification: beads were washed 3 times with 500 µl of 50 mM K_2HPO_4/KH_2PO_4 pH 7.5 containing 150 mM KCl and 20 mM Imidazole. To 120 µl of cross-linked sample, 330 µl of the buffer were added and incubated with Ni-NTA beads during 15 min at 4 °C (under rotation). The flow through fraction was recovered, and beads were washed 5 times with the same buffer. The elution was done with 2 x 250 µl of 50 mM K_2HPO_4/KH_2PO_4 pH 7.5 containing 150 mM KCl and 500 mM Imidazole. When this purification was combined with streptavidin purification, 1 mg of DTT was added to the eluate and heated at 95 °C for 5 min.

Streptavidin purification: To one volume of sample, 2 volumes of 50 mM K_2HPO_4/KH_2PO_4 pH 7.5 were added. DTT was then added (to reach 10 mM) and the sample was denatured by heating 5 min at 95 °C. Streptavidin-conjugated beads were washed 3 times with 500 µl of 50 mM K_2HPO_4/KH_2PO_4, and incubated with denatured sample during 30 min at 20 °C. After incubation, the flow through fraction was collected, and beads were washed twice with 50 mM K_2HPO_4/KH_2PO_4, twice with 50 mM K_2HPO_4/KH_2PO_4/500 mM NaCl, and twice with 50 mM K_2HPO_4/KH_2PO_4. Sample was eluted by heating 5 min at 95 °C with 15 µl of Laemmli dissociating buffer.

3.8.2.3.2. Proteins cross-linked with endogenous mt-AspRS using glutaraldehyde

Anti-mt-AspRS antibody was coupled with unconjugated magnetic beads (PureCube NHS-Activated MagBeads, Cube Biotech) following supplier's instructions. 100 µl of beads (delivered as a 25% suspension) were pelleted using a magnet and the storing buffer was discarded. Beads were then conjugated with 200 µg of anti-mt-AspRS antibody in 625 µl of PBS for 2h at 4 °C under rotation. After that, anti-mt-AspRS conjugated beads were washed twice with PBS and 4 times with H_2O, and then incubate with 1.2 ml of Tris-HCl 1M (pH 7.5) to quench free NHS (N-

hydroxy-succinimide) group. Beads were washed again 4 times with PBS and twice with H_2O, and then incubated with cross-linked mitochondrial extract for 1h at 4 °C and under rotation. After incubation, the flow through fraction was recovered and beads were washed 3 times with 50 mM K_2HPO_4/KH_2PO_4 pH 7.5 containing 150 mM KCl, then 2 times with 50 mM K_2HPO_4/KH_2PO_4 pH 7.5 containing 500 mM KCl. After a last wash with PBS, sample was eluted by heating 5 min at 95 °C with 15 µl of Laemmli dissociating buffer.

3.8.2.3.3. Proteins cross-linked with expressed mt-AspRS using glutaraldehyde

BHK21 cells were transfected with plasmid expressing the WT mt-AspRS construct (see section 3.3.2.), after what mitochondria were purified (see section 3.5.1.2.), and the protein content measured. Mitochondrial extract was cross-linked using glutaraldehyde (see section 3.8.2.1.). Cross-linked mitochondrial extract was then incubated with anti-flag conjugated magnetic beads (Anti-Flag® M2 magnetic beads, Sigma-Aldrich®) for 1h at 4 °C and under rotation. After incubation, the flow through fraction was recovered and beads were washed 3 times with 50 mM K_2HPO_4/KH_2PO_4 pH 7.5 containing 150 mM KCl, then 2 times with 50 mM K_2HPO_4/KH_2PO_4 pH 7.5 containing 500 mM KCl. After a last wash with PBS, sample was eluted by heating 5 min at 95 °C with 15 µl of Laemmli dissociating buffer.

3.8.3. Mass spectrometry analysis

The in-gel digestion procedure was carried out as described in (Rabilloud *et al.* 2001). Briefly, proteins within gel bands were reduced (10 mM DTT), alkylated (25 mM Iodoacetamide) and digested with trypsin (sequencing-grade, Promega, V5111) at a final concentration of 10ng/µl. Tryptic peptides were extracted prior to mass spectrometry analysis. In-solution digestion was performed as described in (Chicher *et al.* 2015). Each sample was precipitated with 0.1 M ammonium acetate in 100% methanol, and proteins were reduced (5 mM DTT), alkylated (Iodoacetamide 10 mM) and digested with sequencing-grade trypsin.

After digestion, peptides mixtures were analyzed using a NanoLC-2DPlus system (with nanoFlex ChiP module; Eksigent, ABSciex, Concord, Ontario, Canada)

coupled to a TripleTOF 5600 mass spectrometer (ABSciex) operating in positive mode. Data were searched against the UniProt database using a fasta file consisting of a forward database (proteins from N- to C-terminal part) and a decoy database (reversed sequences from C- to N-terminal part, obtained by a Perl script, makeDecoyDB.pl from Bruker). We used Mascot as the database search algorithm (version 2.2, Matrix Science, London, UK) through the ProteinScape 3.1 package (Bruker). Peptide modifications allowed during the search were: N-acetyl (protein), carbamidomethylation (C) and oxidation (M). Mass tolerances in MS and MS/MS were set to 30 ppm and 0.5 Da, respectively. Peptide identifications obtained from Mascot were validated with p-value<0.05 and proteins were validated respecting FDR<1% (False-Discovery Rate). Mass spectrometry analyses were performed by Philippe Hammann, Lauriane Kuhn and Johanna Chicher from the "Plateforme Protéomique Strasbourg-Esplanade".

3.9. Sample preparation and analysis by western blotting

Soluble fractions were concentrated up to a volume of 80 µl using Amicon®Ultra-0.5 centrifugal filters (10K, Millipore). Residual fractions and membranes fractions were solubilized in 80 µl of 10 mM K_2HPO_4/KH_2PO_4 pH 7.5 (containing 300 mM Mannitol, 1 mM EDTA). All fractions were supplemented with 20 µl of Laemmli dissociating buffer, heated at 95°C for 10 min. Twenty µl of each fraction were loaded on a 10% SDS-PAGE. Proteins were blotted on a PVDF membrane and detected with specific antibodies. Chemiluminescent detection was carried out using the Pierce Detection Kit low and high sensitivity (ECL Western blotting Substrate, and SuperSignal West Femto Maximum Sensitivity Substrate, respectively) according to manufacturer's instructions. One volume of superoxide buffer was mixed with one volume of Luminol Enhancer solution and put over PVDF membrane. After 1 to 2 min, PVDF membrane was dried and exposed to radiographic film (Fuji Medical X-ray Film, Fujifilm). Autoradiographies were scanned using Epson Perfection 3490 Photo and the relative amount of proteins was estimated from band intensities using ImageJ software (Schneider *et al.* 2012).

REFERENCES

REFERENCES

A

Abhishek, A., A. Bavishi, A. Bavishi and M. Choudhary (2011). "Bacterial genome chimaerism and the origin of mitochondria." Canadian Journal of Microbiology 57(1): 49-61.

Adamek, N. and M. A. Geeves (2014). "Use of pyrene-labelled actin to probe actin-myosin interactions: kinetic and equilibrium studies." EXS 105: 87-104.

Addya, S., H. K. Anandatheerthavarada, G. Biswas, S. V. Bhagwat, J. Mullick and N. G. Avadhani (1997). "Targeting of NH2-terminal-processed microsomal protein to mitochondria: A novel pathway for the biogenesis of hepatic mitochondrial P450MT2." Journal of Cell Biology 139(3): 589-599.

Adrion, J. R., P. S. White and K. L. Montooth (2016). "The Roles of Compensatory Evolution and Constraint in Aminoacyl tRNA Synthetase Evolution." Mol Biol Evol 33(1): 152-161.

Agaronyan, K., Y. I. Morozov, M. Anikin and D. Temiakov (2015). "Mitochondrial biology. Replication-transcription switch in human mitochondria." Science 347(6221): 548-551.

Aguer, C., D. Gambarotta, R. J. Mailloux, C. Moffat, R. Dent, R. McPherson and M. E. Harper (2011). "Galactose enhances oxidative metabolism and reveals mitochondrial dysfunction in human primary muscle cells." PLoS One 6(12): e28536.

Antonicka, H. and E. A. Shoubridge (2015). "Mitochondrial RNA Granules Are Centers for Posttranscriptional RNA Processing and Ribosome Biogenesis." Cell Rep.

Antonicka, H., F. Sasarman, T. Nishimura, V. Paupe and E. A. Shoubridge (2013). "The Mitochondrial RNA-Binding Protein GRSF1 Localizes to RNA Granules and Is Required for Posttranscriptional Mitochondrial Gene Expression." Cell Metabolism 17(3): 386-398.

Antonsson, B., S. Montessuit, S. Lauper, R. Eskes and J. C. Martinou (2000). "Bax oligomerization is required for channel-forming activity in liposomes and to trigger cytochrome c release from mitochondria." Biochemical Journal 345: 271-278.

Aradjanski, M., S. Lotter and A. Trifunovic (2016). "Loss of mitochondrial aspartyl-tRNA synthetase (DARS2) in neurons, but not myelin-producing cells leads to progressive neurodegeneration." EMBO workshop on “Molecular Biology of Mitochondrial Gene expression" Bro, Sweden, 23-26 May, 2016 Poster presentation.

Archibald, J. M. (2015). "Endosymbiosis and Eukaryotic Cell Evolution." Current Biology 25(19): R911-R921.

Arnold, I., H. Folsch, W. Neupert and R. A. Stuart (1998). "Two distinct and independent mitochondrial targeting signals function in the sorting of an inner membrane protein, cytochrome c(1)." Journal of Biological Chemistry 273(3): 1469-1476.

Arnold, S. and B. Kadenbach (1997). "Cell respiration is controlled by ATP, an allosteric inhibitor of cytochrome-c oxidase." Eur J Biochem 249(1): 350-354.

Arnoult, D., F. Soares, I. Tattoli, C. Castanier, D. J. Philpott and S. E. Girardin (2009). "An N-terminal addressing sequence targets NLRX1 to the mitochondrial matrix." J Cell Sci 122(Pt 17): 3161-3168.

B

Balla, S., V. Thapar, S. Verma, T. Luong, T. Faghri, C. H. Huang, S. Rajasekaran, J. J. del Campo, J. H. Shinn, W. A. Mohler, M. W. Maciejewski, M. R. Gryk, B. Piccirillo, S. R. Schiller and M. R. Schiller (2006). "Minimotif Miner: a tool for investigating protein function." Nat Methods 3(3): 175-177.

Banerjee, R., Reynolds, N. M., Yadavalli, S. S., Rice, C., Roy, H., Banerjee, P., Alexander, R. W. and Ibba, M. (2011) “Mitochondrial aminoacyl-tRNA synthetase single-nucleotide polymorphisms that lead to defects in refolding but not aminoacylation.” J Mol Biol 410(2):280-93.

Bec, G., P. Kerjan, X. D. Zha and J. P. Waller (1989). "Valyl-tRNA synthetase from rabbit liver. I. Purification as a heterotypic complex in association with elongation factor 1." J Biol Chem 264(35): 21131-21137.

Berridge, M., M. McConnell, C. Grasso, M. Bajzikova, J. Kovarova and J. Neuzil (2016). "Horizontal transfer of mitochondria between mammalian cells: beyond co-culture approaches." Current Opinion in Genetics & Development 38: 75-82.

Bhaskaran, H., Taniguchi, T., Suzuki, T., Suzuki, T. and Perona, J. J. (2014). "Structural dynamics of a mitochondrial tRNA possessing weak thermodynamic stability." Biochemistry 53(9):1456-65.

Bogenhagen, D. F., D. W. Martin and A. Koller (2014). "Initial Steps in RNA Processing and Ribosome Assembly Occur at Mitochondrial DNA Nucleoids." Cell Metabolism 19(4): 618-629.

Bogenhagen, D. F., Y. S. Wang, E. L. Shen and R. Kobayashi (2003). "Protein components of mitochondrial DNA nucleoids in higher eukaryotes." Molecular & Cellular Proteomics 2(11): 1205-1216.

Bonn, F., T. Tatsuta, C. Petrungaro, J. Riemer and T. Langer (2011). "Presequence-dependent folding ensures MrpL32 processing by the m-AAA protease in mitochondria." EMBO J 30(13): 2545-2556.

Bonnefond, L., A. Fender, J. Rudinger-Thirion, R. Giege, C. Florentz and M. Sissler (2005). "Toward the full set of human mitochondrial aminoacyl-tRNA synthetases: characterization of AspRS and TyrRS." Biochemistry 44(12): 4805-4816.

Bonnefond, L., M. Frugier, E. Touze, B. Lorber, C. Florentz, R. Giege, C. Sauter and J. Rudinger-Thirion (2007). "Crystal structure of human mitochondrial tyrosyl-tRNA synthetase reveals common and idiosyncratic features." Structure 15(11): 1505-1516.

Bonnefond, L., M. Frugier, R. Giege and J. Rudinger-Thirion (2005). "Human mitochondrial TyrRS disobeys the tyrosine identity rules." Rna-a Publication of the Rna Society 11(5): 558-562.

Bonnefoy, N., N. Bsat and T. D. Fox (2001). "Mitochondrial translation of Saccharomyces cerevisiae COX2 mRNA is controlled by the nucleotide sequence specifying the pre-Cox2p leader peptide." Molecular and Cellular Biology 21(7): 2359-2372.

Bradford, M. M. (1976). "A rapid and sensitive method for the quantitation of microgram quantities of protein utilizing the principle of protein-dye binding." Anal Biochem 72: 248-254.

Bradshaw, R. A., W. W. Brickey and K. W. Walker (1998). "N-terminal processing: the methionine aminopeptidase and N-alpha-acetyl transferase families." Trends in Biochemical Sciences 23(7): 263-267.

Bragoszewski, P., M. Wasilewski, P. Sakowska, A. Gornicka, L. Bottinger, J. Qiu, N. Wiedemann and A. Chacinska (2015). "Retro-translocation of mitochondrial intermembrane space proteins." Proc Natl Acad Sci U S A 112(25): 7713-7718.

Branda, S. S. and G. Isaya (1995). "Prediction and identification of new natural substrates of the yeast mitochondrial intermediate peptidase." J Biol Chem 270(45): 27366-27373.

Bullwinkle, T. J. and M. Ibba (2016). "Translation quality control is critical for bacterial responses to amino acid stress." Proceedings of the National Academy of Sciences of the United States of America 113(8): 2252-2257.

Burri, L., Y. Strahm, C. J. Hawkins, I. E. Gentle, M. A. Puryer, A. Verhagen, B. Callus, D. Vaux and T. Lithgow (2005). "Mature DIABLO/Smac is produced by the IMP protease complex on the mitochondrial inner membrane." Molecular Biology of the Cell 16(6): 2926-2933.

Butow, R. A. and N. G. Avadhani (2004). "Mitochondrial signaling: The retrograde response." Molecular Cell 14(1): 1-15.

C

Calvo, S. E. and V. K. Mootha (2010). "The Mitochondrial Proteome and Human Disease." Annual Review of Genomics and Human Genetics, Vol 11 11: 25-44.

Cannino, G., C. M. Di Liegro, I. Di Liegro and A. M. Rinaldi (2004). "Analysis of cytochrome C oxidase subunits III and IV expression in developing rat brain." Neuroscience 128(1): 91-98.

Carpenter, K. L., I. Jalloh and P. J. Hutchinson (2015). "Glycolysis and the significance of lactate in traumatic brain injury." Front Neurosci 9: 112.

Chicher, J., A. Simonetti, L. Kuhn, L. Schaeffer, P. Hammann, G. Eriani and F. Martin (2015). "Purification of mRNA-programmed translation initiation complexes suitable for mass spectrometry analysis." Proteomics 15(14): 2417-2425.

Chimnaronk, S., M. Gravers Jeppesen, T. Suzuki, J. Nyborg and K. Watanabe (2005). "Dual-mode recognition of noncanonical tRNAs(Ser) by seryl-tRNA synthetase in mammalian mitochondria." EMBO J 24(19): 3369-3379.

Claros, M. G. and P. Vincens (1996). "Computational method to predict mitochondrially imported proteins and their targeting sequences." European Journal of Biochemistry 241(3): 779-786.

Cosentino, K. and A. J. Garcia-Saez (2014). "Mitochondrial alterations in apoptosis." Chem Phys Lipids 181: 62-75.

Couvillion, M. T., I. C. Soto, G. Shipkovenska and L. S. Churchman (2016). "Synchronized mitochondrial and cytosolic translation programs." Nature 533(7604): 499-+.

D

Dallabona, C., D. Diodato, S. H. Kevelam, T. B. Haack, L. J. Wong, G. S. Salomons, E. Baruffini, L. Melchionda, C. Mariotti, T. M. Strom, T. Meitinger, H. Prokisch, K. Chapman, A. Colley, H. Rocha, K. Ounap, R. Schiffmann, E. Salsano, M. Savoiardo, E. M. Hamilton, T. E. Abbink, N. I. Wolf, I. Ferrero, C. Lamperti, M. Zeviani, A. Vanderver, D. Ghezzi and M. S. van der Knaap (2014). "Novel (ovario) leukodystrophy related to AARS2 mutations." Neurology 82(23): 2063-2071.

Datler, C., E. Pazarentzos, A. L. Mahul-Mellier, W. Chaisaklert, M. S. Hwang, F. Osborne and S. Grimm (2014). "CKMT1 regulates the mitochondrial permeability transition pore in a process that provides evidence for alternative forms of the complex." Journal of Cell Science 127(8): 1816-1828.

Daum, G., S. M. Gasser and G. Schatz (1982). "Import of Proteins into Mitochondria - Energy-Dependent, 2-Step Processing of the Intermembrane Space Enzyme Cytochrome-B2 by Isolated Yeast Mitochondria." Journal of Biological Chemistry 257(21): 3075-3080.

David, A., N. Netzer, M. B. Strader, S. R. Das, C. Y. Chen, J. Gibbs, P. Pierre, J. R. Bennink and J. W. Yewdell (2011). "RNA binding targets aminoacyl-tRNA synthetases to translating ribosomes." J Biol Chem 286(23): 20688-20700.

Davis, C. H. O., K. Y. Kim, E. A. Bushong, E. A. Mills, D. Boassa, T. Shih, M. Kinebuchi, S. Phan, Y. Zhou, N. A. Bihlmeyer, J. V. Nguyen, Y. J. Jin, M. H. Ellisman and N. Marsh-Armstrong (2014). "Transcellular degradation of axonal mitochondria." Proceedings of the National Academy of Sciences of the United States of America 111(26): 9633-9638.

Deatherage, B. L. and B. T. Cookson (2012). "Membrane vesicle release in bacteria, eukaryotes, and archaea: a conserved yet underappreciated aspect of microbial life." Infect Immun 80(6): 1948-1957.

Delage, L., P. Giege, M. Sakamoto and L. Marechal-Drouard (2007). "Four paralogues of RPL12 are differentially associated to ribosome in plant mitochondria." Biochimie 89(5): 658-668.

Demarquoy, J., A. Fairand, C. Gautier and R. Vaillant (1994). "Demonstration of argininosuccinate synthetase activity associated with mitochondrial membrane: characterization and hormonal regulation." Mol Cell Biochem 136(2): 145-155.

Devaux-Bricout, M., D. Grevent, A. S. Lebre, M. Rio, I. Desguerre, P. De Lonlay, V. Valayannopoulos, F. Brunelle, A. Rotig, A. Munnich and N. Boddaert (2014). "Aspect of brain MRI in mitochondrial respiratory chain deficiency. A diagnostic algorithm of the most common mitochondrial genetic mutations." Revue Neurologique 170(5): 381-389.

Dhar, S. S., K. Johar and M. T. T. Wong-Riley (2013). "Bigenomic transcriptional regulation of all thirteen cytochrome c oxidase subunit genes by specificity protein 1." Open Biology 3.

Diekert, K., G. Kispal, B. Guiard and R. Lill (1999). "An internal targeting signal directing proteins into the mitochondrial intermembrane space." Proceedings of the National Academy of Sciences of the United States of America 96(21): 11752-11757.

DiMauro, S. (2004). "Mitochondrial diseases." Biochim Biophys Acta 1658(1-2): 80-88.
Duchene, A. M., A. Giritch, B. Hoffmann, V. Cognat, D. Lancelin, N. M. Peeters, M. Zaepfel, L. Marechal-Drouard and I. D. Small (2005). "Dual targeting is the rule for organellar aminoacyl-tRNA synthetases in Arabidopsis thaliana." Proceedings of the National Academy of Sciences of the United States of America 102(45): 16484-16489.
Dudek, J., P. Rehling and M. van der Laan (2013). "Mitochondrial protein import: Common principles and physiological networks." Biochimica Et Biophysica Acta-Molecular Cell Research 1833(2): 274-285.

E

Echevarria, L., P. Clemente, R. Hernandez-Sierra, M. E. Gallardo, M. A. Fernandez-Moreno and R. Garesse (2014). "Glutamyl-tRNA(Gln) amidotransferase is essential for mammalian. mitochondrial translation in vivo." Biochemical Journal 460: 91-101.
Edvardson, S., A. Shaag, O. Kolesnikova, J. M. Gomori, I. Tarassov, T. Einbinder, A. Saada and O. Elpeleg (2007). "Deleterious mutation in the mitochondrial arginyl-transfer RNA synthetase gene is associated with pontocerebellar hypoplasia." American Journal of Human Genetics 81(4): 857-862.
Eliseev, R. A., J. Malecki, T. Lester, Y. Zhang, J. Humphrey and T. E. Gunter (2009). "Cyclophilin D interacts with Bcl2 and exerts an anti-apoptotic effect." J Biol Chem 284(15): 9692-9699.
Elo, J. M., Yadavalli, S. S., Euro, L., Isohanni, P., Götz, A., Carroll, C. J., Valanne, L., Alkuraya, F. S., Uusimaa, J., Paetau, A., Caruso, E. M., Pihko, H., Ibba, M., Tyynismaa, H. and Suomalainen, A. (2012)“Mitochondrial phenylalanyltRNA synthetase mutations underlie fatal infantile Alpers enc ephalopathy.” Hum Mol Genet 21(20):4521-9.
Emdal, K. B., A. K. Pedersen, D. B. Bekker-Jensen, K. P. Tsafou, H. Horn, S. Lindner, J. H. Schulte, A. Eggert, L. J. Jensen, C. Francavilla and J. V. Olsen (2015). "Temporal proteomics of NGF-TrkA signaling identifies an inhibitory role for the E3 ligase Cbl-b in neuroblastoma cell differentiation." Sci Signal 8(374): ra40.
Engl, G., S. Florian, L. Tranebjaerg and D. Rapaport (2012). "Alterations in expression levels of deafness dystonia protein 1 affect mitochondrial morphology." Hum Mol Genet 21(2): 287-299.
Ernst, T., M. Hergenhahn, M. Kenzelmann, C. D. Cohen, M. Bonrouhi, A. Weninger, R. Klaren, E. F. Grone, M. Wiesel, C. Gudemann, J. Kuster, W. Schott, G. Staehler, M. Kretzler, M. Hollstein and H. J. Grone (2002). "Decrease and gain of gene expression are equally discriminatory markers for prostate carcinoma: a gene expression analysis on total and microdissected prostate tissue." Am J Pathol 160(6): 2169-2180.
Ersahin, C., A. M. Szpaderska, A. T. Orawski and W. H. Simmons (2005). "Aminopeptidase P isozyme expression in human tissues and peripheral blood mononuclear cell fractions." Arch Biochem Biophys 435(2): 303-310.
Esser, K., B. Tursun, M. Ingenhoven, G. Michaelis and E. Pratje (2002). "A novel two-step mechanism for removal of a mitochondrial signal sequence involves the mAAA complex and the putative rhomboid protease Pcp1." Journal of Molecular Biology 323(5): 835-843.
Eubel, H., H. P. Braun and A. H. Millar (2005). "Blue-native PAGE in plants: a tool in analysis of protein-protein interactions." Plant Methods 1(1): 11.

F

Fadouloglou, V. E., M. Kokkinidis and N. M. Glykos (2008). "Determination of protein oligomerization state: two approaches based on glutaraldehyde crosslinking." Anal Biochem 373(2): 404-406.

Falchi, A. M., V. Sogos, F. Saba, M. Piras, T. Congiu and M. Piludu (2013). "Astrocytes shed large membrane vesicles that contain mitochondria, lipid droplets and ATP." Histochemistry and Cell Biology 139(2): 221-231.

Fan, Y. Q., J. Wu, M. H. Ung, N. De Lay, C. Cheng and J. Q. Ling (2015). "Protein mistranslation protects bacteria against oxidative stress." Nucleic Acids Research 43(3): 1740-1748.

Feagin, J. E. (1992). "The 6-kb element of Plasmodium falciparum encodes mitochondrial cytochrome genes." Mol Biochem Parasitol 52(1):145-8.

Fender, A., A. Gaudry, F. Juhling, M. Sissler and C. Florentz (2012). "Adaptation of aminoacylation identity rules to mammalian mitochondria." Biochimie 94(5): 1090-1097.

Fender, A., C. Sauter, M. Messmer, J. Putz, R. Giege, C. Florentz and M. Sissler (2006). "Loss of a primordial identity element for a mammalian mitochondrial aminoacylation system." J Biol Chem 281(23): 15980-15986.

Finsterer, J. and L. Segall (2010). "Drugs interfering with mitochondrial disorders." Drug and Chemical Toxicology 33(2): 138-151.

Folmes, C. D. L., G. Sawicki, V. J. J. Cadete, G. Masson, A. J. Barr and G. D. Lopaschuk (2010). "Novel O-palmitolylated beta-E1 subunit of pyruvate dehydrogenase is phosphorylated during ischemia/reperfusion injury." Proteome Science 8.

Folsch, H., B. Gaume, M. Brunner, W. Neupert and R. A. Stuart (1998). "C- to N-terminal translocation of preproteins into mitochondria." Embo Journal 17(22): 6508-6515.

Frechin, M., B. Senger, M. Braye, D. Kern, R. P. Martin and H. D. Becker (2009). "Yeast mitochondrial Gln-tRNA(Gln) is generated by a GatFAB-mediated transamidation pathway involving Arc1p-controlled subcellular sorting of cytosolic GluRS." Genes & Development 23(9): 1119-1130.

Freitag, D. G., P. M. Ouimet, T. L. Girvitz and M. Kapoor (1997). "Heat shock protein 80 of Neurospora crassa, a cytosolic molecular chaperone of the eukaryotic stress 90 family, interacts directly with heat shock protein 70." Biochemistry 36(33): 10221-10229.

Fujiki, Y., A. L. Hubbard, S. Fowler and P. B. Lazarow (1982). "Isolation of intracellular membranes by means of sodium carbonate treatment: application to endoplasmic reticulum." J Cell Biol 93(1): 97-102.

Fukasawa, Y., J. Tsuji, S. C. Fu, K. Tomii, P. Horton and K. Imai (2015). "MitoFates: Improved Prediction of Mitochondrial Targeting Sequences and Their Cleavage Sites." Molecular & Cellular Proteomics 14(4): 1113-1126.

G

Gabaldon, T., D. Rainey and M. A. Huynen (2005). "Tracing the evolution of a large protein complex in the eukaryotes, NADH : Ubiquinone oxidoreductase (Complex I)." Journal of Molecular Biology 348(4): 857-870.

Gakh, O., P. Cavadini and G. Isaya (2002). "Mitochondrial processing peptidases." Biochim Biophys Acta 1592(1): 63-77.

Gaudry, A., B. Lorber, A. Neuenfeldt, C. Sauter, C. Florentz and M. Sissler (2012). "Re-designed N-terminus enhances expression, solubility and crystallizability of mitochondrial protein." Protein Eng Des Sel 25(9): 473-481.

Gerhold, J. M., S. Cansiz-Arda, M. Lohmus, O. Engberg, A. Reyes, H. van Rennes, A. Sanz, I. J. Holt, H. M. Cooper and J. N. Spelbrink (2015). "Human Mitochondrial DNA-Protein Complexes Attach to a Cholesterol-Rich Membrane Structure (vol 5, 15292, 2015)." Scientific Reports 5.

Giannone, R. J., H. W. McDonald, G. B. Hurst, R. F. Shen, Y. Wang and Y. Liu (2010). "The protein network surrounding the human telomere repeat binding factors TRF1, TRF2, and POT1." PLoS One 5(8): e12407.

Gilkerson, R., L. Bravo, I. Garcia, N. Gaytan, A. Herrera, A. Maldonado and B. Quintanilla (2013). "The Mitochondrial Nucleoid: Integrating Mitochondrial DNA into Cellular Homeostasis." Cold Spring Harbor Perspectives in Biology 5(5).

Gogvadze, V., S. Orrenius and B. Zhivotovsky (2006). "Multiple pathways of cytochrome c release from mitochondria in apoptosis." Biochimica Et Biophysica Acta-Bioenergetics 1757(5-6): 639-647.
Goldstein, A. C., P. Bhatia and J. M. Vento (2013). "Mitochondrial Disease in Childhood: Nuclear Encoded." Neurotherapeutics 10(2): 212-226.
Gordon, D. M., Q. Shi, A. Dancis and D. Pain (1999). "Maturation of frataxin within mammalian and yeast mitochondria: one-step processing by matrix processing peptidase." Human Molecular Genetics 8(12): 2255-2262.
Gray, M. W. (2015). "Mosaic nature of the mitochondrial proteome: Implications for the origin and evolution of mitochondria." Proceedings of the National Academy of Sciences of the United States of America 112(33): 10133-10138.
Gray, M. W., G. Burger and B. F. Lang (1999). "Mitochondrial evolution." Science 283(5407): 1476-1481.
Greber, B. J., D. Boehringer, A. Leitner, P. Bieri, F. Voigts-Hoffmann, J. P. Erzberger, M. Leibundgut, R. Aebersold and N. Ban (2014). "Architecture of the large subunit of the mammalian mitochondrial ribosome." Nature 505(7484): 515-+.
Guillery, O., F. Malka, T. Landes, E. Guillou, C. Blackstone, A. Lombes, P. Belenguer, D. Arnoult and M. Rojo (2008). "Metalloprotease-mediated OPA1 processing is modulated by the mitochondrial membrane potential." Biology of the Cell 100(5): 315-325.
Guo, M. and P. Schimmel (2013). "Essential nontranslational functions of tRNA synthetases." Nat Chem Biol 9(3): 145-153.
Guo, M., M. Ignatov, K. Musier-Forsyth, P. Schimmel and X. L. Yang (2008). "Crystal structure of tetrameric form of human lysyl-tRNA synthetase: Implications for multisynthetase complex formation." Proceedings of the National Academy of Sciences of the United States of America 105(7): 2331-2336.
Guo, Y., S. M. Srinivasula, A. Druilhe, T. Fernandes-Alnemri and E. S. Alnemri (2002). "Caspase-2 induces apoptosis by releasing proapoptotic proteins from mitochondria." Journal of Biological Chemistry 277(16): 13430-13437.
Gurdon, C., Z. Svab, Y. P. Feng, D. Kumar and P. Maliga (2016). "Cell-to-cell movement of mitochondria in plants." Proceedings of the National Academy of Sciences of the United States of America 113(12): 3395-3400.
Gutell, R. R., J. C. Lee and J. J. Cannone (2002). "The accuracy of ribosomal RNA comparative structure models." Current Opinion in Structural Biology 12(3): 301-310.

H

Halestrap, A. P., G. P. McStay and S. J. Clarke (2002). "The permeability transition pore complex: another view." Biochimie 84(2-3): 153-166.
Halwani, R., S. Cen, H. Javanbakht, J. Saadatmand, S. Kim, K. Shiba and L. Kleiman (2004). "Cellular distribution of Lysyl-tRNA synthetase and its interaction with Gag during human immunodeficiency virus type 1 assembly." J Virol 78(14): 7553-7564.
Hartl, F. U., B. Schmidt, E. Wachter, H. Weiss and W. Neupert (1986). "Transport into Mitochondria and Intramitochondrial Sorting of the Fe/S Protein of Ubiquinol Cytochrome-C Reductase." Cell 47(6): 939-951.
Hatakeyama, H. and Y. Goto (2016). "Concise Review: Heteroplasmic Mitochondrial DNA Mutations and Mitochondrial Diseases: Toward iPSC-Based Disease Modeling, Drug Discovery, and Regenerative Therapeutics." Stem Cells 34(4): 801-808.
Hausmann, C. D. and M. Ibba (2008). "Aminoacyl-tRNA synthetase complexes: molecular multitasking revealed." Fems Microbiology Reviews 32(4): 705-721.
Havrylenko, S. and M. Mirande (2015). "Aminoacyl-tRNA synthetase complexes in evolution." Int J Mol Sci 16(3): 6571-6594.

Hayakawa, K., E. Esposito, X. Wang, Y. Terasaki, Y. Liu, C. Xing, X. Ji and E. H. Lo (2016). "Transfer of mitochondria from astrocytes to neurons after stroke." Nature 535(7613): 551-555.

He, J., H. M. Cooper, A. Reyes, M. Di Re, H. Sembongi, T. R. Litwin, J. Gao, K. C. Neuman, I. M. Fearnley, A. Spinazzola, J. E. Walker and I. J. Holt (2012). "Mitochondrial nucleoid interacting proteins support mitochondrial protein synthesis." Nucleic Acids Research 40(13): 6109-6121.

Hebben, M., J. Brants, C. Birck, J. P. Samama, B. Wasylyk, D. Spehner, K. Pradeau, A. Domi, B. Moss, P. Schultz and R. Drillien (2007). "High level protein expression in mammalian cells using a safe viral vector: modified vaccinia virus Ankara." Protein Expr Purif 56(2): 269-278.

Helm, M., H. Brule, D. Friede, R. Giege, D. Putz and C. Florentz (2000). "Search for characteristic structural features of mammalian mitochondrial tRNAs." Rna-a Publication of the Rna Society 6(10): 1356-1379.

Herget, M. and R. Tampe (2007). "Intracellular peptide transporters in human - compartmentalization of the "peptidome"." Pflugers Archiv-European Journal of Physiology 453(5): 591-600.

Hirschvogel, K., K. Matiasek, K. Flatz, M. Drogemuller, C. Drogemuller, B. Reiner and A. Fischer (2013). "Magnetic resonance imaging and genetic investigation of a case of Rottweiler leukoencephalomyelopathy." BMC Vet Res 9: 57.

Hlatky, R., A. B. Valadka, J. C. Goodman, C. F. Contant and C. S. Robertson (2004). "Patterns of energy substrates during ischemia measured in the brain by microdialysis." J Neurotrauma 21(7): 894-906.

Huang, C. C., S. H. Tu, H. H. Lien, J. Y. Jeng, C. S. Huang, C. J. Huang, L. C. Lai and E. Y. Chuang (2013). "Concurrent gene signatures for han chinese breast cancers." PLoS One 8(10): e76421.

Huot, J. L., L. Enkler, C. Megel, L. Karim, D. Laporte, H. D. Becker, A. M. Duchene, M. Sissler and L. Marechal-Drouard (2014). "Idiosyncrasies in decoding mitochondrial genomes." Biochimie 100: 95-106.

Huss, M. and H. Wieczorek (2007). "Influence of ATP and ADP on dissociation of the V-ATPase into its V-1 and V-O complexes." Febs Letters 581(29): 5566-5572.

Huttlin EL, T. L., Bruckner RJ, Paulo JA, Gygi MP, Rad R, Kolippakkam D, Szpyt J, Zarraga G, Tam S, Gebreab F, Colby G, Pontano-Vaites L, Obar RA, Guarani-Pereira V, Harris T, Artavanis-Tsakonas S, Sowa ME, Harper JW, Gygi SP (2014). "High-Throughput Proteomic Mapping of Human Interaction Networks via Affinity-Purification Mass Spectrometry ".

Huttlin, E. L., L. Ting, R. J. Bruckner, F. Gebreab, M. P. Gygi, J. Szpyt, S. Tam, G. Zarraga, G. Colby, K. Baltier, R. Dong, V. Guarani, L. P. Vaites, A. Ordureau, R. Rad, B. K. Erickson, M. Wuhr, J. Chick, B. Zhai, D. Kolippakkam, J. Mintseris, R. A. Obar, T. Harris, S. Artavanis-Tsakonas, M. E. Sowa, P. De Camilli, J. A. Paulo, J. W. Harper and S. P. Gygi (2015). "The BioPlex Network: A Systematic Exploration of the Human Interactome." Cell 162(2): 425-440.

I

Ilkow, C. S., D. Weckbecker, W. J. Cho, S. Meier, M. D. Beatch, I. S. Goping, J. M. Herrmann and T. C. Hobman (2010). "The rubella virus capsid protein inhibits mitochondrial import." J Virol 84(1): 119-130.

J

Javid, B., F. Sorrentino, M. Toosky, W. Zheng, J. T. Pinkham, N. Jain, M. M. Pan, P. Deighan and E. J. Rubin (2014). "Mycobacterial mistranslation is necessary and sufficient for rifampicin phenotypic resistance." Proceedings of the National Academy of Sciences of the United States of America 111(3): 1132-1137.

Jester, B. C., R. Drillien, M. Ruff and C. Florentz (2011). "Using Vaccinia's innate ability to introduce DNA into mammalian cells for production of recombinant proteins." J Biotechnol 156(3): 211-213.
Jourdain, A. A., E. Boehm, K. Maundrell and J. C. Martinou (2016). "Mitochondrial RNA granules: Compartmentalizing mitochondrial gene expression." J Cell Biol 212(6): 611-614.
Jourdain, A. A., M. Koppen, M. Wydro, C. D. Rodley, R. N. Lightowlers, Z. M. Chrzanowska-Lightowlers and J. C. Martinou (2013). "GRSF1 Regulates RNA Processing in Mitochondrial RNA Granules." Cell Metabolism 17(3): 399-410.

K

Kalousek, F., J. P. Hendrick and L. E. Rosenberg (1988). "Two mitochondrial matrix proteases act sequentially in the processing of mammalian matrix enzymes." Proc Natl Acad Sci U S A 85(20): 7536-7540.
Karnkowska, A., V. Vacek, Z. Zubacova, S. C. Treitli, R. Petrzelkova, L. Eme, L. Novak, V. Zarsky, L. D. Barlow, E. K. Herman, P. Soukal, M. Hroudova, P. Dolezal, C. W. Stairs, A. J. Roger, M. Elias, J. B. Dacks, C. Vlcek and V. Hampl (2016). "A Eukaryote without a Mitochondrial Organelle." Current Biology 26(10): 1274-1284.
Kehrein, K., N. Bonnefoy and M. Ott (2013). "Mitochondrial Protein Synthesis: Efficiency and Accuracy." Antioxidants & Redox Signaling 19(16): 1928-1939.
Kepp, O., A. Gdoura, I. Martins, T. Panaretakis, F. Schlemmer, A. Tesniere, G. M. Fimia, F. Ciccosanti, A. Burgevin, M. Piacentini, P. Eggleton, P. J. Young, L. Zitvogel, P. van Endert and G. Kroemer (2010). "Lysyl tRNA synthetase is required for the translocation of calreticulin to the cell surface in immunogenic death." Cell Cycle 9(15): 3072-3077.
Khachane, A. N., K. N. Timmis and V. A. Martins dos Santos (2007). "Dynamics of reductive genome evolution in mitochondria and obligate intracellular microbes." Mol Biol Evol 24(2): 449-456.
Khan, M., G. H. Syed, S. J. Kim and A. Siddiqui (2015). "Mitochondrial dynamics and viral infections: A close nexus." Biochim Biophys Acta 1853(10 Pt B): 2822-2833.
Kilbride, P., H. J. Woodward, K. B. Tan, N. T. Thanh, K. M. Chu, S. Minogue and M. G. Waugh (2015). "Modeling the effects of cyclodextrin on intracellular membrane vesicles from Cos-7 cells prepared by sonication and carbonate treatment." PeerJ 3: e1351.
Kim, D. G., J. W. Choi, J. Y. Lee, H. Kim, Y. S. Oh, J. W. Lee, Y. K. Tak, J. M. Song, E. Razin, S. H. Yun and S. Kim (2012). "Interaction of two translational components, lysyl-tRNA synthetase and p40/37LRP, in plasma membrane promotes laminin-dependent cell migration." Faseb Journal 26(10): 4142-4159.
Kim, H., S. C. Botelho and K. Park (2015). "Use of carbonate extraction in analyzing moderately hydrophobic transmembrane proteins in the mitochondrial inner membrane." Protein Sci 24(12): 2063-2069.
Klipcan, L., N. Moor, I. Finarov, N. Kessler, M. Sukhanova and M. G. Safro (2012). "Crystal structure of human mitochondrial PheRS complexed with tRNA(Phe) in the active "open" state." J Mol Biol 415(3): 527-537.
Kluck, R. M., E. Bossy-Wetzel, D. R. Green and D. D. Newmeyer (1997). "The release of cytochrome c from mitochondria: a primary site for Bcl-2 regulation of apoptosis." Science 275(5303): 1132-1136.
Kobbi, L., G. Octobre, J. Dias, M. Comisso and M. Mirande (2011). "Association of mitochondrial Lysyl-tRNA synthetase with HIV-1 GagPol involves catalytic domain of the synthetase and transframe and integrase domains of Pol." J Mol Biol 410(5): 875-886.
Koc, E. C., M. E. Haque and L. L. Spremulli (2010). "Current Views of the Structure of the Mammalian Mitochondrial Ribosome." Israel Journal of Chemistry 50(1): 45-59.
Kohler, C., C. Heyer, S. Hoffjan, S. Stemmler, T. Lucke, C. Thiels, A. Kohlschutter, U. Lobel, R. Horvath, S. Kleinle, A. Benet-Pages and A. Abicht (2015). "Early-onset leukoencephalopathy due to a

homozygous missense mutation in the DARS2 gene." Molecular and Cellular Probes 29(5): 319-322.

Konovalova, S. and H. Tyynismaa (2013). "Mitochondrial aminoacyl-tRNA synthetases in human disease." Mol Genet Metab 108(4): 206-211.

Kostiuk, M. A., M. M. Corvi, B. O. Keller, G. Plummer, J. A. Prescher, M. J. Hangauer, C. R. Bertozzi, G. Rajaiah, J. R. Falck and L. G. Berthiaume (2008). "Identification of palmitoylated mitochondrial proteins using a bio-orthogonal azido-palmitate analogue." Faseb Journal 22(3): 721-732.

Kumazawa, Y., T. Yokogawa, E. Hasegawa, K. Miura and K. Watanabe (1989). "The Aminoacylation of Structurally Variant Phenylalanine Transfer-Rnas from Mitochondria and Various Nonmitochondrial Sources by Bovine Mitochondrial Phenylalanyl-Transfer Rna-Synthetase." Journal of Biological Chemistry 264(22): 13005-13011.

Kunz, W. S. (2003). "Different metabolic properties of mitochondrial oxidative phosphorylation in different cell types - important implications for mitochondrial cytopathies." Experimental Physiology 88(1): 149-154.

L

Labauge, P., I. Dorboz, E. Eymard-Pierre, O. Dereeper and O. Boespflug-Tanguy (2011). "Clinically asymptomatic adult patient with extensive LBSL MRI pattern and DARS2 mutations." Journal of Neurology 258(2): 335-337.

Lee, C. M., J. Sedman, W. Neupert and R. K. Stuart (1999). "The DNA helicase, Hmi1p, is transported into mitochondria by a C-terminal cleavable targeting signal." Journal of Biological Chemistry 274(30): 20937-20942.

Lee, J., S. Sharma, J. Kim, R. J. Ferrante and H. Ryu (2008). "Mitochondrial nuclear receptors and transcription factors: Who's minding the cell?" Journal of Neuroscience Research 86(5): 961-971.

Lei, X., Y. Chen, G. Du, W. Yu, X. Wang, H. Qu, B. Xia, H. He, J. Mao, W. Zong, X. Liao, M. Mehrpour, X. Hao and Q. Chen (2006). "Gossypol induces Bax/Bak-independent activation of apoptosis and cytochrome c release via a conformational change in Bcl-2." FASEB J 20(12): 2147-2149.

Li, M. X., Z. Y. Zhong, J. W. Zhu, D. B. Xiang, N. Dai, X. J. Cao, Y. Qing, Z. Z. Yang, J. Y. Xie, Z. P. Li, L. Baugh, G. Wang and D. Wang (2010). "Identification and Characterization of Mitochondrial Targeting Sequence of Human Apurinic/Apyrimidinic Endonuclease 1." Journal of Biological Chemistry 285(20): 14871-14881.

Li, S., L. Wang, B. Fu, M. A. Berman, A. Diallo and M. E. Dorf (2014). "TRIM65 regulates microRNA activity by ubiquitination of TNRC6." Proc Natl Acad Sci U S A 111(19): 6970-6975.

Li, X., W. Wang, J. Wang, A. Malovannaya, Y. Xi, W. Li, R. Guerra, D. H. Hawke, J. Qin and J. Chen (2015). "Proteomic analyses reveal distinct chromatin-associated and soluble transcription factor complexes." Mol Syst Biol 11(1): 775.

Lindenboim, L., C. Borner and R. Stein (2011). "Nuclear proteins acting on mitochondria." Biochimica Et Biophysica Acta-Molecular Cell Research 1813(4): 584-596.

Liu, M. Q. and L. Spremulli (2000). "Interaction of mammalian mitochondrial ribosomes with the inner membrane." Journal of Biological Chemistry 275(38): 29400-29406.

Lo, W. S., E. Gardiner, Z. W. Xu, C. F. Lau, F. Wang, J. J. Zhou, J. D. Mendlein, L. A. Nangle, K. P. Chiang, X. L. Yang, K. F. Au, W. H. Wong, M. Guo, M. J. Zhang and P. Schimmel (2014). "Human tRNA synthetase catalytic nulls with diverse functions." Science 345(6194): 328-332.

Lu, M. Y. and F. Liao (2011). "Interferon-stimulated gene ISG12b2 is localized to the inner mitochondrial membrane and mediates virus-induced cell death." Cell Death and Differentiation 18(6): 925-936.

M

Maniataki, E. and Z. Mourelatos (2005). "Human mitochondrial tRNA(Met) is exported to the cytoplasm and associates with the Argonaute 2 protein." Rna-a Publication of the Rna Society 11(6): 849-852.
Marcondes, M. F., F. M. Alves, D. M. Assis, I. Y. Hirata, L. Juliano, V. Oliveira and M. A. Juliano (2015). "Substrate specificity of mitochondrial intermediate peptidase analysed by a support-bound peptide library." FEBS Open Bio 5: 429-436.
Marnef, A., B. E. Jady and T. Kiss (2016). "Human polypyrimidine tract-binding protein interacts with mitochondrial tRNA(Thr) in the cytosol." Nucleic Acids Research 44(3): 1342-1353.
Martikainen, M. H., U. Ellfolk and K. Majamaa (2013). "Impaired information-processing speed and working memory in leukoencephalopathy with brainstem and spinal cord involvement and elevated lactate (LBSL) and DARS2 mutations: a report of three adult patients." Journal of Neurology 260(8): 2078-2083.
Martin, W. F., S. Garg and V. Zimorski (2015). "Endosymbiotic theories for eukaryote origin." Philosophical Transactions of the Royal Society B-Biological Sciences 370(1678).
Mastrogiacomo, A., S. A. Kohan, J. P. Whitelegge and C. B. Gundersen (1998). "Intrinsic membrane association of Drosophila cysteine string proteins." FEBS Lett 436(1): 85-91.
Matthews, G. D., N. Gur, W. J. Koopman, O. Pines and L. Vardimon (2010). "Weak mitochondrial targeting sequence determines tissue-specific subcellular localization of glutamine synthetase in liver and brain cells." J Cell Sci 123(Pt 3): 351-359.
Mattson, M. P., M. Gleichmann and A. Cheng (2008). "Mitochondria in Neuroplasticity and Neurological Disorders." Neuron 60(5): 748-766.
Mei, Y. D., J. Yong, H. T. Liu, Y. G. Shi, J. Meinkoth, G. Dreyfuss and X. L. Yang (2010). "tRNA Binds to Cytochrome c and Inhibits Caspase Activation." Molecular Cell 37(5): 668-678.
Messmer, M., C. Florentz, H. Schwenzer, G. C. Scheper, M. S. van der Knaap, L. Marechal-Drouard and M. Sissler (2011). "A human pathology-related mutation prevents import of an aminoacyl-tRNA synthetase into mitochondria." Biochem J 433(3): 441-446.
Meyer, A., D. B. Hansen, C. S. Gomes, T. J. Hobley, O. R. Thomas and M. Franzreb (2005). "Demonstration of a strategy for product purification by high-gradient magnetic fishing: recovery of superoxide dismutase from unconditioned whey." Biotechnol Prog 21(1): 244-254.
Meyer, J. N., M. C. K. Leung, J. P. Rooney, A. Sendoel, M. O. Hengartner, G. E. Kisby and A. S. Bess (2013). "Mitochondria as a Target of Environmental Toxicants." Toxicological Sciences 134(1): 1-17.
Minczuk, M., J. Piwowarski, M. A. Papworth, K. Awiszus, S. Schalinski, A. Dziembowski, A. Dmochowska, E. Bartnik, K. Tokatlidis, P. P. Stepien and P. Borowski (2002). "Localisation of the human hSuv3p helicase in the mitochondrial matrix and its preferential unwinding of dsDNA." Nucleic Acids Research 30(23): 5074-5086.
Mirande, M., O. Kellermann and J. P. Waller (1982). "Macromolecular complexes from sheep and rabbit containing seven aminoacyl-tRNA synthetases. II. Structural characterization of the polypeptide components and immunological identification of the methionyl-tRNA synthetase subunit." J Biol Chem 257(18): 11049-11055.
Mirando, A. C., C. S. Francklyn and K. M. Lounsbury (2014). "Regulation of Angiogenesis by Aminoacyl-tRNA Synthetases." International Journal of Molecular Sciences 15(12): 23725-23748.
Mitra, K., N. Rangaraj and S. Shivaji (2005). "Novelty of the pyruvate metabolic enzyme dihydrolipoamide dehydrogenase in spermatozoa: correlation of its localization, tyrosine phosphorylation, and activity during sperm capacitation." J Biol Chem 280(27): 25743-25753.
Miyake, N., S. Yamashita, K. Kurosawa, S. Miyatake, Y. Tsurusaki, H. Doi, H. Saitsu and N. Matsumoto (2011). "A novel homozygous mutation of DARS2 may cause a severe LBSL variant." Clinical Genetics 80(3): 293-296.
Mokranjac, D. and W. Neupert (2010). "The many faces of the mitochondrial TIM23 complex." Biochimica Et Biophysica Acta-Bioenergetics 1797(6-7): 1045-1054.

Monaghan, R. M. and A. J. Whitmarsh (2015). "Mitochondrial Proteins Moonlighting in the Nucleus." Trends in Biochemical Sciences 40(12): 728-735.
Mossmann, D., C. Meisinger and F. N. Vogtle (2012). "Processing of mitochondrial presequences." Biochim Biophys Acta 1819(9-10): 1098-1106.
Motzik, A., H. Nechushtan, S. Y. Foo and E. Razin (2013). "Non-canonical roles of lysyl-tRNA synthetase in health and disease." Trends in Molecular Medicine 19(12): 726-731.
Mudge, S. J., J. H. Williams, H. J. Eyre, G. R. Sutherland, P. J. Cowan and D. A. Power (1998). "Complex organisation of the 5 '-end of the human glycine tRNA synthetase gene." Gene 209(1-2): 45-50.

N

Nagao, A. and T. Suzuki (2007). "Aminoacyl-tRNA surveillance by EF-Tu in mammalian mitochondria." Nucleic Acids Symp Ser (Oxf)(51): 41-42.
Nair, J. R. and J. J. McGuire (2005). "Submitochondrial localization of the mitochondrial isoform of folylpolyglutamate synthetase in CCRF-CEM human T-lymphoblastic leukemia cells." Biochim Biophys Acta 1746(1): 38-44.
Nechushtan, H., S. Kim, G. Kay and E. Razin (2009). "Chapter 1: The physiological role of lysyl tRNA synthetase in the immune system." Adv Immunol 103: 1-27.
Negrutskii, B. S., V. F. Shalak, P. Kerjan, A. V. El'skaya and M. Mirande (1999). "Functional interaction of mammalian valyl-tRNA synthetase with elongation factor EF-1alpha in the complex with EF-1H." J Biol Chem 274(8): 4545-4550.
Nesti, C., M. C. Meschini, B. Meunier, M. Sacchini, S. Doccini, A. Romano, S. Petrillo, I. Pezzini, N. Seddiki, A. Rubegni, F. Piemonte, M. A. Donati, G. Brasseur and F. M. Santorelli (2015). "Additive effect of nuclear and mitochondrial mutations in a patient with mitochondrial encephalomyopathy." Human Molecular Genetics 24(11): 3248-3256.
Nett, J. H. and B. L. Trumpower (1996). "Dissociation of import of the Rieske iron-sulfur protein into Saccharomyces cerevisiae mitochondria from proteolytic processing of the presequence." Journal of Biological Chemistry 271(43): 26713-26716.
Netzer, N., J. M. Goodenbour, A. David, K. A. Dittmar, R. B. Jones, J. R. Schneider, D. Boone, E. M. Eves, M. R. Rosner, J. S. Gibbs, A. Embry, B. Dolan, S. Das, H. D. Hickman, P. Berglund, J. R. Bennink, J. W. Yewdell and T. Pan (2009). "Innate immune and chemically triggered oxidative stress modifies translational fidelity." Nature 462(7272): 522-526.
Neuenfeldt, A., B. Lorber, E. Ennifar, A. Gaudry, C. Sauter, M. Sissler and C. Florentz (2013). "Thermodynamic properties distinguish human mitochondrial aspartyl-tRNA synthetase from bacterial homolog with same 3D architecture." Nucleic Acids Res 41(4): 2698-2708.
Neuspiel, M., A. C. Schauss, E. Braschi, R. Zunino, P. Rippstein, R. A. Rachubinski, M. A. Andrade-Navarro and H. M. McBride (2008). "Cargo-selected transport from the mitochondria to peroxisomes is mediated by vesicular carriers." Curr Biol 18(2): 102-108.
Ng, F. and B. L. Tang (2014). "Pyruvate dehydrogenase complex (PDC) export from the mitochondrial matrix." Mol Membr Biol 31(7-8): 207-210.
Nouws, J., A. V. Goswami, M. Bestwick, B. J. McCann, Y. V. Surovtseva and G. S. Shadel (2016). "Mitochondrial Ribosomal Protein L12 Is Required for POLRMT Stability and Exists as Two Forms Generated by Alternative Proteolysis during Import." Journal of Biological Chemistry 291(2): 989-997.

O

O'Brien, T. W. (2003). "Properties of human mitochondrial ribosomes." IUBMB Life 55(9): 505-513.
O'Toole, J. F., Y. J. Liu, E. E. Davis, C. J. Westlake et al. (2010). "Individuals with mutations in XPNPEP3, which encodes a mitochondrial protein, develop a nephronophthisis-like nephropathy." Journal of Clinical Investigation 120(3): 791-802.

Ofir-Birin, Y., P. F. Fang, S. P. Bennett, H. M. Zhang, J. Wang, I. Rachmin, R. Shapiro, J. Song, A. Dagan, J. Pozo, S. Kim, A. G. Marshall, P. Schimmel, X. L. Yang, H. Nechushtan, E. Razin and M. Guo (2013). "Structural Switch of Lysyl-tRNA Synthetase between Translation and Transcription." Molecular Cell 49(1): 30-42.

Ohtsuki, T. and Y. Watanabe (2007). "T-armless tRNAs and elongated elongation factor Tu." IUBMB Life 59(2): 68-75.

Okorokov, A. L. and J. Milner (1999). "An ATP/ADP-dependent molecular switch regulates the stability of p53-DNA complexes." Mol Cell Biol 19(11): 7501-7510.

Opalinska, M. and C. Meisinger (2015). "Metabolic control via the mitochondrial protein import machinery." Curr Opin Cell Biol 33: 42-48.

Ott, M. and J. M. Herrmann (2010). "Co-translational membrane insertion of mitochondrially encoded proteins." Biochim Biophys Acta 1803(6): 767-775.

P

Pang, Y. L., K. Poruri and S. A. Martinis (2014). "tRNA synthetase: tRNA aminoacylation and beyond." Wiley Interdiscip Rev RNA 5(4): 461-480.

Park, S. G., H. J. Kim, Y. H. Min, E. C. Choi, Y. K. Shin, B. J. Park, S. W. Lee and S. Kim (2005). "Human lysyl-tRNA synthetase is secreted to trigger proinflammatory response." Proceedings of the National Academy of Sciences of the United States of America 102(18): 6356-6361.

Park, S. G., P. Schimmel and S. Kim (2008). "Aminoacyl tRNA synthetases and their connections to disease." Proceedings of the National Academy of Sciences of the United States of America 105(32): 11043-11049.

Petzold, G. C., G. Bohner, R. Klingebiel, N. Amberger, M. S. van der Knaap and R. Zschenderlein (2006). "Adult onset leucoencephalopathy with brain stem and spinal cord involvement and normal lactate." Journal of Neurology Neurosurgery and Psychiatry 77(7): 889-891.

Prabhakaran, K., L. Li, J. L. Borowitz and G. E. Isom (2002). "Cyanide induces different modes of death in cortical and mesencephalon cells." J Pharmacol Exp Ther 303(2): 510-519.

Pratje, E., G. Mannhaupt, G. Michaelis and K. Beyreuther (1983). "A nuclear mutation prevents processing of a mitochondrially encoded membrane protein in Saccharomyces cerevisiae." EMBO J 2(7): 1049-1054.

Q

Quevillon, S., J. C. Robinson, E. Berthonneau, M. Siatecka and M. Mirande (1999). "Macromolecular assemblage of aminoacyl-tRNA synthetases: identification of protein-protein interactions and characterization of a core protein." J Mol Biol 285(1): 183-195.

Quiros, P. M., T. Langer and C. Lopez-Otin (2015). "New roles for mitochondrial proteases in health, ageing and disease." Nature Reviews Molecular Cell Biology 16(6): 345-359.

R

Rabilloud, T., M. Heller, M. P. Rigobello, A. Bindoli, R. Aebersold and J. Lunardi (2001). "The mitochondrial antioxidant defence system and its response to oxidative stress." Proteomics 1(9): 1105-1110.

Rajala, N., F. Hensen, H. J. Wessels, D. Ives, J. Gloerich and J. N. Spelbrink (2015). "Whole cell formaldehyde cross-linking simplifies purification of mitochondrial nucleoids and associated proteins involved in mitochondrial gene expression." PLoS One 10(2): e0116726.

Rajala, N., J. M. Gerhold, P. Martinsson, A. Klymov and J. N. Spelbrink (2014). "Replication factors transiently associate with mtDNA at the mitochondrial inner membrane to facilitate replication." Nucleic Acids Res 42(2): 952-967.

Rangaraju, V., N. Calloway and T. A. Ryan (2014). "Activity-Driven Local ATP Synthesis Is Required for Synaptic Function." Cell 156(4): 825-835.

Ray, P. S., A. Arif and P. L. Fox (2007). "Macromolecular complexes as depots for releasable regulatory proteins." Trends in Biochemical Sciences 32(4): 158-164.

Reed, V. S., M. E. Wastney and D. C. Yang (1994). "Mechanisms of the transfer of aminoacyl-tRNA from aminoacyl-tRNA synthetase to the elongation factor 1 alpha." J Biol Chem 269(52): 32932-32936.

Rendon, A. and A. Waksman (1971). "Intramitochondrial release and binding of mitochondrial aspartate aminotransferase and malate dehydrogenase in the presence and absence of monovalent and bivalent cations." Biochem Biophys Res Commun 42(6): 1214-1219.

Rendon, A. and A. Waksman (1973). "Release and binding of proteins and enzymes with isolated inner mitochondrial membranes." Biochem Biophys Res Commun 50(3): 814-819.

Rhee, H. W., P. Zou, N. D. Udeshi, J. D. Martell, V. K. Mootha, S. A. Carr and A. Y. Ting (2013). "Proteomic mapping of mitochondria in living cells via spatially restricted enzymatic tagging." Science 339(6125): 1328-1331.

Ringwald, M., C. Wu and A. I. Su (2012). "BioGPS and GXD: mouse gene expression data-the benefits and challenges of data integration." Mamm Genome 23(9-10): 550-558.

Roesser, J. R., K. Liittschwager and S. E. Leff (1993). "Regulation of Tissue-Specific Splicing of the Calcitonin Calcitonin Gene-Related Peptide Gene by Rna-Binding Proteins." Journal of Biological Chemistry 268(11): 8366-8375.

Rorbach, J., Yusoff, A. A., Tuppen, H., Abg-Kamaludin, D. P., Chrzanowska-Lightowlers, Z. M., Taylor, R. W., Turnbull, D. M., McFarland, R. and Lightowlers, R. N. (2014). "Overexpression of human mitochondrial valyl tRNA synthetase can partially restore levels of co gnate mt-tRNAVal carrying the pathogenic C25U mutation." Nucleic Acids Res 36(9):3065-74.

Roy, H., J. Q. Ling, J. Alfonzo and M. Ibba (2005). "Loss of editing activity during the evolution of mitochondrial phenylalanyl-tRNA synthetase." Journal of Biological Chemistry 280(46): 38186-38192.

Rytomaa, M. and P. K. Kinnunen (1995). "Reversibility of the binding of cytochrome c to liposomes. Implications for lipid-protein interactions." J Biol Chem 270(7): 3197-3202.

S

Sadacharan, S. K., B. Singh, T. Bowes and R. S. Gupta (2005). "Localization of mitochondrial DNA encoded cytochrome c oxidase subunits I and II in rat pancreatic zymogen granules and pituitary growth hormone granules." Histochem Cell Biol 124(5): 409-421.

Saelens, X., N. Festjens, L. Vande Walle, M. van Gurp, G. van Loo and P. Vandenabeele (2004). "Toxic proteins released from mitochondria in cell death." Oncogene 23(16): 2861-2874.

Sajish, M., Q. Zhou, S. Kishi, D. M. Valdez, Jr., M. Kapoor, M. Guo, S. Lee, S. Kim, X. L. Yang and P. Schimmel (2012). "Trp-tRNA synthetase bridges DNA-PKcs to PARP-1 to link IFN-gamma and p53 signaling." Nat Chem Biol 8(6): 547-554.

Sauter, C., B. Lorber, A. Gaudry, L. Karim, H. Schwenzer, F. Wien, P. Roblin, C. Florentz and M. Sissler (2015). "Neurodegenerative disease-associated mutants of a human mitochondrial aminoacyl-tRNA synthetase present individual molecular signatures." Sci Rep 5: 17332.

Saveliev, S. V., C. C. Woodroofe, G. Sabat, C. M. Adams, D. Klaubert, K. Wood and M. Urh (2013). "Mass Spectrometry Compatible Surfactant for Optimized In-Gel Protein Digestion." Analytical Chemistry 85(2): 907-914.

Schagger, H. and G. von Jagow (1991). "Blue native electrophoresis for isolation of membrane protein complexes in enzymatically active form." Anal Biochem 199(2): 223-231.

Schagger, H., W. A. Cramer and G. von Jagow (1994). "Analysis of molecular masses and oligomeric states of protein complexes by blue native electrophoresis and isolation of membrane protein complexes by two-dimensional native electrophoresis." Anal Biochem 217(2): 220-230.

Scheper, G. C., T. van der Klok, R. J. van Andel, C. G. van Berkel, M. Sissler, J. Smet, T. I. Muravina, S. V. Serkov, G. Uziel, M. Bugiani, R. Schiffmann, I. Krageloh-Mann, J. A. Smeitink, C. Florentz, R. Van Coster, J. C. Pronk and M. S. van der Knaap (2007). "Mitochondrial aspartyl-tRNA synthetase deficiency causes leukoencephalopathy with brain stem and spinal cord involvement and lactate elevation." Nat Genet 39(4): 534-539.

Schlattner, U. and T. Wallimann (2000). "A quantitative approach to membrane binding of human ubiquitous mitochondrial creatine kinase using surface plasmon resonance." J Bioenerg Biomembr 32(1): 123-131.

Schleiff, E. and T. Becker (2011). "Common ground for protein translocation: access control for mitochondria and chloroplasts." Nat Rev Mol Cell Biol 12(1): 48-59.

Schmidt, O., N. Pfanner and C. Meisinger (2010). "Mitochondrial protein import: from proteomics to functional mechanisms." Nat Rev Mol Cell Biol 11(9): 655-667.

Schneider, C. A., W. S. Rasband and K. W. Eliceiri (2012). "NIH Image to ImageJ: 25 years of image analysis." Nat Methods 9(7): 671-675.

Schwenzer, H., G. C. Scheper, N. Zorn, L. Moulinier, A. Gaudry, E. Leize, F. Martin, C. Florentz, O. Poch and M. Sissler (2014). "Released selective pressure on a structural domain gives new insights on the functional relaxation of mitochondrial aspartyl-tRNA synthetase." Biochimie 100: 18-26.

Schwenzer, H., J. Zoll, C. Florentz and M. Sissler (2014). "Pathogenic implications of human mitochondrial aminoacyl-tRNA synthetases." Top Curr Chem 344: 247-292.

Serero, A., C. Giglione, A. Sardini, J. Martinez-Sanz and T. Meinnel (2003). "An unusual peptide deformylase features in the human mitochondrial N-terminal methionine excision pathway." J Biol Chem 278(52): 52953-52963.

Shadel, G. S. and T. L. Horvath (2015). "Mitochondrial ROS Signaling in Organismal Homeostasis." Cell 163(3): 560-569.

Sharma, S., N. Sankhyan, A. Kumar, G. C. Scheper, M. S. van der Knaap and S. Gulati (2011). "Leukoencephalopathy With Brain Stem and Spinal Cord Involvement and High Lactate: A Genetically Proven Case Without Elevated White Matter Lactate." Journal of Child Neurology 26(6): 773-776.

Shutt, T. E. and M. W. Gray (2006). "Bacteriophage origins of mitochondrial replication and transcription proteins." Trends Genet 22(2): 90-95.

Sissler, M., J. Putz, F. Fasiolo and C. Florentz (2000). "Mitochondrial aminoacyl-tRNA synthetases." Georgetown, TX: Landes Biosciences(In: Ibba, M., Francklyn, C. and Cusack, S., eds. Aminoacyl-tRNA synthetases): 271-284.

Skladal, D., J. Halliday and D. R. Thorburn (2003). "Minimum birth prevalence of mitochondrial respiratory chain disorders in children." Brain 126: 1905-1912.

Sloan, D. B., Alverson, A. J., Chuckalovcak, J. P., Wu, M., McCauley, D. E., Palmer, J. D. and Taylor, D.R. (2012).”Rapid evolution of enormous, multichromosomal genomes in flowering plant mitochond ria withexceptionally high mutation rates.” PLoS Biol 10(1):e1001241. doi:10.1371/journal. pbio.1001241.

Small, I., N. Peeters, F. Legeai and C. Lurin (2004). "Predotar: A tool for rapidly screening proteomes for N-terminal targeting sequences." Proteomics 4(6): 1581-1590.

Sohm, B., M. Sissler, H. Park, M. P. King and C. Florentz (2004). "Recognition of human mitochondrial tRNALeu(UUR) by its cognate leucyl-tRNA synthetase." J Mol Biol 339(1): 17-29.

Soltys, B. J. and R. S. Gupta (1999). "Mitochondrial-matrix proteins at unexpected locations: are they exported?" Trends in Biochemical Sciences 24(5): 174-177.

Soubannier, V., G. L. McLelland, R. Zunino, E. Braschi, P. Rippstein, E. A. Fon and H. M. McBride (2012). "A vesicular transport pathway shuttles cargo from mitochondria to lysosomes." Curr Biol 22(2): 135-141.

Stapulionis, R. and M. P. Deutscher (1995). "A channeled tRNA cycle during mammalian protein synthesis." Proc Natl Acad Sci U S A 92(16): 7158-7161.

Steenweg, M. E., D. Ghezzi, T. Haack, T. E. Abbink, D. Martinelli, C. G. van Berkel, A. Bley, L. Diogo, E. Grillo, J. Te Water Naude, T. M. Strom, E. Bertini, H. Prokisch, M. S. van der Knaap and M. Zeviani (2012). "Leukoencephalopathy with thalamus and brainstem involvement and high lactate 'LTBL' caused by EARS2 mutations." Brain 135(Pt 5): 1387-1394.

Sugiura, A., G. L. McLelland, E. A. Fon and H. M. McBride (2014). "A new pathway for mitochondrial quality control: mitochondrial-derived vesicles." EMBO J 33(19): 2142-2156.

Sutendra, G., A. Kinnaird, P. Dromparis, R. Paulin, T. H. Stenson, A. Haromy, K. Hashimoto, N. Zhang, E. Flaim and E. D. Michelakis (2014). "A Nuclear Pyruvate Dehydrogenase Complex Is Important for the Generation of Acetyl-CoA and Histone Acetylation." Cell 158(1): 84-97.

Suzuki, H., T. Ueda, H. Taguchi and N. Takeuchi (2007). "Chaperone properties of mammalian mitochondrial translation elongation factor Tu." Journal of Biological Chemistry 282(6): 4076-4084.

Szczesny, R. J., H. Obriot, A. Paczkowska, R. Jedrzejczak, A. Dmochowska, E. Bartnik, P. Formstecher, R. Polakowska and P. P. Stepien (2007). "Down-regulation of human RNA/DNA helicase SUV3 induces apoptosis by a caspase- and AIF-dependent pathway." Biology of the Cell 99(6): 323-332.

Szczesny, R. J., L. S. Borowski, L. K. Brzezniak, A. Dmochowska, K. Gewartowski, E. Bartnik and P. P. Stepien (2010). "Human mitochondrial RNA turnover caught in flagranti: involvement of hSuv3p helicase in RNA surveillance." Nucleic Acids Res 38(1): 279-298.

T

Taft, R. J., A. Vanderver, R. J. Leventer, S. A. Damiani, C. Simons, S. M. Grimmond, D. Miller, J. Schmidt, P. J. Lockhart, K. Pope, K. L. Ru, J. Crawford, T. Rosser, I. F. M. de Coo, M. Juneja, I. C. Verma, P. Prabhakar, S. Blaser, J. Raiman, P. J. W. Pouwels, M. R. Bevova, T. E. M. Abbink, M. S. van der Knaap and N. I. Wolf (2013). "Mutations in DARS Cause Hypomyelination with Brain Stem and Spinal Cord Involvement and Leg Spasticity." American Journal of Human Genetics 92(5): 774-780.

Tait, S. W. and D. R. Green (2010). "Mitochondria and cell death: outer membrane permeabilization and beyond." Nat Rev Mol Cell Biol 11(9): 621-632.

Takeyama, N., N. Matsuo and T. Tanaka (1993). "Oxidative damage to mitochondria is mediated by the Ca(2+)-dependent inner-membrane permeability transition." Biochem J 294 (Pt 3): 719-725.

Teixeira, P. F. and E. Glaser (2013). "Processing peptidases in mitochondria and chloroplasts." Biochim Biophys Acta 1833(2): 360-370.

Temperley, R. J., M. Wydro, R. N. Lightowlers and Z. M. Chrzanowska-Lightowlers (2010). "Human mitochondrial mRNAs-like members of all families, similar but different." Biochimica Et Biophysica Acta-Bioenergetics 1797(6-7): 1081-1085.

Tezuka, T. and G. G. Laties (1983). "Isolation and Characterization of Inner Membrane-Associated and Matrix NAD-Specific Isocitrate Dehydrogenase in Potato Mitochondria." Plant Physiol 72(4): 959-963.

Tolkunova, E., H. Park, J. Xia, M. P. King and E. Davidson (2000). "The human lysyl-tRNA synthetase gene encodes both the cytoplasmic and mitochondrial enzymes by means of an unusual alternative splicing of the primary transcript." Journal of Biological Chemistry 275(45): 35063-35069.

Tshori, S., E. Razin and H. Nechushtan (2014). "Amino-Acyl tRNA Synthetases Generate Dinucleotide Polyphosphates as Second Messengers: Functional Implications." Aminoacyl-Trna Synthetases in Biology and Medicine 344: 189-206.

Tu, Y. T. and A. Barrientos (2015). "The Human Mitochondrial DEAD-Box Protein DDX28 Resides in RNA Granules and Functions in Mitoribosome Assembly." Cell Reports 10(6): 854-864.

Tylki-Szymanska, A., E. Jurkiewicz, E. Y. Zakharova and B. Bobek-Billewicz (2014). "Leukoencephalopathy with Brain Stem and Spinal Cord Involvement and Lactate Elevation: High Outcome Variation between Two Siblings." Neuropediatrics 45(3): 188-191.

Tzima, E., J. S. Reader, M. Irani-Tehrani, K. L. Ewalt, M. A. Schwartz and P. Schimmel (2005). "VE-cadherin links tRNA synthetase cytokine to anti-angiogenic function." J Biol Chem 280(4): 2405-2408.

Tzoulis, C., G. T. Tran, I. O. Gjerde, J. Aasly, G. Neckelmann, J. Rydland, V. Varga, P. Wadel-Andersen and L. A. Bindoff (2012). "Leukoencephalopathy with brainstem and spinal cord involvement caused by a novel mutation in the DARS2 gene." Journal of Neurology 259(2): 292-296.

V

Vaca Jacome, A. S., T. Rabilloud, C. Schaeffer-Reiss, M. Rompais, D. Ayoub, L. Lane, A. Bairoch, A. Van Dorsselaer and C. Carapito (2015). "N-terminome analysis of the human mitochondrial proteome." Proteomics 15(14): 2519-2524.

Van Berge, L., E. M. Hamilton, T. Linnankivi, G. Uziel, M. E. Steenweg, P. Isohanni, N. I. Wolf, I. Krageloh-Mann, N. J. Brautaset, P. I. Andrews, B. A. de Jong, M. al Ghamdi, W. N. van Wieringen, B. A. Tannous, E. Hulleman, T. Wurdinger, C. G. van Berkel, E. Polder, T. E. Abbink, E. A. Struys, G. C. Scheper and M. S. van der Knaap (2014). "Leukoencephalopathy with brainstem and spinal cord involvement and lactate elevation: clinical and genetic characterization and target for therapy." Brain 137(Pt 4): 1019-1029.

Van Berge, L., J. Kevenaar, E. Polder, A. Gaudry, C. Florentz, M. Sissler, M. S. van der Knaap and G. C. Scheper (2013). "Pathogenic mutations causing LBSL affect mitochondrial aspartyl-tRNA synthetase in diverse ways." Biochem J 450(2): 345-350.

Van Berge, L., S. Dooves, C. G. van Berkel, E. Polder, M. S. van der Knaap and G. C. Scheper (2012). "Leukoencephalopathy with brain stem and spinal cord involvement and lactate elevation is associated with cell-type-dependent splicing of mtAspRS mRNA." Biochem J 441(3): 955-962.

Van der Knaap, M. S., P. van der Voorn, F. Barkhof, R. Van Coster, I. Krageloh-Mann, A. Feigenbaum, S. Blaser, J. S. Vles, P. Rieckmann and P. J. Pouwels (2003). "A new leukoencephalopathy with brainstem and spinal cord involvement and high lactate." Ann Neurol 53(2): 252-258.

Van der Laan, M., S. E. Horvath and N. Pfanner (2016). "Mitochondrial contact site and cristae organizing system." Curr Opin Cell Biol 41: 33-42.

Verweij, B. H., J. P. Muizelaar, F. C. Vinas, P. L. Peterson, Y. Xiong and C. P. Lee (2000). "Impaired cerebral mitochondrial function after traumatic brain injury in humans." J Neurosurg 93(5): 815-820.

Vogtle, F. N., C. Prinz, J. Kellermann, F. Lottspeich, N. Pfanner and C. Meisinger (2011). "Mitochondrial protein turnover: role of the precursor intermediate peptidase Oct1 in protein stabilization." Mol Biol Cell 22(13): 2135-2143.

Vogtle, F. N., S. Wortelkamp, R. P. Zahedi, D. Becker, C. Leidhold, K. Gevaert, J. Kellermann, W. Voos, A. Sickmann, N. Pfanner and C. Meisinger (2009). "Global analysis of the mitochondrial N-proteome identifies a processing peptidase critical for protein stability." Cell 139(2): 428-439.

Vonheijne, G. (1986). "Mitochondrial Targeting Sequences May Form Amphiphilic Helices." Embo Journal 5(6): 1335-1342.

W

Waksman, A. and A. Rendon (1971). "Intramitochondrial release and binding of mitochondrial aspartate aminotransferase and malate dehydrogenase in the presence and absence of exogenous succinate." Biochem Biophys Res Commun 42(4): 745-749.

Waksman, A. and A. Rendon (1974). "Intramitochondrial intermembranal large amplitude protein movements. I. A possible novel aspect of membrane fluidity." Biochimie 56(6-7): 907-924.

Wan, C., B. Borgeson, S. Phanse, F. Tu, K. Drew, G. Clark, X. Xiong, O. Kagan, J. Kwan, A. Bezginov, K. Chessman, S. Pal, G. Cromar, O. Papoulas, Z. Ni, D. R. Boutz, S. Stoilova, P. C. Havugimana, X. Guo, R. H. Malty, M. Sarov, J. Greenblatt, M. Babu, W. B. Derry, E. R. Tillier, J. B. Wallingford, J. Parkinson, E. M. Marcotte and A. Emili (2015). "Panorama of ancient metazoan macromolecular complexes." Nature 525(7569): 339-344.

Wang, D. D. H., Z. Shu, S. A. Lieser, P. L. Chen and W. H. Lee (2009). "Human Mitochondrial SUV3 and Polynucleotide Phosphorylase Form a 330-kDa Heteropentamer to Cooperatively Degrade Double-stranded RNA with a 3 '-to-5 ' Directionality." Journal of Biological Chemistry 284(31): 20812-20821.

Wang, J., K. Huo, L. Ma, L. Tang, D. Li, X. Huang, Y. Yuan, C. Li, W. Wang, W. Guan, H. Chen, C. Jin, J. Wei, W. Zhang, Y. Yang, Q. Liu, Y. Zhou, C. Zhang, Z. Wu, W. Xu, Y. Zhang, T. Liu, D. Yu, L. Chen, D. Zhu, X. Zhong, L. Kang, X. Gan, X. Yu, Q. Ma, J. Yan, L. Zhou, Z. Liu, Y. Zhu, T. Zhou, F. He and X. Yang (2011). "Toward an understanding of the protein interaction network of the human liver." Mol Syst Biol 7: 536.

Wang, M., P. Sips, E. Khin, M. Rotival, X. Sun, R. Ahmed, A. A. Widjaja, S. Schafer, P. Yusoff, P. K. Choksi, N. S. Ko, M. K. Singh, D. Epstein, Y. Guan, J. Houštěk, T. Mracek, H. Nuskova, B. Mikell, J. Tan, F. Pesce, F. Kolar, L. Bottolo, M. Mancini, N. Hubner, M. Pravenec, E. Petretto, C. MacRae and S. A. Cook (2016). "Wars2 is a determinant of angiogenesis." Nat Commun 7: 12061.

Wang, Y. S. and D. F. Bogenhagen (2006). "Human mitochondrial DNA nucleoids are linked to protein folding machinery and metabolic enzymes at the mitochondrial inner membrane." Journal of Biological Chemistry 281(35): 25791-25802.

Wenz, L. S., L. Opalinski, N. Wiedemann and T. Becker (2015). "Cooperation of protein machineries in mitochondrial protein sorting." Biochimica Et Biophysica Acta-Molecular Cell Research 1853(5): 1119-1129.

Williamson, R. M. (1993). "Membrane association of leucyl-tRNA synthetase during leucine starvation in Escherichia coli." Biochem Biophys Res Commun 190(3): 794-800.

Winger, A. M., N. L. Taylor, J. L. Heazlewood, D. A. Day and A. H. Millar (2007). "Identification of intra- and intermolecular disulphide bonding in the plant mitochondrial proteome by diagonal gel electrophoresis." Proteomics 7(22): 4158-4170.

Wittig, I., H. P. Braun and H. Schagger (2006). "Blue native PAGE." Nat Protoc 1(1): 418-428.

Wredenberg, A., M. Lagouge, A. Bratic, M. D. Metodiev, H. Spahr, A. Mourier, C. Freyer, B. Ruzzenente, L. Tain, S. Gronke, F. Baggio, C. Kukat, E. Kremmer, R. Wibom, P. L. Polosa, B. Habermann, L. Partridge, C. B. Park and N. G. Larsson (2013). "MTERF3 Regulates Mitochondrial Ribosome Biogenesis in Invertebrates and Mammals." Plos Genetics 9(1).

X

Xie, W., P. Schimmel and X. L. Yang (2006). "Crystallization and preliminary X-ray analysis of a native human tRNA synthetase whose allelic variants are associated with Charcot-Marie-Tooth disease." Acta Crystallogr Sect F Struct Biol Cryst Commun 62(Pt 12): 1243-1246.

Y

Yadavalli, S. S., L. Klipcan, A. Zozulya, R. Banerjee, D. Svergun, M. Safro and M. Ibba (2009). "Large-scale movement of functional domains facilitates aminoacylation by human mitochondrial phenylalanyl-tRNA synthetase." Febs Letters 583(19): 3204-3208.

Yang, J. C. and G. A. Cortopassi (1998). "dATP causes specific release of cytochrome C from mitochondria." Biochem Biophys Res Commun 250(2): 454-457.

Yang, J. C. and G. A. Cortopassi (1998). "Induction of the mitochondrial permeability transition causes release of the apoptogenic factor cytochrome c." Free Radic Biol Med 24(4): 624-631.

Yang, J., X. Liu, K. Bhalla, C. N. Kim, A. M. Ibrado, J. Cai, T. I. Peng, D. P. Jones and X. Wang (1997). "Prevention of apoptosis by Bcl-2: release of cytochrome c from mitochondria blocked." Science 275(5303): 1129-1132.

Yano, H., S. V. Baranov, O. V. Baranova, J. Kim, Y. Pan, S. Yablonska, D. L. Carlisle, R. J. Ferrante, A. H. Kim and R. M. Friedlander (2014). "Inhibition of mitochondrial protein import by mutant huntingtin." Nat Neurosci 17(6): 822-831.

Yao, P. and P. L. Fox (2013). "Aminoacyl-tRNA synthetases in medicine and disease." EMBO Mol Med 5(3): 332-343.

Yao, Y. N., L. Wang, X. F. Wu and E. D. Wang (2003). "Human mitochondrial leucyl-tRNA synthetase with high activity produced from Escherichia coli." Protein Expression and Purification 30(1): 112-116.

Yogev, O. and O. Pines (2011). "Dual targeting of mitochondrial proteins: Mechanism, regulation and function." Biochimica Et Biophysica Acta-Biomembranes 1808(3): 1012-1020.

Z

Zeng, X. M., W. Neupert and A. Tzagoloff (2007). "The metalloprotease encoded by ATP23 has a dual function in processing and assembly of subunit 6 of mitochondrial ATPase." Molecular Biology of the Cell 18(2): 617-626.

Zhang, X. P., S. Sjoling, M. Tanudji, L. Somogyi, D. Andreu, L. E. Eriksson, A. Graslund, J. Whelan and E. Glaser (2001). "Mutagenesis and computer modelling approach to study determinants for recognition of signal peptides by the mitochondrial processing peptidase." Plant J 27(5): 427-438.

Zhao, H. and A. S. Martinis (2015). "Escherichia coli Secretion of Leucyl-tRNA Synthetase." 10th International Symposium on Aminoacyl-tRNA Synthetases Barcelona, Spain, 18-22 October, 2015: Poster presentation.

Zhao, S., E. R. Aviles, Jr. and D. G. Fujikawa (2010). "Nuclear translocation of mitochondrial cytochrome c, lysosomal cathepsins B and D, and three other death-promoting proteins within the first 60 minutes of generalized seizures." J Neurosci Res 88(8): 1727-1737.

ANNEXES

ANNEXES

Annex 1

Biochimie 100 (2014) 95–106

Contents lists available at ScienceDirect

Biochimie

journal homepage: www.elsevier.com/locate/biochi

Review

Idiosyncrasies in decoding mitochondrial genomes

Jonathan L. Huot [a,1], Ludovic Enkler [a,1], Cyrille Megel [c], Loukmane Karim [b], Daphné Laporte [a], Hubert D. Becker [a,*], Anne-Marie Duchêne [c], Marie Sissler [b,*], Laurence Maréchal-Drouard [c,*]

[a] Unité Mixte de Recherche 7156, Génétique Moléculaire, Génomique, Microbiologie, CNRS, Université de Strasbourg, 21, rue René Descartes, 67084 Strasbourg, France
[b] Architecture et Réactivité de l'ARN, IBMC, CNRS, conventionné avec l'Université de Strasbourg, 15 rue René Descartes, 67084 Strasbourg, France
[c] Institut de Biologie Moléculaire des Plantes, IBMP, CNRS, conventionné avec l'Université de Strasbourg, 12 rue du Général Zimmer, 67084 Strasbourg, France

ARTICLE INFO

Article history:
Received 7 December 2013
Accepted 6 January 2014
Available online 16 January 2014

Keywords:
Mitochondria
Codon usage
Transfer RNA
Aminoacyl-tRNA synthetase

ABSTRACT

Mitochondria originate from the α-proteobacterial domain of life. Since this unique event occurred, mitochondrial genomes of protozoans, fungi, plants and metazoans have highly derived and diverged away from the common ancestral DNA. These resulting genomes highly differ from one another, but all present-day mitochondrial DNAs have a very reduced coding capacity. Strikingly however, ATP production coupled to electron transport and translation of mitochondrial proteins are the two common functions retained in all mitochondrial DNAs. Paradoxically, most components essential for these two functions are now expressed from nuclear genes. Understanding how mitochondrial translation evolved in various eukaryotic models is essential to acquire new knowledge of mitochondrial genome expression. In this review, we provide a thorough analysis of the idiosyncrasies of mitochondrial translation as they occur between organisms. We address this by looking at mitochondrial codon usage and tRNA content. Then, we look at the aminoacyl-tRNA-forming enzymes in terms of peculiarities, dual origin, and alternate function(s). Finally we give examples of the atypical structural properties of mitochondrial tRNAs found in some organisms and the resulting adaptive tRNA-protein partnership.

1. Introduction

In most eukaryotes, mitochondrial (mt) translation is of bacterial type but a certain degree of variation and adaptation has occurred during evolution. While the endosymbiotic genome likely encoded all components of the translational apparatus, genome wide analysis shows that mt DNA has kept only a minimal set of elements (mainly genes encoding a few respiratory chain proteins and rRNAs), but differences can be observed between species [1]. Nevertheless, mitochondria have retained a functional translational apparatus, meaning that almost all genes encoding mt ribosomal proteins, aminoacyl-tRNA synthetases (aaRSs), tRNAs and other translation-related factors were transferred to the nuclear genome. Once translated in the cytosol, these missing mt-encoded products must be imported into the organelle.

Evolutionarily, most components of the mt translation machinery have a bacterial origin and can often be experimentally replaced by bacterial homologs. However, rapid evolution of the mt genomes, numerous post-endosymbiotic lateral gene transfer events (*e.g.* Ref. [2]) as well as an increased flexibility of mt enzymes and tRNAs can make these replacements difficult. For instance, in the case of mt tRNAs from metazoans, significant changes in tertiary structure likely require adaptation of the mt translation machinery (*e.g.* [3]). In addition, nucleus-encoded proteins and RNAs of eukaryotic origin, including many tRNAs, are imported into mitochondria where they also cause divergence from the bacterial "norm" of translation [4]. This presents major drawbacks when trying to establish eukaryotic models for the study of mt functions. The experimental advantages of using eukaryotic models such as the yeast *Saccharomyces cerevisiae*, the land plant *Arabidopsis thaliana* or human cells to study mt dysfunction (in particular respiratory dysfunction) are evident, but require a thorough understanding of the idiosyncrasies of mt translation as they occur between organisms.

To this end, we sought to highlight here unconventional properties of mt translation from different kingdoms of the eukaryotic tree of life (protozoans, fungi, plants and metazoans). We address

* Corresponding authors.
E-mail address: laurence.drouard@ibmp-cnrs.unistra.fr (L. Maréchal-Drouard).
[1] These authors are considered as co-first authors.

0300-9084/$ – see front matter © 2014 Elsevier Masson SAS. All rights reserved.
http://dx.doi.org/10.1016/j.biochi.2014.01.004

this by looking at mt codon usage, and mitochondrion-encoded tRNAs and their peculiarities. We also describe strategies used by species to express mt aaRSs or other aa-tRNA-forming enzymes, as well as the alternative roles of these enzymes.

2. Alternate codon usage

Of the ways in which mt translation differs from the bacterial or cytosolic (cyto) processes, the use of unique genetic codes may be the most familiar. The aaRSs, which determine what tRNAs (and anticodons) are paired with which amino acid (aa), are the molecular embodiment of the genetic code. Once formed, and if recruited by an elongation factor, the identity of the aa moiety of an aminoacyl-tRNA is no longer recognized. This may sometimes cause missense mutations, but it also allows suppression and codon reassignment, which occur at a higher rate in metazoan mitochondria for example. Codon usage is tied to tRNA availability: either the tRNA pool drives codon usage, or codon usage is determined by other factors and changes in the tRNA pool follow suit. Studying codon usage gives considerable insight into which tRNAs are used in mitochondria, and sometimes into their origin.

The number of tRNA genes encoded in the mt genome among related species follows broad trends, with many exceptions (see below for more details, [5–7]). In protozoan species that have been extensively studied, it is typical for the mt genome to have lost several tRNA-coding genes. The loss of mt tRNA genes must therefore be compensated by the import of nucleus-encoded tRNA species [4,8]. In Metazoa, the situation is more complex, but in higher Metazoa the trend is toward the conservation of a single mitochondrion-encoded tRNA for every aa, except leucine and serine, which have two tRNAs. In both these groups, codon usage seems likely to be biased toward those synonymous codons, which can be decoded by a single tRNA for every codon box (a codon box is defined as the set of four triplets sharing the first two nucleotides), which explains the presence of two isoacceptors for Leu and for Ser. While Arg normally also occupies two codon boxes, it has been recently demonstrated that the rare Arg AGA/AGG codons are not used. Instead, a very elegant work from Temperley et al. [9] demonstrated that, in the presence of these codons (and in the absence of any possible $tRNA^{Arg}$), with human mt ribosomes a frameshift occurs resulting in the positioning of a universal UAG stop codon. In plant mitochondria, broadly speaking, between 30 and 50% of the mitochondrion-encoded tRNA genes are well conserved, and sometimes present in more than one copy per codon. This is coupled with the import of several nucleus-encoded tRNA species [8]. How this may influence their codon usage in relation to Protozoa and Metazoa is a complex question.

Pressures defining synonymous codon usage can be pre-translational, such as mRNA secondary structure, abundance, and stability [10–12], and such as the GC-content of the genome [13,14]. These pressures can also be post-transcriptional, like repeating synonymous codon usage in order to maximize tRNA recycling [15], or a 5′ stretch of codons enhancing ribosome “ramp up” shortly after initiation [16]. All of these factors as well as the number of tRNAs available for the decoding of mt genes may vary strongly between different species, but all have retained a translational apparatus tuned to the expression of a small number of genes. The most conserved of these are the respiratory chain proteins of which cytochrome *b* (Cytb) and cytochrome *c* oxidase subunit one (Cox1) are the only genes present in all known mt genomes. The proteins encoded by these genes are hydrophobic, at least transiently membrane-bound, and coordinate the binding of cofactors. These characteristics, in particular strong hydrophobicity, have been hypothesized as having selected these proteins for retention of the corresponding genes in the mt DNA. If these proteins are translated from nucleus-encoded genes it will require import of the pre-proteins into mitochondria that can be impeded by their strong hydrophobicity, particularly in trans-membrane helices [17–19].

When comparing codon usage between diverse organisms, the value of each of those codons, whether it codes for an aa, a stop, or a start, does not need to be known in order to gain insights into mt translation. So long as coding DNA sequences are known, large scale surveys of codon usage can serve as a guide for further work, as shown here with a surface plot representation of three genes from ten species (Fig. 1). The coding DNA sequences for Cytb, Cox1 and for the nucleus-encoded cytochrome *c* subunit 1 (Cyt1) were obtained (GenBank, PlasmoDB, PlantGDB), and their codon usage values calculated using available programs (www.GeneInfinity.org; www.kazusa.or.jp/codon/). Trends are sufficiently conserved among different species for those who diverge from this rough consensus to be readily apparent. The relevance of this type of data representation is demonstrable by how it visually flags idiosyncrasies previously described experimentally. For example, the fact that $tRNA^{Leu}_{CAA}$ in *Chlamydomonas reinhardtii* is a nucleus-encoded tRNA mostly present in mitochondria [20], is likely related to the prevalence of TTG codons in Cox1 and Cytb when compared to Metazoa and Protozoa (Fig. 1, dark gray focus circle). In the mt (maxi-circle) genome of *Leishmania major*, some genes such as Cytb have TAG codons in frame, which do not result in a translational stop [21]. It is possible that this is related to the unusual frequency at which TAG codons occur in *L. major* Cytb when compared to the other organisms surveyed (Fig. 1, light gray focus circle). *Marchantia polymorpha*, *C. reinhardtii* and *A. thaliana* all import a significant number of nucleus-encoded tRNAs, which may explain their partial divergence from codon usage patterns seen in Protozoa and Metazoa. Another aspect that might have influenced codon usage in plant mt genomes is the presence of a second endosymbiotic organelle, the chloroplast. When comparing Protozoa and Metazoa, codon usage is surprisingly well conserved between organisms of these phylae, despite significant differences in the extent of mitochondrion-encoded tRNAs and in mt RNA editing patterns. This is apparent when comparing Cox1 and Cytb to the nucleus-encoded Cyt1, which is one of the components of the same respiratory chain complex in which Cytb participates (complex III). The surface plot of codon usage shows significantly more shifts in codon preference between species in Cyt1 (twists and breaks in the intensity ridges perpendicular to the *X*-axis) than in Cox1 and Cytb, despite well-conserved aa content for all three proteins. The survey presented also reveals other trends, which may guide future work.

3. Peculiarities of mitochondrial tRNAs and aminoacyl-tRNA synthetases

3.1. Mitochondrion-encoded versus nucleus-encoded mitochondrial tRNAs

Since genome sequencing has become commonplace, data on complete mt genomes have steadily increased for a wide range of evolutionarily divergent organisms. In theory, bioinformatics tools allow identification of the set of mitochondrion-encoded tRNA genes in each of these organisms. In practice, this is not always an easy task as several parameters may interfere with tRNA identification and with the characterization of the minimal set of tRNA genes required for mt translation to occur. Among them, we can cite: unknown codon/anticodon rules, deviation from the universal genetic code, post-transcriptional modification such as editing that changes the decoding properties of the tRNA molecule, “bizarre” tRNAs with unconventional cloverleaf secondary structure, which can escape detection [22,23]. Nevertheless, it has become clear that the number of mt tRNA genes varies between organisms, and that

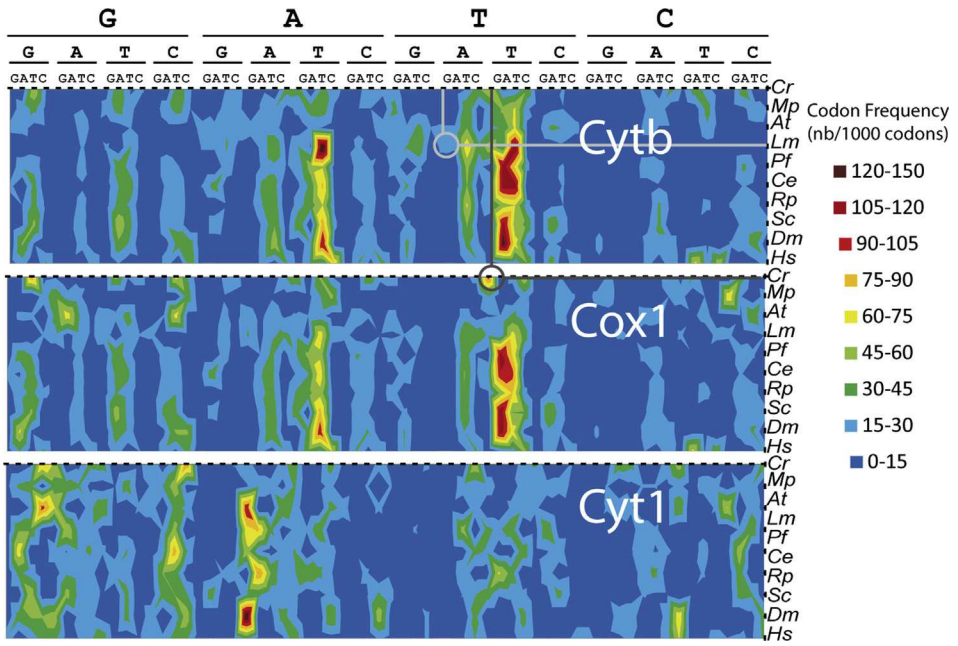

Fig. 1. A small survey of codon usage for three respiratory chain proteins across diverse genera. Organisms surveyed were *Chlamydomonas reinhardtii* (*Cr*), *Marchantia polymorpha* (*Mp*), *Arabidopsis thaliana* (*At*), *Rickettsia prowazekii* (*Rp*), *Caenorhabditis elegans* (*Ce*), *Drosophila melanogaster* (*Dm*), *Saccharomyces cerevisiae* (*Sc*), *Homo sapiens* (*Hs*), *Plasmodium falciparum* (*Pf*), *Leishmania major* (*Lm*). Proteins surveyed were the mitochondrion-encoded cytochrome *b* (Cytb), and cytochrome *c* oxidase sububit 1 (Cox1), as well as the nuclear-encoded cytochrome *c* subunit 1 (Cyt1). The prevalence of each codon is shown as a frequency out of 1000 codons in order to account for the length of the polypeptide chain. Frequencies are plotted as points colored according to a nine-level scale of prevalence. The color between each frequency and its neighboring points corresponds to the value of the slope between each pair of points. Continuous intensity of coloration in a ridge perpendicular to the *X*-axis indicates conservation of codon usage across species: twists in this ridge are caused by bias shifting to codons with different third codon position identities, and breaks are caused by bias shifting toward codons with a different first or second codon position identity. Dark gray and light gray focus circles are examples discussed in Section 2.

those mt tRNA genes missing from the minimal set allowing mt translation must be imported via a correspondingly variable number of nucleus-encoded tRNAs [24]. Indeed, during the last two decades, experimental proof of tRNA mt import has been brought in some organisms and reviews on this topic have been recently written [4,8,25–27]. Major questions that are under debate are the origin of tRNA mt import and the mechanism(s) involved. Here, we only focused our analysis on the great variability of the mt tRNA gene content, and as a consequence, on the potential extent of mt tRNA import in eukaryotes representative of the different kingdoms.

The proto-mitochondrion at the origin of present-day mitochondria likely expressed the full set of mt tRNA genes of the ancestral endosymbiotic α proteobacterium. In contrast to this ancient situation, most mt genomes have now lost at least a few tRNA genes (Fig. 2) [24,27]. From the examples presented in the figure, a few conclusions can be drawn.

i) The presence of an apparently full set of mt tRNA genes (in some Metazoa, fungi and green algae) is rather an exception. Furthermore, having an apparent full set of mt tRNA genes does not mean mitochondria do not need to import nucleus-encoded tRNAs. An illustration is the import of one of the two cyto $tRNA^{Lys}$ isoacceptors into *S. cerevisiae* mitochondria, which becomes essential under heat stress condition [28].

ii) Within all taxa, species *a priori* requiring no or mostly no tRNA import are phylogenetically close to species where many mt tRNA genes are missing. For example, in metazoans, as compared to *Caenorhabditis elegans* or *Drosophila melanogaster*, which contain a full set of mt tRNA genes, only 2 tRNAs are expressed from the mt genome of *Metridium senile* and no tRNA genes were found in *Mnemiopsis leidyi* mt DNA. The same holds true in other clades/taxa (*e.g. S. cerevisiae* versus *Spizellomyces punctatus*) as observed in Fig. 2. Intermediate situations also exist in each kingdom where only a subset of tRNAs are imported.

iii) On a large evolutionary scale, the loss of mt tRNA genes does not seem to follow a pattern. However, once a specific tRNA gene is lost in a certain organism, it is not recovered afterward (see Cycas and related species). To ensure an active mt translation, the loss of a mt tRNA must be preceded by the import of its cyto counterpart. Importantly, once imported, this eukaryotic cyto tRNA needs to be functional in a prokaryotic translational environment. This may strongly limit the loss of some tRNA genes with prokaryotic features. Mt genes encoding $tRNA^{Thr}$ are the ones disappearing the most easily while genes encoding $tRNA^{Met}$ and $tRNA^{Trp}$ seem to be more efficiently retained. Whether these observations reflect biological constraints remains to be elucidated.

iv) The lack of mt tRNA genes is well described in the literature, but the loss of tRNA genes in chloroplasts, the second endosymbiotic organelle present in plants and *apicomplexans*, is less described. In photosynthetic plants, a full set of plastidial tRNA genes is found. By contrast, as briefly mentioned in Fig. 2, the number of plastidial tRNA genes is highly reduced in nonphotosynthetic parasitic plants such as *Epifagus virginiana* or *Rhizanthella gardneri*.

While import of mt proteins is believed to have a monophyletic origin, the origin of tRNA mt import is still under debate. On one hand, looking at the above observations on evolutionary divergent organisms suggests that the process of tRNA import has been created independently many times over the course of eukaryotic evolution, a hypothesis already raised a few years ago [4]. On the other hand, an attractive proposal is that a cryptic RNA import

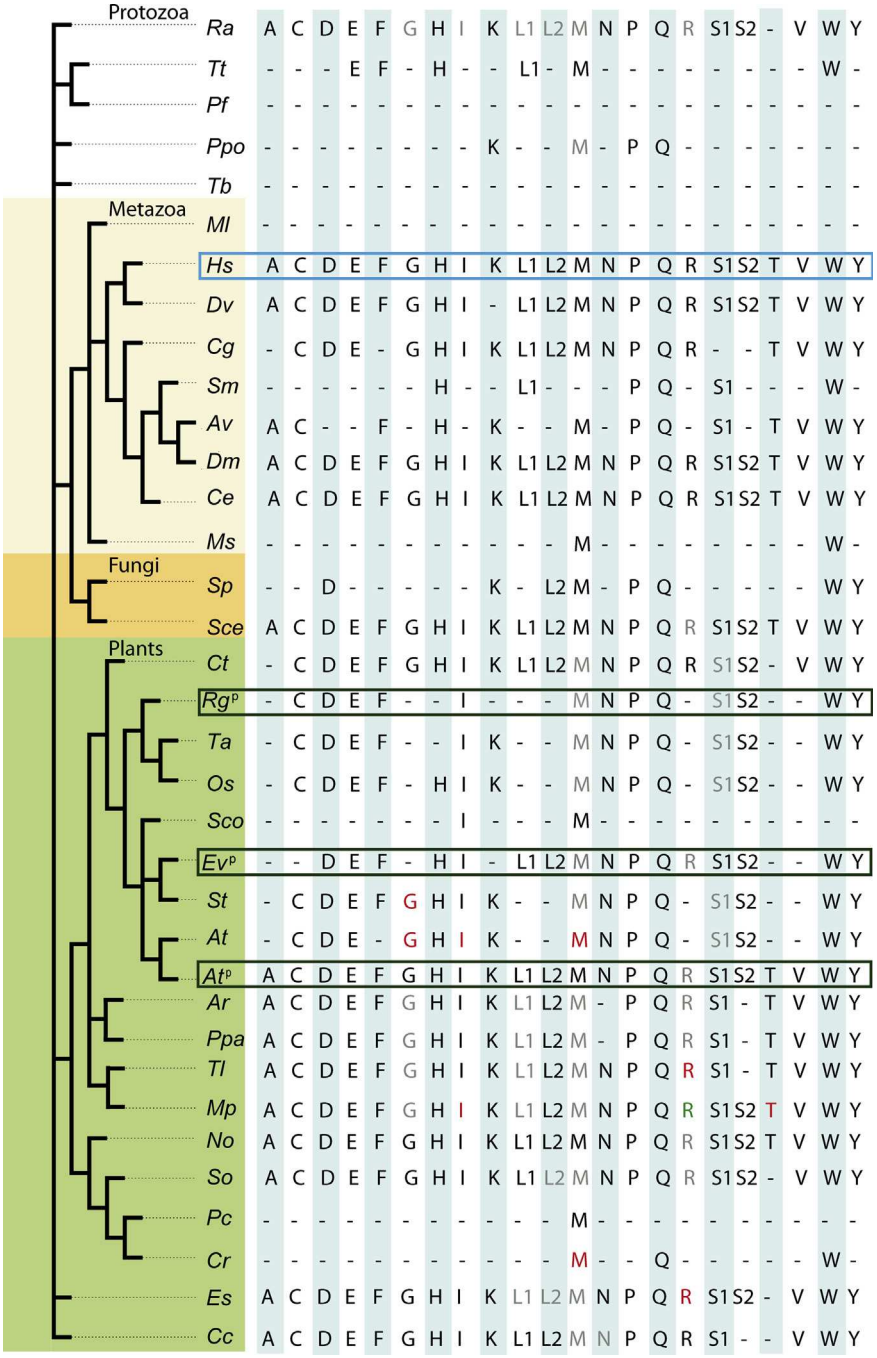

Fig. 2. Transfer RNA genes encoded by mitochondrial genomes of evolutionary divergent organisms. Only a few examples representative of the situation are given. The set of 22 mt tRNA genes of *Homo sapiens* was taken as arbitrary reference (blue frame). Amino acids in gray or green indicate that 2 or 3 isoacceptor tRNA genes respectively are mitochondrion-encoded and necessary to decode all codons of the family and ensure mt translation. Amino acids in red indicate that one isoacceptor tRNA is missing to carry out mt translation. *Hs*, *Homo sapiens* (*J01415*); *Dv*, *Didelphis virginiana* (*Z29573*); *Dm*, *Drosophila melanogaster* (U37541); Ce, *Caenorhabditis elegans* (U37541); Sm, *Steganacarus magnus* (EU935607); Av, *Armadillidium vulgare* (EU935607); Cg, *Crassostrea gigas* (AF177226); Ms, *Metridium senile* (AF000023); Ml, *Mnemiopsis leidyi* (JF760210); Sce, *Saccharomyces cerevisiae* (*AJ011856*); *Sp*, *Spizellomyces punctatus* (*AF404303*; *AF404304*; *AF404305*); *Ppo*, *Physarum polycephalum* (*AB027295*); *Tt*, *Tetrahymena thermophila* (*AB027295*); *Ra*, *Reclinomonas americana* (*AF007261*); *Tb*, *Trypanosoma brucei* [126]; *Pf*, *Plasmodium falciparum* (*AJ276845*); *Cr*, *Chlamydomonas reinhartii* (*AJ276845*); *Pc*, *Polytomella capuana* (*EF645804*); *Nephroselmis olivacea* (*AF110138*); *So*, *Scenedesmus obliquus* (*AF204057*); *Es*, *Ectocarpus siliculosus* (FP885846); Cc, *Chondrus crispus* (Z47547); Ppa, *Physcomitrella patens* (AB251495); Mp, *Marchantia polymorpha* (M68929); Ar, *Anomodon rugelii* (JF973314); Tl, *Treubia lacunosa* (JF973315); Ct, *Cycas taitungensis* (AP009381); At, *Arabidopsis thaliana* (Y08501); St, *Solanum tuberosum* (L. Maréchal-Drouard, personal communication); *Sco*, *Silene conica* [127]; *Ta*, *Tricitum aestivum* (*AP008982*); *Os*, *Oryza sativa* (*BA000029*). The tRNA genes encoded by Rg^p (*Rhizanthella gardneri*, *NC_014874*), Ev^p (*Epifagus virginiana*, *NC_014874*) and At^p (*NC_000932*) plastidial genomes are framed in green.

machinery was created very early during the evolution of the proto-mitochondria (as a matter of fact, the protist *Reclinomonas americana* has already lost mt $tRNA^{Thr}$ genes) or even was pre-existing in the ancestral endosymbiotic bacteria, meaning in that case that mt tRNA import is monophyletic. Under evolutionary pressure, this cryptic machinery could be activated, and could also evolve. If this happens independently in different eukaryotic organisms, from a monophyletic cryptic machinery, the acquisition of various additional import factors can be envisaged. A similar hypothesis is also applicable to the case of plastidial tRNA import. Our

present knowledge does not allow discriminaton between the poly- or monophyletic evolutionary status of tRNA mt import. Deciphering import machineries from phylogenetically distant organisms is essential to answer this question. Experimental evidence from *S. cerevisiae*, plant and *Trypanosoma brucei* shows that tRNA import requires factors of the protein import machinery. Although this may suggest that some of these factors are the common bricks of the cryptic machinery, information is still too fragmentary and controversial today to draw a conclusion.

3.2. Mitochondrial aminoacyl-tRNA synthetases

3.2.1. In photosynthetic organisms and apicomplexans

Over the course of eukaryotic evolution, a first endosymbiotic event led to mitochondria. In plants, subsequent endosymbioses led to chloroplasts and derivatives. Most plastids originate from the endosymbiotic acquisition of a cyanobacterium by a primitive eukaryote. Other plastids originate from the endosymbiosis of a green or red alga into an eukaryote. This is for example the case of apicoplasts in *Apicomplexa* [29]. In plants, algae and apicomplexans, translation occurs in all three compartments: the cytosol, the mitochondrion and the plastid (or relic of plastid). So, all of the components needed for translation should be found in these three compartments. In particular three complete sets of aminoacylated tRNAs have to be generated, implying the need for three complete sets of tRNAs and aaRSs (sixty aaRS activities are thus expected per organism).

The first observation is that all aaRS genes originating from the primitive organellar genomes have been lost or transferred into the nucleus, and all aaRS genes are now localized in the nucleus [2]. The second observation is that the number of putative aaRSs never reaches 60 (Table 1), suggesting that some enzymes are shared between two or three compartments. Among the analysed organisms, the highest number of aaRS genes is found in *Oryza sativa* (53 aaRS genes [30]), and the lowest in *C. reinhardtii* with 33 aaRS genes [6].

The 30 to 50 aaRS genes are distributed so that the most frequent situation is the existence of two aaRSs per aa (70% of aa-aaRS couples, Table 1). In a few cases (15%) only one aaRS has been identified per aa, and in other cases (15%) 3 or 4 aaRS were found per aa. No particular bias was observed at the level of aa, with the notable exception of Gln. In most of the mentioned organisms, only one GlnRS gene is found, probably because Gln-tRNA^{Gln} can be formed by two pathways. In *A. thaliana* cyto tRNAs^{Gln} are charged by cyto GlnRS (direct pathway), but organellar Gln-tRNAs^{Gln} are formed by an indirect transamidation pathway. In mitochondria and chloroplasts, tRNAs^{Gln} are first charged with glutamate by a non-discriminating GluRS, then are converted into Gln-tRNA^{Gln} by a tRNA-dependent amidotransferase (AdT). Both the non-discriminating GluRS and the three AdT subunits are dual imported into mitochondria and chloroplasts [31,32]. AdT subunits have been identified in all the analysed organisms (Table 1), suggesting that the transamidation pathway is functional in one or the other cellular compartment.

The number of aaRSs is particularly high in land plants (*O. sativa*, *A. thaliana*, *Physcomitrella patens*). In these plants, 3 or 4 aaRS genes per aa are often found (Table 1). AaRS localization has been extensively studied in *A. thaliana*. In this plant, synthesis from the same gene of two isoforms that only differ by the presence of a mt targeting sequence (MTS) prior to import, appears to be a general rule (also referred herein as "dual targeting"). Among the 24 identified organellar aaRSs, 17 are shared between mitochondria and plastids, 4 are shared between cytosol and mitochondria, and probably 2 are shared between the 3 compartments (Fig. 3A)

Table 1
Number of aaRS subunits per aa in a few organisms with 3 translating compartments. Amino acids are indicated with the one-letter code. The blue background refers to 3 or 4 aaRS genes, the light brown to 2 genes, and the green background to one unique gene. For PheRSs, one type is composed of one subunit, the other is tetrameric($\alpha 2\beta 2$) yes: at least one out of the 3 AdT subunits has been identified. Os *Oryza sativa* japonica, At *Arabidopsis thaliana*, Pp *Physcomitrella patens*, Es *Ectocarpus siliculosus*, Cr *Chlamydomonas reinhardtii*, Ot *Ostreococcus tauri*, Pt *Phaeodactylum tricornutum*, Pf *Plasmodium falciparum*, Tg *Toxoplasma gondii*.

	Higher plant		Moss	Brown algae	Green algae			Apicomplexa	
	monocot	dicot					diatom (2ary)	plastids (2ary)	
One letter code	Os	At	Pp	Es	Cr	Ot	Pt	Pf	Tg
A	3	2	2	3	2	2	2	1	1
C	3	3	4	3	2	2	2	1	1
D	3	3	3	2	2	2	2	2	1
E	3	2	1	2	2	2	2	2	2
F	3 (type?)	3 (1+a+b)	3 (1+a+b)	4 (type?)	2 (a+b)	3 (1+a+b)	4 (type?)	3 (1+a+b)	3 (1+a+b)
G	2	2	2	2	1	2	2	1	2
H	2	2	2	2	1	2	2	2	2
I	1	2	2	2	1	2	2	2	2
K	2	2	3	2	2	2	2	2	2
L	3	2	2	2	2	2	2	2	2
M	3	2	3	2	2	2	2	2	2
N	3	3	3	2	1	2	2	2	1
P	2	2	2	2	2	2	2	2	1
Q	2	1	1	1	1	1	2	1	1
R	2	2	1	2	1	1	1	2	2
S	3	2	4	2	2	2	2	2	2
T	2	3	4	2	2	2	2	1	2
V	4	2	2	2	2	2	2	2	2
W	3	2	2	2	1	2	2	2	2
Y	4	3	2	2	2	2	2	2	2
# aaRS genes	53	45	49	43	33	39	41	36	35
AdT subunits*	Yes	Yes	Yes	Yes	Yes	Yes	Yes	Yes	Yes

*The diatom Pt and the apicomplexans Pf and Tg have secondary plastids.

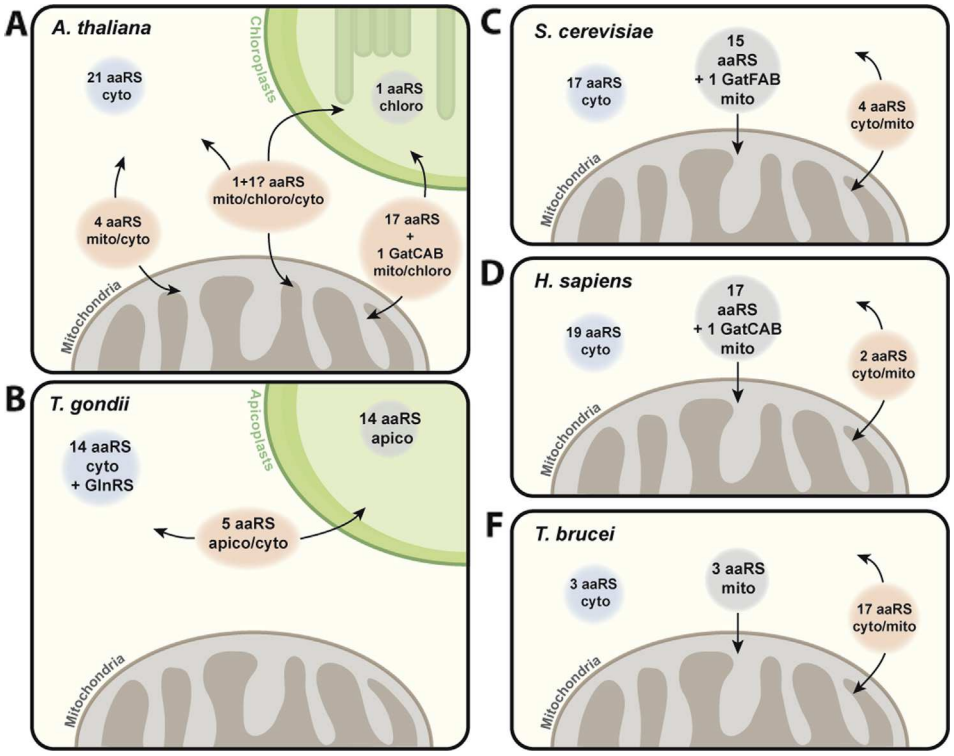

Fig. 3. Aminoacyl-tRNA synthetases (and amidotransferases) localization in *A. thaliana*, *T. gondii*, *S. cerevisiae*, *H. sapiens* and *T. brucei*. In all theses organisms, all the aaRS-encoding genes are localized in the nucleus. A) In *A. thaliana*, most organellar aaRSs are shared between the 2 organelles or between mitochondria and the cytosol. One AlaRS and probably one ArgRS are targeted to the 3 compartments. B) In *T. gondii*, no aaRS have been identified in mitochondria. A few aaRSs are expected to be shared between the cytosol and the apicoplast. But for most of aa, 2 cognate aaRSs have been determined, one potentially targeted to the apicoplast and the other cytosolic. C, D, and E) In *S. cerevisiae*, *H. sapiens* and *T. brucei*, most of the mt aaRSs are encoded by nuclear genes and imported in mitochondria. Some aaRSs are shared between the cytosol and the mitochondria. In *A. thaliana*, *S. cerevisiae* and *H. sapiens*, mt-tRNA^{Gln} is aminoacylated by a non-discriminating GluRS. The misacylated Glu-tRNA^{Gln} is further converted into Gln-tRNA^{Gln} by a tRNA-dependent amido-transferase (AdT) constituted by three subunits (A, B, and either C or F). Thus, these enzymes are named GatCAB or GatFAB.

[27,33–35]. Only 1 was shown to be uniquely chloroplastic, and none to be uniquely mitochondrial. Surprisingly 2 aaRSs with the same aa specificity can also be found in the same compartment, although some of these aaRSs show no aminoacylation activity in the organelle [27,36]. Altogether these results show the complexity of aaRSs localization in *A. thaliana* [37].

In algae, the general situation is also 2 aaRS per aa, suggesting that at least one of these is dual targeted. *C. reinhardtii* appears as an exception because for 8 aa species, a single corresponding aaRS gene was found. *C. reinhardtii* is also the green algae with the lowest tRNA gene content in the mt genome (only 3 tRNA genes, see above). The full set of mt tRNAs is provided by extensive tRNA import from the cytosol [20]. A few aaRSs have been detected in the mitochondrial proteome [38]. These results suggest an extensive sharing of tRNAs and aaRSs between *C. reinhardtii* compartments.

In apicomplexans, even though 2 aaRSs can also be found per aa, the situation is clearly different from that in plants. Translation occurs in the cytosol, mitochondria and the apicoplast but neither tRNAs, nor aaRSs are found in mitochondria [39–42]. Hence it is thought that mt tRNAs are imported from the cytosol in an aminoacylated state. This also implies that aaRSs are shared between the apicoplast and the cytosol (Fig. 3B). For most aa, one cognate aaRS is predicted to be targeted to the apicoplast and the other to the cytosol. A few other aaRSs were shown or are predicted to be dual localized in the cytosol and the apicoplast.

A last example is the unicellular marine algae chlorarachniophytes. This algae has 4 genome-containing compartments due to the presence of a secondary plastid and a relic nucleus derived from the green algal endosymbiont. The relic nucleus, called nucleomorph, is located in a residual cytoplasm named the periplastidial compartment (PPC). The localization of 3 HisRSs and 2 GlyRSs has been studied in *Bigelowiella natans* [43]. One HisRS was located in the cytosol, the second in the PPC and the third one is dual targeted to mitochondria and plastids. One GlyRS is mt and plastidial, the other one is cyto. None are found in PPC. Moreover the nucleomorph in PPC does not contain tRNA^{Gly} sequences, and import of charged tRNA^{Gly} is suggested [43].

These few examples illustrate the complexity of aaRS localization and sharing in organisms with 3 (or more) translating compartments.

3.2.2. In protozoans, fungi and metazoans

The endosymbiotic origin of mitochondria is still under debate. While phylogeny with the α-proteobacteria can be easily retraced for nucleus-encoded genes of the mt respiratory chain, the ancestral "proto-mitochondrial" aaRS genes *a priori* re-targeted to the nuclear genome do not cluster with the α-proteobacteria clade due to horizontal gene transfer, gene deletion or extensive duplication [2]. When looking at genomes of different metazoans, one can see that the general trend seems to be having 2 genes encoding one cyto and one mt aaRS rather than having one gene encoding both the cyto and mt aaRS. When comparing the fungi *S. cerevisiae*, the mammalian *Homo sapiens* and the trypanosomatid *T. brucei*, cyto and mt aaRS encoded by a single gene are different from species to species. One exception is the Cnidaria *Nematostella vectensis*, which shares features between mammalians and trypanosomatids. It only contains 2 putative mt aaRS (mt PheRS and mt TrpRS) genes in the nuclear genome [44]. Consequently, MTSs were identified in every other cyto aaRS, due to their necessity to be dual localized in absence of additional gene encoding the mt aaRSs. This report

demonstrates that some in-between cases exist in which the loss of almost all mt-aaRSs is followed by the subsequent acquisition of MTSs in their cyto homologs.

Interestingly, one pathway that remains evolutionarily similar from yeast to higher eukaryotes is the absence of a mt GlnRS and a specific pathway for Gln-tRNA^{Gln} biogenesis. As seen in *A. thaliana*, mt-tRNA^{Gln} is aminoacylated by a non-discriminating GluRS (the mt one in mammals [45], the cyto GluRS in yeast [32]). The misacylated Glu-tRNA^{Gln} is further converted into Gln-tRNA^{Gln} by a tRNA-dependent amido-transferase (AdT) named GatCAB (GatFAB in yeast), even though import of cyto tRNA glutamine has been proposed for yeast and human [46,47]. There is a particularly interesting feature of one of the components of the yeast transamidation pathway with respect to dual cyto and mt localization of aa-tRNA-forming enzymes. The pool of cyto GluRS participating in mt tRNA^{Gln} charging is imported inside the organelle without any additional targeting signal nor processing; meaning that both cyto and mt pools of GluRS originate from the same cyto translational product and have therefore the same exact aa sequence [32].

In the model organism *S. cerevisiae*, aaRSs are also encoded by the nuclear genome (Fig. 3C). Commonly, this genome contains one gene coding for the cyto aaRS, and another coding for the mt version. This is the case for Trp- [48], Thr- [49], Phe- [50], Leu- [51], Met- [52], Lys- [53], Ile-, Glu-, Arg- [54], Tyr- [55] and AspRS [56]. As for SerRS, ProRS, AsnRS and CysRS they are only shown as putative mt proteins since no work highlighting their real localization was done. But they can also display some differences. For example, cyto PheRS consists of two subunits whereas the mt version has only one subunit and lacks the editing domain [57]. Other exceptions exist: *HTS1* and *VAS1* encode both the cyto and mt HisRS and ValRS respectively [58,59]. These aaRSs are encoded by transcripts harboring different 5′ ends with two alternative in-frame AUG initiation codons: the shorter variant coding for the cyto enzyme and the longer (harboring the MTS sequence) coding for the mt enzyme, a situation often found in plants. Cyto and mt GlyRS and AlaRS are also encoded both by a single gene, but mt GlyRS and mt AlaRS are subjected to alternative translational start [60,61]. Two genes, *GRS1* and *GRS2*, encode GlyRS, but only *GRS1* encodes the mt and cyto isoforms. *GRS2* has been shown to encode a heat stress inducible GlyRS which is more stable and has a lower K_M value for tRNA^{Gly} than the GlyRS1 at 37 °C [62].

In *H. sapiens*, 17 nuclear genes encode mt aaRSs with predicted *bona fide* MTS [63]. These are Met, Leu, Ile, Val, Ser, Pro, Thr, Ala, Tyr, His, Asn, Asp, Glu, Cys, Trp, Phe and Arg (Fig. 3D). It is to be noted that in 2008, Rorbach et al. [64] confirmed *in vivo* that *VARS2* was encoding a mt protein. There are 2 examples of cyto and mt aaRSs isoforms encoded by a single nuclear-gene, namely the human mt GlyRS and the human mt LysRS: i) human mt GlyRS is synthesized from an alternative translational initiation [65]; ii) human mt LysRS transcript is subjected to alternative splicing. Upon splicing, the longer variant gives the mt protein whereas the shorter gives the cyto one [66]. This enzyme is further cleaved upon mt import to give the mature human mt LysRS form [67].

Trypanosomatids are an extreme example of gene transfer from mitochondria to the nucleus. As stated above, unlike in eukaryotes, all tRNA genes were transferred to the nuclear genome and this was accompanied, in *T. brucei*, with the transfer of all aaRS genes to the nuclear genome. Nevertheless, the nuclear genome of *T. brucei* only encodes for 23 aaRSs [68] (Fig. 3E), meaning that almost all aaRSs require a strategy to be dual localized. This was well studied in the case of *T. brucei* IleRS, GluRS and GlnRS, where cyto and mt proteins are produced through alternative *trans*-splicing of the messenger RNA. In these cases, the major long variant allows production of the mt form displaying an MTS, the second produces a shorter variant corresponding to the cyto form [46,69]. *T. brucei* mt TrpRS, AspRS and LysRS are encoded by a specific single gene and are not subjected to any trans-splicing or alternative translation-start. Further *in silico* analyses [46], adapted from *in vivo* studies, showed that Asn-, Pro-, Phe(α)-, Ser-, Ala-, Thr-, Met- and CysRS are translated from alternatively spliced mRNAs transcribed from single genes to express both mt and cyto forms. The remaining aaRSs (Arg-, Gly-, Val-, Phe(β)-, Leu-, Tyr- and HisRS) display no alternative splicing sites and might rather be subjected to alternative translation start [70,71].

Altogether these data point to the fact that from Trypanosomatids to Metazoans, all aaRS genes were transferred from the mt to the nuclear genome. Species then developed their own strategy to express and target each aaRS to the mitochondria. This was followed by many re-arrangements leading to the complex situation that we can observe nowadays.

3.2.3. Alternate functions

3.2.3.1. In photosynthetic organisms. Although gene characterization and subcellular localization have been extensively studied in plants, no work has focused on potential alternative functions for plants aaRSs inside their respective compartments. The vast diversity of additional functions acquired by aaRSs in Metazoa, discussed below, might reflect a similar pattern for plant aaRSs. As an example, the GlyRS1 of *A. thaliana* and *Phaseolus vulgaris* is both cyto and mt but is only active for cyto Gly-tRNA^{Gly} formation [36]. The role of this inactive GlyRS1 remains in question, since GlyRS2 aminoacylates the mt tRNA^{Gly}. This evidence remains insufficient, but careful analysis of each aaRS should unravel their potential alternative roles in plants. This could open a new field of research and lead to a better integration of biological pathways within the plant cell.

3.2.3.2. In yeast and metazoan. Group I introns are self-splicing non-coding nuclear and organellar RNAs. Even though they have an autocatalytic activity, they require the involvement of proteins partners *in vivo*. In *Neurospora crassa* and *Podospora anserina*, one of these cofactors is the mt TyrRS [72]. Genomic analysis and biochemical assays comparing mt TyrRS of different fungal species showed that the bifunctionality of this aaRS is a characteristic of the subphylum *Pezizomycotina* including *Aspergillus nidulans*, and suggests acquisition of this additional role after divergence with the *Saccharomycotina* subphylum [73].

Saccharomycotina subphylum displays another bifunctional mt aaRS. In *S. cerevisiae* and *Saccharomyces douglasii* mt LeuRS is involved in mRNA splicing [51]. This “moonlighting” activity involves the CP1 (connective polypeptide 1) domain, the C-terminus of mt LeuRS and requires participation of the bI4 maturase [74]. Although the human mt genome lacks group I introns, mt LeuRS from *H. sapiens* is able to complement the intron-splicing activity in a yeast strain disrupted for the endogenous mt LeuRS [75].

In human, the HIV-1 virus hijacks the host translational machinery for the production of viral particles. It was first thought that packaging of polyproteins into newly assembled virions relied on the uptake of cyto LysRS and its cognate tRNA^{Lys} [33,76]. However, it was recently shown that human mt LysRS, through its amino-terminal extension, provides a strong scaffold for tRNA$^{Lys}_3$ prior to its interaction with the unprocessed polyprotein GagPol. More especially the catalytic domain of human mt LysRS interacts with the P6- and integrase domains of GagPol. The authors of this discovery also propose that tRNA^{Lys} is contacted by the Reverse Transcriptase domain to further stabilize the complex [77].

Gowher et al. [78] showed that, like in yeast, cytosolic tRNA$^{Lys(cuu)}$ (tRK1) can be imported into human mitochondria. This import is facilitated by the mammalian enolase and mediated by the precursor of human mt LysRS (preKARS2), which has affinity for tRK1.

Some pathogenic mutations reported for human mt aaRSs have a mild effect (if any at all) on their aminoacylation activity, suggesting that they are not related to their aminoacylation activities. Intriguing examples can be found in the literature such as the involvement of mt LysRS and in amyotrophic lateral sclerosis [79]. Other examples include the autosomal recessive disease leukoencephalopathy and the identification of missense mutations in mt AspRS (reviewed in Ref. [80]). One appealing possibility would be that these mutations affect yet unknown non-canonical function(s); therefore the deep characterization and analysis of these mutants would be of great therapeutic interest. The hypothesis of non-canonical function for mt aaRSs would be in line with observations made for their cytosolic homologs. Indeed, numerous studies over the past decade have demonstrated that aside from their canonical/ancestral aminoacylation activities, human cyto aaRSs can fulfill equally important additional tasks upon challenging of the cells by diverse stimuli. They range from translational regulation during immune response [81] to leucine sensing *via* the mTORC1 pathway [82] and many others that are well documented [83–86]. These signaling activities are not only carried by full-length and catalytically active aaRSs but also by splice-variants that are catalytic-null isoforms. These truncated aaRSs or aaRS fragments, also called physiocrines (http://www.atyrpharma.com/physiocrines/), are often used as intracellular regulatory factors but can sometimes be secreted (for a review see Ref. [83]). A recent work lead to the identification of a pool of aaRS gene-derived mRNAs packaged into exosomes, yet the exact role of this set of aaRSs remains to be identified [87].

Finally, it is to be noted that a few studies are highlighting the role of some aaRSs in Insecta mitochondria. One example is the SLIMP (Seryl-tRNA synthetase-like insect mitochondrial protein) identified by Guitart et al. [88], which appears to be a mt protein with essential functions beyond translation.

4. Atypical structural properties of mitochondrial tRNAs and adaptive partnership

Numerous studies on tRNAs have identified common features defining the tRNA canonical structure at different levels: invariant and semi-invariant nucleotides in the primary sequence; D-arm, anticodon arm, variable region, T-arm and acceptor stem allowing the tRNA to adopt a cloverleaf secondary structure and an L-shape tertiary structure stabilized by nine well-defined long-distance interactions (Fig. 4A). Noteworthy are six of these long-distance interactions which build the core of the tRNA molecule. One is inside the T-loop and two bring the D- and the T-loops close to each other. Interestingly, all tRNAs of the different kingdoms adopt this canonical structure except mt ones that display a wide range of unconventional structures and even very unusual tertiary folds (reviewed in *e.g.* Refs. [89,90]). This observation led to the proposal that mt tRNAs are, in some species, 'bizarre' or degenerated when compared to their cyto homologs [91]. Also and as mentioned before, mt translation machinery might either be of dual origin (from nucleus and mitochondria), or of exclusive nuclear origin. Indeed, the set of mt tRNAs is either entirely encoded by the mt DNA (in *e.g.* human), partially encoded by mt DNA and the remaining ones imported from the cytosol (in *e.g. A. thaliana*) or totally imported (*e.g. T. brucei*) [4]. In every situation however, partner proteins are encoded in the nucleus and imported from the cytosol, raising issues about adaptive partnership.

The present part aims to address two questions: how degenerated (or not) are the mt tRNAs? And, how mt tRNAs partner proteins have adapted to this degeneracy? For the sake of simplicity, our analysis is mainly focusing on mt $tRNA^{Ser}$ which nicely exemplifies the large structural variability of mt tRNAs throughout the Tree of Life.

4.1. How degenerated are mitochondrial tRNAs?

All mt tRNAs from plants, fungi and protozoans display canonical secondary structures, despite the existence of few differences in common signature motifs [92,93] (Fig. 4B). The only exception described so far is mt $tRNA^{Met}$ from *Tetrahymena pyriformis* and *Paramecium primaurelia*, characterized by the absence of canonical nucleotides in D-arm and an atypical structure [94,95].

In metazoans, mt tRNAs are mainly non-canonical and lack some or most of the common features. Metazoans usually have two mt $tRNA^{Ser}$ isoacceptors, one of them commonly lacks its D-arm (Fig. 4C and D) (except mt $tRNAs^{Ser}$ from some arthropods *e.g. Diaphania pyloalis* [96]). In vertebrates, the second mt $tRNA^{Ser}$ isoacceptor has a cloverleaf-like secondary structure (4 arms with, however, strong deviations from the canonical definition) (Fig. 4C), as it is the case for all mt tRNAs of other specificities [89,97]. The most noticeable exception concerns mt $tRNA^{Cys}$ from Lepidosaurians, which lacks the D-arm as well [98]. In invertebrates, the second mt $tRNA^{Ser}$ isoacceptor is either D-armless (in most species), T-armless (in *e.g.* the nematode *Ascaris suum* [99] Fig. 4D; or the arthropod *Heptathela hangzhouensis* [100]), or cloverleaf-like (in some arthropods as *e.g. D. pyloalis* [96]). This diversity of structures is collectively found in mt tRNAs from other specificities, with most of them lacking the T-arm (in arthropods, nematodes, mollusks, plathelminthes, brachiopods, bryozoans and acanthocephalans [101]). The situation in Enoplea (Nematode) is presently the most puzzling, with most unusual mt tRNAs. For some species, both mt $tRNA^{Ser}$ are D-armless, more than half of the other mt tRNAs are T-armless, and the rest is D- and T-armless. The extreme situation concerns mt $tRNA^{Ala}$, $tRNA^{Cys}$, $tRNA^{Phe}$, $tRNA^{His}$, $tRNA^{Ile}$, $tRNA^{Asn}$, $tRNA^{Arg}$, $tRNA^{Thr}$, $tRNA^{Val}$, and $tRNA^{Tyr}$, which are the smallest functional mt tRNAs, containing only 45 nucleotides (Fig. 4E) ([23,102], this special issue).

Access to native mt tRNAs is difficult because the amount of mt tRNAs is extremely low as compared to the amount of cyto tRNAs in eukaryotic cells. Also, the absence of post-transcriptional modifications within *in vitro* transcribed mt tRNAs was shown to have a drastic incidence on the proper folding of the tRNA [103]. As a consequence, only a few investigations have so far been performed to establish in solution the 2D structures of mt tRNAs and to build models of their 3D structures (*e.g.* Refs. [103–108]). It has also been shown that truncated mt tRNAs of metazoans display more flexibility than their conventional homologs, due to *e.g.* the absence of some long distance interactions between D- and T-loops [108], or the decrease of Mg^{2+} ions binding [90,109]. Thus, 2D representations of mt tRNAs are today mostly established using bioinformatics prediction. The reactivity of these mt atypical structures remains, however, to be proven for several instances. This was the case for the marsupial mitochondrion-encoded $tRNA^{Lys}$ that was first predicted to be D-armless, but experimentally proven to be non functional and compensated by a mt $tRNA^{Lys}$ imported from cytosol and with a typical cloverleaf structure [110,111].

4.2. How have partner proteins been adapted to the degeneracy of mitochondrial tRNAs?

The crystal structure of mt SerRS from *Bos taurus* has been resolved [112] and allowed us to understand the exact mechanism by which both mt $tRNA^{Ser}$ isoacceptors are recognized and aminoacylated [113,114], although these isoacceptors share neither the same structure nor the same anticodon-acceptor inter-stem angle [115]. In fact, mt SerRS possesses an additional N-terminal helix and

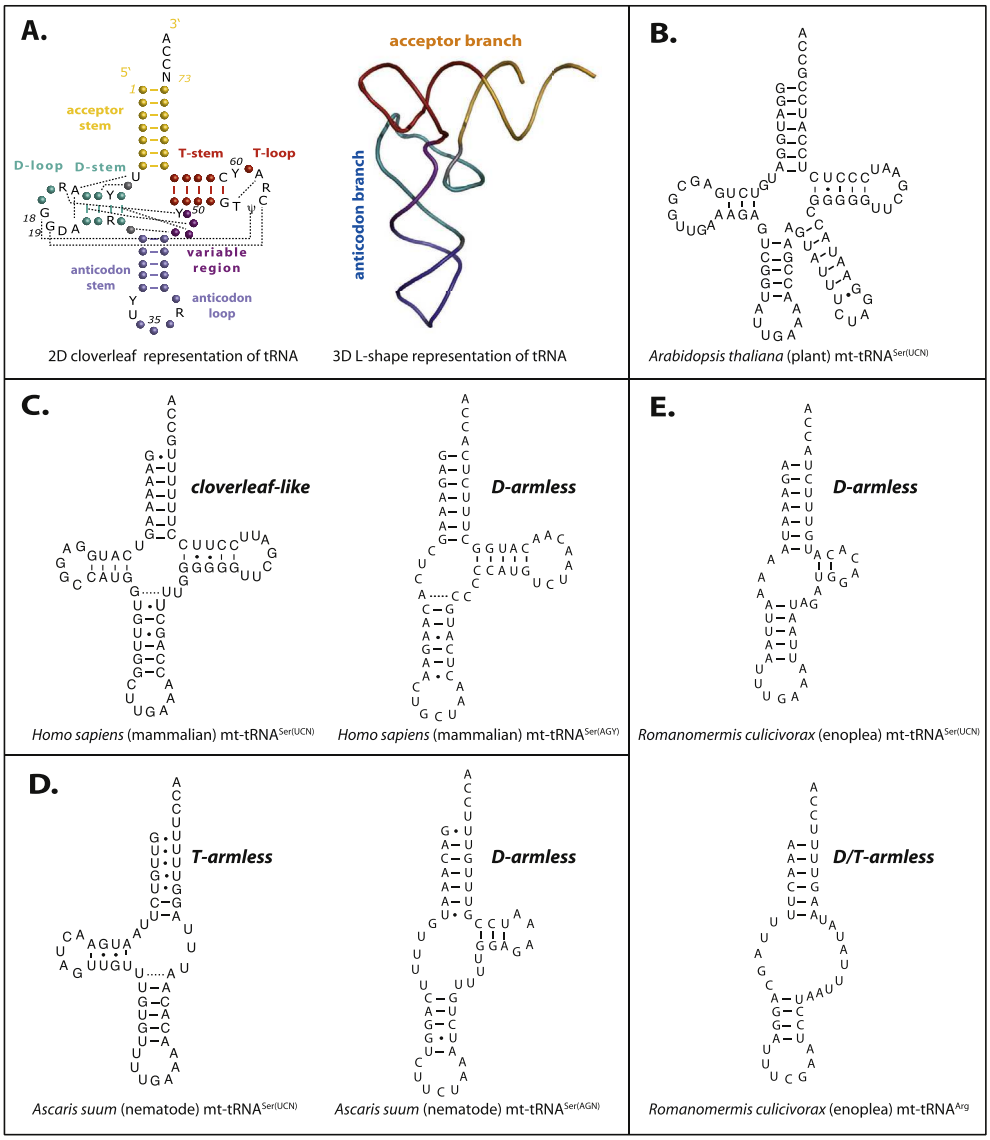

Fig. 4. Atypical structural properties of mitochondrial tRNAs. A) 2D and 3D representations of canonical tRNA [89,90]. tRNA's domains are colored and named. Conserved and semi-conserved nucleotides are indicated. Long distance interactions are displayed using dashed lines. B) Mt $tRNA^{Ser(UCN)}$ from *Arabidopsis thaliana* (taken from http://plantrna.ibmp.cnrs.fr/ [127]), as a representative of the three tRNAs accepting serine in plant mitochondria. Of note, this mt-tRNA displays all canonical features and a long variable region, which is typical for canonical $tRNA^{Ser}$. C and D) Mt $tRNA^{Ser(UCN)}$ and $tRNA^{Ser(AGY)}$ in *Homo sapiens* (as a representative of mammals) and *Ascaris suum* (as a representative of Nematodes), respectively. E) The extreme case of Enoplea (group of Nematodes) is illustrated by the T-armless $tRNA^{Ser(UCN)}$ (from Ref. [7]) and the D/T-armless $tRNA^{Arg}$ (from Ref. [23], this special issue).

a C-terminal extension when compared to its bacterial homolog, and these elements are responsible for the recognition of the two isoacceptors. It has also been shown that the human mt AspRS displays a reduced catalytic efficiency [63], a reduced thermal stability [116], an increased cross-aminoacylation activity (*i.e.* can aminoacylate tRNAs of different origins [117,118]), a more electropositive surface potential, and an increased plasticity [116] compared to its *Escherichia coli* homolog, despite the fact that the two enzymes have common evolutionary ancestry and highly similar tertiary structures [116]. Those functional and physicochemical differences have been suggested to be evolutionary adaptations necessary to accommodate the more flexible and structurally degenerated/relaxed mt tRNAs.

After aminoacylation, mt tRNAs are delivered to the ribosome in order to decode their corresponding codons. The unique mammalian mt EF-Tu recognizes all cloverleaf-like mt tRNAs including the D-armless mt $tRNA^{Ser}$ [119]. In contrast, two mt EF-Tu have been identified in *C. elegans* and *Trichinella spiralis* (Enoplea) [101]. While mt EF-Tu2 recognizes specifically the D-armless mt $tRNA^{Ser}$ in the two organisms, mt EF-Tu1 is specific to the T-armless tRNAs in *C. elegans*, but recognizes mt tRNAs of different structures (cloverleaf-like, lacking D- or T-arm) in *T. spiralis*. Notably, both mt EF-Tu1 and mt EF-Tu2 possess a C-terminal extension (of 57 and 16 aa respectively) absent from canonical EF-Tu. These C-terminal extensions compensate the absence of the tRNA T- or D- arms and keep recognition specificity [120,121]. However, whether the duplication of the mt EF-Tu gene is an adaptation to D- or T-armless tRNAs, or the truncation of tRNAs is an adaptation to mt EF-Tu duplication remains ambiguous. It also remains puzzling why mammals do not have a mt EF-Tu2-like factor specific to the D-armless mt $tRNA^{Ser}$. It has to be mentioned that an EF-Tu pseudogene was discovered in different mammals and could be a remnant of EF-Tu gene duplication [122]. Finally, the persistent existence of two mt EF-Tu in all arthropods [101] may not exclusively account

for the appearance of T-armless tRNAs. Indeed, large combinations of mt tRNAs exist in these organisms (including or excluding T-armless tRNAs): only cloverleaf-like tRNAs (in *e.g. D. pyloalis* [96]), D-armless and cloverleaf-like tRNAs (in *e.g. D. melanogaster* [123]), D- and T-armless tRNAs (in *e.g. Paratemnoides elongatus* [124]), or a mixture of all structures (in *e.g. H. hangzhouensis* [100]).

Truncation of mt RNAs is a hallmark of mt evolution, which tends to be compensated by accretive addition of new domains or extensions to the proteins binding these truncated RNAs (*e.g.* compensation of truncated mt rRNAs by ribosomal proteins [125]). This compensatory interplay is illustrated here by mt SerRS and mt EF-Tu but might plausibly be extended to ribosomal proteins or other unknown RNA-binding proteins.

5. Conclusion

Access to a growing number of sequenced genomes over the past decades has allowed us to explore and analyze content in tRNA genes, aaRS genes, and in mt-related proteins on a large scale. Despite this vast amount of data, the question of how organellar translation is regulated remains poorly understood, because genetic content only gives an incomplete picture of the molecular basis of codon usage, organellar import and protein-tRNA recognition. Large-scale data has made clear that the genomic content of each species has evolved closely to suit its specific environment, but that it nonetheless shares similar patterns between species, such as the dual localization of mt-aaRSs, and the specificity of tRNAs most often retained in the mt genome. These patterns help us to understand the most basic evolutionary adaptations that are necessary to interconnect the mt bacteria-like and eukaryotic translation systems. The challenge of the post-genomic era will be to understand the various layers of crosstalks connecting the mitochondria and the nucleus genomes.

Acknowledgments

The work was supported by the French National Program “Investissement d’Avenir” administered by the “Agence National de la Recherche” (ANR) (“MitoCross” Laboratory of Excellence (Labex), funded as ANR-10-IDEX-0002-02), the University of Strasbourg and the CNRS. L.E. is recipient of a fellowship from the Ministère de l’Education Nationale, de la Recherche et de la Technologie. C.M., L.K. and D.L. are recipients of doctoral fellowship and J.L.H. is recipient of a postdoctoral fellowship, all four supported by the ANR-10-IDEX-0002-02 “Investissements d’Avenir” program.

References

[1] M.W. Gray, G. Burger, B.F. Lang, The origin and early evolution of mitochondria, Genome Biol. 2 (2001) 1–5.
[2] B. Brindefalk, J. Viklund, D. Larsson, M. Thollesson, S.G. Andersson, Origin and evolution of the mitochondrial aminoacyl-tRNA synthetases, Mol. Biol. Evol. 24 (2007) 743–756.
[3] H. Schwenzer, G.C. Scheper, N. Zorn, L. Moulinier, A. Gaudry, E. Leize, F. Martin, C. Florentz, O. Poch, M. Sissler, Released selective pressure on a structural domain gives new insights on the functional relaxation of mitochondrial aspartym-tRNA synthetase, Biochimie 100 (2014) 18–26.
[4] A. Schneider, Mitochondrial tRNA import and its consequences for mitochondrial translation, Annu. Rev. Biochem. 80 (2011) 1033–14053.
[5] T. Abe, T. Ikemura, J. Sugahara, A. Kanai, Y. Ohara, H. Uehara, M. Kinouchi, S. Kanaya, Y. Yamada, A. Muto, H. Inokuchi, tRNADB-CE 2011: tRNA gene database curated manually by experts, Nucleic Acids Res. 39 (2011) D210–D213.
[6] V. Cognat, G. Pawlak, A.M. Duchêne, M. Daujat, A. Gigant, T. Salinas, M. Michaud, B. Gutmann, P. Giege, A. Gobert, L. Maréchal-Drouard, PlantRNA, a database for tRNAs of photosynthetic eukaryotes, Nucleic Acids Res. 41 (2013) D273–D279.
[7] F. Juhling, J. Putz, C. Florentz, P.F. Stadler, Armless mitochondrial tRNAs in enoplea (nematoda), RNA Biol. 9 (2012) 1161–1166.
[8] F. Sieber, A.M. Duchêne, L. Maréchal-Drouard, Mitochondrial RNA import: from diversity of natural mechanisms to potential applications, Int. Rev. Cell Mol. Biol. 287 (2011) 145–190. Elsevier.
[9] R. Temperley, R. Richter, S. Dennerlein, R.N. Lightowlers, Z.M. Chrzanowska-Lightowlers, Hungry codons promote frameshifting in human mitochondrial ribosomes, Science 327 (2010) 301.
[10] S.A. Shabalina, N.A. Spiridonov, A. Kashina, Sounds of silence: synonymous nucleotides as a key to biological regulation and complexity, Nucleic Acids Res. 41 (2013) 2073–2094.
[11] E. Trotta, Selection on codon bias in yeast: a transcriptional hypothesis, Nucleic Acids Res. 41 (2013) 9382–9395.
[12] H. Zur, T. Tuller, Strong association between mRNA folding strength and protein abundance in *S. cerevisiae*, EMBO Rep. 13 (2012) 272–277.
[13] M.M. Fonseca, S. Rocha, D. Posada, Base-pairing versatility determines wobble sites in tRNA anticodons of vertebrate mitogenomes, PLoS One 7 (2012) e36605.
[14] Z. Sun, L. Ma, R.W. Murphy, X. Zhang, D. Huang, Factors affecting mito-nuclear codon usage interactions in the OXPHOS system of *Drosophila melanogaster*, J. Genet. Genomics 35 (2008) 729–735.
[15] G. Cannarozzi, N.N. Schraudolph, M. Faty, P. von Rohr, M.T. Friberg, A.C. Roth, P. Gonnet, G. Gonnet, Y. Barral, A role for codon order in translation dynamics, Cell 141 (2010) 355–367.
[16] K. Fredrick, M. Ibba, How the sequence of a gene can tune its translation, Cell 141 (2010) 227–229.
[17] M. Bietenhader, A. Martos, E. Tetaud, R.S. Aiyar, C.H. Sellem, R. Kucharczyk, S. Clauder-Münster, M.F. Giraud, F. Godard, B. Salin, I. Sagot, J. Gagneur, M. Déquard-Chablat, V. Contamine, S. Hermann-Le Denmat, A. Sainsard-Chanet, L.M. Steinmetz, J.P. di Rago, Experimental relocation of the mitochondrial ATP9 gene to the nucleus reveals forces underlying mitochondrial genome evolution, PLoS Genet. 8 (2012) e1002876.
[18] E. Perales-Clemente, P. Fernández-Silva, R. Acín-Pérez, A. Pérez-Martos, J.A. Enríquez, Allotopic expression of mitochondrial-encoded genes in mammals: achieved goal, undemonstrated mechanism or impossible task? Nucleic Acids Res. 39 (2011) 225–234.
[19] L. Supekova, F. Supek, J.E. Greer, P.G. Schultz, A single mutation in the first transmembrane domain of yeast COX2 enables its allotopic expression, Proc. Natl. Acad. Sci. U. S. A. 104 (2010) 5047–5052.
[20] E. Vinogradova, T. Salinas, V. Cognat, C. Remacle, L. Maréchal-Drouard, Steady-state levels of imported tRNAs in *Chlamydomonas* mitochondria are correlated with both cytosolic and mitochondrial codon usages, Nucleic Acids Res. 37 (2009) 1521–1528.
[21] L. Yatawara, T.H. Le, S. Wickramasinghe, T. Agatsuma, Maxicircle (mitochondrial) genome sequence (partial) of *Leishmania major*: gene content, arrangement and composition compared with *Leishmania tarentolae*, Gene 424 (2008) 80–86.
[22] M. Michaud, V. Cognat, A.M. Duchêne, L. Maréchal-Drouard, A global picture of tRNA genes in plant genomes, Plant J. 66 (2011) 80–93.
[23] S. Wende, E.G. Platzer, F. Jühling, J. Putz, C. Florentz, P.F. Stadler, M. Mörl, Biological evidence for the world’s smallest tRNAs, Biochimie 100 (2014) 151–158.
[24] T. Lithgow, A. Schneider, Evolution of macromolecular import pathways in mitochondria, hydrogenosomes and mitosomes, Philos. Trans. R. Soc. B 365 (2010) 799–817.
[25] T. Salinas, A.M. Duchêne, L. Maréchal-Drouard, Recent advances in tRNA mitochondrial import, Trends Biochem. Sci. 33 (2008) 320–329.
[26] J.D. Alfonzo, D. Söll, Mitochondrial tRNA import – the challenge to understand has just begun, Biol. Chem. 390 (2009) 717–722.
[27] A.K. Berglund, C. Pujol, A.M. Duchêne, E. Glaser, Defining the determinants for dual targeting of aminoacyl-tRNA synthetases to mitochondria and chloroplasts, J. Mol. Biol. 393 (2009) 803–814.
[28] P. Kamenski, O. Kolesnikova, V. Jubenot, N. Entelis, I.A. Krasheninnikov, R.P. Martin, I. Tarassov, Evidence for an adaptation mechanism of mitochondrial translation via tRNA import from the cytosol, Mol. Cell 26 (2007) 625–637.
[29] R.G. Dorrell, C.J. Howe, What makes a chloroplast? Reconstructing the establishment of photosynthetic symbioses, J. Cell Sci. 125 (2012) 1865–1875.
[30] C.V. Morgante, R.A. Rodrigues, P.A. Marbach, C.M. Borgonovi, D.S. Moura, M.C. Silva-Filho, Conservation of dual-targeted proteins in Arabidopsis and rice points to a similar pattern of gene-family evolution, Mol. Genet. Genomics 281 (2009) 525–538.
[31] C. Pujol, M. Bailly, D. Kern, L. Maréchal-Drouard, H. Becker, A.M. Duchêne, Dual-targeted tRNA-dependent amidotransferase ensures both mitochondrial and chloroplastic Gln-tRNA^{Gln} synthesis in plants, Proc. Natl. Acad. Sci. U. S. A. 105 (2008) 6481–6485.
[32] M. Frechin, A.M. Duchêne, H.D. Becker, Translating organellar glutamine codons: a case by case scenario? RNA Biol. 6 (2009) 31–34.
[33] U. Ahting, C. Thun, R. Hegerl, D. Typke, F.E. Nargang, W. Neupert, S. Nussberger, The TOM core complex: the general protein import pore of the outer membrane of mitochondria, J. Cell Biol. 147 (1999) 959–968.
[34] A.M. Duchêne, A. Giritch, B. Hoffmann, V. Cognat, D. Lancelin, N.M. Peeters, M. Zaepfel, L. Maréchal-Drouard, I.D. Small, Dual targeting is the rule for organellar aminoacyl-tRNA synthetases in *Arabidopsis thaliana*, Proc. Natl. Acad. Sci. U. S. A. 102 (2005) 16484–16489.
[35] M.M. Brandao, M.C. Silva-Filho, Evolutionary history of *Arabidopsis thaliana* aminoacyl-tRNA synthetase dual-targeted proteins, Mol. Biol. Evol. 28 (2011) 79–85.

[36] A.M. Duchêne, N. Peeters, A. Dietrich, A. Cosset, I.D. Small, H. Wintz, Overlapping destinations for two dual targeted glycyl-tRNA synthetases in *Arabidopsis thaliana* and *Phaseolus vulgaris*, J. Biol. Chem. 276 (2001) 15275–15283.

[37] K. Hammani, G. Bonnard, A. Bouchoucha, A. Gobert, F. Pinsker, T. Salinas, P. Giegé, Helical repeats modular proteins are major players for organelle gene expression, Biochimie 100 (2014) 141–150.

[38] A. Atteia, A. Adrait, S. Brugiere, M. Tardif, R. van Lis, O. Deusch, T. Dagan, L. Kuhn, B. Gontero, W. Martin, J. Garin, J. Joyard, N. Rolland, A proteomic survey of *Chlamydomonas reinhardtii* mitochondria sheds new light on the metabolic plasticity of the organelle and on the nature of the alpha-proteobacterial mitochondrial ancestor, Mol. Biol. Evol. 26 (2009) 1533–1548.

[39] A. Gupta, A. Haider, S. Vaishya, S. Habib, Translation in mitochondria and apicoplasts of apicomplexan parasites, in: D. A. M. (Ed.), Translation in Mitochondria and Other Organelles, Springer, 2013, pp. 159–179.

[40] P. Pino, E. Aeby, B.J. Foth, L. Sheiner, T. Soldati, A. Schneider, D. Soldati-Favre, Mitochondrial translation in absence of local tRNA aminoacylation and methionyl tRNA Met formylation in Apicomplexa, Mol. Microbiol. 76 (2010) 706–718.

[41] K.E. Jackson, S. Habib, M. Frugier, R. Hoen, S. Khan, J.S. Pham, L. Ribas de Pouplana, M. Royo, M.A. Santos, A. Sharma, S.A. Ralph, Protein translation in *Plasmodium* parasites, Trends Parasitol. 27 (2011) 467–476.

[42] K.E. Jackson, J.S. Pham, M. Kwek, N.S. De Silva, S.M. Allen, C.D. Goodman, G.I. McFadden, L.R. de Pouplana, S.A. Ralph, Dual targeting of aminoacyl-tRNA synthetases to the apicoplast and cytosol in *Plasmodium falciparum*, Int. J. Parasitol. 42 (2012) 177–186.

[43] Y. Hirakawa, F. Burki, P.J. Keeling, Dual targeting of aminoacyl-tRNA synthetases to the mitochondrion and complex plastid in chlorarachniophytes, J. Cell Sci. 125 (2012) 6176–6184.

[44] K.M. Haen, W. Pett, D.V. Lavrov, Parallel loss of nuclear-encoded mitochondrial aminoacyl-tRNA synthetases and mt DNA-encoded tRNAs in Cnidaria, Mol. Biol. Evol. 27 (2010) 2216–2219.

[45] A. Nagao, T. Suzuki, T. Katoh, Y. Sakaguchi, Biogenesis of glutaminyl-mt $tRNA^{Gln}$ in human mitochondria, Proc. Natl. Acad. Sci. U. S. A. 106 (2009) 16209–16214.

[46] J. Rinehart, E.K. Horn, D. Wei, D. Soll, A. Schneider, Non-canonical eukaryotic glutaminyl- and glutamyl-tRNA synthetases form mitochondrial aminoacyl-tRNA in *Trypanosoma brucei*, J. Biol. Chem. 279 (2004) 1161–1166.

[47] M.A. Rubio, J.J. Rinehart, B. Krett, S. Duvezin-Caubet, A.S. Reichert, D. Soll, J.D. Alfonzo, Mammalian mitochondria have the innate ability to import tRNAs by a mechanism distinct from protein import, Proc. Natl. Acad. Sci. U. S. A. 105 (2008) 9186–9191.

[48] A.M. Myers, A. Tzagoloff, MSW, a yeast gene coding for mitochondrial tryptophanyl-tRNA synthetase, J. Biol. Chem. 260 (1985) 15362–15370.

[49] L.K. Pape, T.J. Koerner, A. Tzagoloff, Characterization of a yeast nuclear gene (MST1) coding for the mitochondrial threonyl-tRNA1 synthetase, J. Biol. Chem. 260 (28) (1985) 15362–15370.

[50] T.J. Koerner, A.M. Myers, S. Lee, A. Tzagoloff, Isolation and characterization of the yeast gene coding for the a subunit of mitochondrial phenylalanyl-tRNA synthetase, J. Biol. Chem. 262 (1987) 3690–3696.

[51] C.J. Herbert, M. Labouesse, G. Dujardin, P. Slonimski, The NAM2 proteins from *Saccharomyces cerevisiae* and *Spiraea douglasii* are mitochondrial leucyl-tRNA synthetases, and are involved in mRNA splicing, EMBO J. 7 (1988) 473–483.

[52] A. Tzagoloff, A. Vambutas, A. Akai, Characterization of MSM1, the structural gene for yeast mitochondrial methionyl-tRNA synthetase, Eur. J. Biochem. 179 (1989) 365–371.

[53] D.L. Gatti, A. Tzagaloff, Structure of a group of related aminoacyl-tRNA synthetases, J. Mol. Biol. 218 (1991) 557–568.

[54] A. Tzagoloff, A. Shtanko, Mitochondrial and cytoplasmic isoleucyl-, glutamyl and arginyl-tRNA synthetases of yeast are encoded by separated genes, Eur. J. Biochem. 230 (1995) 582–586.

[55] C.M. Chow, U.L. RajBhandary, *Saccharomyces cerevisiae* cytoplasmic tyrosyl-tRNA synthetase gene. Isolation by complementation of a mutant *Escherichia coli* suppressor tRNA defective in aminoacylation and sequence analysis, J. Biol. Chem. 268 (1993) 12855–12863.

[56] I. Landrieu, M. Vandenbol, M. Hartlein, D. Portetelle, Mitochondrial asparaginyl-tRNA synthetase is encoded by the yeast nuclear gene YCR24c, Eur. J. Biochem. 243 (1997) 268–273.

[57] A. Sanni, C. Houtondji, S. Blanquet, J.-P. Ebel, Y. Boulanger, F. Fasiolo, Interaction of the tRNA(Phe) acceptor end with the synthetase involves a sequence common to yeast and *Escherichia coli* phenylalanyl-tRNA synthetases, Biochemistry 30 (1991) 2448–2453.

[58] X. Jordana, B. Chatton, M. Paz-Weisshaar, J.M. Buhler, F. Cramer, J.P. Ebel, F. Fasiolo, Structure of the yeast valyl-tRNA synthetase gene (VASI) and the homology of its translated amino acid sequence with *Escherichia coli* isoleucyl-tRNA synthetase, J. Biol. Chem. 262 (1987) 7189–7194.

[59] G. Natsoulis, F. Hilger, G.R. Fink, The HTS1 gene encodes both the cytoplasmic and mitochondrial histidine tRNA synthetases of *S. cerevisiae*, Cell 46 (1986) 235–243.

[60] H.L. Tang, L.S. Yeh, N.K. Chen, T. Ripmaster, P. Schimmel, C.C. Wang, Translation of a yeast mitochondrial tRNA synthetase initiated at redundant non-AUG codons, J. Biol. Chem. 279 (2004) 49656–49663.

[61] R.J. Turner, M. Lovato, P. Schimmel, One of two genes encoding glycyl-tRNA synthetase in *Saccharomyces cerevisiae* provides mitochondrial and cytoplasmic functions, J. Biol. Chem. 275 (2000) 27681–27688.

[62] S.J. Chen, Y.H. Wu, H.Y. Huang, C.C. Wang, *Saccharomyces cerevisiae* possesses a stress-inducible glycyl-tRNA synthetase gene, PLoS One 7 (2012) e33363.

[63] L. Bonnefond, A. Fender, J. Rudinger-Thirion, R. Giegé, C. Florentz, M. Sissler, Towards the full set of human mitochondrial aminoacyl-tRNA synthetases: characterization of AspRS and TyrRS, Biochemistry 44 (2005) 4805–4816.

[64] J. Rorbach, A.A. Yusoff, H. Tuppen, D.P. Abg-Kamaludin, Z.M. Chrzanowska-Lightowlers, R.W. Taylor, D.M. Turnbull, R. McFarland, R.N. Lightowlers, Overexpression of human mitochondrial valyl tRNA synthetase can partially restore levels of cognate mt-tRNAVal carrying the pathogenic C25U mutation, Nucleic Acids Res. 36 (2008) 3065–3074.

[65] K. Shiba, P. Schimmel, H. Motegi, T. Noda, Human glycyl-tRNA synthetase. Wide divergence of primary structure from bacterial counterpart and species-specific aminoacylation, J. Biol. Chem. 269 (1994) 30049–30055.

[66] E. Tolkunova, H. Park, J. Xia, M.P. King, E. Davidson, The human lysyl-tRNA synthetase gene encodes both the cytoplasmic and mitochondrial enzymes by means of an unusual splicing of the primary transcript, J. Biol. Chem. 275 (2000) 35063–35069.

[67] J. Dias, G. Octobre, L. Kobbi, M. Comisso, S. Flisiak, M. Mirande, Activation of human mitochondrial lysyl-tRNA synthetase upon maturation of its pre-mitochondrial precursor, Biochemistry 51 (2012) 909–916.

[68] M. Berriman, E. Ghedin, C. Hertz-Fowler, G. Blandin, H. Renauld, D.C. Bartholomeu, N.J. Lennard, E. Caler, N.E. Hamlin, B. Haas, U. Böhme, L. Hannick, M.A. Aslett, J. Shallom, L. Marcello, L. Hou, B. Wickstead, U.C. Alsmark, C. Arrowsmith, R.J. Atkin, A.J. Barron, F. Bringaud, K. Brooks, M. Carrington, I. Cherevach, T.J. Chillingworth, C. Churcher, L.N. Clark, C.H. Corton, A. Cronin, R.M. Davies, J. Doggett, A. Djikeng, T. Feldblyum, M.C. Field, A. Fraser, I. Goodhead, Z. Hance, D. Harper, B.R. Harris, H. Hauser, J. Hostetler, A. Ivens, K. Jagels, D. Johnson, J. Johnson, K. Jones, A.X. Kerhornou, H. Koo, N. Larke, S. Landfear, C. Larkin, V. Leech, A. Line, A. Lord, A. Macleod, P.J. Mooney, S. Moule, D.M. Martin, G.W. Morgan, K. Mungall, H. Norbertczak, D. Ormond, G. Pai, C.S. Peacock, J. Peterson, M.A. Quail, E. Rabbinowitsch, M.A. Rajandream, C. Reitter, S.L. Salzberg, M. Sanders, S. Schobel, S. Sharp, M. Simmonds, A.J. Simpson, L. Tallon, C.M. Turner, A. Tait, A.R. Tivey, S. Van Aken, D. Walker, D. Wanless, S. Wang, B. White, O. White, S. Whitehead, J. Woodward, J. Wortman, M.D. Adams, T.M. Embley, K. Gull, E. Ullu, J.D. Barry, A.H. Fairlamb, F. Opperdoes, B.G. Barrell, J.E. Donelson, N. Hall, C.M. Fraser, S.E. Melville, N.M. El-Sayed, The genome of the African trypanosome *Trypanosoma brucei*, Science 309 (2005) 416–422.

[69] J. Rettig, Y. Wang, A. Schneider, T. Ochsenreiter, Dual targeting of isoleucyl-tRNA synthetase in *Trypanosoma brucei* is mediated through alternative trans-splicing, Nucleic Acids Res. 40 (2012) 1299–1306.

[70] N.G. Kolev, J.B. Franklin, S. Carmi, H. Shi, S. Michaeli, C. Tschudi, The transcriptome of the human pathogen *Trypanosoma brucei* at single-nucleotide resolution, PLoS Pathog. 6 (2010) e1001090.

[71] T.N. Siegel, D.R. Hekstra, X. Wang, S. Dewell, G.A. Cross, Genome-wide analysis of mRNA abundance in two life-cycle stages of *Trypanosoma brucei* and identification of splicing and polyadenylation sites, Nucleic Acids Res. 38 (2010) 4946–4957.

[72] U. Kamper, U. Kuck, A.D. Cherniack, A.M. Lambowitz, The mitochondrial tyrosyl-tRNA synthetase of *Podospora anserina* is a bifunctional enzyme active in protein synthesis and RNA splicing, Mol. Cell. Biol. 12 (1992) 499–511.

[73] P.J. Paukstelis, A.M. Lambowitz, Identification and evolution of fungal mitochondrial tyrosyl-tRNA synthetases with group I intron splicing activity, Proc. Natl. Acad. Sci. U. S. A. 105 (2008) 6010–6015.

[74] S.B. Rho, T.L. Lincecum Jr., S.A. Martinis, An inserted region of leucyl-tRNA synthetase plays a critical role in group I intron splicing, EMBO J. 21 (2002) 6874–6881.

[75] F. Houman, S.B. Rho, J. Zhang, X. Shen, C.-C. Wang, P. Schimmel, S.A. Martinis, A prokaryote and human tRNA synthetase provide an essential RNA splicing function in yeast mitochondria, Proc. Natl. Acad. Sci. U. S. A. 97 (2000) 13743–13748.

[76] M. Kaminska, V. Shalak, M. Francin, M. Mirande, Viral hijacking of mitochondrial lysyl-tRNA synthetase, J. Virol. 81 (2007) 68–73.

[77] L. Kobbi, G. Octobre, J. Dias, M. Comisso, M. Mirande, Association of mitochondrial Lysyl-tRNA synthetase with HIV-1 GagPol involves catalytic domain of the synthetase and transframe and integrase domains of Pol, J. Mol. Biol. 410 (2011) 875–886.

[78] A. Gowher, A. Smirnov, I. Tarassov, N. Entelis, Induced tRNA import into human mitochondria: implication of a host aminoacyl-tRNA-synthetase, PLoS One 8 (2013) e66228.

[79] H. Kawamata, J. Magrané, C. Kunst, M.P. King, G. Manfredi, Lysyl-tRNA synthetase is a target for mutant SOD1 toxicity in mitochondria, J. Biol. Chem. 283 (2008) 28321–28328.

[80] H. Schwenzer, J. Zoll, C. Florentz, M. Sissler, Pathogenic implications of human mitochondrial aminoacyl-tRNA synthetases, Top. Curr. Chem. (2013), (Epub ahead of print).

[81] A. Arif, J. Jia, R. Mukhopadhyay, B. Willard, M. Kinter, P.L. Fox, Two-site phosphorylation of EPRS coordinates multimodal regulation of noncanonical translational control activity, Mol. Cell 35 (2009) 164–180.

[82] J.M. Han, S.J. Jeong, M.C. Park, G. Kim, N.H. Kwon, H.K. Kim, S.H. Ha, S.H. Ryu, S. Kim, Leucyl-tRNA synthetase is an intracellular leucine sensor for the mTORC1-signaling pathway, Cell 149 (2012) 410–424.
[83] M. Guo, P. Schimmel, Essential nontranslational functions of tRNA synthetases, Nat. Chem. Biol. 9 (2013) 145–153.
[84] M. Guo, X.L. Yang, P. Schimmel, New functions of aminoacyl-tRNA synthetases beyond translation, Nat. Rev. Mol. Cell. Biol. 11 (2010) 668–674.
[85] C.D. Hausmann, M. Ibba, Aminoacyl-tRNA synthetase complexes: molecular multitasking revealed, FEMS Microbiol. Rev. 32 (2008) 705–721.
[86] E.V. Smirnova, V.A. Lakunina, I. Tarassov, I.A. Krasheninnikov, P.A. Kamenski, Noncanonical functions of aminoacyl-tRNA synthetases, Biochemistry (Moscow) 77 (2012) 15–25.
[87] F. Wang, Z. Xu, J. Zhou, W.S. Lo, C.F. Lau, L.A. Nangle, X.L. Yang, M. Zhang, P. Schimmel, Regulated capture by exosomes of mRNAs for cytoplasmic tRNA synthetases, J. Biol. Chem. 288 (2013) 29223–29228.
[88] T. Guitart, T. Leon Bernardo, J. Sagalés, T. Stratmann, J. Bernués, L. Ribas de Pouplana, New aminoacyl-tRNA synthetase-like protein in insecta with an essential mitochondrial function, J. Biol. Chem. 285 (2010) 38157–38166.
[89] G. Dirheimer, G. Keith, P. Dumas, E. Westhof, Primary, secondary, and tertiary structures of tRNAs, in: D. Söll, U.L. RajBhandary (Eds.), tRNA: Structure, Biosynthesis, and Function, American Society for Microbiology, Washington DC, 1995, pp. 93–126.
[90] R. Giegé, F. Juhling, J. Pütz, P. Stadler, C. Sauter, C. Florentz, Structure of transfer RNAs: similarity and variability, Wiley Interdiscip. Rev. RNA 3 (2012) 37–61.
[91] M. Helm, H. Brulé, D. Friede, R. Giegé, J. Pütz, C. Florentz, Search for characteristic structural features of mammalian mitochondrial tRNAs, RNA 6 (2000) 1356–1379.
[92] D.O. Clary, J.M. Goddard, S.C. Martin, C.M. Fauron, D.R. Wolstenholme, Drosophila mitochondrial DNA: a novel gene order, Nucleic Acids Res. 10 (1982) 6619–6637.
[93] L. Maréchal-Drouard, J.H. Weil, A. Dietrich, Transfer-RNAs and transfer-RNA genes in plants, Annu. Rev. Plant Physiol. 44 (1993) 13–32.
[94] J.J. Seilhamer, D.J. Cummings, Structure and sequence of the mitochondrial 20S rRNA and tRNA^{Tyr} gene of *Paramecium primaurelia*, Nucleic Acids Res. 9 (1981) 6391–6406.
[95] M.N. Schnare, S.J. Greenwood, M.W. Gray, Primary sequence and post-transcriptional modification pattern of an unusual mitochondrial tRNA^{Met} from *Tetrahymena pyriformis*, FEBS Lett. 362 (1995) 24–28.
[96] B.J. Zhu, Q.N. Liu, L.S. Dai, L. Wang, Y. Sun, K.Z. Lin, G.Q. Wei, C.L. Liu, Characterization of the complete mitochondrial genome of *Diaphania pyloalis* (Lepidoptera: Pyralididae), Gene 527 (2013) 283–291.
[97] T. Ueda, T. Ohta, K. Watanabe, Large scale isolation and some properties of AGY-specific serine tRNA from bovine heart mitochondria, J. Biochem. 98 (1985) 1275–1284.
[98] J.R. Macey, A. Larson, N.B. Ananjeva, T.J. Papenfuss, Evolutionary shifts in three major structural features of the mitochondrial genome among iguanian lizards, J. Mol. Evol. 44 (1997) 660–674.
[99] D.R. Wolstenholme, J.L. Macfarlane, R. Okimoto, D.O. Clary, J.A. Wahleithner, Bizarre tRNAs inferred from DNA sequences of mitochondrial genomes of nematode worms, Proc. Natl. Acad. Sci. U. S. A. 84 (1987) 1324–1328.
[100] Y. Qiu, D. Song, K. Zhou, H. Sun, The mitochondrial sequences of *Heptathela hangzhouensis* and *Ornithoctonus huwena* reveal unique gene arrangements and atypical tRNAs, J. Mol. Evol. 60 (2005) 57–71.
[101] T. Ohtsuki, Y. Watanabe, T-armless tRNAs and elongated elongation factor Tu, IUBMB Life 59 (2007) 68–75.
[102] M. Bernt, A. Donath, F. Juhling, F. Externbrink, C. Florentz, G. Fritzsch, J. Pütz, M. Middendorf, P.F. Stadler, MITOS: improved de novo metazoan mitochondrial genome annotation, Mol. Phylogenet. Evol. 69 (2013) 313–319.
[103] M. Helm, H. Brulé, F. Degoul, C. Cepanec, J.-P. Leroux, R. Giegé, C. Florentz, The presence of modified nucleotides is required for cloverleaf folding of a human mitochondrial tRNA, Nucleic Acids Res. 26 (1998) 1636–1643.
[104] M.H.L. de Bruijn, A. Klug, A model for the tertiary structure of mammalian mitochondrial transfer RNAs lacking the entire 'dihydrouridine' loop and stem, EMBO J. 2 (1983) 1309–1321.
[105] M. Helm, R. Giegé, C. Florentz, A Watson–Crick base-pair disrupting methyl group (m^1A9) is sufficient for cloverleaf folding of human mitochondrial tRNA^{Lys}, Biochemistry 38 (1999) 13338–13346.
[106] L.M. Wittenhagen, M.D. Roy, S.O. Kelley, The pathogenic U3271C human mitochondrial tRNA$^{Leu(UUR)}$ mutation disrupts a fragile anticodon stem, Nucleic Acids Res. 31 (2003) 596–601.
[107] R. Hao, M.W. Zhao, Z.X. Hao, Y.N. Yao, E.D. Wang, A T-stem slip in human mitochondrial tRNA$^{Leu(CUN)}$ governs its charging capacity, Nucleic Acids Res. 33 (2005) 3606–3613.
[108] M. Messmer, J. Pütz, T. Suzuki, T. Suzuki, C. Sauter, M. Sissler, C. Florentz, Tertiary network in mammalian mitochondrial tRNA^{Asp} revealed by solution probing and phylogeny, Nucleic Acids Res. 37 (2009) 6881–6895.
[109] A.A. Frazer-Abel, P.J. Hagerman, Variation of the acceptor-anticodon interstem angles among mitochondrial and non-mitochondrial tRNAs, J. Mol. Biol. 343 (2004) 313–325.
[110] A. Janke, G. Feldmaier-Fuchs, W.K. Thomas, A. von Haeseler, S. Paabo, The marsupial mitochondrial genome and the evolution of placental mammals, Genetics 137 (1994) 243–256.
[111] M. Dorner, M. Altmann, S. Paabo, M. Morl, Evidence for import of a lysyl-tRNA into marsupial mitochondria, Mol. Biol. Cell 12 (2001) 2688–2698.
[112] S. Chimnaronk, M. Gravers Jeppesen, T. Suzuki, J. Nyborg, K. Watanabe, Dual-mode recognition of noncanonical tRNAs^{Ser} by seryl-tRNA synthetase in mammalian mitochondria, EMBO J. 24 (2005) 3369–3379.
[113] N. Shimada, T. Suzuki, K. Watanabe, Dual mode recognition of two isoacceptor tRNAs by mammalian mitochondrial seryl-tRNA synthetase, J. Biol. Chem. 276 (2001) 46770–46778.
[114] T. Hanada, T. Suzuki, T. Yokogawa, C. Takemoto-Hori, M. Sprinzl, K. Watanabe, Translation ability of mitochondrial tRNAs^{Ser} with unusual secondary structures in an *in vitro* translation system of bovine mitochondria, Genes Cells 6 (2001) 1019–1030.
[115] A.A. Frazer-Abel, P.J. Hagerman, Determination of the angle between the acceptor and anticodon stems of a truncated mitochondrial tRNA, J. Mol. Biol. 285 (1999) 581–593.
[116] A. Neuenfeldt, B. Lorber, E. Ennifar, A. Gaudry, C. Sauter, M. Sissler, C. Florentz, Thermodynamic properties distinguish human mitochondrial aspartyl-tRNA synthetase from bacterial homolog with same 3D architecture, Nucleic Acids Res. 41 (2013) 2698–2708.
[117] Y. Kumazawa, H. Himeno, K. Miura, K. Watanabe, Unilateral aminoacylation specificity between bovine mitochondria and eubacteria, J. Biochem. 109 (1991) 421–427.
[118] A. Fender, A. Gaudry, F. Juhling, M. Sissler, C. Florentz, Adaptation of aminoacylation identity rules to mammalian mitochondria, Biochimie 94 (2012) 1090–1097.
[119] T. Ohtsuki, A. Sato, Y. Watanabe, K. Watanabe, A unique serine-specific elongation factor Tu found in nematode mitochondria, Nat. Struct. Biol. 9 (2002) 669–673.
[120] M. Sakurai, Y. Watanabe, K. Watanabe, T. Ohtsuki, A protein extension to shorten RNA: elongated elongation factor-Tu recognizes the D-arm of T-armless tRNAs in nematode mitochondria, Biochem. J. 399 (2006) 249–256.
[121] D.K. Willkomm, R.K. Hartmann, Intricacies and surprises of nuclear-mitochondrial co-evolution, Biochem. J. 399 (2006) e7–e9.
[122] M. Ling, F. Merante, H.S. Chen, C. Duff, A.M. Duncan, B.H. Robinson, The human mitochondrial elongation factor Tu (EF-Tu) gene: cDNA sequence, genomic localization, genomic structure, and identification of a pseudogene, Gene 197 (1997) 325–336.
[123] D.L. Lewis, C.L. Farr, L.S. Kaguni, *Drosophila melanogaster* mitochondrial DNA: completion of the nucleotide sequence and evolutionary comparisons, Insect Mol. Biol. 4 (1995) 263–278.
[124] S. Ovchinnikov, S.E. Masta, Pseudoscorpion mitochondria show rearranged genes and genome-wide reductions of RNA gene sizes and inferred structures, yet typical nucleotide composition bias, BMC Evol. Biol. 12 (2012) 31.
[125] O. Rackham, A. Filipovska, Supernumerary proteins of mitochondrial ribosomes, Biochim. Biophys. Acta (2013), http://dx.doi.org/10.1016/j.bbagen.2013.08.010.
[126] K. Hancock, S.L. Hajduk, The mitochondrial tRNAs of *Trypanosoma brucei* are nuclear encoded, J. Biol. Chem. 265 (1990) 19208–19215.
[127] D.B. Sloan, A.J. Alverson, J.P. Chuckalovcak, M. Wu, D.E. McCauley, J.D. Palmer, D.R. Taylor, Rapid evolution of enormous, multichromosomal genomes in flowering plant mitochondria with exceptionally high mutation rates, PLoS Biol. 10 (2012) e1001241.

Annex 2

SCIENTIFIC REPORTS

OPEN

Received: 11 June 2015
Accepted: 29 October 2015
Published: 01 December 2015

Neurodegenerative disease-associated mutants of a human mitochondrial aminoacyl-tRNA synthetase present individual molecular signatures

Claude Sauter[1,*], Bernard Lorber[1,*], Agnès Gaudry[1], Loukmane Karim[1], Hagen Schwenzer[1,†], Frank Wien[2], Pierre Roblin[2,3], Catherine Florentz[1] & Marie Sissler[1]

Mutations in human mitochondrial aminoacyl-tRNA synthetases are associated with a variety of neurodegenerative disorders. The effects of these mutations on the structure and function of the enzymes remain to be established. Here, we investigate six mutants of the aspartyl-tRNA synthetase correlated with leukoencephalopathies. Our integrated strategy, combining an ensemble of biochemical and biophysical approaches, reveals that mutants are diversely affected with respect to their solubility in cellular extracts and stability in solution, but not in architecture. Mutations with mild effects on solubility occur in patients as allelic combinations whereas those with strong effects on solubility or on aminoacylation are necessarily associated with a partially functional allele. The fact that all mutations show individual molecular and cellular signatures and affect amino acids only conserved in mammals, points towards an alternative function besides aminoacylation.

Mitochondria are the powerhouses of the eukaryotic cell, hosting the production of energy in the form of ATP by oxidative phosphorylation of ADP. They possess their own genome (mt-DNA), which codes in humans for 13 of the respiratory chain subunits, 22 tRNAs and 2 rRNAs. More than one thousand proteins, encoded by the nuclear genome, synthesized in the cytosol and subsequently imported into mitochondria, are also required for mitochondrial biogenesis and functioning (reviewed in e.g.[1]). Defects in mt-DNA were correlated to human disorders more than 25 years ago[2]. More recently, mitochondrial disorders were also associated with mutations within imported molecules, like factors of the mitochondrial translation machinery[3–5]. Among these are mitochondrial aminoacyl-tRNA synthetases (mt-aaRSs), which catalyze the esterification of tRNAs with cognate amino acids, and are key actors of the synthesis of the 13 respiratory chain subunits.

In 2007, it was shown for the first time that a mt-aaRS is implicated in a disease when mutations were found in the *DARS2* gene coding for the mitochondrial aspartyl-tRNA synthetase (mt-AspRS)[6]. This attracted the attention of the medical community and the steadily growing number of cases reported since then led to the current statement that all mt-aaRS genes (except *WARS2*) are affected by pathology-related mutations[1,7–12]. Mt-aaRSs are impacted in various ways, despite being ubiquitously

[1]Architecture et Réactivité de l'ARN, CNRS, Université de Strasbourg, IBMC, 15 rue René Descartes, 67084 STRASBOURG Cedex, France. [2]Synchrotron SOLEIL, L'Orme des Merisiers Saint Aubin, 91410 Gif-sur-Yvette, France. [3]URBIA-Nantes, INRA Centre de Nantes, 60 rue de la Géraudière, 44316 Nantes, France. *These authors contributed equally to the work. †Present address: The Wohl Virion Centre, Division of Infection & Immunity, UCL, Cruciform Building, 90 Gower Street, London WC1E 6BT, UK. Correspondence and requests for materials should be addressed to C.S. (email: c.sauter@ibmc-cnrs.unistra.fr) or M.S. (email: m.sissler@ibmc-cnrs.unistra.fr)

expressed and having a common role in protein biosynthesis. Mutations cause an unexpected variety of phenotypic expressions, including mainly neurological disorders but also non-neurological symptoms in some cases. In every case, however, they have tissue-specific phenotypic imprints. The cause of this selective vulnerability is not understood (reviewed in e.g.[1,5,8,13]), and neither is the way mutations affect the structure and/or function of mt-aaRSs.

Human mt-AspRS is the most prominent case with the largest number of reported mutations (60). These are spread throughout the *DARS2* gene within a cohort of 78 patients belonging to 58 families[6,14–19]. All these mutations are correlated with Leukoencephalopathy with Brain stem and Spinal cord involvement and Lactate elevation (LBSL), an autosomal recessive neurological disorder most often manifesting in early childhood and showing a wide spectrum of clinical phenotypes[20]. LBSL patients suffer from impairment of motor function and manual ability and loss of cognitive function to various degrees. Magnetic resonance imaging reveals characteristic abnormalities in the cerebral white matter, the cerebellum, brainstem, and spinal cord. In general, if the first neurological signs of disease appear in infancy (infantile/early onset LBSL), they are followed by severe neurological deterioration and the loss of the ability to walk in adolescence. If symptoms appear later (adult/late onset LBSL), the disease evolves at a slower pace but the patients need support for walking or become wheelchair dependent at the end of their lives (reviewed in[19]). LBSL patients are mainly compound heterozygous[19], but cases of homozygous mutations have been described in two families[17,21]. More than two thirds of the compound heterozygotes carry a mutation in a poly-pyrimidine tract at the 3′ end of intron 2 in one allele that affects the correct splicing of the third exon. This leads to a frameshift and a premature stop, but the defect is called "leaky" because it does not fully stop the expression of full-length mt-AspRS[6].

Initial *in vitro* analyses of an initial set of human mt-AspRS mutants revealed that only some of them had lower aminoacylation activities[22,23] suggesting that the protein synthesis housekeeping function is not a general target of the mutations. Further investigation showed that any step in the life of the enzyme can be impacted, as shown for pre-mRNA splicing[24], protein expression and dimerization[23], and protein translocation from the cytosol into mitochondria[25]. However, the link between the consequence of a mutation at the protein level and the observed clinical phenotype remains unclear.

We recently determined the X-ray structure of human mt-AspRS[26]. This class II homodimeric synthetase shares a common architecture with its bacterial homologs, but is more thermolabile and exhibits a higher plasticity for the binding of tRNA[26]. Based on this knowledge we selected six clinically relevant single point mutations (Fig. 1) located in the N-terminal anticodon-binding domain (R58G, T136S), in the catalytic domain (Q184K, R263Q) or in the C-terminal extension (L613F, L626Q). Phenotypes of corresponding patients are listed in Supplementary Table 1. Previous *in vitro* assays had shown that R263Q is the only mutation of these six that significantly impairs the aminoacylation property of recombinant protein[23]. To investigate if and how these mutations change the solubility, thermal stability and structure in solution of mt-AspRS, we applied an integrated strategy based on comparative biochemical and biophysical analyses. The implications of these observations are discussed in the context of LBSL clinical pictures.

Results

In the present study, wild-type (WT) mt-AspRS and six mutants (Fig. 1) were produced in *E. coli* for *in vitro* biophysical analysis. Proteins were expressed without the first 40 N-terminal amino-acids, corresponding to the putative MTS, and with a His-tag appended at the C-terminus. After purification as initially reported for the WT enzyme[27], all were homogeneous according to dynamic light scattering (DLS) and SDS-PAGE criteria, with masses expected from their amino acid compositions. Aminoacylation activities were in agreement with those reported[23]. The same set of WT and mutant mt-AspRS was expressed in mammalian cells for *in cellulo* solubility analysis as full-length sequences flanked by a C-terminal Flag®-tag for immunodetection. In this case, the MTS was naturally cleaved after import into mitochondria.

For both *in vitro* and *in cellulo* experiments, the mutants and the WT synthetase were prepared in parallel and treated in the same way for strictly comparative biochemical and biophysical analyses of solubility (by protein quantification), thermal stability (by DLS; differential scanning fluorimetry, DSF; and synchrotron radiation circular dichroism, SRCD), 2D and 3D structure in solution (by SRCD and small angle X-ray scattering, SAXS). The stabilizing effect of a synthetic inhibitor derived from the aspartyl-adenylate (Asp-AMS), which binds to the active site of the enzyme[26], was also assessed by DSF.

Structural properties of recombinant proteins in solution. Particle size distributions by intensity derived from DLS measurements performed independently in two instruments indicated that WT and mutants had mean hydrodynamic diameters of $d_h = 10 \pm 1$ nm, except Q184K whose size was slightly greater (Fig. 2A and Supplementary Fig. 1). Concentration dependence analysis confirmed that the d_h of this mutant was ~12 ± 1 nm after extrapolation to zero concentration (Fig. 2B). SLS analyses also showed that Q184K was distinguished from other samples by a ~20% higher mean molecular mass (results not shown). The content of secondary structure elements in all seven proteins was investigated by SRCD. Far-UV spectra indicated that all contain α-helices, ß-sheets and less structured regions in similar proportions (Fig. 2C, and Supplementary Fig. 2 and Table 2).

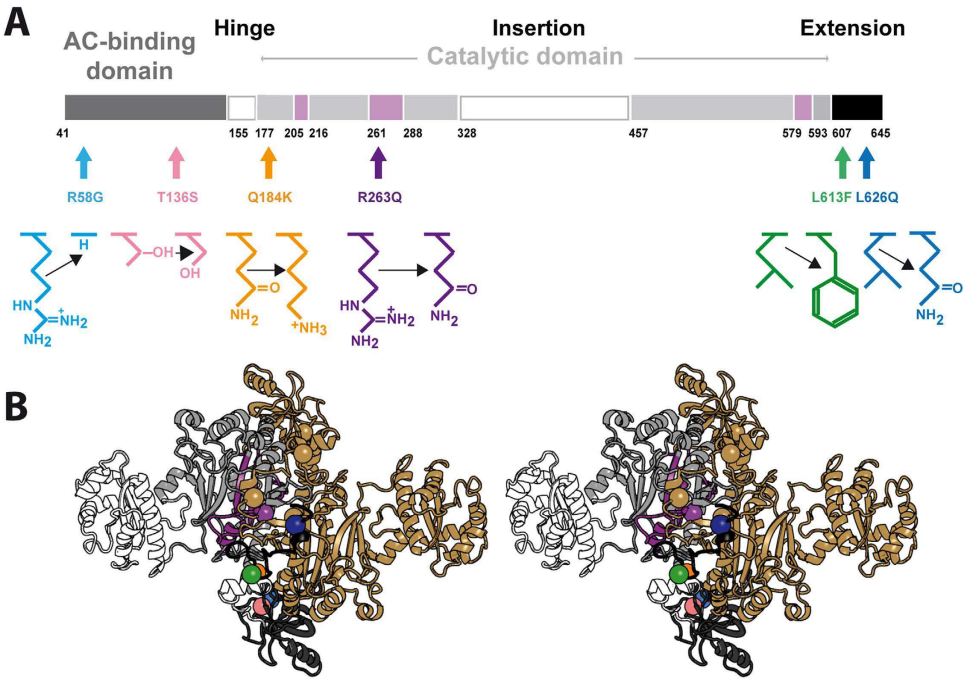

Figure 1. Locations and chemical nature of the amino acid substitutions of LBSL-associated mutations within functional domains of mt-AspRS. (**A**) Schematic representation of the modular organization of the human mt-AspRS (adapted from[23]). Structural modules are the anticodon (AC) binding domain (dark grey), the hinge region (white), and the catalytic domain (light grey). –Insertion– and –Extension– stands for bacterial-type insertion (white) and C-terminal extension (black) domains, respectively. Numbers correspond to amino acid positions flanking the different domains. Pink boxes situate catalytic motifs 1, 2, and 3, specific from class II aaRSs[48]. (**B**) Stereo view of the crystal structure of mt-AspRS (PDBid: 4AH6) with the positions of the studied mutations highlighted by color spheres. Color code on one monomer is as in panel (**A**). The second monomer is shown in gold. All molecular representations were prepared with PyMOL (Schrödinger, Inc.).

Thermal stability. The stability of WT and mutant proteins was compared by heating them gradually from 24 °C to 80 °C and monitoring either their aggregation by DLS, the binding of a fluorescent dye by DSF, or the effect on their secondary structures by SRCD (Supplementary Fig. 3). The temperatures at which aggregation started in DLS were 40 ± 1 °C for the WT mt-AspRS, 41 ± 1 °C for mutant R263Q, 39 ± 1 °C for mutants R58G, T136S, L613F and L626Q, and 38 ± 1 °C for mutant Q184K. Visual inspection revealed that at the end of these experiments the solutions of mutants Q184K and R263Q had the appearance of boiled egg-white while those of all other proteins contained a layer of aggregated material at the bottom of the DLS cells (results not shown).

In DSF experiment, the transition mid-point temperatures derived from increase of fluorescence intensity of R263Q, L613F, and L626Q were comparable to that of WT mt-AspRS (Tm = 47 to 48 ± 1 °C) (Fig. 3A). The Tm of Q184K was lower by ~2 °C and those of R58G and T136S lower by as much as 3 °C. In the presence of Asp-AMS, the Tm values of WT and R58G were 54 ± 1 °C and 53 ± 1 °C, respectively. Those of T136S, L613F, and L626Q were 52 ± 1 °C. The stabilizing effect of Asp-AMS on WT mt-AspRS[26] was also strong on R58G and T136S (ΔTm = +7 to +8 °C), but lower on L613F and L626Q (ΔTm = +4 to +5 °C), very low on Q184K (ΔTm = +2 °C), and negligible on R263Q (ΔTm = 0 °C) (Fig. 3A).

The structural stability of WT and mutant mt-AspRSs was further characterized by recording SRCD spectra as a function of the temperature to monitor the loss of secondary structure elements during unfolding. CD spectra are displayed in Supplementary Fig. 3. The Tm derived from the variation of ellipticity at 209 nm wavelength corresponding to CD minimum of the native state (Fig. 3B) was 51 °C for the WT, 50° for Q184K, 48 °C for T136S, 47 °C for R263Q and L613F, 46 °C for R58G, and 45 °C for L626Q. These last two mutants were most affected with Tm values up to 5 to 6 °C below that of the WT enzyme.

Solubility of mt-AspRS mutants *in cellulo*. WT and mutants of mt-AspRS were expressed in BHK21 cells and their abundance in soluble and insoluble fraction in either whole cell extracts or enriched mitochondria was determined by western blot (Fig. 4B). Histograms displaying relative amounts of mt-AspRS in the various fractions are shown in Fig. 4C. Similar trends were found in whole cell extracts and enriched mitochondria: mutant L613F is slightly more soluble than the WT mt-AspRS, L626Q is not

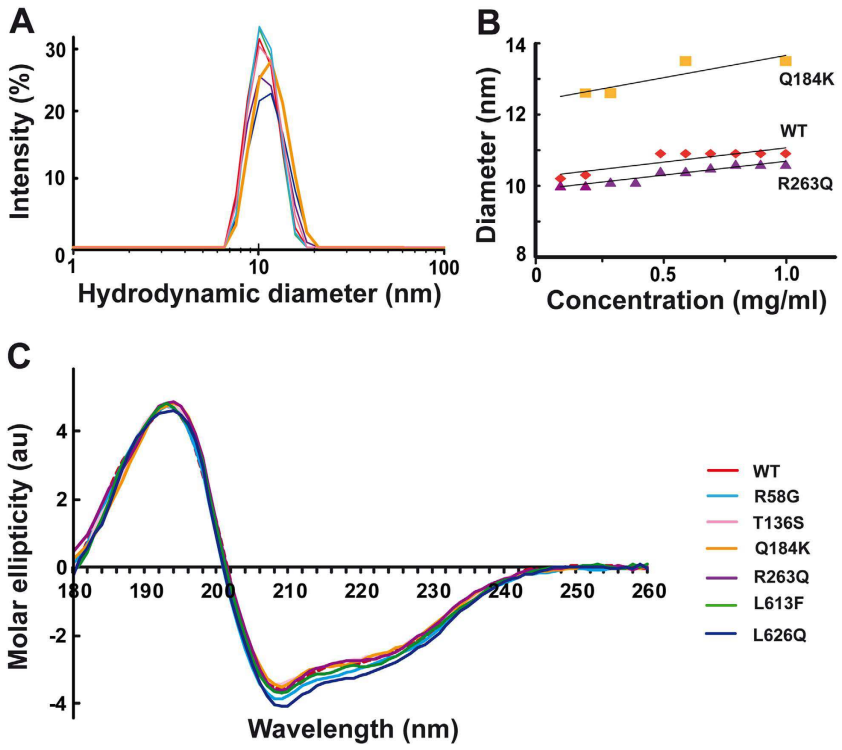

Figure 2. Comparative size and secondary structure elements of WT and mutant mt-AspRSs. (**A**) Particle hydrodynamic diameter distribution by intensity as measured by DLS. (**B**) Concentration dependence of particle diameter of WT, Q184K and R263Q as determined by DLS. (**C**) Overlay of the SRCD spectra of WT and mutants at 24°C. Color code is the same in all panels, as indicated in panel (**C**).

significantly impacted, and R58G, T136S and R263Q are slightly less soluble. The most statistically significant decrease in solubility (with p-values ≤ 0.01) was only observed for mutant Q184K.

Solution structure of mutants Q184K and R263Q *versus* WT. Mutants Q184K and R263Q, showing respectively the highest impact on protein solubility in cellular extracts (either whole cells or enriched mitochondria) and the highest impact on aminoacylation *in vitro*[23], were compared to that of the WT enzyme by SAXS analyses. Each sample was subjected to size exclusion chromatography (HPLC-SEC) directly upstream the SAXS cell to separate aggregates of various sizes from oligomers, allowing individual characterization of each species. The WT enzyme eluted from the SEC column essentially as a single population of particles (UV-absorbance peak 3 in Fig. 5A) while both mutants also contained a significant amount of high molecular-weight particles eluting earlier as peaks 1 and 2 (Fig. 5A). The X-ray scattering signal recorded during the elution of these three protein samples revealed that each peak was composed of well-defined particles yielding similar SAXS curves (Fig. 5B).

The major component of the three protein samples eluting as peak 3 consisted of mt-AspRS dimers with an Rg of 40 ± 1 Å, slightly larger than the Rg (36 Å) calculated from the crystal structure (PDBid: 4AH6), which does not include the C-terminal tails. These tails were not visible by X-ray crystallography probably because they do not adopt a fixed position in the crystal packing. In solution, however, their presence was revealed by the maximal interatomic distance (dmax = 150–155 Å) in the distance distribution function p(r) of the dimer (Table 1). Accordingly, we generated a complete atomic model based on the crystal structure with a C-terminal tail added to each monomer. A series of derived models were selected using DADIMODO (see Methods) that fitted well the experimental SAXS data (Fig. 5C) and gave a much better goodness-of-fit than the crystal structure (Supplementary Fig. 5). Figure 5C shows a superposition of the eight best models and illustrates how the 70 Å long tails extend in the solvent. In the AspRS from *E. coli*, the C-terminal tail encompasses only ten residues and is thus slightly shorter. The last five residues are also not visible in the crystal structure of the free enzyme (PDBid: 1C0A), confirming the flexible nature of C-terminal regions in bacterial-type AspRSs.

The particles eluting in peaks 1 and 2 found in the mutants corresponded to high-order assemblies. While *ab initio* bead modeling did not converge to a satisfactory representation of these entities, the similarity of their SAXS profiles clearly indicated that they were not random aggregates. According to their radii of gyration (Rg = 71 Å and 56 Å, respectively) and their Porod molecular volumes, these large complexes correspond to hexamers of dimers in peak 1 and dimers of dimers in peak 2 (Table 1, Supplementary Fig. 4). A comparison of the integration of the absorbance peaks 1, 2, and 3 of mutant

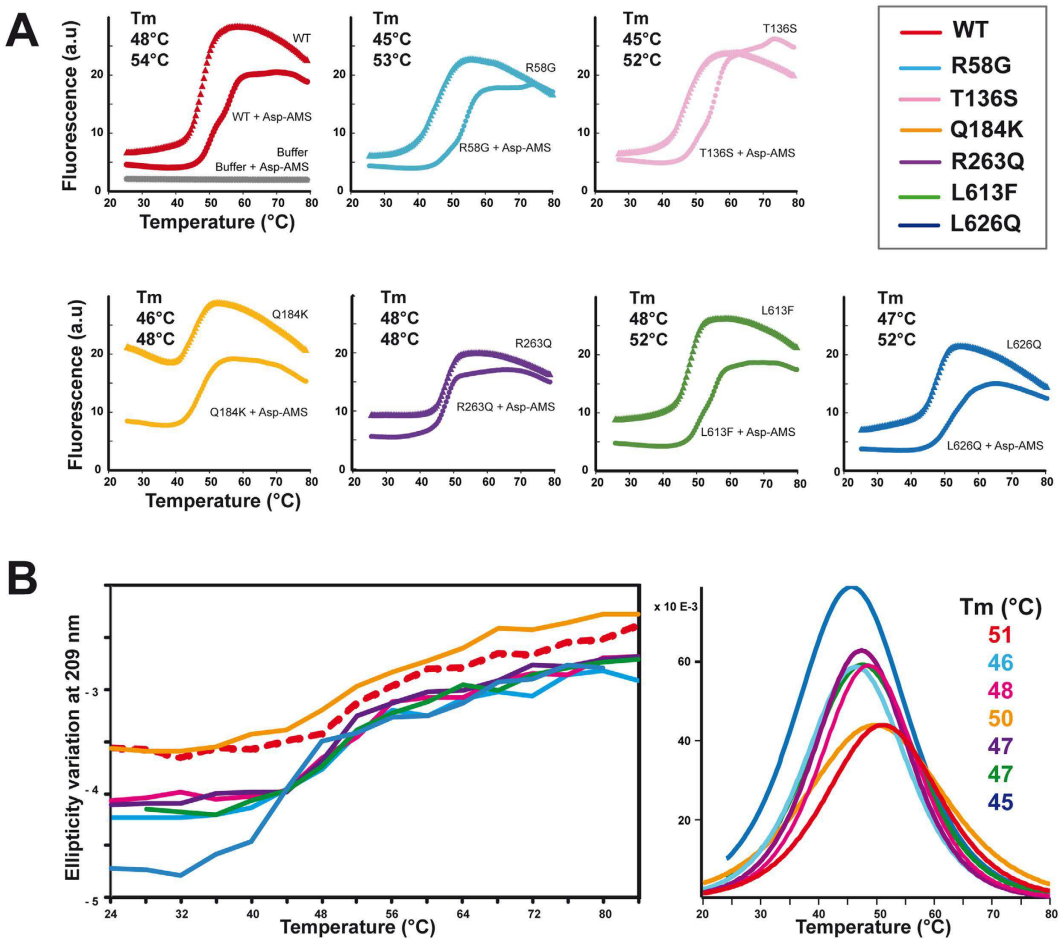

Figure 3. Differential thermal stability of WT mt-AspRS and mutants. (**A**) Temperature-dependent binding of a fluorescent hydrophobic dye measured by DSF, in the absence and in the presence of an aminoacyl-adenylate analog 5′-O-[N-(L-aspartyl)sulfamoyl]adenosine (Asp-AMS). (**B**) Thermal stability of structural secondary elements. (Left) Temperature dependent variation of the molar ellipticity at 209 nm measured by SRCD. (Right) Derivatives of sigmoidal fits of curves displayed in the left panel with maxima corresponding to the Tm. Color code is as in Fig. 1.

Sample	Peak	Rg Guinier (Å)	Rg p(r) (Å)	dmax (Å)	Porod Vol. (Å^3)	Oligomer
WT	#3	38.5	39.2	150	230.E3	dimer
R263Q	#1	71.1	71.2	220	145.E4	6× dimer
	#2	53.5	55.0	220	430.E3	2× dimer
	#3	38.7	39.3	155	230.E3	dimer
Q184K	#1	70.8	68.5	200	145.E4	6× dimer
	#2	53.7	56.7	220	430.E3	2× dimer
	#3	40.0	41.3	155	230.E3	dimer

Table 1. SAXS analysis of WT mt-AspRS and mutants.

Q184K indicated that the two first high-molecular weight assemblies represent ~11 and 23% of the protein respectively (Fig. 5A). This indicates a strong potential for self-assembly and/or aggregation of this mutant. Under the same experimental conditions, the R263Q sample eluted mainly as dimers (peak 3 contained ~88% of the total protein and peaks 2 and 1 only 9% and 2%, respectively). This mutant interacted with the column matrix as revealed by the reproducible slightly retarded elution. Otherwise, the particle sizes in the three peaks matched with those determined for mutant Q184K. Overall, these results correlate well with the greater size observed in DLS and the predominant occurrence of Q184K in the insoluble fraction *in cellulo*.

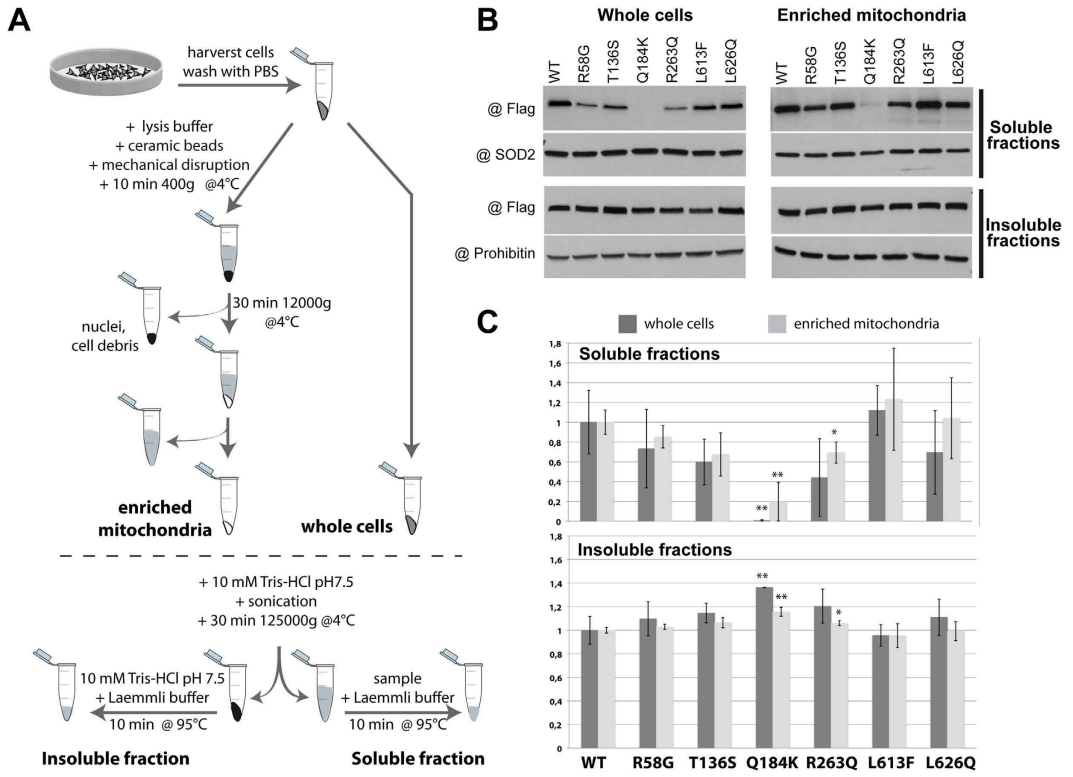

Figure 4. Solubility of WT *versus* mutant mt-AspRSs *in cellulo*. (**A**) Flowchart of experimental procedure. (**B**) Representative western blots of WT and mutant mt-AspRS (detected with anti-Flag antibodies) in soluble and insoluble fractions, within whole cells or enriched mitochondria. Detections of SOD2 (a mitochondrial matrix protein) and prohibitin (a mitochondrial membrane protein) were performed as loading controls for the soluble and the insoluble fractions, respectively. Three sets of independent experiments for whole cells and three sets of independent experiments for enriched mitochondria were analyzed. (**C**) Relative abundance of mutant proteins as compared to WT mt-AspRS in soluble (top) and insoluble (bottom) fractions. Relative amounts of polypeptides were estimated as described in the methods section and normalized according to the WT mt-AspRS, arbitrarily set to a value of 1 in both soluble and insoluble fractions. Errors bars illustrate the standard deviations calculated from the three sets of independent experiments. *$p < 0.05$ and **$p \leq 0.01$ based on Student's *t*-test.

Discussion

Previous studies on human mt-AspRS had shown that mutations associated with the LBSL pathology have various impacts on the molecular and cellular properties of the enzyme, but reduce only marginally the catalytic activity of mt-AspRS and are thus not always deleterious to the housekeeping function[22–25]. Here, we focused on a set of six mutations and explored how they modify the biophysical properties of the mt-AspRS, specifically its 2D and 3D folds and thermal stability, as well as solubility *in vitro* and *in cellulo*. These clinically relevant mutations, distributed throughout the enzyme sequence, are located either in the anticodon-binding domain opposite to the tRNA binding interface (R58G, T136S), in the catalytic domain at the dimer interface (Q184K, R263Q) or in the C-terminal extension (L613F, L626Q) involved in subunit dimerization within bacterial-type AspRSs.

Mutations in mt-AspRS sequence context. It is widely believed that mutation of strictly conserved residues would be detrimental to the architecture or activity (in the present case, aminoacylation). Therefore we investigated the amino acid conservation of relevant residues in structural sequence alignments made of 180 sequences of bacterial-type AspRSs (60 mitochondrial and 120 bacterial AspRSs). We found that none of them are strictly conserved (Supplementary Table 3), indicating that no gross structural and/or functional perturbations are likely to occur. As seen in Fig. 1A, amino acid substitutions either extend, shorten or delete side chains with either a gain or loss of positive charge or of hydrophobicity. Because of changes in size or the introduction of attractive or repulsive interactions, mutations may compact or expand locally the structure. However, homology models based on the X-ray structure of human WT mt-AspRS suggest that these modifications do not perturb the overall 2D and 3D fold (Fig. 6A,B and Supplementary Table 3). This lack of perturbation is clear for T136S, where mutation replaces a side chain with one of similar volume, and for R58G and L613F where side chains are directed toward the solvent. L613F is the only one occurring in the vicinity of the tRNA binding site

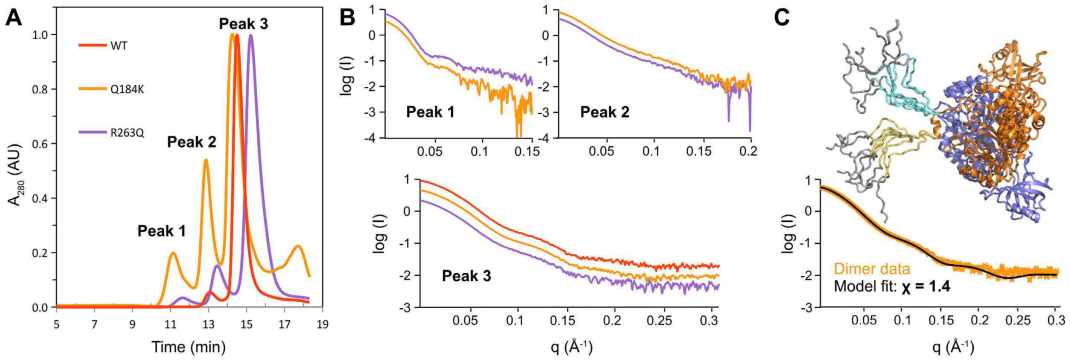

Figure 5. Comparison of WT, Q184K and R263Q mt-AspRSs by SAXS. (**A**) Overlay of normalized SEC absorbance profiles and SAXS curves recorded for each absorbance peak. The WT protein (plots in red) forms essentially a dimer present in peak 3 (93% of the sample), while mutants Q184K (in orange) and R263Q (in violet) also form entities of higher molecular sizes that elute faster in peak 1 (11%, 2% of overall population, respectively) and peak 2 (23%, 9%, respectively). (**B**) SAXS profiles of AspRS populations in peaks 1, 2 and 3. For clarity of presentation, the curves are offset. (**C**) Modeling of mt-AspRS dimer in peak 3 by atomic models generated from the X-ray structure of mt-AspRS (PDBid: 4AH6) to which flexible C-terminal tails were added. In this example, data from Q184K mutant are represented as orange crosses and a typical profile calculated from one of conformers generated under SAXS data constrains by DADIMODO is shown in black. Eight conformations of C-terminal extensions with lowest Chi values (see also Supplementary Fig. 5) are depicted: yellow and cyan tails belong to orange and blue subunit, respectively. The gray region corresponds to the tag used for affinity purification.

but the introduction of a phenyl group at this position is possible without clash with the ligand. In the case of Q184K, R263Q and L626Q at the heart of the dimerization interface, the local structure may cope with the new side chains presenting conformers that do not cause any steric hindrance (Supplementary Table 3).

Mutations do not affect enzyme architecture. The particle diameters determined by DLS showed that the tested mutants were dimers like the WT mt-AspRS, but that mutant Q184K was of slightly greater size. SAXS data confirmed that mutants Q184K and R263Q, like the WT, are predominantly composed of dimers (Fig. 5). The similarity of SRCD spectra indicated that the secondary structure elements composing the six mutants are present in the same proportions as in the WT enzyme. Altogether, these experimental results demonstrate that the polypeptide chains of all mutants are properly folded and that the 3D architecture of mt-AspRS is not significantly altered by these single point mutations. These results are consistent with the moderate impacts on the ability of the mutants to perform tRNA aminoacylation in the test tube[23].

SAXS analysis further confirmed the floppy nature of the C-terminal tails in the mt-AspRS dimer that were not visible in the X-ray structure. These extensions pointing into the solvent (Figs 5C and 6A) may provide interaction platforms for putative partners linking the enzyme with alternate mitochondrial networks. The mutations R58G and T136S located on the face opposite to that interacting with the tRNAs could also impair the binding of partner molecules onto mt-AspRS.

Mutants differ in their stability. All enzymes, WT and mutant mt-AspRSs, sharing the same structure were subjected to thermal denaturation in order to detect differences in stability. Three approaches were used to assess the propensity to aggregate (recorded by DLS), to unfold (visualized by SRCD) and to expose hydrophobic regions to the solvent upon unfolding (monitored by DSF). Interestingly, every mutant behaved in a different manner in response to thermal denaturation. This response varied from one analytical method to the other as summarized in Fig. 6C. The common point was that all mutants were more fragile than the WT protein. These observations raised the question of the stability of the mutants in the cellular environment and at body temperature.

Our previous analyses of human WT mt-AspRS had revealed that the synthetic analog of the aminoacylation intermediate aspartyl-adenylate, Asp-AMS, binds cooperatively[28] and increases the thermal stability of the protein by as much as 6 °C[26]. This family of compounds is commonly used in crystallographic studies to rigidify the region around the catalytic site[29,30]. Here, mutants R58G, T136S, L613F and L626Q were stabilized to the same extent as the WT protein, whereas mutants Q184K and R263Q were not stabilized at all by Asp-AMS. The latter two mutations are located at the dimer interface and may thus hinder the allosteric communication between the two active sites of the synthetase dimer.

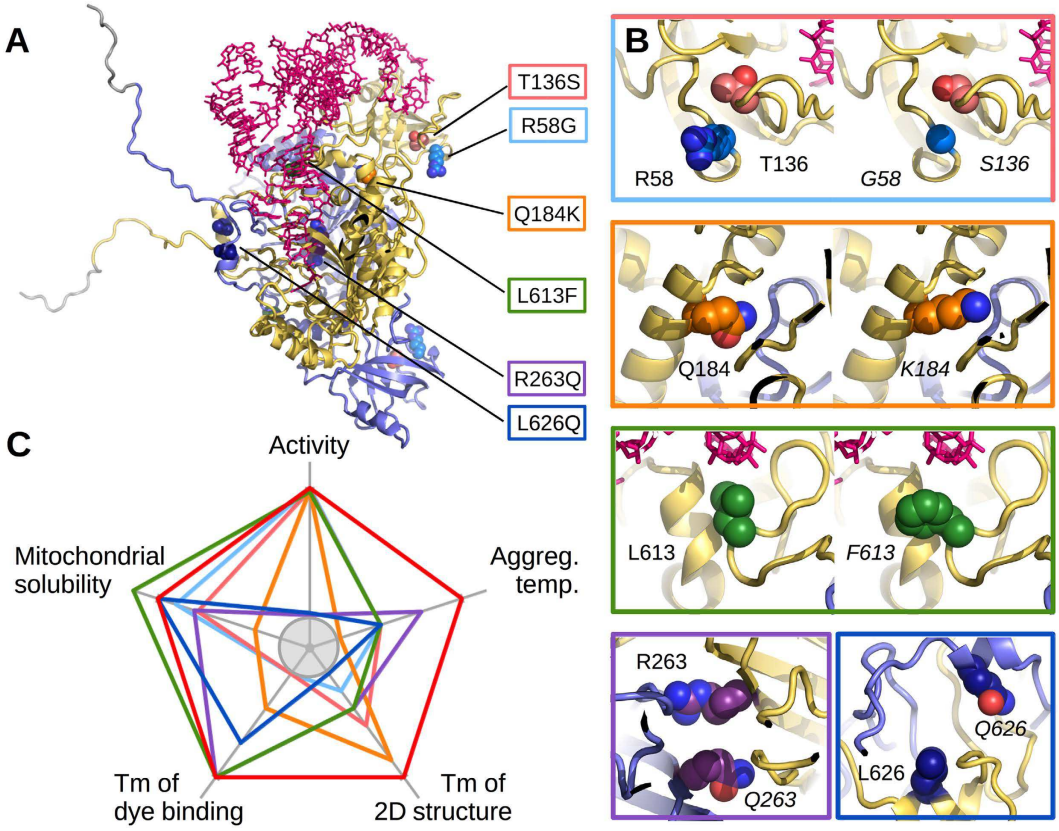

Figure 6. mt-AspRS WT *versus* mutants. (**A**) Positions of single point mutations on the 3D model of mt-AspRS including the two C-terminal extensions and a tRNA molecule docked onto the yellow subunit to show its interaction area (adapted from[26]). (**B**) Close up views showing the original and the mutated side chains in space filling representation. The color of carbon atoms is the same as in other figures. Oxygen and nitrogen atoms depicted in red and blue, respectively. All substitutions are possible without significant steric hindrance. R263Q and L626Q being close to the enzyme 2-fold axis, WT and mutated residues are shown in the same inset. (**C**) Five intrinsic properties ranked relative to the WT (red pentagon = 100% of scale). The enzymatic activity of all mutants was comparable to that of the WT, except that of L626Q and R263Q for which moderate 40 and 140-fold decreases were measured, respectively[23]. Ranges of aggregation temperature determined by DLS, Tm of 2D structure unfolding in SRCD and Tm of dye binding in DSF ranged are 38–41 °C, 45–51 °C and 45–48 °C, respectively. Mitochondrial protein solubilities are taken from top histogram in Fig. 4C. The gray circle delineates the lowest values of each interval. The color code for mutants is indicated. All molecular representations were prepared with PyMOL (Schrödinger, Inc.).

***In cellulo* solubility of WT and mutant mt-AspRSs.** The differential thermal stability and effect of Asp-AMS led us to examine the stability of the mutants in the mitochondria of mammalian cells. All recombinant proteins produced in *E. coli* were soluble *in vitro* up to at least 10 mg/ml in standard solvent conditions. The situation was different in BHK cells grown at 37 °C. As shown in Fig. 4, WT and mutant mt-AspRSs were present in the soluble fraction of cellular extracts or of purified mitochondria, except mutant Q184K, which was more abundant in the insoluble fractions. The propensity of this mutant to form insoluble material is consistent with the presence of high-molecular weight objects suspected in DLS analyses and visualized in SEC. SAXS analyses confirmed that the particles in SEC peaks 1 and 2 are not random aggregates but have well defined sizes and shapes (Fig. 5 and Supplementary Fig. 4). These entities correspond to various assemblies of mt-AspRS dimers, e.g. dimers and/or hexamers of dimers (Table 1).

mt-AspRS mutations in LBSL patients. Selected mutations are found in LBSL patients as compound heterozygous states, meaning that patients *a priori* possess a mixture of homo- and hetero-dimers. Here we examined homodimers composed of either two WT or two mutated monomers, which represent two-thirds of the possible combinations (boxed in Supplementary Fig. 6). Although our approach did not consider heterodimers, it sheds light on the correlation between the strength of the impact of a mutation and the expression of a phenotype.

Q184K and R263Q, the two missense mutations that show the strongest impacts on solubility and activity respectively, are each combined in patients with a splicing defect on the second allele (named R76Serfs*5; Supplementary Table 1). The leakiness of the splicing defect allows the expression of a reduced amount of functional WT enzyme, likely sufficient to sustain mitochondrial translation and to compensate for the depletion in soluble mt-AspRS caused by the presence of aggregation-prone mutants. This hypothesis is supported by the description of another patient, whose allelic composition associates the leaky splicing defect (R76Serfs*5) with the nonsense mutation R263X. The latter generates a completely non-functional molecule. Interestingly, patients R76Serfs*5/R263X and R76Serfs*5/R263Q display similar phenotypes and disease courses (Supplementary Table 1).

Additional compound heterozygous states exist in which the allelic composition combines two missense mutations, i.e. R58G/T136S and L613F/L626Q[19] (Supplementary Table 1). If we consider our homodimeric mutants R58G, T136S, L613F and L626Q individually, their effects *in cellulo* and *in vitro* are relatively mild with regard to solubility, thermal stability and structure in solution. This suggests that their pathogenicity is likely due to the combination of these effects in patient cells, leading to cumulative deficiencies in their mitochondria.

Altogether, the occurrence of LBSL phenotype seems to be related to the amount of soluble AspRS available in the mitochondria. We observe that allelic compositions in patients (with comparable phenotypes and disease courses, Supplementary Table 1) associate either two mutations with mild individual impacts (i.e. R58G/T136S and L613F/L626Q) or a more deleterious with a non-symptomatic one (i.e. R263Q/R76Serfs*5 and Q184K/R76Serfs*5). This indicates that the strength of the impact of a mutation necessarily falls into a narrow window. In the case of LBSL patients, this window starts where the symptoms become detectable and goes up to a level that is still compatible with a life expectancy greater than 20 years. This is not a general trend since mutations identified in other mt-aaRSs can lead to faster disease courses. In the case of mt-ArgRS for instance, mutations cause severe neonatal or early-infantile epileptic encephalopathy[31]. Strikingly, most of those mutations concern residues that are highly conserved throughout phylogeny.

Conclusions and perspectives. The main results of the present analysis of six LBSL mutants of human mitochondrial aspartyl-tRNA synthetase (mt-AspRS) can be summarized as follows:

- *In vitro*, mutations have diverse effects on protein solubility and stability, but do not affect enzyme architecture.
- *In cellulo*, five mutants R58G, T136S, R263Q, L613F and L626Q are present like the WT in the soluble fraction of cellular extracts, while mutant Q184K is more abundant in the insoluble fractions.
- In patients, four of the mutants with mild effects on solubility occur as heterozygous pairs in allelic compositions. The two mutants with strongest solubility or activity defect are each combined with a splicing defect on the second allele that allows the expression, albeit at reduced levels, of functional WT enzyme.
- Mutated positions are not strictly conserved throughout phylogeny, in agreement with the fact that none of them leads to gross structural and/or functional perturbations. The exception is residue R263, which is mainly but not strictly conserved. Its mutation causes the strongest impact on aminoacylation.

Up to now LBSL is the neurodegenerative disease correlated with the greatest number of mutations in a human mitochondrial aminoacyl-tRNA synthetase, and with the largest cohort of diagnosed patients. All investigations performed thus far on the possible impacts of LBSL-causing mutations on molecular, cellular, and in the present contribution on biophysical properties of the mt-AspRS, highlight that each mutation has an individual signature (as illustrated in Fig. 6C for those examined here). These observations strengthen the need to further explore cellular properties of mt-AspRS and to search for possible alternative functions, beyond mitochondrial translation. For instance, the C-terminal flexible extensions of mt-AspRS observed by SAXS and pointing into the solvent may provide interaction platforms for putative partners connecting the enzyme with alternate mitochondrial networks. The hypothesis of a non-translational role of mt-AspRS is in agreement with the observation that impacted residues are solely conserved within mammals mt-AspRSs indicating a selective pressure restricted to higher eukaryotes (Supplementary Table 3). This observation holds true as well for additional 18 clinically relevant missense mutations, mainly reported since the beginning of the present work (Supplementary Table 4). While a few of them affect positions highly or strictly conserved throughout all phylogeny, all of them affect positions strictly conserved within mammals. Notably, numerous functions besides translation (often qualified as 'moonlighting activities') of cytosolic aaRSs have been described during the past decade (e.g.[32–34]). Interestingly, these functions appeared to have emerged from new selective pressures or new architectural elaborations mainly in vertebrates, and have been shown to be involved in autoimmune disorders, cancers and neurological disorders.

Material and Methods

Cells, biochemicals and chemicals. Baby Hamster Kidney cells strain 21 (BHK21) (ATCC # CRL-12072) and modified Vaccinia Ankara strain (MVA-EM24) were generous gifts from Robert Drillien (IGBMC, Strasbourg). Bacterial strain Rosetta™2(DE3) was purchased from Merck Millipore, Anti-Flag® antibody and Tris(2-carboxyethyl)phosphine hydrochloride (TCEP) were from Sigma, anti-SOD2 (human) and anti-prohibitin (human) antibodies were from Abcam®, goat anti-rabbit secondary antibody conjugated to horseradish peroxidase [HRP] was from BioRad, chemiluminescent detection kit from Pierce (Thermo Scientific), aminoacyl-adenylate analog 5′-O-[N-(L-aspartyl)sulfamoyl]adenosine (Asp-AMS) from Integrated DNA Technologies (Belgium), and SYPRO Orange™ from Molecular Probes Invitrogen. Mini-Protean® TGX Precast polyacrylamid gels, Trans-Blot Turbo system and SEC protein standard (lyophilized mix containing thyroglobulin, bovine γ-globulin, chicken ovalbumin, equine myoglobin and vitamin B12, MW 1,350–670,000–Cat. No. 151–1901) were from BioRad. Arrest™ protease inhibitor cocktail and polyethylenimine (PEI, linear 25 kDa) were purchased from GBiosciences and Polysciences, respectively.

Production of recombinant WT and mutant mt-AspRSs. The genes for wild-type mt-AspRS and those carrying the mutations 172C > G (R58G), 406A > T (T136S), 550C > A (Q184K), 788G > A (R263Q), 1837C > T (L613F) and 1876T > A (626Q) were cloned in bacterial strain Rosetta™2(DE3) as previously described[23,27]. The wild-type mt-AspRS and the six mutants lacked the 40 N-terminal amino acids and had a VMYLE sequence before the C-terminal 6-His tag. They were purified to homogeneity by affinity and size exclusion chromatography as reported for the WT enzyme[26,27].

Dynamic (DLS) and static light scattering (SLS). Samples containing 2 mg/ml mt-AspRS in standard buffer (100 mM potassium phosphate pH 7.5, 50 mM KCl, 0.1 mM EDTA, 10 mM β-mercaptoethanol, and 10% v/v glycerol) were ultracentrifuged for 1 h at 45 000 rpm or 100 000 × g. The supernatant was transferred into 2 μl or 20 μl quartz cells for parallel analyzes at 20 °C in Wyatt Technology Nanostar™ and Malvern Zetasizer™ NanoS light scattering instruments, respectively[35]. Hydrodynamic diameters determined by DLS were corrected for solvent refractive index 1.351 and absolute viscosity 1.463×10^{-3} Pa.s. Particle masses determined by SLS were corrected for refractive index concentration dependence dn/dc 0.185 ml/g. The behavior of samples subjected to a temperature gradient from 20 °C to 60 °C was monitored by DLS in the Zetasizer. A shift in the autocorrelation function towards greater times was indicative of the onset of aggregation.

Differential scanning fluorimetry (DSF). Twenty μl of mt-AspRS solution containing 2 mg/ml were mixed with 0.5 μl dye (SYPRO Orange™ 5000X stock solution diluted 20-fold in dimethylsulfoxide) in 0.2 ml transparent plastic qPCR tubes. Fluorescence variation was monitored along a temperature gradient from 20 to 90 °C using an Agilent Stratagene Mx3005P instrument. The inflection point of the fluorescence intensity *versus* temperature plot was considered to be the transition mid-point (Tm).

Synchrotron radiation circular dichroism (SRCD). SRCD spectra were recorded on the DISCO beamline[36] at synchrotron SOLEIL (Saint-Aubin, France). The experimental setup was calibrated for magnitude and polarization with a 6.1 mg/ml D-10-camphorsulfonic acid solution. Two μl of WT mt-AspRS or mutants solution at 10 mg/ml in 100 mM potassium phosphate pH 7.5, 50 mM KCl, 10% (v/v) glycerol and 1 mM TCEP were transferred in a CaF_2 cuvette with an optical path of 8 μm. Three spectra from 170 to 280 nm were recorded at temperatures ranging from 24 to 80 °C with 4 °C steps. They were averaged, solvent baseline subtracted, scaled and normalized to molar ellipticities using CDtool[37]. Protein stability was determined by plotting the variation of the CD minimum at 209 nm as a function of temperature. IGOR software (WaveMetrics) was used to model this variation by a sigmoid and the temperature corresponding to the maximum of its derivative defined a structural transition or melting temperature (Tm). Secondary structure content was estimated from SRCD spectra collected at 24 °C using CONTINLL in Dichroweb and SELCON3 in CDPro using the SP175 reference data set[38–40]. A data cutoff at 180 nm was applied based on photomultiplier high-tension viability. Values were compared to those in the X-ray structure of the WT human mt-AspRS (PDBid: 4AH6).

Small-angle X-ray scattering (SAXS). SAXS experiments were performed on the SWING beamline[41] at synchrotron SOLEIL (Saint-Aubin, France). The beam wavelength was $\lambda = 1.033$ Å. The 17×17 cm^2 low-noise Aviex CCD detector was positioned at a distance of 2107 mm from the sample with the direct beam off-centered. The resulting exploitable q-range was 0.005–0.35 Å^{-1}, where the wave vector $q = 4\pi \sin\theta/\lambda$ and 2θ is the scattering angle.

WT mt-AspRS and mutants Q184K and R263Q at, respectively, 7.4, 10 and 14 mg/ml in 50 mM HEPES-Na pH 7.5, 150 mM NaCl, 10% (v/v) glycerol, 0.1 mM EDTA and 1 mM DTT, were separated by SEC and analyzed by SAXS online. Thus, 45 μl protein solution was loaded onto an Agilent Bio SEC-3 column (300 Å, 4.6 × 300 mm, 3 μm) installed on an Agilent HPLC system and maintained at 15 °C. Proteins were eluted at a flow rate of 0.2 ml/min with a mobile phase containing 100 mM HEPES-Na pH 7.5, 250 mM NaCl, 5% (v/v) glycerol and 1 mM TCEP. The eluate was analyzed by SAXS in a continuous

flow capillary cell with a frame duration of 1000 ms at intervals of 500 ms. Data processing, analysis and modeling step were done with PRIMUS and other programs of the ATSAS suite[42].

Radii of gyration (R_g) were derived from Guinier approximation and used to estimate the molecular Porod volume. R_g was also calculated from the entire scattering pattern using the indirect transform package GNOM[43], which provides the distance distribution function p(r) of the particle. A dimeric mt-AspRS model including all residues (two polypeptide chains encompassing residues 41–645 plus a linker of 5 residues and a 6-His-tag) were derived from the X-ray structure (PDBid: 4AH6). The C-terminal tails added to the monomers consisted of the last 15 residues not visible in the crystal structure and of the 11 amino acid affinity tag. The conformational space of these tails was modeled under SAXS constraints using DADIMODO[44], a genetic algorithm-based refinement analysis program. The core of the dimer corresponding to the crystal structure was treated as a rigid body while the conformation of the C-terminal tails was explored by simulated annealing. A set of eight models were selected that best fit the experimental data. The goodness-of-fit was estimated using CRYSOL[45].

Analysis of the soluble/insoluble state of mt-AspRS *in cellulo*. WT and mutants constructs were generated by directed mutagenesis from pBCJ749.77 plasmid, derived from described pBCJ739.14[46] with the sequence coding for the Flag® tag DYKDDDDK added downstream of the coding sequence of the full-length mt-AspRS including the mitochondrial sequence (MTS) (Consensus CDS Gene CCDS1311.1). Constructs were introduced in BHK21 using a protocol adapted from the transfection-infection approach[46], under conditions where protein expression is moderate. Cells were washed with PBS and infected with modified vaccinia virus expressing IPTG-inducible T7 polymerase, and subsequently transfected. For transfection, plasmid/PEI complexes were prepared in a mass ratio of 1:4.5 and incubated for 15 min at 20 °C. Protein expression was induced by 1 mM IPTG. 36 h post-transfection, ~5.10^6 cells were harvested, washed with PBS.

A flowchart of the experimental procedure to investigate soluble/insoluble state of the proteins is given in Fig. 4A. For mitochondrial enrichment, cells were mechanically disrupted using 2 mm diameter ceramic beads in a FastPrep-24™ 5G machine (MP biomedicals), in 1.5 ml of an isotonic lysis buffer (220 mM mannitol, 70 mM sucrose, 1 mM EDTA, 1 mM $MgCl_2$, 10 mM HEPES-KOH pH 7.4) containing a protease inhibitor cocktail. Mechanically lysed cells were centrifuged 10 min at 400 g (4 °C). The pellet (nuclei and cell debris) was discarded, and the supernatant was centrifuged 10 min at 12 000 g (4 °C) to pellet mitochondria. Whole cells and mitochondria were sonicated (6×10 s) on ice in 160 µl of 10 mM Tris-HCl pH 7.5 containing a protease inhibitor cocktail. The lysates were then ultracentrifuged 30 min at 125 000 g (4 °C) and the soluble fractions (supernatants) were separated from the insoluble fractions (pellets). An aliquot of each soluble fraction (16 µl) was withdrawn and added to 4 µl of Laemmli denaturing buffer, heated to 95 °C for 10 min and loaded on a 10% (m/v) polyacrylamide gel. Pellets were solubilized in 160 µl of 10 mM Tris-HCl pH 7.5 to which 40 µl Laemmli buffer was added before heating and 20 µl of this mixture was analyzed on a gel. Proteins were blotted onto a PVDF membrane and recombinant proteins were detected with an antibody specific for the Flag® tag peptide. Chemiluminescent detection was carried out using the Pierce Detection Kit according to manufacturer's instructions. Exposed films were digitized using Epson Perfection 3490 Photo scanner and band intensities were quantified on images using ImageJ software[47].

Mt-AspRS in each sample distributed in either soluble or insoluble fraction, the total corresponding to 100%. The blots of these fractions were developed simultaneously in the same bath to allow for strict comparison of protein amounts and determination of relative distribution in both fractions. In that way, the result was independent of expression. The loading controls, SOD2 or prohibitin respectively for soluble or insoluble fractions, were used to adjust the amount of mt-AspRS in every lane of a given blot. Resulting mt-AspRS intensities were converted to percentages of protein amount (WT or mutants) in soluble and insoluble fractions.

Mean values and standard deviations were derived from three independent experiments. Histograms were normalized with regard to WT mt-AspRS to compare the relative abundance of the mutated proteins in whole cell extracts and enriched mitochondria.

References

1. Schwenzer, H., Zoll, J., Florentz, C. & Sissler, M. Pathogenic implications of human mitochondrial aminoacyl-tRNA synthetases. In *Topics in Current Chemistry-Aminoacyl-tRNA Synthetases: Applications in Chemistry, Biology and Medicine*, Vol. 344 (ed. Kim, S.) 247–292 (Springer, 2014).
2. Wallace, D., Brown, M. & Lott, M. Mitochondrial DNA variation in human evolution and disease. *Gene* **238,** 211–230 (1999).
3. Thorburn, D. R. Mitochondrial disorders: prevalence, myths and advances. *J. Inherit. Metab. Dis.* **27,** 349–362 (2004).
4. Rötig, A. Genetic bases of mitochondrial respiratory chain disorders. *Diabetes Metab.* **36,** 97–107 (2010).
5. Boczonadi, V. & Horvath, R. Mitochondria: impaired mitochondrial translation in human disease. *Int J Biochem Cell Biol.* **48,** 77–84 (2014).
6. Scheper, G. C. *et al.* Mitochondrial aspartyl-tRNA synthetase deficiency causes leukoencephalopathy with brain stem and spinal cord involvement and lactate elevation. *Nat Genet* **39,** 534–539 (2007).
7. Suzuki, T., Nagao, A. & Suzuki, T. Human mitochondrial tRNAs: biogenesis, function, structural aspects, and diseases. *Annu. Rev. Genet.* **45,** 299–329 (2011).
8. Konovalova, S. & Tyynismaa, H. Mitochondrial aminoacyl-tRNA synthetases in human disease. *Mol Genet Metab.* **108,** 206–211 (2013).

9. Diodato, D., Ghezzi, D. & Tiranti, V. The Mitochondrial Aminoacyl tRNA Synthetases: Genes and Syndromes. *Int J Cell Biol.* **2014,** 787956 (2014).
10. Schwartzentruber, J. *et al.* Mutation in the Nuclear Encoded Mitochondrial Isoleucyl tRNA-Synthetase IARS2 in Patients with Cataracts, Growth Hormone Deficiency with Short Stature, Partial Sensorineural Deafness and Peripheral Neuropathy or with Leigh Syndrome. *Hum. Mutat.* **35,** 1285–1289 (2014).
11. Hallmann, K. *et al.* A homozygous splice-site mutation in CARS2 is associated with progressive myoclonic epilepsy. *Neurology* **83,** 2183–2187 (2014).
12. Sofou, K. *et al.* Whole exome sequencing reveals mutations in NARS2 and PARS2, encoding the mitochondrial asparaginyl-tRNA synthetase and prolyl-tRNA synthetase, in patients with Alpers syndrome. *Mol Genet Genomic Med.* **3,** 59–68 (2015).
13. Lombès, A., Auré, K., Bellanné-Chantelot, C., Gilleron, M. & Jardel, C. Unsolved issues related to human mitochondrial diseases. *Biochimie* **100,** 171–176 (2014).
14. Isohanni, P. *et al.* DARS2 mutations in mitochondrial leucoencephalopathy and multiple sclerosis. *J. Med. Genet.* **47,** 66–70 (2010).
15. Lin, J. *et al.* Leukoencephalopathy With Brainstem and Spinal Cord Involvement and Normal Lactate: A New Mutation in the DARS2 Gene. *J. Child. Neurol.* **25,** 1425–1428 (2010).
16. Labauge, P., Dorboz, I., Eymard-Pierre, E., Dereeper, O. & Boespflug-Tanguy, O. Clinically asymptomatic adult patient with extensive LBSL MRI pattern and DARS2 mutations. *J. Neurol.* **258,** 335–337 (2011).
17. Miyake, N. *et al.* A novel homozygous mutation of DARS2 may cause a severe LBSL variant. *Clin. Genet.* **80,** 293–296 (2011).
18. Tzoulis, C. *et al.* Leukoencephalopathy with brainstem and spinal cord involvement caused by a novel mutation in the DARS2 gene. *J. Neurol.* **259,** 292–296 (2012).
19. van Berge, L. *et al.* Leukoencephalopathy with brainstem and spinal cord involvement and lactate elevation: clinical and genetic characterization and target for therapy. *Brain* **137,** 1019–1029 (2014).
20. van der Knaap, M. S. *et al.* A new leukoencephalopathy with brainstem and spinal cord involvement and high lactate. *Ann. Neurol.* **53,** 252–258 (2003).
21. Synofzik, M. *et al.* Acetazolamide-responsive exercise-induced episodic ataxia associated with a novel homozygous DARS2 mutation. *J. Med. Genet.* **48,** 713–715 (2011).
22. Scheper, G. C., van der Knaap, M. S. & Proud, C. G. Translation matters: protein synthesis defects in inherited disease. *Nat. Rev. Genet.* **8,** 711–723 (2007).
23. van Berge, L. *et al.* Pathogenic mutations causing LBSL affect mitochondrial aspartyl-tRNA synthetase in diverse ways. *Biochemical Journal* **450,** 345–350 (2013).
24. van Berge, L. *et al.* Leukoencephalopathy with brain stem and spinal cord involvement and lactate elevation is associated with cell-type-dependent splicing of mtAspRS mRNA. *Biochem J.* **441,** 955–962 (2012).
25. Messmer, M. *et al.* A human pathology-related mutation prevents import of an aminoacyl-tRNA synthetase into mitochondria. *Biochem J.* **433,** 441–446 (2011).
26. Neuenfeldt, A. *et al.* Thermodynamic properties distinguish human mitochondrial aspartyl-tRNA synthetase from bacterial homolog with same 3D architecture. *Nucleic Acids Res.* **41,** 2698–2708 (2013).
27. Gaudry, A. *et al.* Redesigned N-terminus enhances expression, solubility, and crystallisability of mitochondrial enzyme. *Protein Engineering, Design and Selection* **25,** 473–481 (2012).
28. Messmer, M. *et al.* Peculiar inhibition of human mitochondrial aspartyl-tRNA synthetase by adenylate analogs. *Biochimie* **91,** 596–603 (2009).
29. Giegé, R., Touzé, E., Lorber, B., Théobald-Dietrich, A. & Sauter, C. Crystallogenesis trends of free and liganded aminoacyl-tRNA synthetases. *Crystal Growth & Design* **8,** 4297–4306 (2008).
30. Bonnefond, L. *et al.* Exploiting Protein Engineering and Crystal Polymorphism for Successful X-ray Structure Determination. *Crystal Growth & Design* **11,** 4334–4343 (2011).
31. Cassandrini, D. *et al.* Pontocerebellar hypoplasia type 6 caused by mutations in RARS2: definition of the clinical spectrum and molecular findings in five patients. *J Inherit Metab Dis.* **36,** 43–53 (2013).
32. Guo, M., Schimmel, P. & Yang, X.-L. Functional expansion of human tRNA synthetases achieved by structural inventions. *FEBS Lett.* **584,** 434–442 (2010).
33. Kim, S., You, S. & Hwang, D. Aminoacyl-tRNA synthetases and tumorigenesis: more than housekeeping. *Nat Rev Cancer.* **11,** 708–718 (2011).
34. Guo, M. & Schimmel, P. Essential nontranslational functions of tRNA synthetases. *Nature Chemical Biology* **9,** 145–153 (2013).
35. Lorber, B., Fischer, F., Bailly, M., Roy, H. & Kern, D. Protein analysis by dynamic light scattering: Methods and techniques for students. Biochem. *Mol. Biol. Educ.* **40,** 372–382 (2012).
36. Réfrégiers, M. *et al.* DISCO synchrotron-radiation circular-dichroism endstation at SOLEIL. *J Synchrotron Radiat.* **19,** 831–835 (2012).
37. Lees, J. G., Smith, B. R., Wien, F., Miles, A. J. & Wallace, B. A. CDtool-an integrated software package for circular dichroism spectroscopic data processing, analysis, and archiving. *Anal. Biochem.* **332,** 285–289 (2004).
38. Sreerama, N. & Woody, R. W. Estimation of protein secondary structure from circular dichroism spectra: comparison of CONTIN, SELCON, and CDSSTR methods with an expanded reference set. *Anal. Biochem* **287,** 252–260 (2000).
39. Whitmore, L. & Wallace, B. A. DICHROWEB, an online server for protein secondary structure analyses from circular dichroism spectroscopic data. *Nucleic Acids Research* **32,** W668–W673 (2004).
40. Lees, J. G., Miles, A. J., Wien, F. & Wallace, B. A. A reference database for circular dichroism spectroscopy covering fold and secondary structure space. *Bioinformatics* **22,** 1955–1962 (2006).
41. David, G. & Pérez, J. Combined sampler robot and high-performance liquid chromatography: a fully automated system for biological small-angle X-ray scattering experiments at the Synchrotron SOLEIL SWING beamline. *J. Appl. Cryst.* **42,** 892–900 (2009).
42. Konarev, P. V., Petoukhov, M. V., Volkov, V. V. & Svergun, D. I. ATSAS 2.1, a program package for small-angle scattering data analysis. *J. Appl. Crystallogr.* **39,** 277–286 (2006).
43. Svergun, D. I. Determination of the regularization parameter in indirect-transform methods using perceptual criteria. *J. Appl. Cryst.* **25,** 495–503 (1992).
44. Evrard, G., Mareuil, F., Bontems, F., Sizun, C. & Pérez, J. DADIMODO: a program for refining the structure of multidomain proteins and complexes against small-angle scattering data and NMR-derived restraints. *J. Appl. Cryst.* **44,** 1264–1271 (2011).
45. Svergun, D. I., Barberato, C. & Koch, M. H. J. CRYSOL – a Program to Evaluate X-ray Solution Scattering of Biological Macromolecules from Atomic Coordinates. *J. Appl. Crystallogr.* **28,** 768–773 (1995).
46. Jester, B. C., Drillien, R., Ruff, M. & Florentz, C. Using Vaccinia's innate ability to introduce DNA into mammalian cells for production of recombinant proteins. *J. Biotechnol.* **156,** 211–213 (2011).
47. Schneider, C. A., Rasband, W. S. & Eliceiri, K. NIH Image to ImageJ: 25 years of image analysis. *Nat Methods.* **9,** 671–675 (2012).
48. Cusack, S., Berthet-Colominas, C., Härtlein, M., Nassar, N. & Leberman, R. A second class of synthetase structure revealed by X-ray analysis of *Escherichia coli* seryl-tRNA synthetase at 2.5 A. *Nature* **347,** 249–255 (1990).

Acknowledgements

The authors are grateful to Anne Neuenfeldt for her contribution at an early step of this project, Julie Lopès for technical assistance and Joseph Chihade for linguistic improvements of the manuscript. They thank the teams of SWING-SAXS and DISCO-SRCD beamlines at Synchrotron SOLEIL for the beamtime allocation and support. They also thank Robert Drillien (IGBMC, Illkirch) for a generous gift of BHK cells and modified vaccinia virus. This work was supported by Centre National de la Recherche Scientifique (CNRS), Université de Strasbourg (UNISTRA), France Diplomatie (no. 200930), ANR-09-BLAN-0091-01/03, ANR-PCV07-187047, the French National Program "Investissement d'Avenir" (Labex MitoCross), administered by the "Agence National de la Recherche", and referenced [ANR-11-LABX-0057_MITOCROSS]. H.S. was supported by Région Alsace, Université de Strasbourg, AFM and Fondation des Treilles. L.K. was supported by LabEx MitoCross.

Author Contributions

C.S., B.L., C.F. and M.S. conceived the original idea and designed the experiments. A.G. expressed and purified WT and mutant proteins. B.L. performed DLS and SLS experiments. B.L. and A.G. performed DSF experiments. C.S., B.L. and F.W. performed SRCD experiments. C.S. and P.R. performed SAXS experiments. L.K. and H.S. performed solubility experiments using cellular extracts. C.S., B.L. and M.S. wrote the manuscript. All authors analyzed and discussed the results, and commented on the manuscript.

Additional Information

Supplementary information accompanies this paper at http://www.nature.com/srep

Competing financial interests: The authors declare no competing financial interests.

How to cite this article: Sauter, C. *et al.* Neurodegenerative disease-associated mutants of a human mitochondrial aminoacyl-tRNA synthetase present individual molecular signatures. *Sci. Rep.* **5**, 17332; doi: 10.1038/srep17332 (2015).

SUPPLEMENTARY MATERIAL

Title: Neurodegenerative disease-associated mutants of a human mitochondrial aminoacyl-tRNA synthetase present individual molecular signatures

Author list: Claude SAUTER[1†]*, Bernard LORBER[1†], Agnès GAUDRY[1], Loukmane KARIM[1], Hagen SCHWENZER[1#], Frank WIEN[2], Pierre ROBLIN[2,3], Catherine FLORENTZ[1] and Marie SISSLER[1]*

[1] Architecture et Réactivité de l'ARN, CNRS, Université de Strasbourg, IBMC, 15 rue René Descartes, 67084 STRASBOURG Cedex, France

[2] Synchrotron SOLEIL, L'Orme des Merisiers Saint Aubin, 91410 Gif-sur-Yvette, France;

[3] URBIA-Nantes, INRA Centre de Nantes, 60 rue de la Géraudière, 44316 Nantes, France.

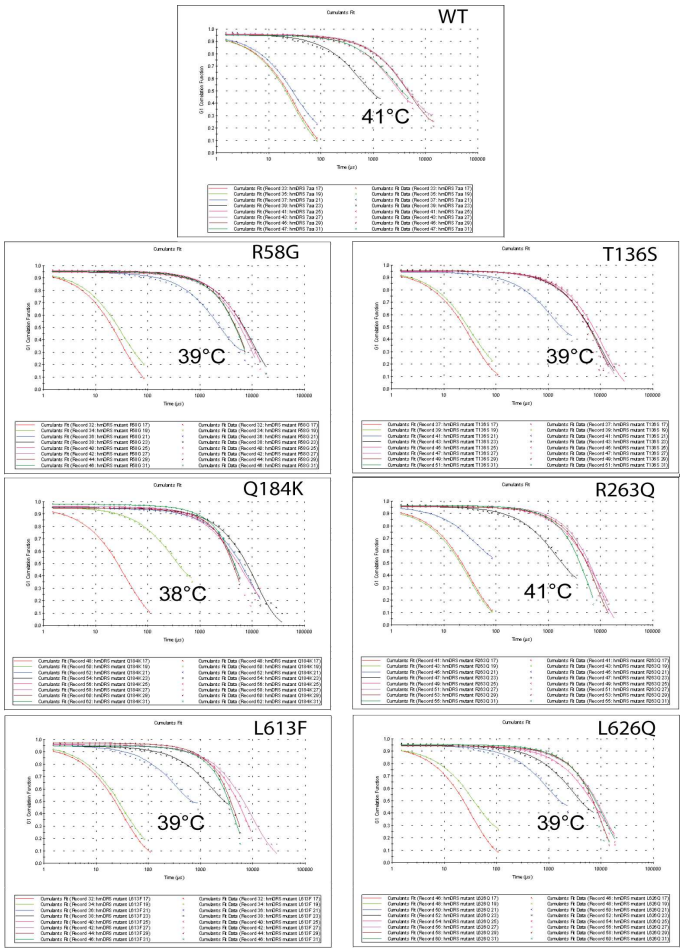

Supplementary Figure 1: DLS analysis of WT mt-AspRS and mutants as a function of temperature. A shift in the auto-correlation function indicates a drop in diffusion coefficient (i.e. increase in size). The temperature at which the shift starts is highlighted.

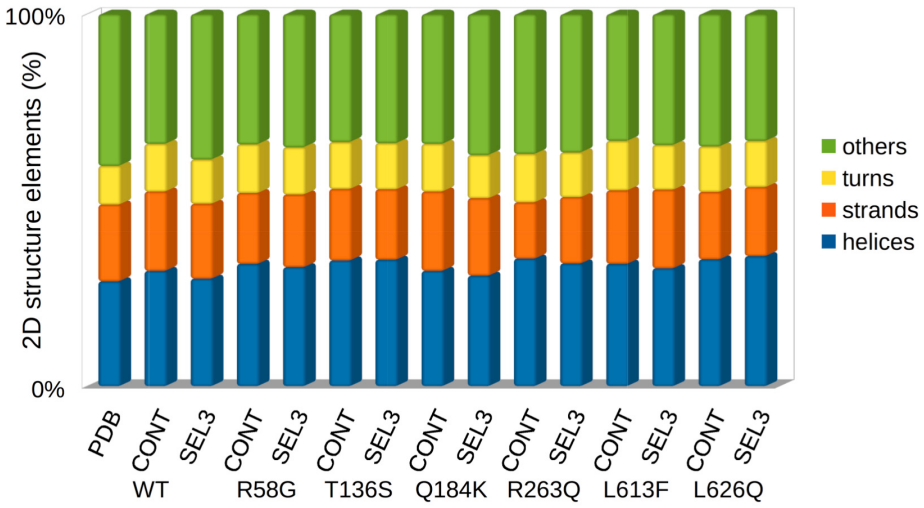

Supplementary Figure 2: Secondary structure contents of WT mt-AspRS and mutants. The percentage of helices, beta strands and turns was determined from SRCD spectra collected at 24°C (as displayed in Figure 2) using CONTINLL and SELCON3 (see methods). The distribution of 2D elements in the X-ray structure of mt-AspRS (PDBid: 4AH6) was determined using DSSP[49]. Numerical data are listed in **Supplementary Table 2**.

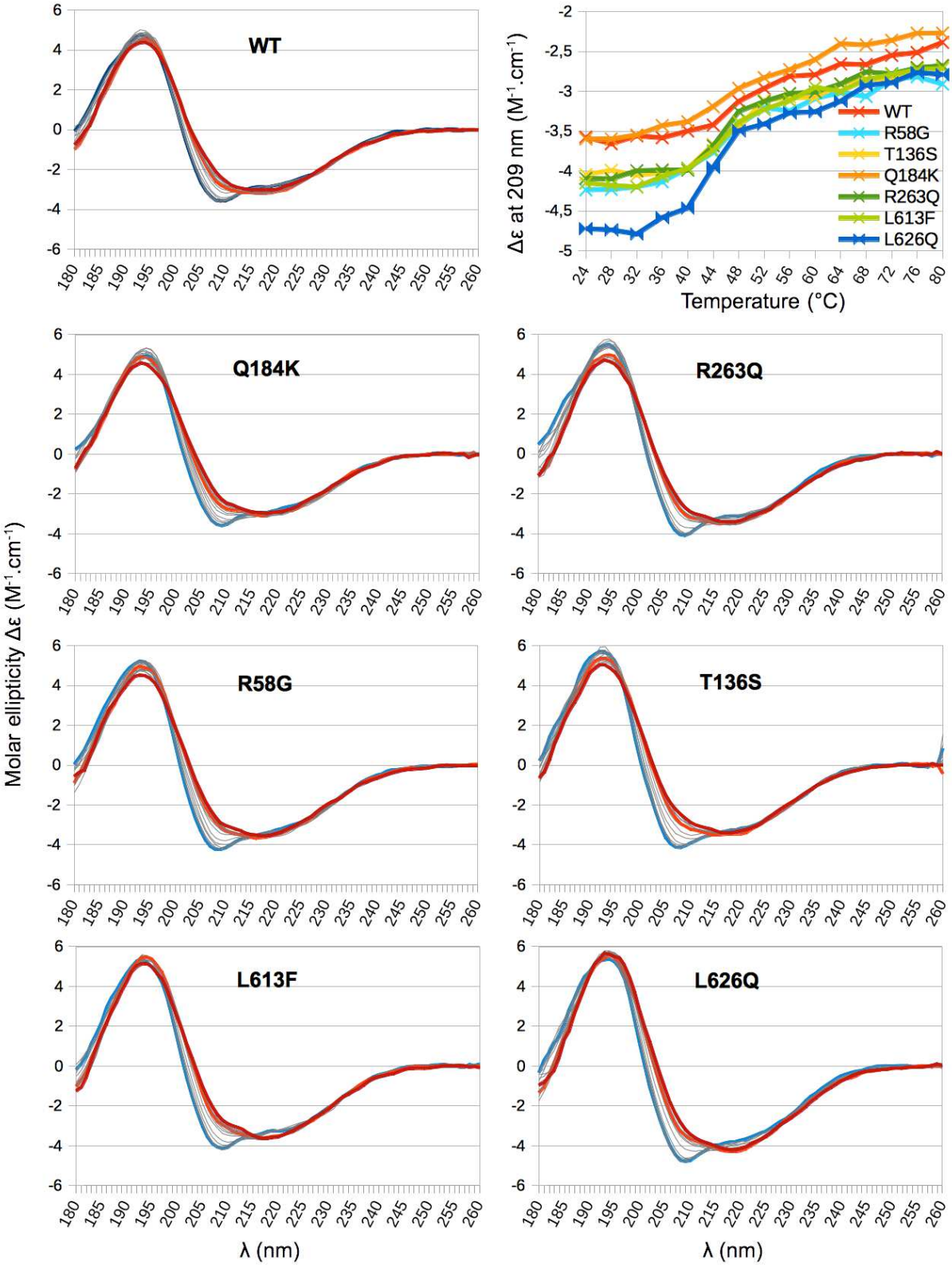

Supplementary Figure 3: SRCD spectra of WT mt-AspRS and mutants as a function of temperature. The temperature was stepwise increased from 24°C (blue curve) to 80°C (red curve). (Top right panel) Variation of ellipticity at 209 nm is plotted for each variant as a function of temperature.

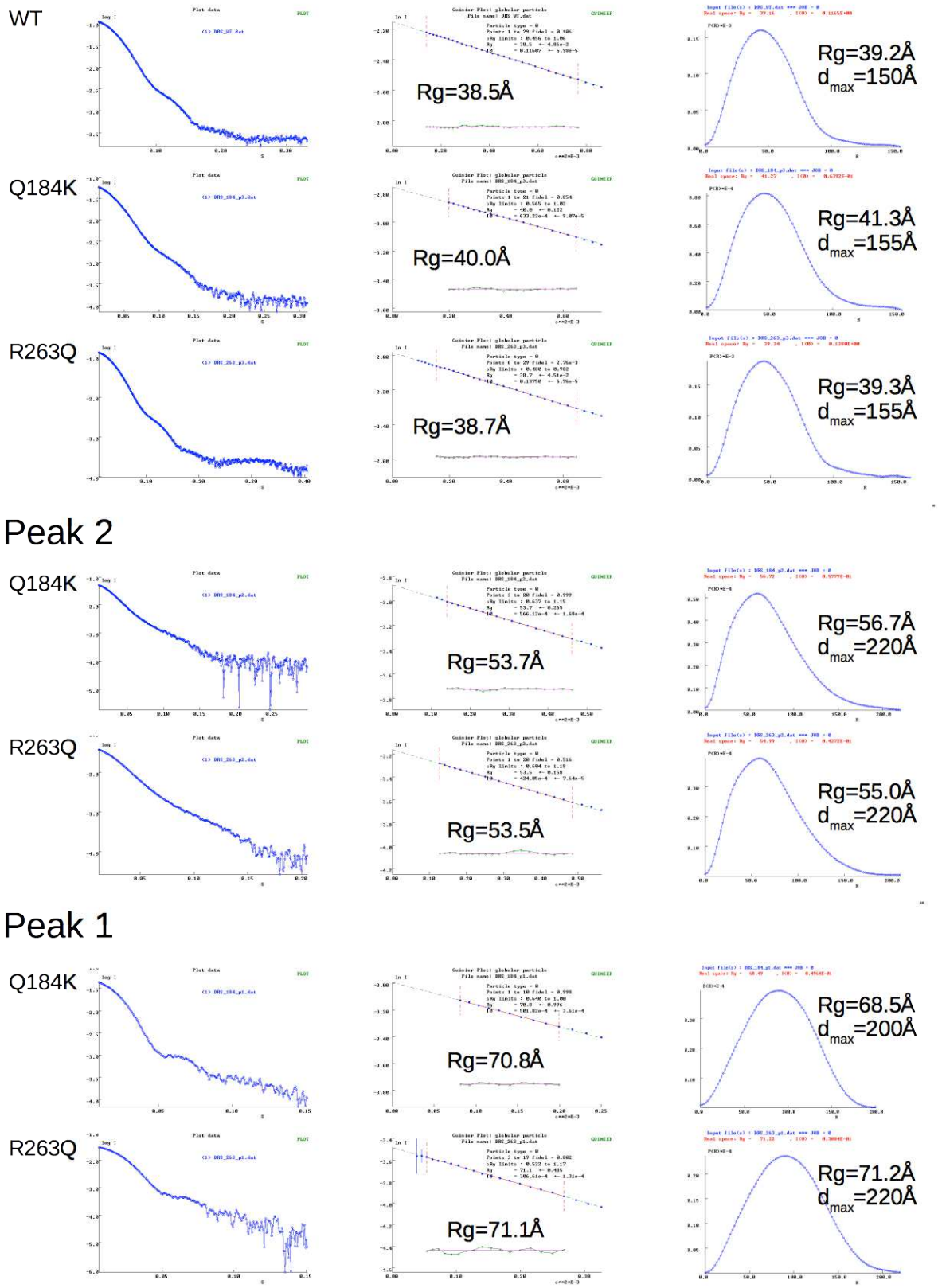

Supplementary Figure 4: SAXS analysis of WT mt-AspRS and Q184K and R263Q mutants. (Left, center, right) Experimental SAXS profiles, Guinier plots and P(r) distance distribution functions for each protein population isolated by SEC in peaks 1-3.

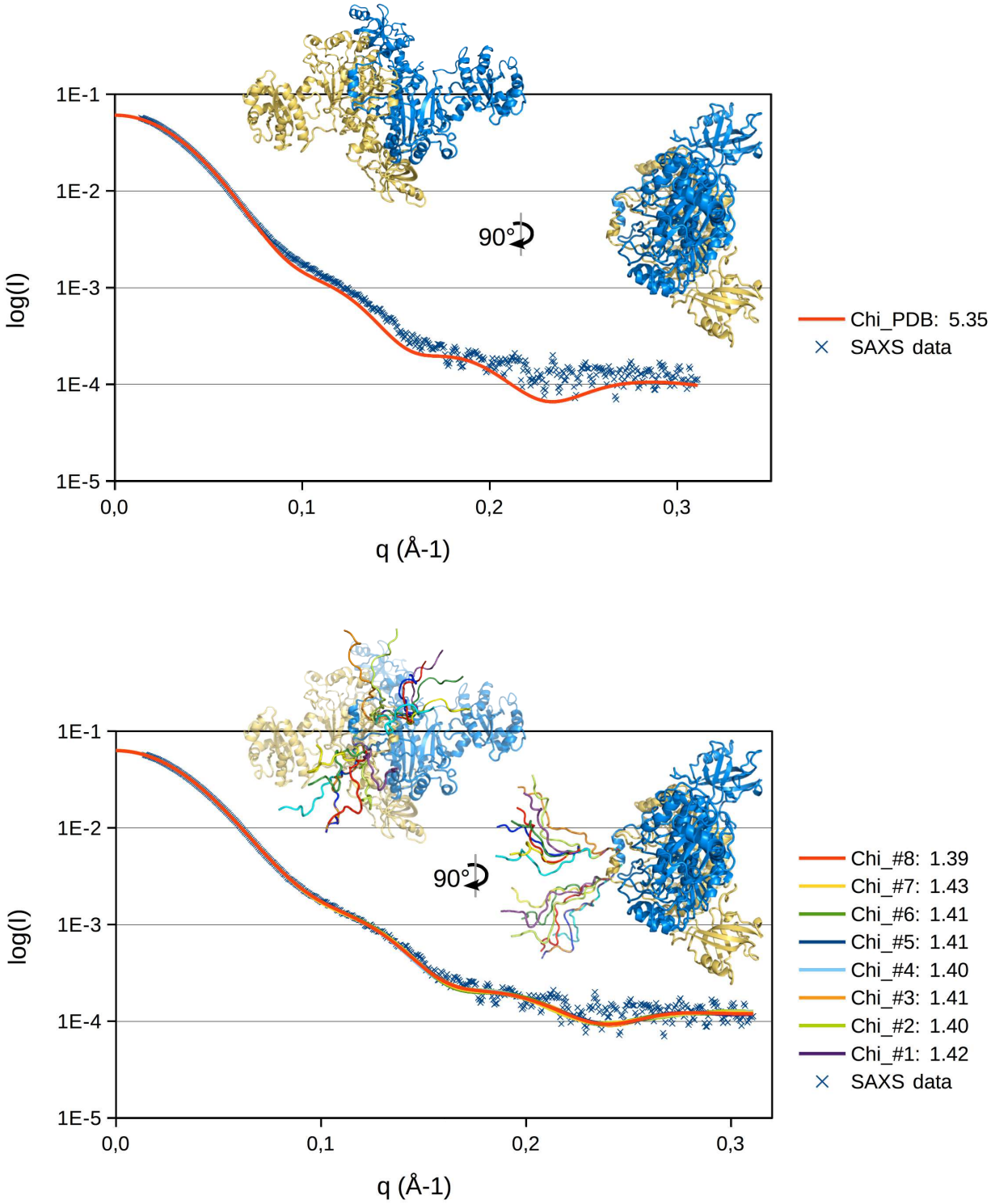

Supplementary Figure 5: Structure of mt-AspRS dimers in solution. Experimental SAXS profile of mtAspRS (Q184K mutant - blue dots) was compared to theoretical curves computed for atomic models corresponding to the crystal structure (PDBid: 4AH6) lacking the C-terminal extensions (Top) and to a series of complete models generated by DADIMODO (Bottom). C-terminal extension models and corresponding curves are depicted with the same color. The goodness-of-fit (Chi) was determined using CRYSOL. Models including the C-terminal extensions display a better fit with the data as indicated by lower Chi values.

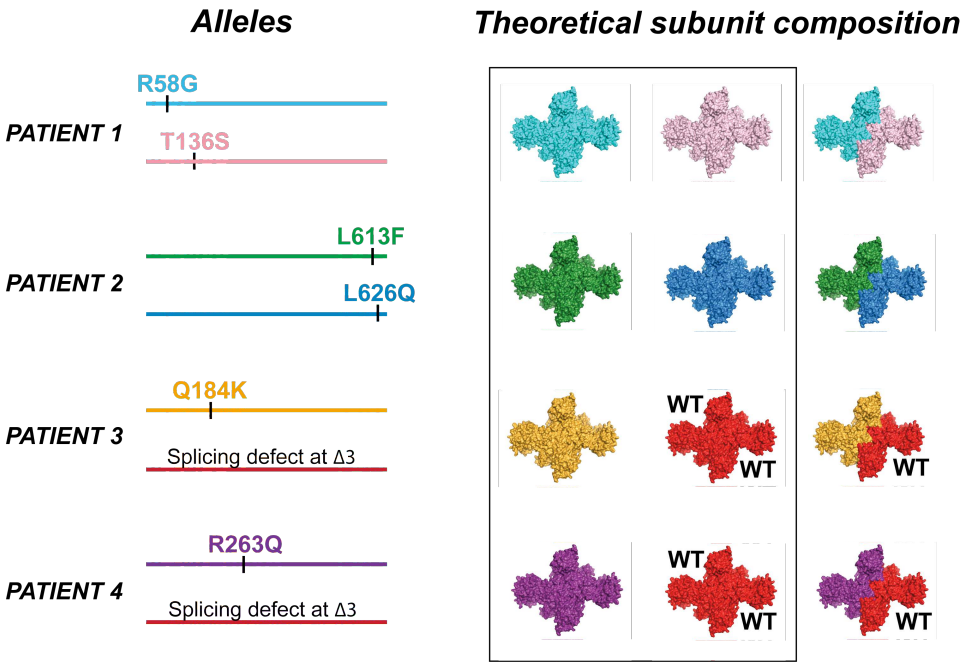

Supplementary Figure 6: Theoretical subunit composition of mt-AspRS dimers resulting from LBSL associated mutations in alleles of heterozygote patients. Situations explored in this study are boxed.

Supplementary Table 1: Phenotypes of LBSL patients with selected mutations

Allelic composition		First neurological Signs at years	Loss of unsupported walking at years	Full wheelchair dependency at years	Age in 2013 in years
Mutation 1	Mutation 2				
R58G	T136S	3	-	-	23
R58G	T136S	2	-	-	15
L613F	L626Q	12	28	-	36
Q184K	R76Serfs*5	6	-	-	22
Q184K	R76Serfs*5	7	18	-	20
R263Q	R76Serfs*5	3	8	20	33
R263Q	R76Serfs*5	5	28	-	29
R263X [a)]	R76Serfs*5	2	6	-	20
R263X [a)]	R76Serfs*5	1	14	22	24

Adapted from [50]. [a)] not analyzed in the present study but added for comparison.

Supplementary Table 2: Secondary structure contents derived from SRCD spectra

Sample		WT-mt-AspRS	R58G	T136S	Q184K	R263Q	L613F	L626Q
Method	PDB	CONT / SEL3	CONT / SEL3	CONT / SEL3	CONT / SEL3	CONT / SEL3	CONT / SEL3	CONT / SEL3
Helices	28,2	31,0 / 28,9	32,9 / 32,0	33,8 / 34,0	31,0 / 29,7	34,3 / 33,0	32,9 / 31,7	34,1 / 35,0
Strands	20,6	21,3 / 20,1	19,0 / 19,5	19,2 / 18,9	21,3 / 20,8	15,1 / 17,8	19,7 / 21,1	18,1 / 18,5
Turns	10,4	12,8 / 11,9	13,1 / 12,7	12,6 / 12,4	12,8 / 11,6	13,0 / 12,0	13,3 / 12,0	12,2 / 12,4
Others	40,8	34,9 / 39,1	35,0 / 35,8	34,4 / 34,7	34,9 / 37,9	37,6 / 37,2	34,1 / 35,2	35,6 / 34,1
RMSD		9,8 / 14,6	0,1 / 12,2	13,1 / 12,8	9,8 / 14,6	13,0 / 19,0	12,2 / 13,5	13,9 / 13,4

The percentage of 2D elements was assessed from the PDB entry of WT mt-AspRS using DSSP[49] and determined from SRCD spectra collected at 24°C using CONTINLL (CONT) and SELCON3 (SEL3). The RMSD of the 2D element estimation is indicated for each method.

Supplementary Table 3: Analysis of amino acid conservation and changes in mt-AspRS sequences

Mutations		**R58G**	**T136S**	**Q184K**	**R263Q**	**L613F**	**L626Q**
Location		Anticodon-binding domain	Anticodon-binding domain	Catalytic domain	Catalytic domain	C-terminal extension	C-terminal extension
WT residue conservation	**all seq.** (180)	no	no	no	**R/K** (~97%)	no	no
	mt mammals (11)	mainly **R**	yes	yes	yes	only **L/V**	yes
	mt others (49)	no	no	no	mainly **R**	**L** (~60%), **P** (~40%)	**L** (~80%), **R** (~20%)
	bacteria (120)	no	mainly **T** – a few **S**	no	mainly **R**	**L** (~60%), **P** (~40%)	**L** (~80%), **R** (~20%)
Natural occurrence of substituting residue		**G** in some bacteria	**S** in some bacteria	**R/K** in some bacteria; **R** in mt of fungi	**Q** in one bacterium and one mt arthropod	no	no
Structural environment of WT residue		Exposed to solvent. No visible interaction with neighbor residues	Hydrophobic environment. Near **L**, **V** and **M** residues	At the beginning of dimerization helix. Involved in a network of hydrogen bonds (G253 from other chain; L178 and R188 of the same chain)	Close to the enzyme 2-fold axis. Interacts with E277 (from same monomer) and T212 (from opposite monomer)	In the vicinity of tRNA binding site	Close to the enzyme 2-fold axis. In the dimerization mini-helix
Theoretical structural impact of the mutation		Loss of one positive charge. No local rearrangement	Loss of a methyl group and of van der Waals interactions, but compatible with hydrophobic environment.	15 out of 18 theoretical conformers lead to steric hindrances.	Loss of a positive charge. Leaves a negative charge with no interactant	2 out of 4 theoretical conformers lead to steric hindrances.	4 out of 16 theoretical conformers lead to steric hindrances.

–Conservation of WT residue– and –Natural occurrence of substitution– were analyzed in a multiple sequence alignment composed of 180 bacterial–type AspRSs, as generated in[51]. This alignment is made of 120 sequences of AspRS proteins from bacteria (encompassing all bacterial subgroups) and 60 sequences of mt-AspRS proteins from eukaryotes (with representatives of mammals, arthropods, fungi and protists). For an objective evaluation of the sequence conservation or divergence, redundancy was avoided by considering only non-identical sequences.

Supplementary Table 4: Analysis of amino acid conservation of mt-AspRS positions impacted by disease-associated missense mutations

	Mutations	**N52S** (ref.[50])	**R125H** (ref.[50])	**I139T** (ref.[50])	**C152F** (ref.[52])	**R179H** (ref.[52])	**G206E** (ref.[50])	**L239P** (ref.[53])	**Q248K** (ref.[52])	**L249I** (ref.[54])
	Location	anticodon-binding domain	anticodon-binding domain	anticodon-binding domain	anticodon-binding domain	helix of dimerization	catalytic domain (motif 1)	catalytic domain	catalytic domain	catalytic domain
WT residue conservation	**all seq. (180)**	no	**R/K** (~97%)	no	no	yes (100%)	no	yes (100%)	yes (100%)	no
	mt mammals (11)	**yes (100%)**	**yes (100%)**	**yes (100%)**	**yes (100%)**	**yes (100%)**	**yes (100%)**	**yes (100%)**	**yes (100%)**	**yes (100%)**
	mt others (49)	no	no (mainly **K**)	no	no	yes (100%)	no	yes (100%)	yes (100%)	no (**L/I/M/T**)
	bacteria (120)	no (never a **N**)	yes (100% **R**)	mainly **I/V**	no	yes (100%)	no	yes (100%)	yes (100%)	no (**L/I/M/V**)
	natural occurrence of substituting res.	no	no	no	no	no	**E** in some mt others, and in some bacteria	no	no	**I** in some mt others, and in some bacteria
	allelic composition	**C152F**	Exon 3 splicing defect	Exon 3 splicing defect	**N52S**	Exon 3 splicing defect	Exon 3 splicing defect	Exon 3 splicing defect	Exon 3 splicing defect	Exon 3 splicing defect

	Mutations	**L250P** (ref.[50])	**G254S** (ref.[50])	**E284K** (ref.[55])	**R336H** (ref.[50])	**P576S** (ref.[50])	**D560V** (ref.[52])	**R609W** (ref.[56])	**L626V** (ref.[52])	**Y629C** (ref.[52])
	Location	catalytic domain	catalytic domain	catalytic domain (motif 2)	catalytic domain	catalytic domain	catalytic domain	bacterial-type C-terminal extension	bacterial-type C-terminal extension	bacterial-type C-terminal extension
WT residue conservation	**all seq. (180)**	**L** (~97%)	**G** (~97%)	yes (100%)	**R** (~97%)	yes (100%)	no	no	no	no
	mt mammals (11)	**yes (100%)**	**yes (100%)**	**yes (100%)**	**yes (100%)**	**yes (100%)**	**yes (100%)**	**yes (100%)**	**yes (100%)**	**yes (100%)**
	mt others (49)	yes (100%)	mainly **G** (some **S/A**)	yes (100%)	mainly **R** (some **C/G**)	yes (100%)	no	no	no	yes (100%)
	bacteria (120)	mainly **L** (some **M/C**)	yes (100%)	yes (100%)	yes (100%)	yes (100%)	no	no	no	no
	natural occurrence of substituting res.	no	no	no	no	no	no	no	no	no
	allelic composition	Exon 3 splicing defect	Exon 3 splicing defect	Exon 3 splicing defect	Exon 3 splicing defect	Exon 3 splicing defect	Exon 3 splicing defect	**R609W**	**L613F**	Exon 3 splicing defect

Mutations were taken from references [50, 52-56] as indicated. They were reported after the beginning of the present work (except for those from ref. [52]). –Conservation of WT residue– and –Natural occurrence of substitution– were analyzed in a multiple sequence alignment composed of 180 bacterial–type AspRSs, as generated in[51]. This alignment is made of 120 sequences of AspRS proteins from bacteria (encompassing all bacterial subgroups) and 60 sequences of mt-AspRS proteins from eukaryotes (with representatives of mammals, arthropods, fungi and protists). For an objective evaluation of the sequence conservation or divergence, redundancy was avoided by considering only non-identical sequences. Allelic composition recalls the situation found in patients.

References

49. Joosten, R.P. et al. A series of PDB related databases for everyday needs. *Nucleic Acids Research* **3**, D411-D419 (2011).
50. van Berge, L. et al. Leukoencephalopathy with brainstem and spinal cord involvement and lactate elevation: clinical and genetic characterization and target for therapy. *Brain* **137**, 1019-1029 (2014).
51. Schwenzer, H. et al. Released selective pressure on a structural domain gives new insights on the functional relaxation of mitochondrial aspartyl-tRNA synthetase. *Biochimie (Special Issue "Mitochondria: an organelle for life")* **100**, 18-26 (2014).
52. Scheper, G.C. et al. Mitochondrial aspartyl-tRNA synthetase deficiency causes leukoencephalopathy with brain stem and spinal cord involvement and lactate elevation. *Nat Genet* **39**, 534-539 (2007).
53. Lin, J. et al. Leukoencephalopathy with brainstem and spinal cord involvement and normal lactate: a new mutation in the DARS2 gene. *J. Child. Neurol.* **25**, 1425-1428 (2010).
54. Labauge, P., Dorboz, I., Eymard-Pierre, E., Dereeper, O. & Boespflug-Tanguy, O. Clinically asymptomatic adult patient with extensive LBSL MRI pattern and DARS2 mutations. *J. Neurol.* **258**, 335-337 (2011).
55. Cheng, F.B. et al. Adult-onset leukoencephalopathy with brain stem and spinal cord involvement in Chinese Han population: a case report and literature review. *Neurol India.* **61**, 161-163 (2013).
56. Synofzik, M. et al. Acetazolamide-responsive exercise-induced episodic ataxia associated with a novel homozygous DARS2 mutation. *J. Med. Genet.* **48**, 713-715 (2011).

Methods xxx (2016) xxx–xxx

Annex 3

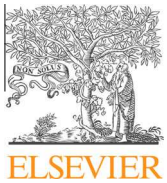

Contents lists available at ScienceDirect

Methods

journal homepage: www.elsevier.com/locate/ymeth

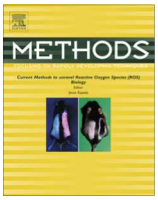

Two proteomic methodologies for defining N-termini of mature human mitochondrial aminoacyl-tRNA synthetases

Christine Carapito [a,1], Lauriane Kuhn [b,1], Loukmane Karim [c], Magali Rompais [a], Thierry Rabilloud [d], Hagen Schwenzer [c,2], Marie Sissler [c,*]

[a] Laboratoire de Spectrométrie de Masse BioOrganique, Université de Strasbourg, CNRS, IPHC, UMR 7178, F-67000 Strasbourg, France
[b] Plateforme Protéomique Strasbourg – Esplanade, Institut de Biologie Moléculaire et Cellulaire, CNRS, FRC 1589, 15 rue Descartes, F-67084 Strasbourg Cedex, France
[c] Université de Strasbourg, CNRS, Architecture et Réactivité de l'ARN, UPR 9002, F-67000 Strasbourg, France
[d] Laboratoire de Chimie et Biologie des Métaux, UMR CNRS-CEA-UGA 5249, iRTSV/LCBM, CEA Grenoble, Grenoble, France

ARTICLE INFO

Article history:
Received 22 August 2016
Received in revised form 21 October 2016
Accepted 24 October 2016
Available online xxxx

Keywords:
Mitochondrial targeting sequence
Maturation
Aminoacyl-tRNA synthetases
Human
Mitochondria
Shotgun proteomics
N-terminomics

ABSTRACT

Human mitochondrial aminoacyl-tRNA synthetases (mt-aaRSs) are encoded in the nucleus, synthesized in the cytosol and targeted for importation into mitochondria by a N-terminal mitochondrial targeting sequence. This targeting sequence is presumably cleaved upon entry into the mitochondria, following a process still not fully deciphered in human, despite essential roles for the mitochondrial biogenesis. Maturation processes are indeed essential both for the release of a functional enzyme and to route correctly the protein within mitochondria. The absence of consensus sequences for cleavage sites and the discovery of possible multiple proteolytic steps render predictions of N-termini difficult. Further, the knowledge of the cleavages is key for the design of protein constructions compatible with efficient production in bacterial strains. Finally, full comprehension becomes essential because a growing number of mutations are found in genes coding for mt-aaRS. In the present study, we take advantage of proteomic methodological developments and identified, in mitochondria, three N-termini for the human mitochondrial aspartyl-tRNA synthetase. This first description of the co-existence of different forms opens new perspectives in the biological understanding of this enzyme. Those methods are extended to the whole set of human mt-aaRSs and methodological advice are provided for further investigations.

1. Introduction

Mitochondria are the powerhouse of eukaryotic cells. They host essential metabolic pathways and harbor a genome (mt-DNA) that codes in human for only 13 proteins. Thus, the vast majority of proteins (>99%) necessary for mitochondrial (mt) biogenesis and functions (estimated number ~ 1500 [1]) are encoded by the nucleus, expressed as precursor proteins in the cytosol, and targeted to the mitochondria thanks to a sorting signal (reviewed in *e.g.* [2]). Among imported proteins, the human mitochondrial aminoacyl-tRNA synthetases (mt-aaRSs) are key actors of the mitochondrial translation apparatus by catalyzing the aminoacylation of tRNAs with cognate amino acids. Mt-aaRSs are encoded by a set of genes mainly distinct from the ones coding for the cytosolic aaRSs [3]. The only two exceptions concern the GlyRSs and LysRSs encoded by single genes but produced by, respectively, alternate starting codons [4] and alternate splicing of pre-mRNA [5].

In general, mitochondrial precursor proteins are translocated into mitochondria through the outer mitochondrial membrane (*via* the TOM complex, the mitochondria entry gate) and, depending on sorting signals, further internalized towards the matrix through the translocase of the inner membrane (TIM), or alternatively integrated into the inner or the outer membrane, or released in the inter-membranes space. More than four different import pathways of precursor proteins are presently reported (reviewed in *e.g.* [6–9]). The sorting signals include mitochondrial targeting sequences (MTSs), either in a form of an internal or a C-terminal signal that is non-cleavable and remains in the mature protein, or as a N-terminal pre-sequence that is often proteolytically

Abbreviations: aaRS, aminoacyl-tRNA synthetase; mt, mitochondrial; MTS, mitochondrial targeting sequence; TMPP, trimethoxyphenyl phosphonium.

* Corresponding author at: IBMC – 15 rue René Descartes, 67084 Strasbourg Cedex, France.
E-mail address: M.Sissler@ibmc-cnrs.unistra.fr (M. Sissler).

[1] These authors contributed equally to this work and should be considered as co-first-authors. Their names are listed alphabetically.

[2] Present address: Division of Infection and Immunity, University College London (UCL), Cruciform Building, 90 Gower Street, London WC1E 6BT, UK.

http://dx.doi.org/10.1016/j.ymeth.2016.10.012
1046-2023/

removed after import (reviewed in *e.g.* [10]). Among the identified peptidases, the mitochondrial processing peptidase (MPP) cleaves pre-sequences of most incoming precursor proteins (*e.g.* [11]). As illustrated in Fig. 1, additional cleavages can subsequently occur to remove *e.g.* newly exposed N-terminal sorting peptides (inner membrane peptidase, IMP; mitochondrial intermediate peptidase, MIP; *e.g.* [6,12]) or destabilizing residues (the yeast intermediate cleaving peptidases Icp55 [13] or the human Aminopeptidase P APP3 [14]). Although several peptidases have been identified, deciphering the proteolytic cleavage site of N-terminal MTS remains a challenging task. Some studies were performed to decode cleavable motifs recognized by the MPP [11], to profile the constitutive proteolytic events *in vivo* [15], or to determine the mature N-termini of the majority of the known yeast mitochondrial proteins (named "N-proteome" [13]). However, the absence of consensus sequences for cleavage sites and the discovery of possible multiple proteolytic steps render predictions difficult.

Import/maturation pathways were mainly studied using fungal model organisms but are far from being fully deciphered in higher eukaryotic organisms. The identification of N-terminal amino acids of mature proteins is, however, essential not only to understand the mechanisms underlying the mitochondrial biogenesis [6], but also to design sequences compatible with efficient expression in bacterial strains (*e.g.* [16–18]). It also becomes a necessity at a time where a growing number of pathology-related mutations are discovered in proteins involved in mitochondrial biogenesis (reviewed in *e.g.* [19–23]), and more specifically in mt-aaRSs (reviewed in [24,25]).

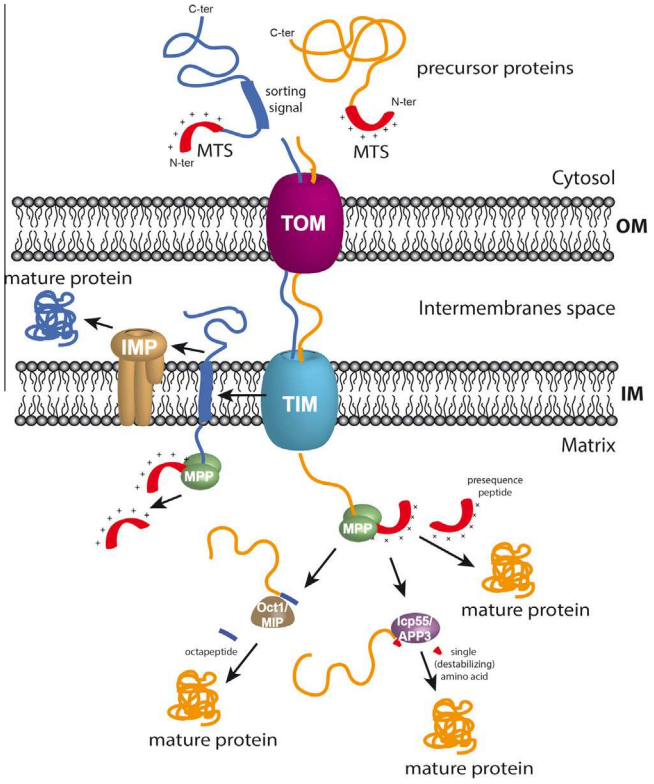

Fig. 1. Schematic overview of mitochondrial processing of precursor proteins with N-terminal targeting sequence (MTS). Mitochondrial precursor proteins are translated on cytosolic ribosomes and transported into mitochondria through the translocase of the outer-membrane (TOM) and the translocase of the inner-membrane (TIM) complexes. The N-terminal MTS is proteolytically removed upon import by several proteases, localized in the mitochondrial matrix and the inner membrane (IM). MPP: mitochondrial processing peptidase; IMP: inner membrane peptidase; Oct1: octapeptidyl aminopeptidase (yeast); MIP: mitochondrial intermediate peptidase; Icp55: intermediate cleaving peptidase 55 (yeast); and AAP3: Aminopeptidase P 3 (human). The illustration is adapted from Ref. [10].

Here, we take advantage of recent developments in proteomic methodologies to characterize mature N-termini of mt-aaRSs, with a focus on mt-AspRS. We applied two strategies that both led to the same results helping to open biological understanding of the enzyme. Further, we extended the strategy to the whole family of human mt-aaRSs.

2. Experimental procedures

2.1. Mitochondria purification and mt-AspRS enrichment

Mitochondria from human U937 cells were prepared essentially as described in [26]. Briefly, cells were harvested, rinsed three times in phosphate-buffered saline (PBS) solution and re-suspended in ten-fold pellet volume of hypotonic buffer (10 mM Hepes-NaOH pH 7.5, 2 mM $MgCl_2$, 1 mM EGTA, 50 mM KCl). After 10 min on ice, cells were lysed by ten strokes of a Dounce homogenizer (tight pestle). One-tenth volume of 2 M sucrose was then added, and the mixture was homogenized by two additional strokes. The suspension was centrifuged at 1000*g* for 5 min to pellet the nuclei and unbroken cells. The supernatant was then centrifuged at 7000*g* for 10 min to pellet the mitochondria. The mitochondrial pellet was re-suspended in washing buffer (10 mM Hepes-NaOH pH 7.5, 2 mM $MgCl_2$, 250 mM sucrose) and recentrifuged at 7000*g* for 10 min.

For the shotgun strategy, mt-AspRS was enriched by immunoprecipitation from crude mitochondrial extract from HEK293 cells. To do so, HEK293 cells, grown in ten to fifteen T175 culture flasks, were harvested when at a confluence of 80% and washed twice in PBS buffer. The cell pellet was resuspended in 10 ml buffer A (220 mM mannitol, 70 mM sucrose, 10 mM Hepes-KOH pH 7.5, 1 mM $MgCl_2$, 1 mM EDTA and 1% BSA) and ruptured using a Waring blender (5 × 10 s). The lysate was centrifuged for 10 min at 800*g* to remove unbroken cells. The supernatant was centrifuged for 30 min at 8600*g*. The obtained pellet was re-suspended in buffer A and centrifuged sequentially at 800*g* and 8600*g*. The mitochondrial pellet was washed in buffer B (20 mM Hepes-KOH pH 7.5, 200 mM KAc, 0.2% Triton X100) and cracked by sonication (5 strokes at 6 watts for 10 s). The lysate was diluted twice in buffer C (20 mM Hepes-KOH pH 7.5, 200 mM KAc) in order to reduce the Triton concentration below 0.05%, which is suitable for downstream immunoprecipitation experiment. Contaminating membranes were removed by centrifugation at 100,000*g* for 45 min at 4 °C. The crude mitochondrial extract was first incubated for 1 h at 4 °C with protein A agarose beads, and second with non-specific IgG covalently coupled with protein A agarose beads. The pre-cleared lysate was then incubated for 2 h at 4 °C with human mt-AspRS-specific IgG cross-linked protein A agarose beads. The beads were then incubated with 10 volumes of PBS for 30 min at 4 °C, loaded on a gravity-flow column, and further washed with five volumes of PBS. Mt-AspRS-enriched sample was recovered from the beads by two incubations of 5 min at 50 °C in 250 mM Tris-HCl pH 7.5 and 2% Sodium dodecyl sulfate (SDS), concentrated using Centricon centrifugal filter device (10 kDa, Millipore), and loaded on a large 10% SDS-PAGE.

2.2. Shotgun proteomics

2.2.1. Sample preparation

Twenty-five protein bands, systematically excised from the SDS-PAGE lane, were transferred into a 96-well microtiter plate. Gel slices were washed with three cycles of incubations in 25 mM ammonium bicarbonate for 15 min and then in 25 mM ammonium bicarbonate containing 50% (v/v) acetonitrile for 15 min. Samples were dehydrated with 100% acetonitrile and then

reduced with 10 mM DTT for 1 h at 56 °C. Proteins were then alkylated with 55 mM iodoacetamide for 1 h in the dark at room temperature. Gel pieces were washed again with the destaining solutions described above. Twenty nanograms of sequencing-grade porcine trypsin (5 ng/µl, V5111, Promega, Madison, WI) in 25 mM ammonium bicarbonate were added to each dehydrated gel piece. After 30 min of rehydration at room temperature, 30 µl of 25 mM ammonium bicarbonate was added on gel pieces before trypsin digestion, overnight at room temperature. The resulting peptides were then extracted from the gel pieces in 30 µl of 60% acetonitrile and 5% formic acid. The initial digestion and extraction supernatants were pooled and vacuum-dried in a SpeedVac.

2.2.2. Liquid chromatography-tandem mass spectrometry (LC-MS/MS) analyses

The dried peptides were re-suspended in 15 µl of water containing 0.1% formic acid (solvent A). Peptide mixtures were analyzed using a NanoLC-2DPlus system (with nanoFlex ChiP module; Eksigent, ABSciex, Concord, Ontario, Canada) coupled to a TripleTOF 5600 mass spectrometer (ABSciex) operating in positive mode. After 10 min of desalting and concentration, the pre-column was switched online with the analytical ChIP C-18 analytical column (75 µm ID × 15 cm ChromXP; Eksigent). Peptides were eluted using a 5%–40% gradient of solvent B (0.1% formic acid in ACN) for 60 min at a flow rate of 300 nl/min. The TripleTOF 5600 was operated in data-dependent acquisition. Up to 20 of the most intense multiply charged ions were selected for CID fragmentation: this "Top20" method had a constant cycle time of 3.3 s and was set to a high-sensitivity mode.

2.2.3. Data interpretation

MS/MS data were searched against the human UniProtKB-SwissProt database (release 2016-01-21, 22105 sequences) using the Mascot algorithm (version 2.2, Matrix Science, London, UK). Peptide modifications allowed during the search were: N-acetyl (protein N-term), carbamidomethylation (C) and oxidation (M). Mass tolerances in MS and MS/MS were set to 20 ppm and 0.5 Da, respectively; the instrument setting was specified as ESI-QUAD-TOF and three missed cleavages were allowed. Semi-trypsin (allowing only one tryptic end) was used for enzyme specificity. Proteins were validated at FDR <1% at the protein level (Proteinscape 3.1, Bruker Daltonics, Bremen, Germany) using a decoy database strategy. MS/MS spectra matching on the N-terminal part of proteins were carefully manually inspected.

2.3. Doublet N-terminal oriented proteomics (dN-TOP)

2.3.1. Doublet TMPP-labeling and SDS-PAGE separation

The protocol used here was adapted from previous work [26,27]. The pellets of purified mitochondria were re-suspended in labeling buffer (50 mM Tris-HCl, 8 M urea, 2 M thiourea, SDS 1%, pH 8.2), reduced (5 mM tributylphosphine (TBP), 1 h) and alkylated (50 mM iodoacetamide (IAA), 1 h, room temperature). An equimolar solution of 0.1 M of 12C-TMPP-Ac-OSu ((N-succinimidyloxycarbonylmethyl)tris(2,4,6-trimethoxyphenyl)phosphonium bromide) and 13C9-TMPP-Ac-OSu in acetonitrile:water (8:2; v/v) was added at a molar ratio of 200:1 and incubated for 1 h at room temperature. Residual derivatizing reagent was quenched by adding a solution of 0.1 M hydroxylamine at room temperature for 1 h. Glycerol (10%) and bromophenol blue (1%) were added to the samples before loading on a 12% monodimensional SDS-PAGE (10.1 cm × 7.3 cm) on a mini PROTEAN (Bio-Rad) apparatus at 50 V for 20 min and 120 V until the complete migration of the blue front. Molecular mass markers (10–250 kDa, Precision Plus Protein™ Unstained Standards, Bio-Rad) were used as migration control. After migration, the gels were washed with water and fixed using 3% Phosphoric acid in 50:50 ethanol:water (v:v). Gels were stained by a colloidal blue method (G250, Fluka, Buchs, Switzerland) and whole lanes were systematically cut in 27 2 mm-bands using a disposable grid-cutter (The Gel-Company, Tübingen, Germany). Slices were divided into three pieces, in-gel reduced and alkylated using the MassPrep Station (Waters, Milford, MA, USA) and in-gel digested overnight at 37 °C using porcine trypsin (Promega, Madison, WI). Resulting tryptic peptides were extracted using 60% ACN in 0.1% formic acid for 1 h at room temperature. The volume was reduced in a vacuum centrifuge and re-suspended using 0.1% formic acid in water before nanoLC-MS/MS analysis.

2.3.2. Liquid chromatography-tandem mass spectrometry (LC-MS/MS) analyses

NanoLC-MS/MS analyses were performed on a NanoAcquity LC-system (Waters) coupled to a Q-Exactive Plus Orbitrap (Thermo Fisher Scientific) mass spectrometer equipped with a nanoelectrospray ion source. The HPLC system consisted of a solvent degasser nanoflow pump, a thermostated column oven kept at 60 °C and a thermostated autosampler kept at 10 °C. Mobile phase A (99.9% water and 0.1% FA) and mobile phase B (99.9% acetonitrile and 0.1% FA) were delivered at 450 nl/min by the nanoAcquity. Samples were loaded into a Symmetry C18 precolumn (0.18 × 20 mm, 5 µm particle size, Waters) over 3 min in 1% buffer B at a flow rate of 5 µl/min. This step was followed by reverse-phase separation at a flow rate of 450 nl/min using an ACQUITY UPLC® BEH130 C18 separation column (200 mm × 75 µm id, 1.7 µm particle size, Waters). Peptides were eluted using a gradient from 1% B to 8% B in 2 min, from 8% B to 40% B in 28 min, from 40% B to 90% B in 1 min, 90% B for 5 min and the column was reconditioned at 1% B. The Q-Exactive plus Orbitrap instrument was operated in data dependent mode by automatically switching between full MS and consecutive MS/MS acquisitions. Survey full scan MS spectra (mass range 300–1800) were acquired in the Orbitrap at a resolution of 70 K at 200 m/z with an automatic gain control (AGC) fixed at 3×10^6 ions and a maximal injection time set at 50 ms. The ten most intense peptide ions in each survey scan with a charge state $\geqslant 2$ were selected for MS/MS. MS/MS spectra were acquired at 17,500 resolution at 200 m/z with a fixed first mass at 100 m/z, AGC was fixed at 1×10^5 and the maximal injection time was set to 100 ms. Peptides were fragmented in the HCD cell by higher-energy collisional dissociation with a normalized collision energy set to 27. Peaks selected for fragmentation were automatically put on a dynamic exclusion list for 60 s and peptide match selection was turned on. MS data were saved in RAW file format (Thermo Fisher Scientific) using XCalibur.

2.3.3. Data interpretation

The data interpretation workflow was adapted from Vaca Jacome et al. [26]. A first search round was done using Mascot run on a local server (version 2.5.1) and OMSSA (version 2.1.9) run through the in-house developed MSDA (Mass Spectrometry Data Analysis) interface [28], against a concatenated target/decoy human UniProtKB-SwissProt database (release-2015_02_12 containing 20282 target sequences) that was generated with the database toolbox from MSDA. Full trypsin enzyme specificity was used, one missed cleavage was allowed and carbamidomethylation of cysteine (+57 Da) was set as a fixed modification. Oxidation of methionine (+16 Da) and protein N-terminal acetylation (+42 Da) were set as variable modifications. Mass tolerance for precursor ions was set at 5 ppm, and at 0.07 Da for fragment ions. Mascot and OMSSA results files were loaded into Proline software (http://proline.profiproteomics.fr/ [29]) and proteins were validated on pretty rank (as defined by Mascot) equal to 1, 1% FDR

on peptide spectrum matches (PSM) based on PSM score and 1% FDR on protein sets based on protein set score. High-quality spectra were recovered from all non-assigned spectra during the first search round thanks to the Recover module of MSDA [28]. A second search round using Mascot and OMSSA was performed using semi-trypsin enzyme specificity on the recovered spectra. In the second search round, the N-terminal modification and side chain derivatization of Tyr and Lys with TMPP were set for light and heavy TMPP (+572.18 Da and +581.21 Da, respectively) and the oxidation of methionine residues were set as variable modifications. Search results files were loaded into Proline and further validated as described in Vaca Jacome et al. [26].

3. Results

3.1. Analytical workflow

Fig. 2 summarizes the analytical strategy developed in this study to characterize mature mt-aaRSs N-termini. First, a classical shotgun proteomics workflow was applied on a mt-AspRS-enriched fraction obtained by immunoprecipitation. The protein extract was separated on a 1D-SDS-PAGE gel and bands were systematically cut and analyzed using high performing nanoLC-MS/MS analysis on a Q-TOF instrument. The generated LC-MS/MS data were searched using semi-trypsin specificity in the human UniProtKB-SwissProt database in order to be able to detect potential mature N-termini as semi-tryptic peptides.

Second, in order to target N-termini more specifically, the doublet N-Terminal Oriented Proteomics (dN-TOP) strategy was applied on a total mitochondrial preparation. The double labeling of free protein's N-termini was performed using simultaneous chemical labeling with light and heavy trimethoxyphenyl phosphonium (TMPP). Validation of the detected TMPP-peptides requires very stringent criteria to be met: both the light and heavy labeled forms of the potential N-terminal peptide need to be identified using database searches, both peptides need to be perfectly co-eluted and the peptide sequence must be unique in the searched database. The labeled sample was loaded on a 1D-SDS-PAGE gel. The systematic analysis of 27 gel bands using a nanoLC-Q-Orbitrap coupling and interpretation of generated LC-MS/MS data were performed as described in [26]. One of the major advantages of this approach resides in the fact that internal peptides are not removed and thus contribute to the identifications of the proteins, while the specifically labeled N-terminal peptides are unequivocally validated using the doublet of labeled peptides.

3.2. N-termini identified for mt-AspRS

To identify the mature N-termini of the mt-AspRS, the protein was first enriched by immuno-precipitation out of a crude mitochondrial protein extract obtained from 10^8 HEK293 cells and in-gel-digested with Trypsin (Fig. 2). Shotgun LC-MS/MS analyses followed by semi-trypsin searches identified two fully-tryptic peptides at positions 40 and 41 (R_{40}IPEFSSFVVR with a mass of 446.2497 Th (m/z) with one missed cleavage and I_{41}PEFSSFVVR with a mass of 590.8184 Th (m/z)), as the peptides closest to the N-terminus of mt-AspRS (Table 1). Additionally, two semi-tryptic peptides were identified: L_{33}LQSSQR with a mass of 416.237 Th

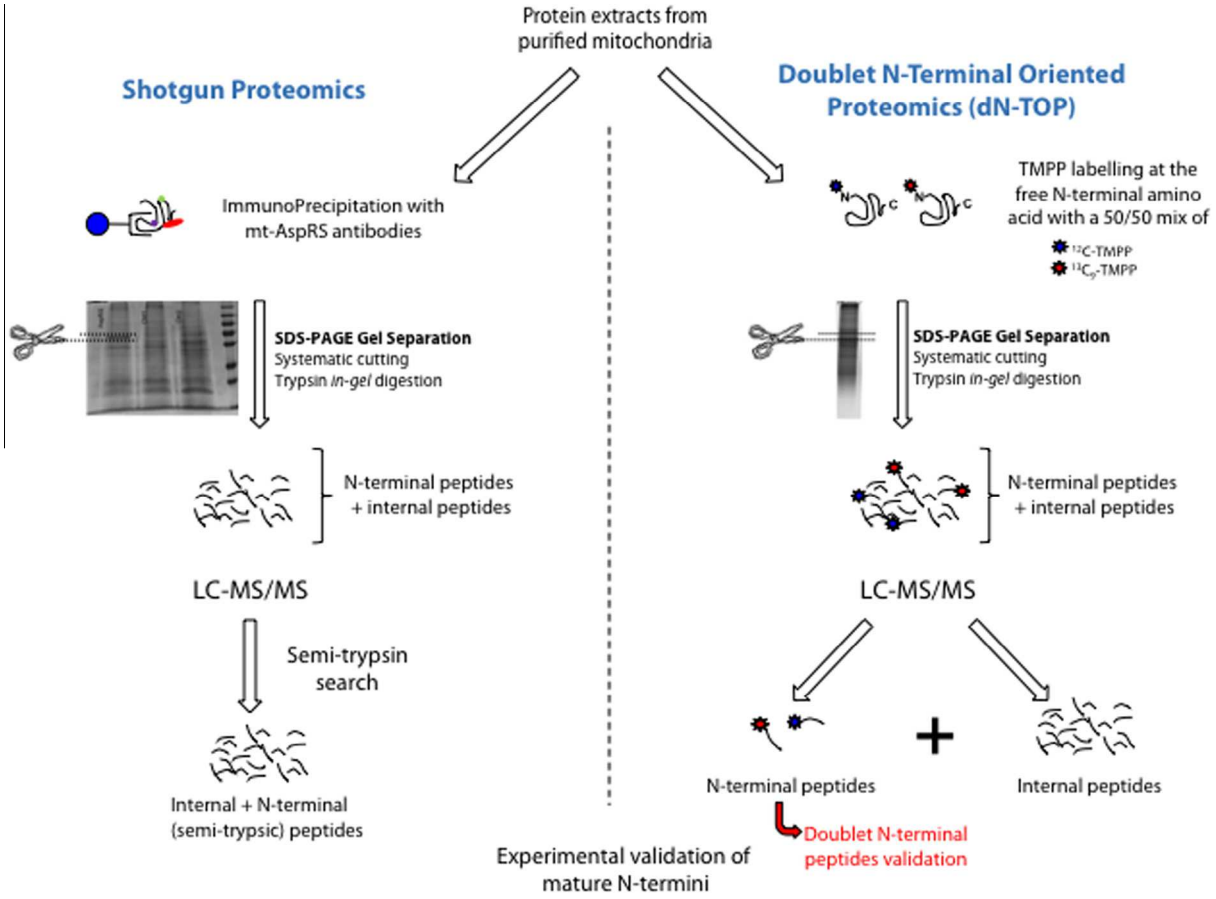

Fig. 2. Experimental workflow. Protein extracts are either mt-AspRS enriched sample, obtained by immunoprecipitation, or total mitochondrial extract. Left: classical shotgun proteomics approach with semi-trypsin searches. Right: Doublet N-Terminal Oriented Proteomics with light/heavy TMPP labeling. (adapted from Ref. [26]).

Please cite this article in press as: C. Carapito et al., Methods (2016), http://dx.doi.org/10.1016/j.ymeth.2016.10.012

Table 1
Identified human mt-aaRSs peptides using Shotgun Proteomics on a mt-AspRS enriched sample or Doublet N-terminal oriented Proteomics on mitochondrial protein extracts. Gene names, UniProt accession numbers and protein sizes are given for the 19 human mt-aaRSs. Sequences of the most upstream tryptic internal peptides are given, when detected. Validated N-terminal peptides indicative of N-terminal mature sequence after processing within mitochondria are highlighted in bold characters. Nd stands for not determined.

Gene name	Short name	UniProt accession	Protein size number of aa (Da)	Shotgun Proteomics on mt-AspRS enriched sample			Doublet N-terminal oriented Proteomics on mitochondrial protein extracts			
				Number of internal unique peptides	Most upstream tryptic internal peptide (sequence)	N-term. semi-tryptic peptide (sequence)	Number of internal unique peptides	Most upstream tryptic internal peptide (sequence)	TMPP labeled N-term. peptide (Number)	Mature start positions (start sequence)
AARS2	AlaRS	Q5JTZ9	985 (107340)	7	E_{251}ADGSLQPLPQR	nd	50	A_{44}AFLNFFR	Yes (2)	**S_{26}HRPLSSEPPAAK** **S_{31}SEPPAAK**
CARS2	CysRS	Q9HA77	564 (62224)	nd	nd	nd	23	E_{49}TGVQVYNSLTGR	No	nd
DARS2	AspRS	Q6PI48	645 (73563)	31	R_{40}IPEFSSFVVR **I_{41}PEFSSFVVR**	**L_{33}LQSSQR** **P_{42}EFSSFVVR**	34	R_{40}IPEFSSFVVR	Yes (3)	**L_{33}LQSSQR** **I_{41}PEFSSFVVR** **P_{42}EFSSFVVR**
EARS2	GluRS	Q5JPH6	523 (58689)	nd	nd	nd	2	F_{41}APSPTGFLHLGGLR	No	nd
FARS2	PheRS	O95363	451 (52357)	nd	nd	nd	10	A_{46}PGSVVELLGK	No	nd
GARS	GlyRS	P41250	762 (83166)	nd	nd	nd	44	S_{76}SMDGAGAEEVLAPLR	Yes (2)	**G_{80}AGAEEVLAPLR** **T_{514}VNVVQFEPSKGAIGK**
HARS2	HisRS	P49590	506 (56888)	6	E_{160}SPTIVQGR	**S_{35}QVAEAVLTSQLK**	17	D_{65}LSPQHMVVR	Yes (1)	**S_{35}QVAEAVLTSQLK**
IARS2	IleRS	Q9NSE4	1012 (113792)	3	Q_{79}QPDTELEIQQK	nd	65	Y_{60}RDTVLLPQTSFPMK	Yes (2)	**V_{45}SGASNHQPNSNSGR** **T_{63}VLLPQTSFPMK**
KARS	LysRS	Q15046-2	625 (71497)	nd	nd	nd	28	F_{99}HVDISLTDFIQK	No	nd
LARS2	LeuRS	Q15031	903 (101976)	nd	nd	nd	29	F_{84}YVLSMFPYPSGK	Yes (1)	**I_{40}YSATGK**
MARS2	MetRS	Q96GW9	593 (66591)	1	L_{569}GPETGLLFPR	nd	11	A_{45}YFTTPIFYVNAAPHIGH-LYSALLADALCR	Yes (1)	**S_{30}SGSLSAGDDACDVR**
NARS2	AsnRS	Q96I59	477 (54090)	nd	nd	nd	11	D_{32}ALGAQNASGER	No	nd
PARS2	ProRS	Q7L3T8	475 (53263)	nd	nd	nd	8	V_{45}FQPQNLR	No	nd
RARS2	ArgRS	Q5T160	578 (65505)	7	L_{72}RCDTVVSEISTGQR	nd	15	D_{53}NDHSRPDIQVQAK	No	nd
SARS2	SerRS	Q9NP81	518 (58283)	2	G_{254}FTPMTVPDLLR	nd	23	E_{50}GYLSALPQLDIER	No	nd
TARS2	ThrRS	Q9BW92	718 (81036)	13	**L_{20}HTAVVSTPPR**	nd	23	L_{36}GLFEELWAAQVKR	Yes (2)	**L_{20}HTAVVSTPPR** **S_{277}GISFPTTELLR**
VARS2	ValRS	Q5ST30	1063 (118490)	nd	nd	nd	14	S_{285}AISDIEVENRPLPGHTQLR	No	nd
WARS2	TrpRS	Q9UGM6	360 (40147)	nd	nd	nd	11	V_{37}FSGIQPTGILHLGN-YLGAIESWVR	No	nd
YARS2	TyrRS	Q9Y2Z4	477 (53199)	2	I_{59}ELPELFDR	nd	18	A_{31}HSGAQGLLAAQK	No	nd

(m/z) and P_{42}EFSSFVVR with a mass of 534.2785 Th (m/z). All these peptides were validated with the stringent FDR criteria applied and show high quality MS/MS spectra (Supplementary Fig. 1, Table 1). It is of note that these two peptides were the only semi-tryptic peptides validated for mt-AspRS, which strengthens the confidence in the identification of these potential sites as start positions.

In order to confirm and refine these results, a targeted approach named dN-TOP (recently developed and described in [26]), which uses simultaneous chemical labeling with light and heavy TMPP of free protein's N-termini, was applied on total mitochondrial protein extracts (Fig. 2). This strategy allowed unequivocally confirming three N-termini at positions Leu_{33}, Ile_{41} and Pro_{42}. All full-scan MS/MS spectra of the non-labeled and TMPP-labeled peptides supporting the identification of these three start positions are provided in Supplementary Fig. 1.

3.3. Searching for N-terminal peptides for the full set of mt-aaRSs

As the AspRS-enriched sample was prepared under non-stringent experimental conditions, other mt-aaRSs were searched within the same sample. To do so, the SDS-PAGE gel was systematically cut from the top of the gel to the front of migration. All bands of the gel were analyzed in LC-MS/MS and interpreted using the shotgun approach. This allowed identifying eight additional mt-aaRSs, with yet lower sequence coverage than for mt-AspRS (as reflected by the number of detected internal peptides, Table 1). Interestingly, one semi-tryptic peptide was validated for mt-HisRS at position 35, as demonstrated by the observation of the peptide S_{35}QVAEAVLTSQLK with a doubly charged mass of 687.3802 Th (m/z). Interestingly, no other semi-tryptic peptide was identified downstream this residue on mt-HisRS sequence, as for mt-AspRS. Again, the detection of this potential mt-HisRS N-terminus was further confirmed by the dN-TOP approach.

In the same way, as the dN-TOP approach was applied on total purified mitochondria analyzed in a systematic way, complementary data on all other members of the mt-aaRSs family were generated. Table 1 summarizes the results obtained. Overall, at least two unique internal peptides were identified for each of the 19 proteins providing here a unique experimental proof of expression of the complete family. Besides, TMPP-labeled peptides, thus mature N-termini, were identified for 8 of the 19 proteins, and for 5 of them multiple start positions were validated.

4. Discussion

4.1. Complementary strategies

Two complementary proteomic strategies have been undertaken in the present study to identify natural N-termini of mt-aaRS after import into mitochondria and maturation (Fig. 2). The first strategy combines the immuno-enrichment of the protein sample with classical shotgun LC-MS/MS analysis and semi-trypsin database searching; the second strategy, named dN-TOP, uses the N-terminal chemical modification of the mitochondrial proteome, prior to LC-MS/MS analysis and specific identification of chemically modified N-terminal peptides.

The shotgun approach conducted on a mt-AspRS-enriched sample is an efficient way to achieve high sequence coverage on the enriched protein (as shown in Table 1) and to propose potential N-termini. However, these potential N-termini can only be identified by semi-trypic peptides and no conclusion can be drawn on fully tryptic peptides. Indeed, if the maturation of the precursor protein occurs after a lysine or an arginine, the N-terminal peptide will be detected as a fully-tryptic peptide. In such a situation, one cannot distinguish whether this peptide is an internal peptide (properly cleaved on both ends by trypsin) or a newly generated mature N-terminus (cleaved only on C-terminal end by trypsin). For these ambiguous peptides, the dN-TOP approach is a more conclusive strategy, thanks to the specific chemical labeling of the N-termini. This is illustrated on peptides I_{41}PEFSSFVVR on mt-AspRS and L_{20}HTAVVSTPPR on ThrRS: these two fully-tryptic peptides were confirmed to be real mature N-termini thanks to the dN-TOP approach.

The combination of both strategies allowed providing evidence of expression for all 19 members of the family with at least 2 unique peptides. Though, some mature N-termini still remain undetected. This could be due to poor LC-MS compatibility of concerned protein sequences: to be detectable in LC-MS/MS, peptides need to be compatible in terms of hydrophobicity, size and modification status. In order to attempt going further in this characterization one could try systematically enriching individual mt-aaRSs, apply the dN-TOP approach on enriched samples in combination with multiple enzymatic digestions with the objective of generating and detecting MS-friendly peptides for the enriched mt-aaRS.

4.2. The two proteomic approaches reveal three N-termini for human mt-AspRS

The characterization of the cleavage site after *in organello* maturation of mitochondrial targeting sequence (MTS) remains a challenging task. Concerning the human mt-AspRS, several attempts were performed. For instance, the protein was enriched by immunoprecipitation out of a crude mitochondrial protein extract obtained from ~120 × 10^8 HEK293 cells, but the quality and quantity of the enriched sample were not sufficient for sequencing by Edman degradation. MTS of mt-AspRS was predicted *in silico* (Predotar [30] and MitoProt [31]) to be cleaved between residues Val_{48} and Val_{49}; or based on multiple sequence alignment to be cleaved between residues Phe_{47} and Val_{48} [3]. The recombinant protein expressed in *E. coli* based on the last prediction turned out to have reduced solubility [18]. More recently, a new program MitoFates predicts mt-AspRS MTS to be cleaved between residue Ser_{32} and Leu_{33} [32] (Fig. 3A). The two complementary proteomic approaches applied in this study allowed demonstrating the presence in mitochondrial extracts of three forms of mt-AspRS with N-termini unequivocally identified at residues Leu_{33}, Ile_{41} and Pro_{42} (Fig. 3B).

Multiple N-termini were foreseen by previous *in vitro* import experiment of ^{35}S- radiolabelled protein into mitochondria purified from HEK293 cells, in which processed forms of mt-AspRS were detected [33]. An inspection of the gel from Fig. 3 in reference [33] reveals two bands corresponding to processed forms of mt-AspRS, while only one is visible for the control experiment. This previous experiment did not allow a more precise identification of the nature of the processed forms. The pattern obtained was, however, similar to the one obtained by others with the yeast mt Rieske Iron-sulfur protein, shown to be successively cleaved by the mitochondrial processing peptidase (MPP) and the mitochondrial intermediate peptidase (MIP) [34]. It has been reported afterwards that mitochondrial protein precursors, processed in two sequential steps by MPP and MIP, are characterized by a motif at the C-terminus of the leader peptide named R-10 with the following characteristic sequence: **R**$_{-10}$x↓(**F/L/I**)$_{-8}$xx(**S/T/G**)$_{-5}$xxxx$_{-1}$↓x$_{+1}$ (reviewed in [11,35]). Alternatively, MPP was shown also to cleave precursor proteins at the level of R-2 or R-3 motifs, both with a conserved arginine residue upstream of the cleavage sites (respectively, **R**$_{-2}$x↓x$_{+1}$

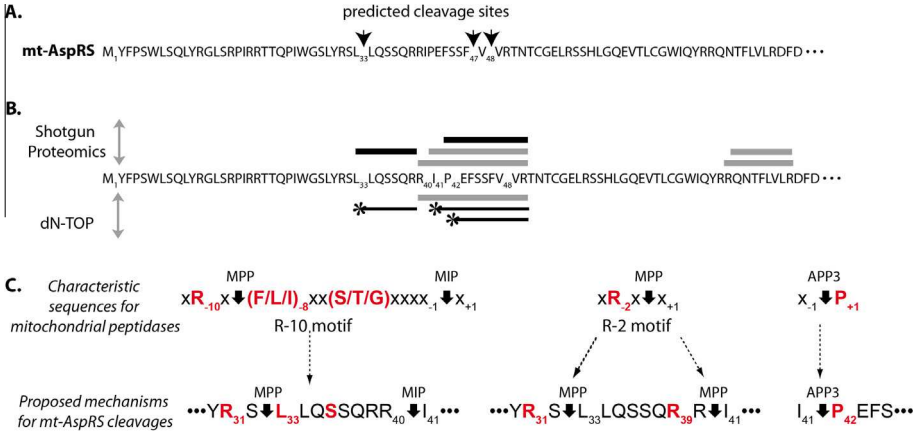

Fig. 3. N-termini for human mitochondrial aspartyl-tRNA synthetase. A. N-terminal sequence of the human mt-AspRS precursor. Cleavage sites, predicted *in silico* (MitoFates [32] for L_{33}; Predotar [30] and MitoProt [31] for F_{47}; based on multiple sequence alignment for V_{48} [3]) are shown with black arrowheads. B. Peptides identified experimentally, by the shotgun Proteomics approach on mt-AspRS enriched sample (above the sequence), and by the doublet N-terminal oriented Proteomics (below the sequence). Tryptic peptides are in gray, semi-tryptic peptides in black, and TMPP-modified peptides in black with asterisks. C. Sequence motifs for peptidases implicated in MTS processing. Upper part: characteristic sequences of R-10 motif, known to be cleaved by mitochondrial processing peptidase (MPP) and mitochondrial intermediate peptidase (MIP); of R-2 motif, cleaved by the MPP (reviewed in [11,35]); and of sequence cleaved by the Aminopeptidase P APP3 [14,39]. Lower part: inspection of mt-AspRS sequence and possible cleavages in agreement with N-terminal peptides experimentally validated.

Please cite this article in press as: C. Carapito et al., Methods (2016), http://dx.doi.org/10.1016/j.ymeth.2016.10.012

and $\mathbf{R}_{-3}$x(F/Y/L)$_{-1}$↓(A/S)$_{+1}$x). The possibility of two independent cleavages by MPP has been observed for instance within the precursor of the human Frataxin and the yeast Frataxin homolog, Yfh1P [36–38]. Thus, inspection of N-terminal sequence of the human mt-AspRS indicates that forms starting at Leu_{33} and Ile_{41} can be produced either in response to a R-10 motif ($\mathbf{R}_{-31}S_{32}$↓$\mathbf{L}_{-33}$LQ$\mathbf{S}_{37}$SQRR$_{41}$↓I$_{42}$) that would thus be cleaved successively by MPP and MIP between residues Ser_{32} and Leu_{33}, and residues Arg_{40} and Ile_{41}, respectively; or in response to two R-2 motifs ($\mathbf{R}_{-31}S_{32}$↓L_{-33} and $\mathbf{R}_{40}R_{41}$↓I_{42}) independently cleaved by MPP at the same two positions (Fig. 3C).

Regarding mt-AspRS starting at Pro_{42}, the most probable hypothesis is a subsequent cleavage of the protein starting at Ile_{41} by the Aminopeptisase P (APP), for which a mitochondrial isoform (APP3 or XPNPEP3) has been described [14,39] (Fig. 3C). This metalloaminopeptidase is related to the yeast Icp55, known to remove destabilizing N-terminal residues [13], which might contribute to prevent from N-end rule-mediated degradation process [40]. APP3 has, however, a restricted specificity, and removes one N-terminal residue upstream a proline [14,39].

The question now is to consider the biological relevance of the different forms. Are some of them intermediates within a sequential maturation process, or do they all co-exist in mitochondria? It is widely acknowledged that maturation of MTS is a fast mechanism and that intermediates are rarely observed *in vivo* [41], and usually barely *in vitro* under low temperature conditions and reduced incubation times [42–44]. The only exception known so far concerns Icp55 (the yeast homolog of APP3) substrates, for which intermediate forms have been detected in addition to mature ones, yet to a lesser extent [13]. Following the latter observation, it can be assumed that mt-AspRS starting at Ile_{41} is an intermediate of mt-AspRS starting at Pro_{42}. Altogether, the identification of three forms of mt-AspRS using the two proteomic approaches presented here, as well as the observation of processed forms after *in vitro* import experiments extended to 30 min of incubation time [33] favors the hypothesis of the co-existence in mitochondria of at least two mature forms of mt-AspRS, with N-termini identified at residues Leu_{33} and Pro_{42}. This is in line with the recent discovery of two mature forms of the mammalian MRPL12, generated by a two-step cleavage during import by MPP and a second cleavage, less efficient or regulated, by MIP [45]. The authors suggest that "the long and short forms of MRPL12 have distinct properties and/or function", and also "that the two-steps processing may be a general mechanism to allow the production of multiple forms of mitochondrial matrix proteins destined to perform different functions". We now have to decipher the biological roles of the long and short mature forms of mt-AspRS.

4.3. Human mitochondrial aminoacyl-tRNA synthetases have idiosyncratic processing patterns

In the present study, besides the detection of all of the 19 human mt-aaRSs by at least two internal peptides, we identified and validated N-termini for eight of them. Noteworthy, some of the N-termini correlate with specific experimental trials, performed to search for the most soluble recombinant mt-aaRS expressed in bacterial strains. For instance, Wang and coworkers tested the solubility of four isoforms of the mt-ThrRS (mt-ThrRSΔ19 *i.e.* deleted of the 19 N-terminal amino acids, mt-ThrRSΔ25, the theoretically predicted mt-ThrRSΔ39, and mt-ThrRSΔ58) but found mt-ThrRSΔ19 as the only soluble protein [46]. This observation is in agreement with the identification here of a N-terminus at position 20 for mt-ThrRS. Similarly, Yao and coworkers showed that mt-LeuRSΔ39, the form identified as being processed in insect cells [17] and further identified here, is drastically more soluble and active than the theoretically predicted mt-LeuRSΔ21 [47]. These observations further illustrate that criteria used to predict MTS cleavage sites should be optimized and would benefit from a more systematic effort to experimentally determine the precise N-termini of mature mitochondrial proteins [18]. Among the eight newly identified N-termini, only the one validated for mt-HisRS is in accordance with predictions [3].

Our data further emphasize the great heterogeneity regarding the lengths of MTS (ranking from 19 amino acids for mt-ThrRS to 80 amino acids for mt-GlyRS) and regarding the processing steps with one N-terminus observed for mt-HisRS, mt-LeuRS, mt-MetRS; two N-termini for mt-AlaRS, mt-GlyRS, mt-IleRS and mt-ThrRS; and three N-termini for mt-AspRS. For mt-GlyRS and mt-ThrRS, the two N-termini are unexpectedly found widely apart from each other, and were therefore named proximal and distal N-termini. Inspection of surrounded sequences indicates that N-termini are most likely generated following a R-2 motif (for mt-IleRS, mt-LeuRS, and for the distal N-terminus of mt-ThrRS), a R-3 motif (for mt-AlaRS and mt-MetRS), an altered R-3 motif (for mt-HisRS), or a R-none motif (for mt-GlyRS and for the proximal N-terminus of mt-ThrRS). The distal N-termini of mt-GlyRS and mt-ThrRS are puzzling. A N-terminus at position 514 for mt-GlyRS would isolate the anticodon binding domain of the enzyme, and at position 277 for mt-ThrRS would liberate the N-terminal TGS-additional domain and restrict mt-ThrRS to its catalytic and anticodon binding domains. The question now is whether these distal N-termini are (i) produced by directed processing or (ii) result from another mechanism known to extend the protein diversity such as alternative splicing or alternative starting codon or (iii) reflect a proteolytic cleavage occurring during the degradation of the protein. In any case, the biological relevance of those isoforms has to be further investigated, as they represent potential new contributors to widen the mitochondrial protein repertoire and may contribute to functional diversity. Supporting this view, truncated versions of human cytosolic aaRSs have already been reported with functions unrelated to the aminoacylation process (*e.g.* [48,49]).

5. Conclusions

A peculiarity of MTSs is the non-conservation of lengths, sequences and amino acid compositions (*e.g.* [6,11,35]), rendering the characterization of N-terminal residues of every mitochondrial protein a unique issue, and sometimes a challenge. A cleavage site is indicative of the processing steps and, thus, gives information about sub-mitochondrial destiny and likely functional properties. Altogether, this knowledge is essential to contribute answering emerging questions not only under wild-type situations/conditions but also to explore the impact(s) of a growing number of pathology-related mutations within nucleus-encoded genes coding for proteins involved in mitochondrial biogenesis (reviewed in *e.g.* [19–23]). Some of the observed mutations, for example the replacement of an Arg residue by another amino acid, could lead to the disappearance or the appearance of a cleavage site with subsequent mislocalization or degradation of the enzyme.

In the present study, we considered a family of enzymes, all devoted to the same cellular process, but which displays a surprising diversity of maturation processes. One can anticipate that this diversity may reflect diversity in mitochondrial location and/or of function(s), as hypothesized for the human mt-AspRS.

Please cite this article in press as: C. Carapito et al., Methods (2016), http://dx.doi.org/10.1016/j.ymeth.2016.10.012

Acknowledgments

This work was supported by Centre National de la Recherche Scientifique (CNRS), Université de Strasbourg (UNISTRA) and by the French National Program "Investissement d'Avenir" (Labex MitoCross), administered by the "Agence National de la Recherche", and referenced [ANR-11-LABX-0057_MITOCROSS]. The work was also supported by the ANR project eNergiome (ANR-13-BSV6-0004-03) and the French Proteomic Infrastructure ProFI (ANR-10-INBS-08-03). H.S was supported by Région Alsace, Université de Strasbourg, AFM, and Fondation des Treilles. L.Ka. was supported by LabEx MitoCross.

Appendix A. Supplementary data

Supplementary data associated with this article can be found, in the online version, at http://dx.doi.org/10.1016/j.ymeth.2016.10.012.

References

[1] D.J. Pagliarini, S.E. Calvo, B. Chang, S.A. Sheth, S.B. Vafai, S.E. Ong, G.A. Walford, C. Sugiana, A. Boneh, W.K. Chen, D.E. Hill, M. Vidal, J.G. Evans, D.R. Thorburn, S. A. Carr, V.K. Mootha, A mitochondrial protein compendium elucidates complex I disease biology, Cell 134 (2008) 112–123.
[2] W. Neupert, J.M. Herrmann, Translocation of proteins into mitochondria, Annu. Rev. Biochem. 76 (2007) 723–749.
[3] L. Bonnefond, A. Fender, J. Rudinger-Thirion, R. Giegé, C. Florentz, M. Sissler, Toward the full set of human mitochondrial aminoacyl-tRNA synthetases: characterization of AspRS and TyrRS, Biochemistry 44 (2005) 4805–4816.
[4] S.J. Mudge, J.H. Williams, H.J. Eyre, G.R. Sutherland, P.J. Cowan, D.A. Power, Complex organisation of the 5'-end of the human glycine tRNA synthetase gene, Gene 209 (1998) 45–50.
[5] E. Tolkunova, H. Park, J. Xia, M.P. King, E. Davidson, The human lysyl-tRNA synthetase gene encodes both the cytoplasmic and mitochondrial enzymes by means of an unusual splicing of the primary transcript, J. Biol. Chem. 275 (2000) 35063–35069.
[6] A. Chacinska, C.M. Koehler, D. Milenkovic, T. Lithgow, N. Pfanner, Importing mitochondrial proteins: machineries and mechanisms, Cell 1387 (2009) 628–644.
[7] O. Schmidt, N. Pfanner, C. Meisinger, Mitochondrial protein import: from proteomics to functional mechanisms, Nat. Rev. Mol. Cell Biol. 11 (2010) 655–667.
[8] T. Becker, L. Böttinger, N. Pfanner, Mitochondrial protein import: from transport pathways to an integrated network, Trends Biochem. Sci. 37 (2012) 85–91.
[9] L.S. Wenz, Ł. Opaliński, N. Wiedemann, T. Becker, Cooperation of protein machineries in mitochondrial protein sorting, Biochim. Biophys. Acta 1853 (2015) 1119–1129.
[10] D. Mossmann, C. Meisinger, F.N. Vögtle, Processing of mitochondrial presequences, Biochim. Biophys. Acta 1819 (2012) 1098–1106.
[11] O. Gakh, P. Cavadini, G. Isaya, Mitochondrial processing peptidases, Biochim. Biophys. Acta 1592 (2002) 63–77.
[12] G. Isaya, F. Kalousek, W.A. Fenton, L.E. Rosenberg, Cleavage of precursors by the mitochondrial processing peptidase requires a compatible mature protein or an intermediate octapeptide, J. Cell Biol. 113 (1991) 65–76.
[13] F.N. Vögtle, S. Wortelkamp, R.P. Zahedi, D. Becker, C. Leidhold, K. Gevaert, J. Kellermann, W. Voos, A. Sickmann, N. Pfanner, C. Meisinger, Global analysis of the mitochondrial N-proteome identifies a processing peptidase critical for protein stability, Cell 139 (2009) 428–439.
[14] C. Erşahin, A.M. Szpaderska, A.T. Orawski, W.H. Simmons, Aminopeptidase P isozyme expression in human tissues and peripheral blood mononuclear cell fractions, Arch. Biochem. Biophys. 435 (2005) 303–310.
[15] J.C. Timmer, M. Enoksson, E. Wildfang, W. Zhu, Y. Igarashi, J.B. Denault, Y. Ma, B. Dummitt, Y.H. Chang, A.E. Mast, A. Eroshkin, J.W. Smith, W.A. Tao, G.S. Salvesen, Profiling constitutive proteolytic events in vivo, Biochem. J. 407 (2007) 41–48.
[16] J.M. Bullard, Y.-C. Cai, L.L. Spremulli, Expression and characterization of the human mitochondrial leucyl-tRNA synthetase, Biochem. Biophys. Acta 1490 (2000) 245–258.
[17] Y.N. Yao, L. Wang, X.F. Wu, E.D. Wang, The processing of human mitochondrial leucyl-tRNA synthetase in the insect cells, FEBS Lett. 534 (2003) 139–142.
[18] A. Gaudry, B. Lorber, M. Messmer, A. Neuenfeldt, C. Sauter, C. Florentz, M. Sissler, Redesigned N-terminus enhances expression, solubility, and crystallisability of mitochondrial enzyme, Protein Eng. Des. Sel. 25 (2012) 473–481.
[19] H.T. Jacobs, D.M. Turnbull, Nuclear genes and mitochondrial translation: a new class of genetic disease, Trends Genet. 21 (2005) 312–314.
[20] G.C. Scheper, M.S. van der Knaap, C.G. Proud, Translation matters: protein synthesis defects in inherited disease, Nat. Rev. Genet. 8 (2007) 711–723.
[21] S.R. Pieczenik, J. Neustadt, Mitochondrial dysfunction and molecular pathways of disease, Exp. Mol. Pathol. 83 (2007) 84–92.
[22] A. Rötig, Human diseases with impaired mitochondrial protein synthesis, Biochim. Biophys. Acta 1807 (2011) 1198–1205.
[23] J. Nunnari, A. Suomalainen, Mitochondria: in sickness and in health, Cell 148 (2012) 1145–1159.
[24] S. Konovalova, H. Tyynismaa, Mitochondrial aminoacyl-tRNA synthetases in human disease, Mol. Genet. Metab. 108 (2013) 206–211.
[25] H. Schwenzer, J. Zoll, C. Florentz, M. Sissler, Pathogenic implications of human mitochondrial aminoacyl-tRNA synthetases, in: S. Kim (Ed.), Topics in Current Chemistry-Aminoacyl-tRNA Synthetases: Applications in Chemistry, Biology and Medicine, Springer, 2014, pp. 247–292.
[26] A.S. Vaca Jacome, T. Rabilloud, C. Schaeffer-Reiss, M. Rompais, D. Ayoub, L. Lane, A. Bairoch, A. Van Dorsselaer, C. Carapito, N-terminome analysis of the human mitochondrial proteome, Proteomics 15 (2015) 2519–2524.
[27] S. Gallien, E. Perrodou, C. Carapito, C. Deshayes, J.M. Reyrat, A. Van Dorsselaer, O. Poch, C. Schaeffer, O. Lecompte, Ortho-proteogenomics: multiple proteomes investigation through orthology and a new MS-based protocol, Genome Res. 19 (2009) 128–135.
[28] C. Carapito, A. Burel, P. Guterl, A. Walter, F. Varrier, F. Bertile, A. Van Dorsselaer, SDA, a proteomics software suite for in-depth Mass Spectrometry Data Analysis using grid computing, Proteomics 14 (2014) 1014–1019.
[29] C. Carapito, L. Lane, M. Benama, A. Opsomer, E. Mouton-Barbosa, L. Garrigues, A. Gonzalez de Peredo, A. Burel, C. Bruley, A. Gateau, D. Bouyssié, M. Jaquinod, S. Cianferani, O. Burlet-Schiltz, A. Van Dorsselaer, J. Garin, Y. Vandenbrouck, Computational and mass-spectrometry-based workflow for the discovery and validation of missing human proteins: application to chromosomes 2 and 14, J. Proteome Res. 14 (2015) 3621–3634.
[30] I. Small, N. Peeters, F. Legeai, C. Lurin, Predotar: a tool for rapidly screening proteomes for N-terminal targeting sequences, Proteomics 4 (2004) 1581–1590.
[31] M.G. Claros, MitoProt, a Macintosh application for studying mitochondrial proteins, Comput. Appl. Biosci. 11 (1995) 441–447.
[32] Y. Fukasawa, J. Tsuji, S.C. Fu, K. Tomii, P. Horton, K. Imai, MitoFates: improved prediction of mitochondrial targeting sequences and their cleavage sites, Mol. Cell. Proteomics 14 (2015) 1113–1126.
[33] M. Messmer, C. Florentz, H. Schwenzer, G.C. Scheper, M.S. van der Knaap, L. Maréchal-Drouard, M. Sissler, A human pathology-related mutation prevents import of an aminoacyl-tRNA synthetase into mitochondria, Biochem. J. 433 (2011) 441–446.
[34] J. Nett, B. Trumpower, Dissociation of import of the Rieske iron-sulfur protein into *Saccharomyces cerevisiae* mitochondria from proteolytic processing of the presequence, J. Biol. Chem. 271 (1996) 26713–26716.
[35] P.F. Teixeira, E. Glaser, Processing peptidases in mitochondria and chloroplasts, Biochim. Biophys. Acta 1833 (2013) 360–370.
[36] S.S. Branda, P. Cavadini, J. Adamec, F. Kalousek, F. Taroni, G. Isaya, Yeast and human frataxin are processed to mature form in two sequential steps by the mitochondrial processing peptidase, J. Biol. Chem. 274 (1999) 11763–22769.
[37] P. Cavadini, J. Adamec, F. Taroni, O. Gakh, G. Isaya, Two-step processing of human frataxin by mitochondrial processing peptidase. Precursor and intermediate forms are cleaved at different rates, J. Biol. Chem. 275 (2000) 41469–41475.
[38] D.M. Gordon, M. Kogan, S.A. Knight, A. Dancis, D. Pain, Distinct roles for two N-terminal cleaved domains in mitochondrial import of the yeast frataxin homolog, Yfh1p, Hum. Mol. Genet. 10 (2001) 259–269.
[39] J.F. O'Toole, Y. Liu, E.E. Davis, C.J. Westlake, M. Attanasio, E.A. Otto, D. Seelow, G. Nurnberg, C. Becker, M. Nuutinen, M. Kärppä, J. Ignatius, J. Uusimaa, S. Pakanen, E. Jaakkola, L.P. van den Heuvel, H. Fehrenbach, R. Wiggins, M. Goyal, W. Zhou, M.T. Wolf, E. Wise, J. Helou, S.J. Allen, C.A. Murga-Zamalloa, S. Ashraf, M. Chaki, S. Heeringa, G. Chernin, B.E. Hoskins, H. Chaib, J. Gleeson, T. Kusakabe, T. Suzuki, R.E. Isaac, L.M. Quarmby, B. Tennant, H. Fujioka, H. Tuominen, I. Hassinen, H. Lohi, J.L. van Houten, A. Rotig, J.A. Sayer, B. Rolinski, P. Freisinger, S.M. Madhavan, M. Herzer, F. Madignier, H. Prokisch, P. Nurnberg, P.K. Jackson, H. Khanna, N. Katsanis, F. Hildebrandt, Individuals with mutations in XPNPEP3, which encodes a mitochondrial protein, develop a nephronophthisis-like nephropathy, J. Clin. Invest. 120 (2010) 791–802.
[40] S.M. Sriram, B.Y. Kim, Y.T. Kwon, The N-end rule pathway: emerging functions and molecular principles of substrate recognition, Nat. Rev. Mol. Cell Biol. 12 (2011) 735–747.
[41] F.U. Hartl, B. Schmidt, E. Wachter, H. Weiss, W. Neupert, Transport into mitochondria and intramitochondrial sorting of the Fe/S protein of ubiquinol-cytochrome c reductase, Cell 47 (1986) 939–951.
[42] G. Daum, S.M. Gasser, G. Schatz, Import of proteins into mitochondria. Energy-dependent, two-step processing of the intermembrane space enzyme cytochrome b2 by isolated yeast mitochondria, J. Biol. Chem. 257 (1982) 13075–13080.
[43] F. Kalousek, J.P. Hendrick, L.E. Rosenberg, Two mitochondrial matrix proteases act sequentially in the processing of mammalian matrix enzymes, Proc. Natl. Acad. Sci. USA. 85 (1988) 7536–7540.
[44] D.M. Gordon, Q. Shi, A. Dancis, D. Pain, Maturation of frataxin within mammalian and yeast mitochondria: one-step processing by matrix processing peptidase, Hum. Mol. Genet. 8 (1999) 2255–2262.
[45] J. Nouws, A.V. Goswami, M. Bestwick, B.J. McCann, Y.V. Surovtseva, G.S. Shadel, Mitochondrial Ribosomal Protein L12 Is required for POLRMT stability and exists as two forms generated by alternative proteolysis during import, J. Biol. Chem. 291 (2016) 989–997.

[46] Y. Wang, X.L. Zhou, Z.R. Ruan, R.J. Liu, G. Eriani, E.D. Wang, A human disease-causing point mutation in mitochondrial threonyl-tRNA synthetase induces both structural and functional defects, J. Biol. Chem. 291 (2016) 6507–6520.

[47] Y.N. Yao, L. Wang, X.F. Wu, E. Wang, Human mitochondrial leucyl-tRNA synthetase with high activity produced from *Escherichia coli*, Protein Expr. Purif. 30 (2003) 112–116.

[48] E. Tzima, J.S. Reader, K.L. Ewalt, M.A. Schwartz, P. Schimmel, Biologically active fragment of a human tRNA synthetase inhibits fluid shear stress-activated responses of endothelial cells, Proc. Natl. Acad. Sci. U.S.A. 100 (2003) 14903–14907.

[49] P. Yao, P.L. Fox, A truncated tRNA synthetase directs a "translational trickle" of gene expression, Cell Cycle 11 (2012) 186–1869.

A.1 Start position 33 (LLQSSQR, 2+)

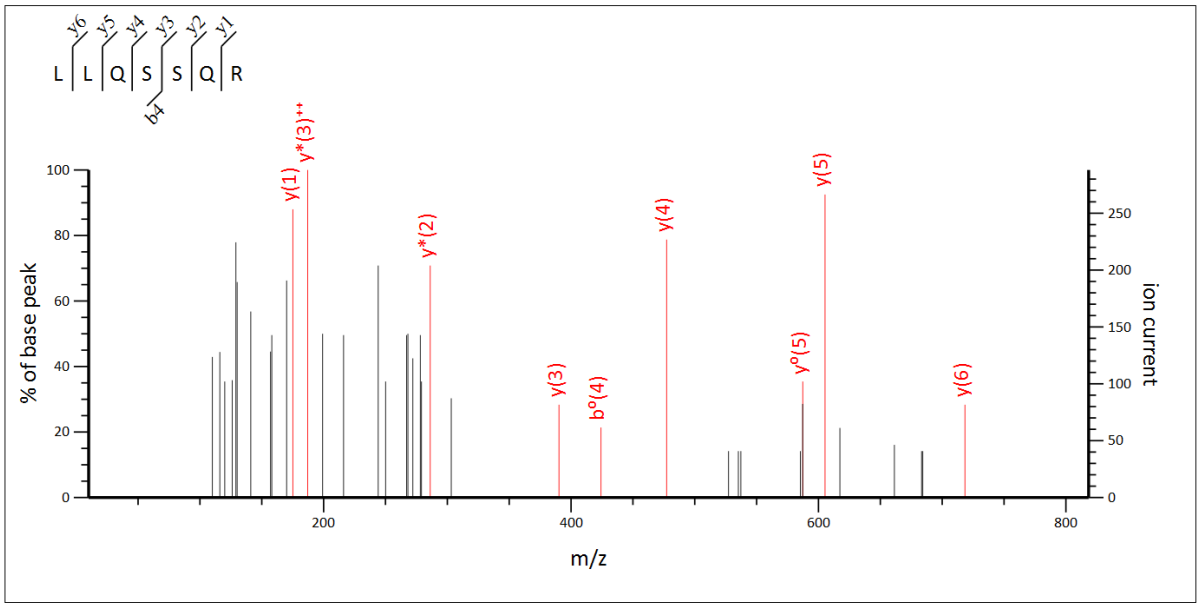

A.2 Start position 33 (LLQSSQR, 2+)

TMPP-C12

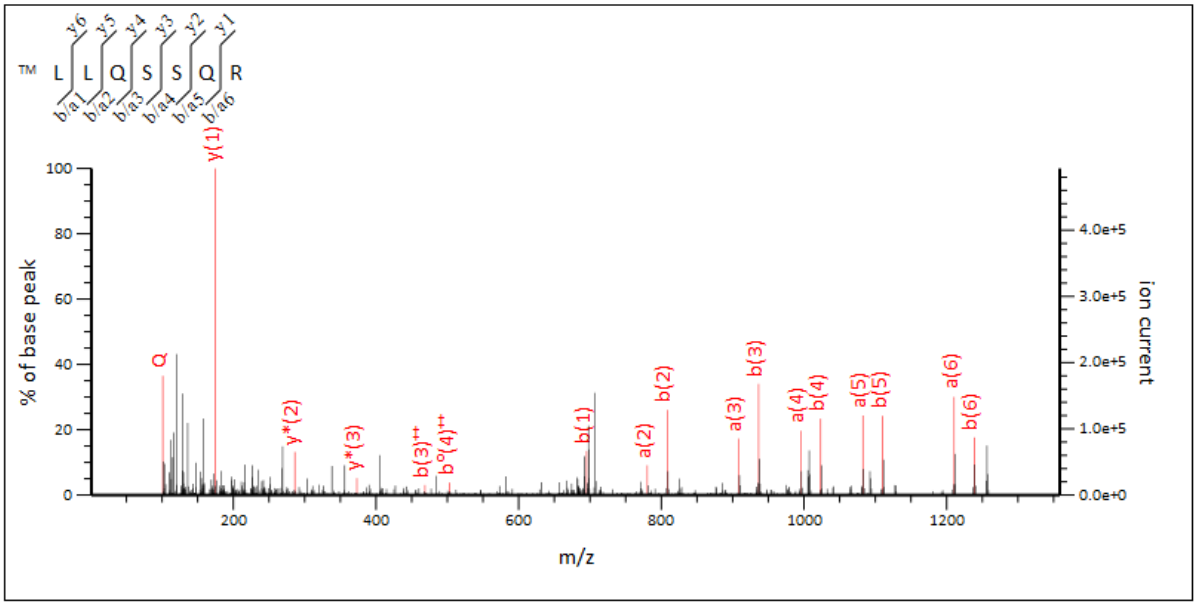

TMPP-C13

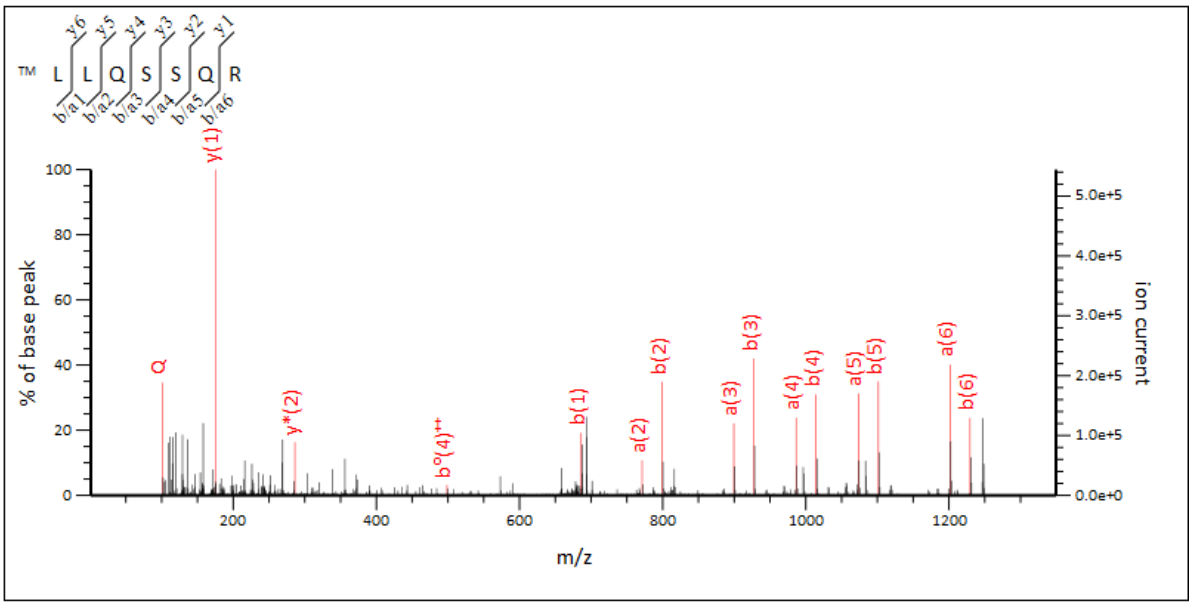

B.1 Start position 41 (IPEFSSFVVR, 2+)

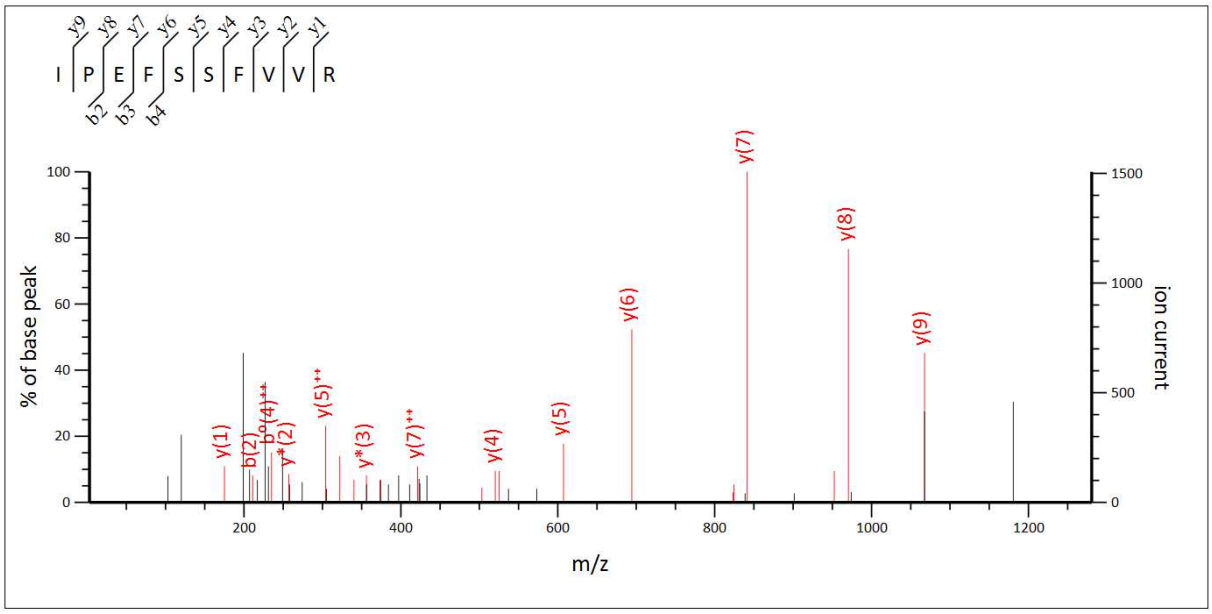

B.2 Start position 41 (IPEFSSFVVR, 2+)

TMPP-C12

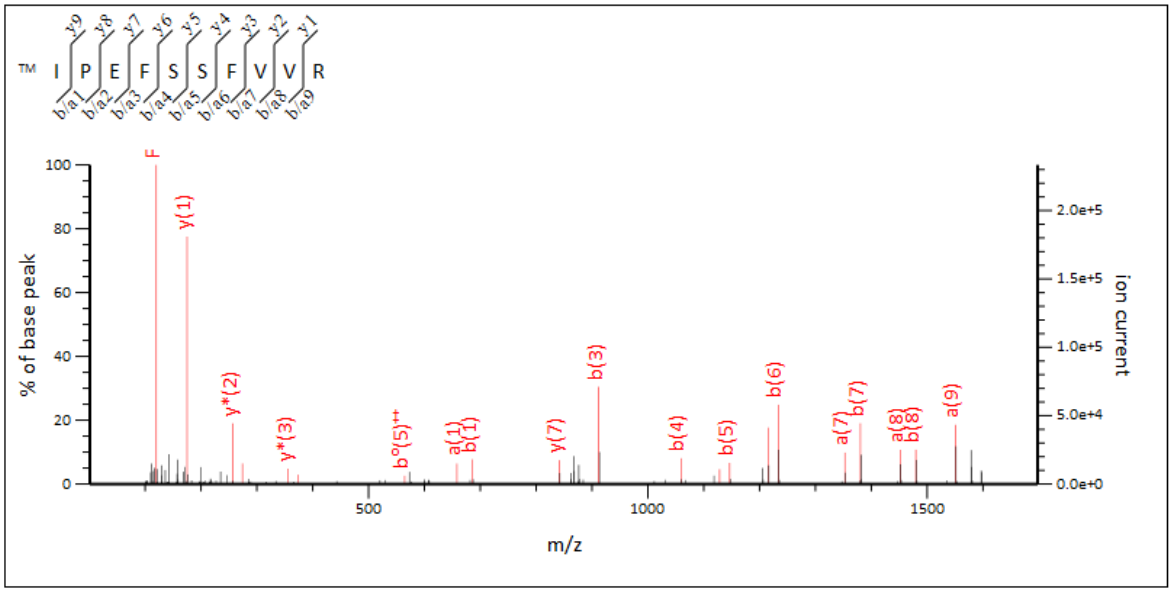

TMPP-C13

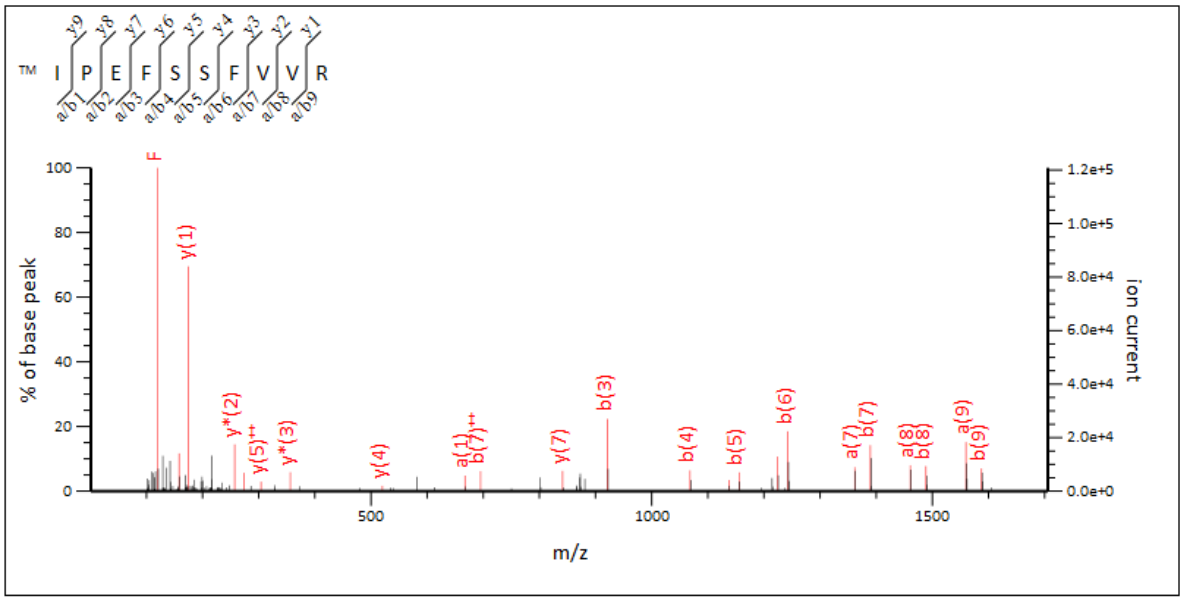

C.1 Start position 42 (PEFSSFVVR, 2+)

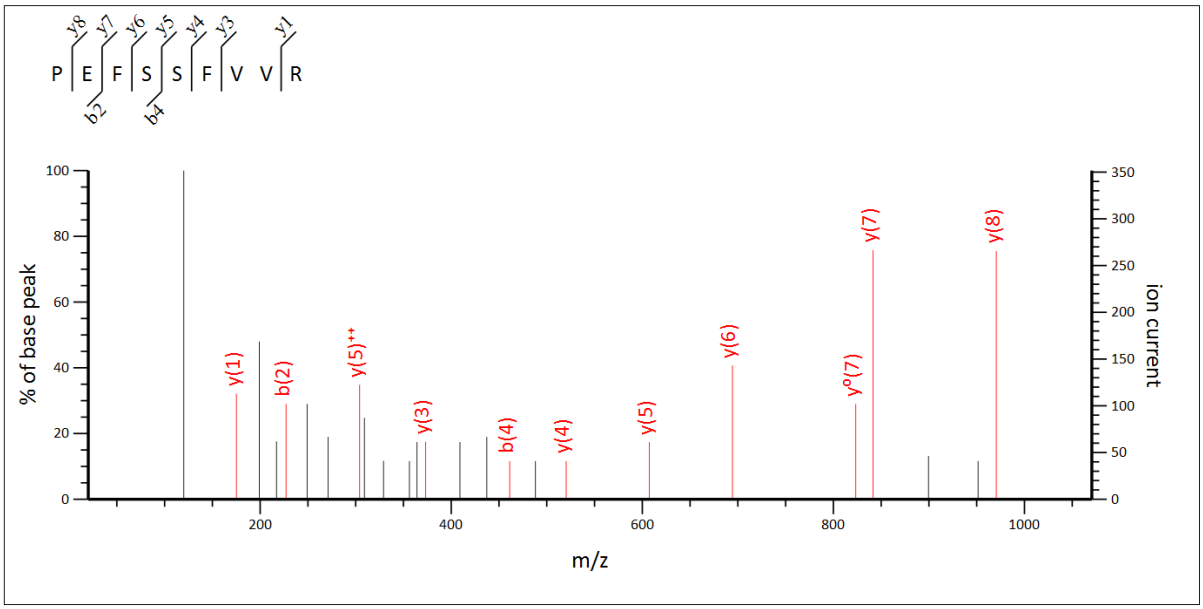

C.1 Start position 42 (PEFSSFVVR, 2+)

TMPP-C12

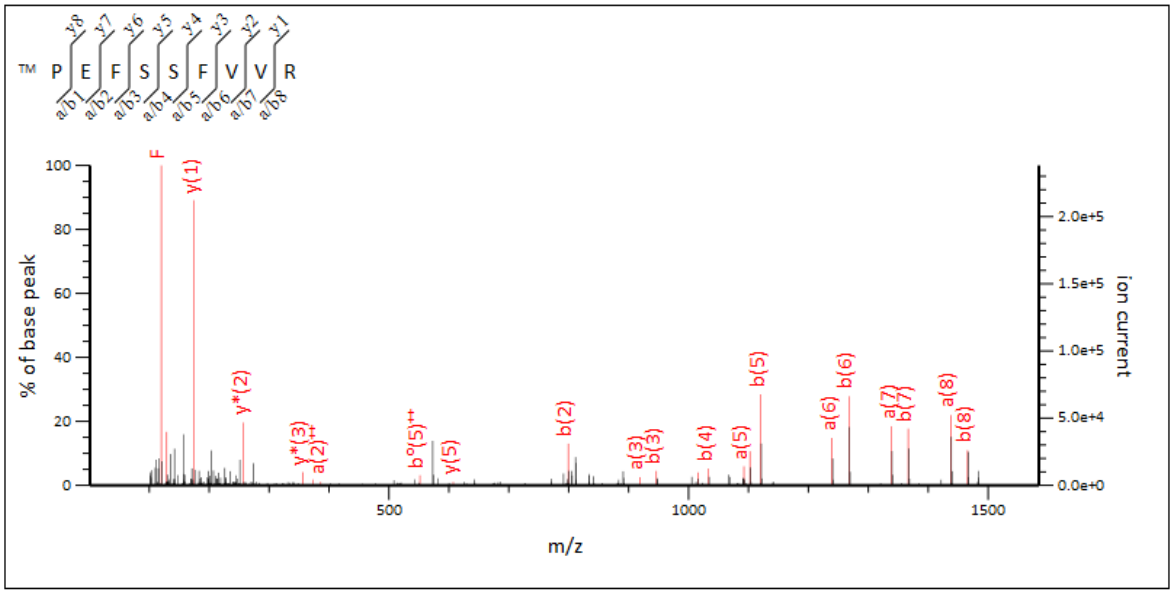

TMPP-C13

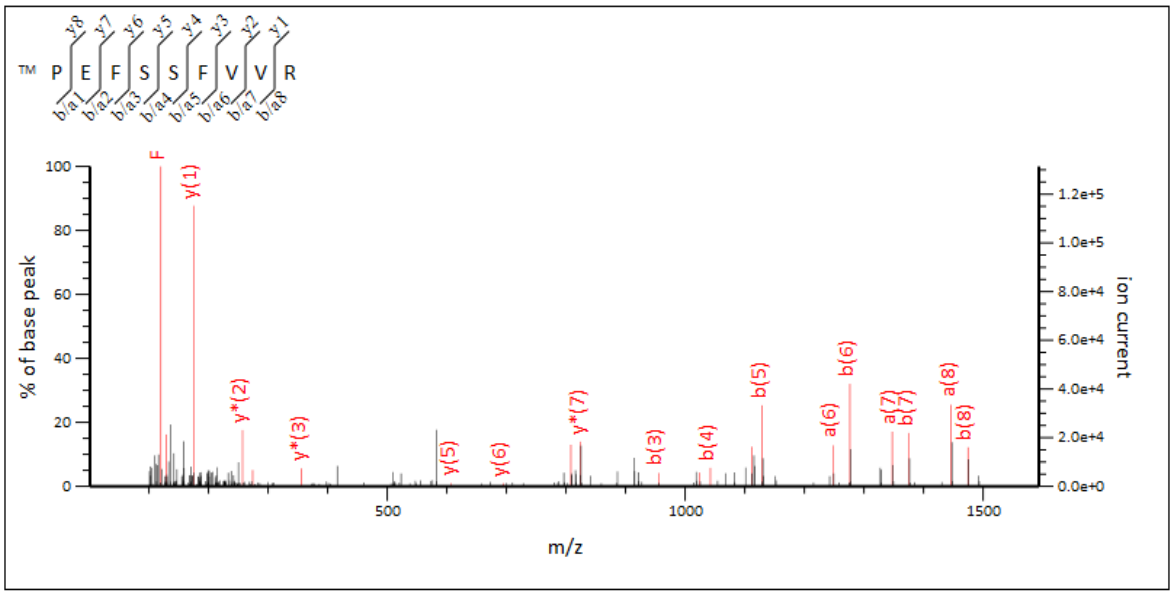

Supplementary Figure 1: **MS/MS spectra identifying the three N-terminal peptides for human mitochondrial aspartyl-tRNA synthetase (UniProt Access Q6PI48) at positions 33 (A.), 41 (B.) and 42 (C.).**

A.1, B.1, C.1: spectra of the semi-tryptic peptides identified with the shotgun approach.

A.2, B.2, C.2: spectra of both light and heavy labeled TMPP peptides identified with the dN-TOP approach

Annex 4

Multiple localizations of the human mitochondrial aspartyl-tRNA synthetase and impact of disease-associated mutations

Loukmane KARIM[1], Hagen SCHWENZER[1,2], Ligia Elena GONZALEZ-SERRANO[1], Agnès RÖTIG[3], Arnold MUNNICH[3], Marie SISSLER[1]*

[1] Architecture et Réactivité de l'ARN, CNRS, Université de Strasbourg, IBMC, 15 rue René Descartes, 67084 Strasbourg Cedex, France
[2] Present address: The Wohl Virion Centre, Virology, Division of Infection & Immunity, UCL, Cruciform Building, 90 Gower Street, London WC1E 6BT, UK
[3] INSERM UMR 1163, Laboratory of Genetics of Mitochondrial Disorders, Paris Descartes - Sorbonne Paris Cité University, Imagine Institute, Paris, France

*To whom correspondence should be addressed:
Marie Sissler, IBMC - 15 rue René Descartes, 67084 Strasbourg Cedex – France, Phone: +33 (0)3 88 41 70 62; Fax: +33 (0)3 88 60 22 18; E-mail: m.sissler@ibmc-cnrs.unistra.fr

ABSTRACT

Human mitochondria (mt) have an own translation machinery. Among factors implicated in mt translation, aminoacyl-tRNA synthetases (mt-aaRSs) play a crucial role by charging amino acids on their cognate tRNA. Increasing numbers of mutations affecting mt-aaRSs and leading to severe disorders have been reported in recent years, but the link between the mutations and phenotypic expressions remains unclear. Several of the reported mutations affect the mt-aspartyl-tRNA synthetase (mt-AspRS) and cause the LBSL (Leukoencephalopathy with Brainstem and Spinal cord involvement and Lactate elevation). Most LBSL-causing mutations, studied so far, slightly impact the structure and activity of mt-AspRS, raising the need to characterize mt-AspRS properties at the cellular level. We investigated the sub-mitochondrial localization of mt-AspRS in human cell lines and in fibroblasts isolated from an LBSL patient bearing an unreported G338E mutation. We demonstrated that mt-AspRS displays matrix and membrane localizations, in addition to an extra-mitochondrial localization similarly to the cytochrome c, under stress conditions. Finally, we assessed the impact of eight LBSL-related mutations among which the unreported G338E mutation, on the multiple localizations of mt-AspRS. For the first time we show that mt-AspRS is dually localized in mitochondria and can be "exported" under stress conditions, strongly suggesting the existence of an alternative function for mt-AspRS. Moreover, despite an impact of some mutations on solubility, no effect was observed on the multiple localizations of mt-AspRS. Our results open new perspectives and may shed new light on the link between mt-AspRS mutations and LBSL disease.

						CTRL-1		CTRL-2		CTRL-3		CTRL-4		ATP-1		ATP-2		ATP-3		ATP-4	
ACCESSION Nb	Description	MW(kDa)	pI	Gene ID	Symbol	Score	#Spectres	Score	#Spectres	Score	#Spectres	Score	#Spectres	Score	#Spectres	Score	#Spectres	Score	#Spectres	Score	#Spectres
DYHC1_HUMAN	Cytoplasmic dynein 1 heavy chain 1 OS=Homo sapiens GN=DYNC1H1 PE=1 SV=5	532.1	6.0	1778	DYNC1H1									4845.9	162	2454.4	79	3205.3	107	7057.9	217
TPR_HUMAN	Nucleoprotein TPR OS=Homo sapiens GN=TPR PE=1 SV=3	267.1	4.8	7175	TPR									2719.6	99	2050.6	68	1938.2	68	2813.7	80
MSH6_HUMAN	DNA mismatch repair protein Msh6 OS=Homo sapiens GN=MSH6 PE=1 SV=2	152.7	6.5	2956	MSH6									1512.1	55	1013.7	31	1356.2	54	1892.9	67
MYH10_HUMAN	Myosin-10 OS=Homo sapiens GN=MYH10 PE=1 SV=3	228.9	5.3	4628	MYH10									2220.6	68	1642.0	48	1795.3	53	2198.2	59
DNMT1_HUMAN	DNA (cytosine-5)-methyltransferase 1 OS=Homo sapiens GN=DNMT1 PE=1 SV=2	183.0	8.9	1786	DNMT1									1037.4	31	701.6	22	831.0	30	1752.3	57
SMC4_HUMAN	Structural maintenance of chromosomes protein 4 OS=Homo sapiens GN=SMC4 PE=1 SV=2	147.1	6.4	10051	SMC4									1393.7	58	931.9	29	1111.8	38	2016.9	54
KINH_HUMAN	Kinesin-1 heavy chain OS=Homo sapiens GN=KIF5B PE=1 SV=1	109.6	6.1	3799	KIF5B									1350.1	46	764.1	32	979.0	31	1437.1	46
HCFC1_HUMAN	Host cell factor 1 OS=Homo sapiens GN=HCFC1 PE=1 SV=2	208.6	7.9	3054	HCFC1									955.0	29	613.6	20	779.7	27	1212.7	45
SMRC1_HUMAN	SWI/SNF complex subunit SMARCC1 OS=Homo sapiens GN=SMARCC1 PE=1 SV=3	122.8	5.4	6599	SMARCC1									442.9	12	264.1	6	340.4	9	1157.6	44
SYTC_HUMAN	Threonine--tRNA ligase, cytoplasmic OS=Homo sapiens GN=TARS PE=1 SV=3	83.4	6.2	6897	TARS									1097.8	43	758.9	31	852.2	32	1274.3	42
DHE3_HUMAN	Glutamate dehydrogenase 1, mitochondrial OS=Homo sapiens GN=GLUD1 PE=1 SV=2	61.4	8.5	2746	GLUD1									611.5	23	366.6	10	301.9	8	1036.9	41
TCRG1_HUMAN	Transcription elongation regulator 1 OS=Homo sapiens GN=TCERG1 PE=1 SV=2	123.8	9.3	10915	TCERG1									450.4	10	165.8	5	305.7	8	1150.4	41
RAD50_HUMAN	DNA repair protein RAD50 OS=Homo sapiens GN=RAD50 PE=1 SV=1	153.8	6.5	10111	RAD50									570.7	17	363.9	4	605.5	16	1240.5	40
RECQ1_HUMAN	ATP-dependent DNA helicase Q1 OS=Homo sapiens GN=RECQL PE=1 SV=3	73.4	9.0	5965	RECQL									364.0	8	31	1	201.4	5	1074.2	38
DHB4_HUMAN	Peroxisomal multifunctional enzyme type 2 OS=Homo sapiens GN=HSD17B4 PE=1 SV=3	79.6	9.6	3295	HSD17B4									1351.3	43	665.0	19	777.2	26	1122.9	37
VRK1_HUMAN	Serine/threonine-protein kinase VRK1 OS=Homo sapiens GN=VRK1 PE=1 SV=1	45.4	9.6	7443	VRK1									515.3	29	315.9	15	437.2	30	853.4	37
SYDM_HUMAN	Aspartate--tRNA ligase, mitochondrial OS=Homo sapiens GN=DARS2 PE=1 SV=1	73.5	9.0	55157	DARS2									434.5	20	101.2	5	119.2	9	888.9	35
CD027_HUMAN	UPF0609 protein C4orf27 OS=Homo sapiens GN=C4orf27 PE=1 SV=2	39.4	6.4	54969	C4orf27									694.0	39	420.8	18	589.1	28	780.1	34
SMRC2_HUMAN	SWI/SNF complex subunit SMARCC2 OS=Homo sapiens GN=SMARCC2 PE=1 SV=1	132.8	5.4	6601	SMARCC2									242.9	7	150.6	4	197.3	5	944.3	34
CYC_HUMAN	Cytochrome c OS=Homo sapiens GN=CYCS PE=1 SV=2	11.7	10.1	54205	CYCS									683.0	90	611.1	119	531.2	116	641.8	33
MCTS1_HUMAN	Malignant T-cell-amplified sequence 1 OS=Homo sapiens GN=MCTS1 PE=1 SV=1	20.5	9.7	28985	MCTS1									656.8	48	502.6	41	589.3	60	688.5	33
NTPCR_HUMAN	Cancer-related nucleoside-triphosphatase OS=Homo sapiens GN=NTPCR PE=1 SV=1	20.7	10.5	84284	NTPCR									579.6	26	400.4	17	435.2	19	677.4	33
KI67_HUMAN	Antigen KI-67 OS=Homo sapiens GN=MKI67 PE=1 SV=2	358.5	10.1	4288	MKI67									2219.7	71	795.7	24	1054.7	33	1169.3	32
TXLNA_HUMAN	Alpha-taxilin OS=Homo sapiens GN=TXLNA PE=1 SV=3	61.9	6.1	200081	TXLNA									786.8	31	630.7	29	731.3	21	856.9	27
MCM5_HUMAN	DNA replication licensing factor MCM5 OS=Homo sapiens GN=MCM5 PE=1 SV=5	82.2	9.5	4174	MCM5									790.2	30	383.5	8	713.6	23	966.2	27
SYNC_HUMAN	Asparagine--tRNA ligase, cytoplasmic OS=Homo sapiens GN=NARS PE=1 SV=1	62.9	5.9	4677	NARS									631.8	22	365.5	10	465.3	18	862.5	26
PNKP_HUMAN	Bifunctional polynucleotide phosphatase/kinase OS=Homo sapiens GN=PNKP PE=1 SV=1	57.0	9.6	11284	PNKP									513.4	17	458.8	16	509.5	19	672.0	26
CHD1L_HUMAN	Chromodomain-helicase-DNA-binding protein 1-like OS=Homo sapiens GN=CHD1L PE=1 SV=2	100.9	6.5	9557	CHD1L									356.0	11	266.4	6	331.7	9	931.4	26
CYFP1_HUMAN	Cytoplasmic FMR1-interacting protein 1 OS=Homo sapiens GN=CYFIP1 PE=1 SV=1	145.1	6.5	23191	CYFIP1									343.8	9	109.3	3	194.2	5	850.0	25
DENR_HUMAN	Density-regulated protein OS=Homo sapiens GN=DENR PE=1 SV=2	22.1	5.1	8562	DENR									826.6	55	828.5	49	772.5	58	639.0	24
SYHC_HUMAN	Histidine--tRNA ligase, cytoplasmic OS=Homo sapiens GN=HARS PE=1 SV=2	57.4	5.6	3035	HARS									491.6	24	216.9	9	337.1	13	570.3	24
SYSC_HUMAN	Serine--tRNA ligase, cytoplasmic OS=Homo sapiens GN=SARS PE=1 SV=3	58.7	6.0	6301	SARS									421.9	28	280.9	15	394.3	19	647.6	24
KCRU_HUMAN	Creatine kinase U-type, mitochondrial OS=Homo sapiens GN=CKMT1A PE=1 SV=1	47.0	9.4	1159	CKMT1B									1082.6	63	721.7	48	796.7	42	779.1	23
PDS5A_HUMAN	Sister chromatid cohesion protein PDS5 homolog A OS=Homo sapiens GN=PDS5A PE=1 SV=1	150.7	9.0	23244	PDS5A									658.9	22	237.3	6	351.3	8	839.6	21
BUB3_HUMAN	Mitotic checkpoint protein BUB3 OS=Homo sapiens GN=BUB3 PE=1 SV=1	37.1	6.4	9184	BUB3									580.4	22	285.2	7	365.5	13	579.8	21
MRE11_HUMAN	Double-strand break repair protein MRE11A OS=Homo sapiens GN=MRE11A PE=1 SV=3	80.5	5.5	4361	MRE11A									425.8	18	275.6	6	280.5	11	659.0	21
TXLNG_HUMAN	Gamma-taxilin OS=Homo sapiens GN=TXLNG PE=1 SV=2	60.5	7.9	55787	TXLNG									649.9	17	345.4	7	509.2	13	753.1	21
DNLI3_HUMAN	DNA ligase 3 OS=Homo sapiens GN=LIG3 PE=1 SV=2	112.8	10.0	3980	LIG3									242.6	10	32	1	119.8	4	779.7	21
WDR5_HUMAN	WD repeat-containing protein 5 OS=Homo sapiens GN=WDR5 PE=1 SV=1	36.6	9.4	11091	WDR5									529.0	20	406.8	16	349.2	13	483.7	20
CUL1_HUMAN	Cullin-1 OS=Homo sapiens GN=CUL1 PE=1 SV=2	89.6	8.9	8454	CUL1									441.6	15	199.6	4	399.0	10	717.2	20
CND1_HUMAN	Condensin complex subunit 1 OS=Homo sapiens GN=NCAPD2 PE=1 SV=3	157.1	6.2	9918	NCAPD2									378.9	9	180.8	6	258.4	5	706.6	20
PP1A_HUMAN	Serine/threonine-protein phosphatase PP1-alpha catalytic subunit OS=Homo sapiens GN=PPP1CA PE=1 S	37.5	5.9	5499	PPP1CA									239.7	7	77.3	3	154.7	5	679.4	20
KCC2D_HUMAN	Calcium/calmodulin-dependent protein kinase type II subunit delta OS=Homo sapiens GN=CAMK2D PE=1	56.3	6.9	817	CAMK2D									450.2	10	329.3	7	470.3	14	618.2	19
SYVC_HUMAN	Valine--tRNA ligase OS=Homo sapiens GN=VARS PE=1 SV=4	140.4	8.4	7407	VARS									260.0	4	85.2	3	123.2	2	883.7	19
P5CR2_HUMAN	Pyrroline-5-carboxylate reductase 2 OS=Homo sapiens GN=PYCR2 PE=1 SV=1	33.6	9.0	29920	PYCR2									465.3	21	364.2	10	407.5	14	591.9	18
SEP10_HUMAN	Septin-10 OS=Homo sapiens GN=SEPT10 PE=1 SV=2	52.6	6.4	151011	SEPT10									159	9	167.6	8	268.1	10	542.5	18
P5CR1_HUMAN	Pyrroline-5-carboxylate reductase 1, mitochondrial OS=Homo sapiens GN=PYCR1 PE=1 SV=2	33.3	8.0	5831	PYCR1									543.4	14	374.9	8	486.4	12	459.8	17
RAD21_HUMAN	Double-strand-break repair protein rad21 homolog OS=Homo sapiens GN=RAD21 PE=1 SV=2	71.6	4.4	5885	RAD21									328.9	6	187.9	6	178.9	5	616.6	17
HELLS_HUMAN	Lymphoid-specific helicase OS=Homo sapiens GN=HELLS PE=1 SV=1	97.0	8.9	3070	HELLS									523.4	15	156.9	4	382.1	12	599.2	15
DC1I2_HUMAN	Cytoplasmic dynein 1 intermediate chain 2 OS=Homo sapiens GN=DYNC1I2 PE=1 SV=3	71.4	4.9	1781	DYNC1I2									410.7	12	285.4	6	316.1	10	642.4	15
LRWD1_HUMAN	Leucine-rich repeat and WD repeat-containing protein 1 OS=Homo sapiens GN=LRWD1 PE=1 SV=2	70.8	7.1	222229	LRWD1									243.0	11	118.4	5	183.7	6	365.2	14
API5_HUMAN	Apoptosis inhibitor 5 OS=Homo sapiens GN=API5 PE=1 SV=3	59.0	7.7	8539	API5									272.6	10	211.2	7	216.3	9	569.3	14
FKBP3_HUMAN	Peptidyl-prolyl cis-trans isomerase FKBP3 OS=Homo sapiens GN=FKBP3 PE=1 SV=1	25.2	9.8	2287	FKBP3									473.0	25	367.3	15	364.6	14	324.0	13
CUTC_HUMAN	Copper homeostasis protein cutC homolog OS=Homo sapiens GN=CUTC PE=1 SV=1	29.3	9.6	51076	CUTC									395.7	17	271.9	13	266.9	12	412.6	13
CAND1_HUMAN	Cullin-associated NEDD8-dissociated protein 1 OS=Homo sapiens GN=CAND1 PE=1 SV=2	136.3	5.4	55832	CAND1									611.4	16	239.2	6	328.2	5	474.9	13
TOM34_HUMAN	Mitochondrial import receptor subunit TOM34 OS=Homo sapiens GN=TOMM34 PE=1 SV=2	34.5	9.8	10953	TOMM34									541.9	16	380.5	11	435.6	16	395.4	13
AMPM1_HUMAN	Methionine aminopeptidase 1 OS=Homo sapiens GN=METAP1 PE=1 SV=2	43.2	6.9											169.4	5	94.4	3	82.9	3	491.0	13
EDF1_HUMAN	Endothelial differentiation-related factor 1 OS=Homo sapiens GN=EDF1 PE=1 SV=1	16.4	10.4	8721	EDF1									437.1	24	398.2	23	447.9	28	292.2	12
IF2P_HUMAN	Eukaryotic translation initiation factor 5B OS=Homo sapiens GN=EIF5B PE=1 SV=4	138.7	5.3	9669	EIF5B									319.1	9	120.2	3	215.9	5	493.0	12
LIS1_HUMAN	Platelet-activating factor acetylhydrolase IB subunit alpha OS=Homo sapiens GN=PAFAH1B1 PE=1 SV=2	46.6	7.2	5048	PAFAH1B1									352.2	6	134.5	2	154.4	4	380.0	12
TMA7_HUMAN	Translation machinery-associated protein 7 OS=Homo sapiens GN=TMA7 PE=1 SV=1	7.1	10.5	51372	TMA7									354.8	25	288.2	29	291.0	19	209.4	11
SEPT3_HUMAN	Neuronal-specific septin-3 OS=Homo sapiens GN=SEPT3 PE=1 SV=3	40.7	6.9	55964	SEPT3									430.6	21	192.1	11	316.9	15	228.7	11
SYFA_HUMAN	Phenylalanine--tRNA ligase alpha subunit OS=Homo sapiens GN=FARSA PE=1 SV=3	57.5	7.9	2193	FARSA									198.4	6	113.2	5	142.4	5	306.0	11
THOC2_HUMAN	THO complex subunit 2 OS=Homo sapiens GN=THOC2 PE=1 SV=2	182.7	9.4	57187	THOC2									376.9	3	231.7	6	270.3	4	373.9	11
SUV3_HUMAN	ATP-dependent RNA helicase SUPV3L1, mitochondrial OS=Homo sapiens GN=SUPV3L1 PE=1 SV=1	87.9	9.1	6832	SUPV3L1									165.0	4	102.0	3	110.6	4	351.3	11
SMCE1_HUMAN	SWI/SNF-related matrix-associated actin-dependent regulator of chromatin subfamily E member 1 OS=Hon	46.6	4.7	6605	SMARCE1									164.3	4	44.3	1	64.8	1	413.5	11
DNJC2_HUMAN	DnaJ homolog subfamily C member 2 OS=Homo sapiens GN=DNAJC2 PE=1 SV=4	72.0	9.5	27000	DNAJC2									122.9	3	130.1	2	223.5	7	370.5	11
DECR_HUMAN	2,4-dienoyl-CoA reductase, mitochondrial OS=Homo sapiens GN=DECR1 PE=1 SV=1	36.0	10.1	1666	DECR1									121.2	2	39.3	1	138.9	2	387.7	11
BAZ1B_HUMAN	Tyrosine-protein kinase BAZ1B OS=Homo sapiens GN=BAZ1B PE=1 SV=2	170.8	9.4	9031	BAZ1B									191.1	6	114.0	5	245.4	9	331.4	10
MACD1_HUMAN	O-acetyl-ADP-ribose deacetylase MACROD1 OS=Homo sapiens GN=MACROD1 PE=1 SV=2	35.5	10.4	28992	MACROD1									202.7	6	102.8	2	118.2	4	374.6	10
NEP1_HUMAN	Ribosomal RNA small subunit methyltransferase NEP1 OS=Homo sapiens GN=EMG1 PE=1 SV=4	26.7	10.0	10436	EMG1									179.8	5	57.5	2	97.3	3	351.2	10
KCC2G_HUMAN	Calcium/calmodulin-dependent protein kinase type II subunit gamma OS=Homo sapiens GN=CAMK2G PE=	62.6	8.9	818	CAMK2G									148	5	112	4	146	7	300.4	10
THOC6_HUMAN	THO complex subunit 6 homolog OS=Homo sapiens GN=THOC6 PE=1 SV=1	37.5	7.9	79228	THOC6									200.5	4	45.3	2	62.6	1	385.4	10

Annex 5

ATM_HUMAN	Serine-protein kinase ATM OS=Homo sapiens GN=ATM PE=1 SV=3	350.5	6.4	472	ATM							166.9	2	128.3	2	75.3	1	634.7	10
MANF_HUMAN	Mesencephalic astrocyte-derived neurotrophic factor OS=Homo sapiens GN=MANF PE=1 SV=3	20.7	9.8	7873	MANF							695.8	32	345.3	18	396.9	20	379.3	10
CLPB_HUMAN	Caseinolytic peptidase B protein homolog OS=Homo sapiens GN=CLPB PE=1 SV=1	78.7	9.8	81570	CLPB							578.3	18	267.6	8	472.5	12	327.5	9
SEPT5_HUMAN	Septin-5 OS=Homo sapiens GN=SEPT5 PE=1 SV=1	42.7	6.2	5413	SEPT5							318.1	12	198.6	7	253.6	9	327.4	9
REQU_HUMAN	Zinc finger protein ubi-d4 OS=Homo sapiens GN=DPF2 PE=1 SV=2	44.1	5.9	5977	DPF2							72	2	126.6	4	96.0	3	251.0	9
SNF5_HUMAN	SWI/SNF-related matrix-associated actin-dependent regulator of chromatin subfamily B member 1 OS=Hon	44.1	5.8	6598	SMARCB1							83.7	3	46.3	2	66.2	2	219.2	9
PPIF_HUMAN	Peptidyl-prolyl cis-trans isomerase F, mitochondrial OS=Homo sapiens GN=PPIF PE=1 SV=1	22.0	10.4	10105	PPIF							413.3	17	270.5	13	305.6	9	242.0	9
SBDS_HUMAN	Ribosome maturation protein SBDS OS=Homo sapiens GN=SBDS PE=1 SV=4	28.7	9.7	51119	SBDS							266.2	12	177.2	4	148.3	5	382.0	9
CDK2_HUMAN	Cyclin-dependent kinase 2 OS=Homo sapiens GN=CDK2 PE=1 SV=2	33.9	9.4	1017	CDK2							313.4	9	167.0	5	207.1	7	380.0	9
SYYM_HUMAN	Tyrosine--tRNA ligase, mitochondrial OS=Homo sapiens GN=YARS2 PE=1 SV=2	53.2	9.7	51067	YARS2							230.9	6	113.9	2	105.0	2	315.2	9
LAMB1_HUMAN	Laminin subunit beta-1 OS=Homo sapiens GN=LAMB1 PE=1 SV=2	197.9	4.7	3912	LAMB1							195.0	4	240.6	4	239.7	5	434.1	8
THIL_HUMAN	Acetyl-CoA acetyltransferase, mitochondrial OS=Homo sapiens GN=ACAT1 PE=1 SV=1	45.2	9.6	38	ACAT1							482.9	17	197.6	7	242.4	6	285.4	8
OARD1_HUMAN	O-acetyl-ADP-ribose deacetylase 1 OS=Homo sapiens GN=OARD1 PE=1 SV=2	17.0	9.5	221443	OARD1							213.8	8	85.6	4	179.3	4	287.7	8
LAMC1_HUMAN	Laminin subunit gamma-1 OS=Homo sapiens GN=LAMC1 PE=1 SV=3	177.5	4.9	3915	LAMC1							363.1	7	289.0	9	389.4	6	378.6	8
CSRP2_HUMAN	Cysteine and glycine-rich protein 2 OS=Homo sapiens GN=CSRP2 PE=1 SV=3	20.9	10.0	1466	CSRP2							578.1	29	501.7	21	522.8	24	275.1	7
PDIA5_HUMAN	Protein disulfide-isomerase A5 OS=Homo sapiens GN=PDIA5 PE=1 SV=1	59.6	8.9	10954	PDIA5							229.9	6	39.8	3	83.6	3	262.5	7
AN32B_HUMAN	Acidic leucine-rich nuclear phosphoprotein 32 family member B OS=Homo sapiens GN=ANP32B PE=1 SV=	28.8	3.8	10541	ANP32B							274.9	5	92.2	1	172.3	4	216.2	7
BUD31_HUMAN	Protein BUD31 homolog OS=Homo sapiens GN=BUD31 PE=1 SV=2	17.0	10.1	8896	BUD31							145.6	5	96.2	5	103.5	2	210.7	7
NU155_HUMAN	Nuclear pore complex protein Nup155 OS=Homo sapiens GN=NUP155 PE=1 SV=1	155.1	5.7	9631	NUP155							78.3	4	122.2	2	93.7	2	323.7	7
P66B_HUMAN	Transcriptional repressor p66-beta OS=Homo sapiens GN=GATAD2B PE=1 SV=1	65.2	10.4	57459	GATAD2B							71	2	56	2	87	2	248.4	7
BZW2_HUMAN	Basic leucine zipper and W2 domain-containing protein 2 OS=Homo sapiens GN=BZW2 PE=1 SV=1	48.1	6.3	28969	BZW2							221.8	8	121.4	4	54	5	236.6	7
SK2L2_HUMAN	Superkiller viralicidic activity 2-like 2 OS=Homo sapiens GN=SKIV2L2 PE=1 SV=3	117.7	6.1	23517	SKIV2L2							285.1	8	107.5	3	308.0	3	349.2	7
NAA25_HUMAN	N-alpha-acetyltransferase 25, NatB auxiliary subunit OS=Homo sapiens GN=NAA25 PE=1 SV=1	112.2	6.2	80018	NAA25							342.4	7	214.5	4	202.6	3	310.0	7
RRP44_HUMAN	Exosome complex exonuclease RRP44 OS=Homo sapiens GN=DIS3 PE=1 SV=2	108.9	6.7	22894	DIS3							77.7	1	58.1	1	86.0	3	273.4	7
BZW1_HUMAN	Basic leucine zipper and W2 domain-containing protein 1 OS=Homo sapiens GN=BZW1 PE=1 SV=1	48.0	5.6	9689	BZW1							327.6	13	192.5	2	285.1	9	215.0	6
TCEA1_HUMAN	Transcription elongation factor A protein 1 OS=Homo sapiens GN=TCEA1 PE=1 SV=2	33.9	9.6	6917	TCEA1							366.3	12	209.4	6	200.3	7	278.4	6
CND2_HUMAN	Condensin complex subunit 2 OS=Homo sapiens GN=NCAPH PE=1 SV=3	82.5	4.8	23397	NCAPH							345.1	9	168.1	2	155.7	2	321.6	6
CDC73_HUMAN	Parafibromin OS=Homo sapiens GN=CDC73 PE=1 SV=1	60.5	10.1	79577	CDC73							183.2	4	172.6	4	155.2	3	219.3	6
SYFB_HUMAN	Phenylalanine--tRNA ligase beta subunit OS=Homo sapiens GN=FARSB PE=1 SV=3	66.1	6.4	10056	FARSB							234.5	6	194.2	7	294.0	7	235.1	6
SC23A_HUMAN	Protein transport protein Sec23A OS=Homo sapiens GN=SEC23A PE=1 SV=2	86.1	6.7	10484	SEC23A							79.4	4	39.2	1	36.9	1	237.7	6
RBM26_HUMAN	RNA-binding protein 26 OS=Homo sapiens GN=RBM26 PE=1 SV=3	113.5	9.7	64062	RBM26							315.9	10	151.1	2	219.5	2	245.9	5
SNUT2_HUMAN	U4/U6.U5 tri-snRNP-associated protein 2 OS=Homo sapiens GN=USP39 PE=1 SV=2	65.3	9.6	10713	USP39							120.7	6	108.9	5	111.9	2	184.7	5
TPX2_HUMAN	Targeting protein for Xklp2 OS=Homo sapiens GN=TPX2 PE=1 SV=2	85.6	9.9	22974	TPX2							232.5	5	226.9	5	224.3	6	199.6	5
PDIA6_HUMAN	Protein disulfide-isomerase A6 OS=Homo sapiens GN=PDIA6 PE=1 SV=1	48.1	4.8	10130	PDIA6							87.6	4	84.3	3	69.0	4	130.7	5
IF5A1_HUMAN	Eukaryotic translation initiation factor 5A-1 OS=Homo sapiens GN=EIF5A PE=1 SV=2	16.8	4.9	1984	EIF5A							433.1	21	230.1	17	252.1	20	229.3	5
NBN_HUMAN	Nibrin OS=Homo sapiens GN=NBN PE=1 SV=1	84.9	6.5	4683	NBN							108.9	4	79.6	2	101.9	1	156.0	5
DD19B_HUMAN	ATP-dependent RNA helicase DDX19B OS=Homo sapiens GN=DDX19B PE=1 SV=1	53.9	5.9	11269	DDX19B							435.3	12	218	7	273	12	167.1	4
HAP28_HUMAN	28 kDa heat- and acid-stable phosphoprotein OS=Homo sapiens GN=PDAP1 PE=1 SV=1	20.6	9.4	11333	PDAP1							295.8	10	316.7	12	211.2	9	234.9	4
DC1L1_HUMAN	Cytoplasmic dynein 1 light intermediate chain 1 OS=Homo sapiens GN=DYNC1LI1 PE=1 SV=3	56.5	6.0	51143	DYNC1LI1							173.4	9	127.9	5	140.9	7	202.7	4
ARPC3_HUMAN	Actin-related protein 2/3 complex subunit 3 OS=Homo sapiens GN=ARPC3 PE=1 SV=3	20.5	9.5	10094	ARPC3							159.3	8	132.0	6	136.8	5	79.7	4
TIM13_HUMAN	Mitochondrial import inner membrane translocase subunit Tim13 OS=Homo sapiens GN=TIMM13 PE=1 SV	10.5	9.7	26517	TIMM13							225.5	5	286.2	16	343.5	16	166.6	4
EML4_HUMAN	Echinoderm microtubule-associated protein-like 4 OS=Homo sapiens GN=EML4 PE=1 SV=3	108.8	5.9	27436	EML4							130.6	5	141.3	3	107.0	4	100.9	4
DYL2_HUMAN	Dynein light chain 2, cytoplasmic OS=Homo sapiens GN=DYNLL2 PE=1 SV=1	10.3	7.7	140735	DYNLL2							49	5	42	3	41	5	138.8	4
KCD12_HUMAN	BTB/POZ domain-containing protein KCTD12 OS=Homo sapiens GN=KCTD12 PE=1 SV=1	35.7	5.4	115207	KCTD12							139.1	5	114.6	6	112.5	5	114.5	4
TCEA2_HUMAN	Transcription elongation factor A protein 2 OS=Homo sapiens GN=TCEA2 PE=1 SV=1	33.6	10.4	6919	TCEA2							109	5	53	2	102	4	133	4
CALD1_HUMAN	Caldesmon OS=Homo sapiens GN=CALD1 PE=1 SV=3	93.2	5.5	800	CALD1							821.9	25	777.7	21	813.5	27	132.8	4
CACP_HUMAN	Carnitine O-acetyltransferase OS=Homo sapiens GN=CRAT PE=1 SV=5	70.8	9.3	1384	CRAT							252.3	8	174.6	3	246.2	4	185.2	4
GLCM_HUMAN	Glucosylceramidase OS=Homo sapiens GN=GBA PE=1 SV=3	59.7	7.9	2629	GBA							202.0	5	40.1	2	100.0	2	136.1	4
TCOF_HUMAN	Treacle protein OS=Homo sapiens GN=TCOF1 PE=1 SV=3	152.0	9.6	6949	TCOF1							327.6	12	248.8	7	376.7	11	129.4	3
ERF1_HUMAN	Eukaryotic peptide chain release factor subunit 1 OS=Homo sapiens GN=ETF1 PE=1 SV=3	49.0	5.4	2107	ETF1							210.0	7	119.3	3	171.1	5	148.1	3
CAF17_HUMAN	Putative transferase CAF17, mitochondrial OS=Homo sapiens GN=IBA57 PE=1 SV=1	38.1	10.8	200205	IBA57							177.2	5	100.0	3	144.6	5	110.6	3
SRC8_HUMAN	Src substrate cortactin OS=Homo sapiens GN=CTTN PE=1 SV=2	61.5	5.1	2017	CTTN							376.6	15	63.6	2	133.7	4	82.3	3
RS28_HUMAN	40S ribosomal protein S28 OS=Homo sapiens GN=RPS28 PE=1 SV=1	7.8	11.6	6234	RPS28							191.6	11	114.6	12	50.3	7	110.5	3
STRAP_HUMAN	Serine-threonine kinase receptor-associated protein OS=Homo sapiens GN=STRAP PE=1 SV=1	38.4	4.8	11171	STRAP							187.6	5	35	2	35	1	174.1	3
LYRIC_HUMAN	Protein LYRIC OS=Homo sapiens GN=MTDH PE=1 SV=2	63.8	9.8	92140	MTDH							219.2	15	152.8	6	152.8	11	75.7	2
DD19A_HUMAN	ATP-dependent RNA helicase DDX19A OS=Homo sapiens GN=DDX19A PE=1 SV=1	53.9	6.2	55308	DDX19A							312	12	246.7	7	404.5	15	43	2
DLRB2_HUMAN	Dynein light chain roadblock-type 2 OS=Homo sapiens GN=DYNLRB2 PE=1 SV=1	10.8	7.8	83657	DYNLRB2							118.4	7	119.6	7	106.7	5	43	2
SPF27_HUMAN	Pre-mRNA-splicing factor SPF27 OS=Homo sapiens GN=BCAS2 PE=1 SV=1	26.1	5.4	10286	BCAS2							311.0	6	175.7	4	201.8	2	43	2
CKAP2_HUMAN	Cytoskeleton-associated protein 2 OS=Homo sapiens GN=CKAP2 PE=1 SV=1	76.9	10.1	26586	CKAP2							138.3	5	109.9	4	134.4	2	107.5	2
SUMO1_HUMAN	Small ubiquitin-related modifier 1 OS=Homo sapiens GN=SUMO1 PE=1 SV=1	11.5	5.2	7341	SUMO1							98.9	5	35	3	67.6	3	37	2
DNJC8_HUMAN	DnaJ homolog subfamily C member 8 OS=Homo sapiens GN=DNAJC8 PE=1 SV=2	29.8	9.5	22826	DNAJC8							286.8	11	93.1	2	195.3	5	127.6	2
SRP09_HUMAN	Signal recognition particle 9 kDa protein OS=Homo sapiens GN=SRP9 PE=1 SV=2	10.1	9.1	6726	SRP9							131.4	5	67.8	1	73.9	3	63	2
ARP3_HUMAN	Actin-related protein 3 OS=Homo sapiens GN=ACTR3 PE=1 SV=3	47.3	5.5	10096	ACTR3							244.0	5	33	1	67	2	219.0	2
MYPT1_HUMAN	Protein phosphatase 1 regulatory subunit 12A OS=Homo sapiens GN=PPP1R12A PE=1 SV=1	115.2	5.2	4659	PPP1R12A							245.9	4	359.1	6	238.3	5	147.4	2
NELFA_HUMAN	Negative elongation factor A OS=Homo sapiens GN=WHSC2 PE=1 SV=3	57.2	9.7	7469	NELFA							128.3	6	68.2	4	107.3	4	50.3	1
CO040_HUMAN	UPF0235 protein C15orf40 OS=Homo sapiens GN=C15orf40 PE=1 SV=1	13.3	10.1	123207	C15orf40							90.9	5	83.8	5	81.2	5	53.3	1
EIF1_HUMAN	Eukaryotic translation initiation factor 1 OS=Homo sapiens GN=EIF1 PE=1 SV=1	12.7	7.8	10209	EIF1							234.1	13	98.6	9	88.0	14	65.2	1
SET_HUMAN	Protein SET OS=Homo sapiens GN=SET PE=1 SV=3	33.5	4.1	6418	SET							156.0	8	126.0	7	117.5	6	40.4	1
CCD50_HUMAN	Coiled-coil domain-containing protein 50 OS=Homo sapiens GN=CCDC50 PE=1 SV=1	35.8	6.2	152137	CCDC50							245.0	5	32	1	91.4	1	74.7	1
PPP5_HUMAN	Serine/threonine-protein phosphatase 5 OS=Homo sapiens GN=PPP5C PE=1 SV=1	56.8	5.9	5536	PPP5C							98.8	3	35	1	78.7	5	79.2	1

Introduction

Les mitochondries jouent un rôle primordial dans la respiration et le métabolisme énergétique cellulaires, et les dysfonctionnements mitochondriaux sont souvent associés à diverses maladies. La mitochondrie (mt) possède sa propre machinerie de transcription/traduction. Le génome mt code chez l'Homme pour 13 protéines de la chaine respiratoire, 22 ARNt et 2 ARNr. Le reste des protéines, codé par le génome nucléaire, est importé après traduction dans le cytosol. Parmi les protéines importées figurent les aminoacyl-ARNt synthétases (aaRS), enzymes clés de la traduction mitochondriale, responsables de l'attachement spécifique de chaque acide aminé à son ARNt correspondant.

En 2007, en collaboration avec des médecins, le laboratoire d'accueil a contribué à la première description corrélant des mutations dans le gène nucléaire d'une aaRS mt à une leucoencéphalopathie (LBSL pour « Leukoencephalopathy with brainstem and spinal cord involvment with lactate elevation »). Le gène en cause, *DARS2*, code pour l'aspartyl-ARNt synthétase mitochondriale (AspRS mt). Aujourd'hui, 18 des 19 aaRS mt sont impliquées dans des maladies aux conséquences souvent sévères. L'AspRS mt a été caractérisée fonctionnellement et structuralement au laboratoire et sa structure cristallographique établie. En plus du volet fondamental, le laboratoire essaie de comprendre le lien entre les mutations « pathologiques » et les phénotypes observés. Le fait que certaines mutations n'affectent ni la structure ni la fonction d'aminoacylation soulève des interrogations quant à l'existence d'autres propriétés, non découvertes à ce jour, pouvant constituer le chainon manquant du lien

mutation/phénotype. Ces propriétés peuvent être : 1) une appartenance à un complexe macromoléculaire ou à un réseau de régulation nécessitant l'interaction avec un ou plusieurs partenaires; 2) une fonction alternative additionnelle de celle canonique d'aminoacylation, comme cela a été décrit pour les aaRS cytosoliques. Il devient de ce fait nécessaire d'explorer les propriétés de l'AspRS mt au niveau cellulaire.

Le travail de cette thèse s'inscrit dans cette démarche et s'articule autour de 3 axes : la recherche de partenaires et de fonctions alternatives de l'AspRS mt, l'établissement et la compréhension de l'organisation sous-mitochondriale de cette dernière, ainsi que l'étude de l'impact de mutations « pathologiques » sur ses différentes propriétés.

Résultats et discussion

1) Recherche de partenaires cellulaires de l'AspRS mt : identification d'au moins un complexe

Les doctorants précédents du laboratoire ont fourni des efforts considérables dans la recherche de partenaires pour l'AspRS mt, en utilisant des techniques d'immunoprécipitation et de « pull down ». Cependant, ces efforts n'ont pas permis d'identifier de manière reproductible une protéine partenaire. Ma contribution dans cet objectif a été d'apporter la preuve que l'AspRS mt interagit bel et bien avec des partenaires. Pour cela, j'ai utilisé deux techniques expérimentales complémentaires : la séparation d'extraits mitochondriaux sur gel natif, et des expériences de « cross-link » afin de fixer les complexes polypeptidiques par des pontages covalents. Dans ces deux

expériences, l'AspRS mt, révélée par western blot, est visible dans 3 bandes : une correspondant vraisemblablement à la forme dimérique native de l'enzyme, et deux autres de haut poids moléculaires correspondant probablement à deux différents complexes. La purification par immunoprécipitation du complexe lié par «cross-link » a cependant été infructueuse pour l'identification du ou des partenaire(s).

J'ai ensuite testé un autre cross-linker (Sulfo-SBED) dont les propriétés permettent (en théorie) l'enrichissement et la détection du partenaire. L'AspRS mt recombinante conjuguée au cross-linker biotinylé est incubée avec un extrait mitochondrial. Quand l'AspRS mt interagit avec son partenaire, le complexe est immobilisé grâce aux rayons UV. Cette dernière action permet également le transfert de la biotine du cross-linker sur le partenaire permettant ainsi son enrichissement sur bille de streptavidine et sa détection par spectrométrie de masse. Là encore, aucun partenaire n'a pu être identifié de manière reproductible.

En parallèle, j'ai exploré les banques d'interactomique et analysé les interactants de l'AspRS mt identifiés soit par des techniques expérimentales à haut débit, soit prédits par des logiciels. Bien que la fiabilité des données contenues dans ces banques soit sujette à caution, certains interactants constituent des partenaires pertinents qui mériteront une exploration expérimentale approfondie.

2) Organisation sous-mitochondriale de l'AspRS mt : identification de deux formes matures et découverte de localisations multiples

La maturation (coupure du signal d'adressage quand il est en N-terminal) après l'import est une étape primordiale pour certaines protéines mitochondriales, et le

signal d'adressage (MTS) renferme dans certains cas des informations quant à la sous-localisation. Connaître le signal d'adressage et sa taille s'avère donc crucial notamment pour l'expression des protéines et leur étude *in vitro*. Cependant, ce n'est pas une tâche aisée techniquement. Dans ce sens, des résultats antérieurs du laboratoire et mes propres résultats montrent que l'AspRS mt possède au moins deux produits de maturation, issus du clivage du MTS après soit l'acide aminé 31 soit l'acide aminé 40. Il sera à présent intéressant de savoir si ce résultat original a une signification biologique.

En outre, il a été démontré que la traduction mitochondriale se fait au niveau de la membrane interne puisque plusieurs facteurs mt, dont le ribosome, interagissent avec cette dernière. Quant est-il des aaRS mt ? Des travaux antérieurs du laboratoire ont mis en évidence 3 groupes d'aaRS mt : certaines sont détectées exclusivement à la membrane, d'autres exclusivement dans la matrice, et la majorité est doublement localisée à la fois à la membrane et à la matrice. L'AspRS mt fait partie de ce dernier groupe. Ma contribution était d'explorer comment l'AspRS mt interagit avec la membrane interne étant donné qu'aucune hélice transmembranaire ne lui est prédite. Après l'exploration de différentes pistes, j'ai démontré que l'AspRS mt est une protéine périphérique interagissant avec la membrane *via* des interactions électrostatiques. D'autres protéines à double localisation mt ont été décrites dans la littérature, avec des fonctionnalités différentes selon leur sous-localisation. Une première analyse en vue de comprendre la signification fonctionnelle de la double localisation a été d'explorer si elle est dynamique. Pour ce faire j'ai criblé plusieurs molécules et réactifs chimiques en les incubant à différentes concentrations avec des

mitochondries isolées de cellules humaines (HEK293T), comme il a été procédé dans d'autres études. Après traitement, les mitochondries sont fractionnées en fraction soluble (contenant des protéines de la matrice et de l'espace intermembranaire) et membranaire (contenant des protéines des membranes interne et externe). La distribution de l'AspRS mt entre fraction soluble et membranaire est alors évaluée par rapport au contrôle (sans aucun traitement). Certaines molécules modifient, de façon peu prononcée, la distribution de l'AspRS mt entre fraction soluble et membranaire, soulignant vraisemblablement le caractère dynamique de cette distribution. Par contre, certains réactifs (e.g. ATP, GTP) provoquent le relargage de l'AspRS mt (sous la forme d'un complexe) à l'extérieur de la mitochondrie, dans des conditions expérimentales qui maintiennent pourtant l'intégrité de l'organelle. La « fuite » concerne un nombre restreint de protéines, dont le cytochrome c (Cyt c). Sachant que le relargage du Cyt c est un effecteur pro-apoptotique, la localisation extra-mitochondriale de l'AspRS mt pourrait signifier que cette dernière joue un rôle dans le processus de mort cellulaire. Bien que d'autres expériences soient nécessaires pour étayer cette hypothèse, il y a là un premier indice expérimental d'une potentielle fonction alternative.

3) Impact des mutations pathologiques sur les propriétés de l'AspRS mt : chaque mutation présente une signature qui lui est spécifique

Afin d'évaluer l'impact de mutations sur les différentes propriétés de l'AspRS mt, j'ai utilisé un système d'expression reposant sur l'infection des cellules de hamster (BHK21) avec le virus de la vaccine, avant de les transfecter avec les différentes

constructions plasmidiques (WT et mutants). J'ai tout d'abord validé l'utilisation de ce système, et démontré que l'expression de l'AspRS mt, son adressage et son internalisation se font correctement. J'ai également démontré que l'enzyme est doublement localisée et son interaction avec la membrane se fait *via* des interactions électrostatiques, de façon identique à l'AspRS mt endogène.

Ce système d'expression me permet d'analyser l'impact de mutations pathologiques sur différents paramètres cellulaires, tels la solubilité, la localisation et le relargage de l'AspRS mt. J'ai ainsi pu démontrer que la solubilité de seulement un des mutants de l'AspRS mt testés (mutant Q184K) est sévèrement affectée *in cellulo*. Par contre, aucune des mutations n'affecte la double localisation mitochondriale de l'AspRS, ni le relargage de l'enzyme vers le milieu extra-mitochondrial, bien que ce dernier résultat ne soit pour l'instant que préliminaire. En parallèle, des fibroblastes issus de patient atteint de la maladie de LBSL, sont étudiés au laboratoire concernant les mêmes paramètres décrits auparavant (solubilité, double localisation et relargage dans le milieu extra-mitochondrial). Ce travail étant en cours, aucune conclusion ne peut être formulée pour l'instant.

L'ensemble de ces résultats complètent des analyses *in vitro* faites au laboratoire sur l'impact des mutations sur les propriétés fonctionnelles et structurales de l'enzyme et révèle que chacune des mutations a une signature moléculaire qui lui est propre.

Conclusion et perspectives

Mon travail de thèse est une contribution importante dans l'analyse de l'AspRS mt humaine et la compréhension de pathologie liée. **D'un point de vue fondamental**, j'ai initié la caractérisation cellulaire de l'enzyme et apporté la preuve qu'elle fait partie d'au moins un complexe. L'identification du ou des partenaires permettrait de découvrir si l'AspRS mt est régulée par des cofacteurs protéiques dans sa fonction canonique d'aminoacylation et/ou d'avoir des indices sur une éventuelle fonction alternative. La combinaison de mes résultats avec ceux antérieurs du laboratoire a permis de décrire deux produits de maturation de l'AspRS mt. Concernant sa double localisation, j'ai démontré que l'AspRS mt est une protéine périphérique interagissant avec la membrane interne *via* des interactions électrostatiques, et que cette double localisation est probablement dynamique. La signification biologique de ce résultat et sa corrélation avec les deux produits de maturation restent à explorer. Un des points forts de mon travail de thèse est la découverte que, dans certaines conditions, la mitochondrie relargue l'AspRS ainsi que d'autres facteurs connus pour leur implication dans le processus de l'apoptose. Ce résultat, encore préliminaire, est également un indice fort d'une fonction alternative (Figure).

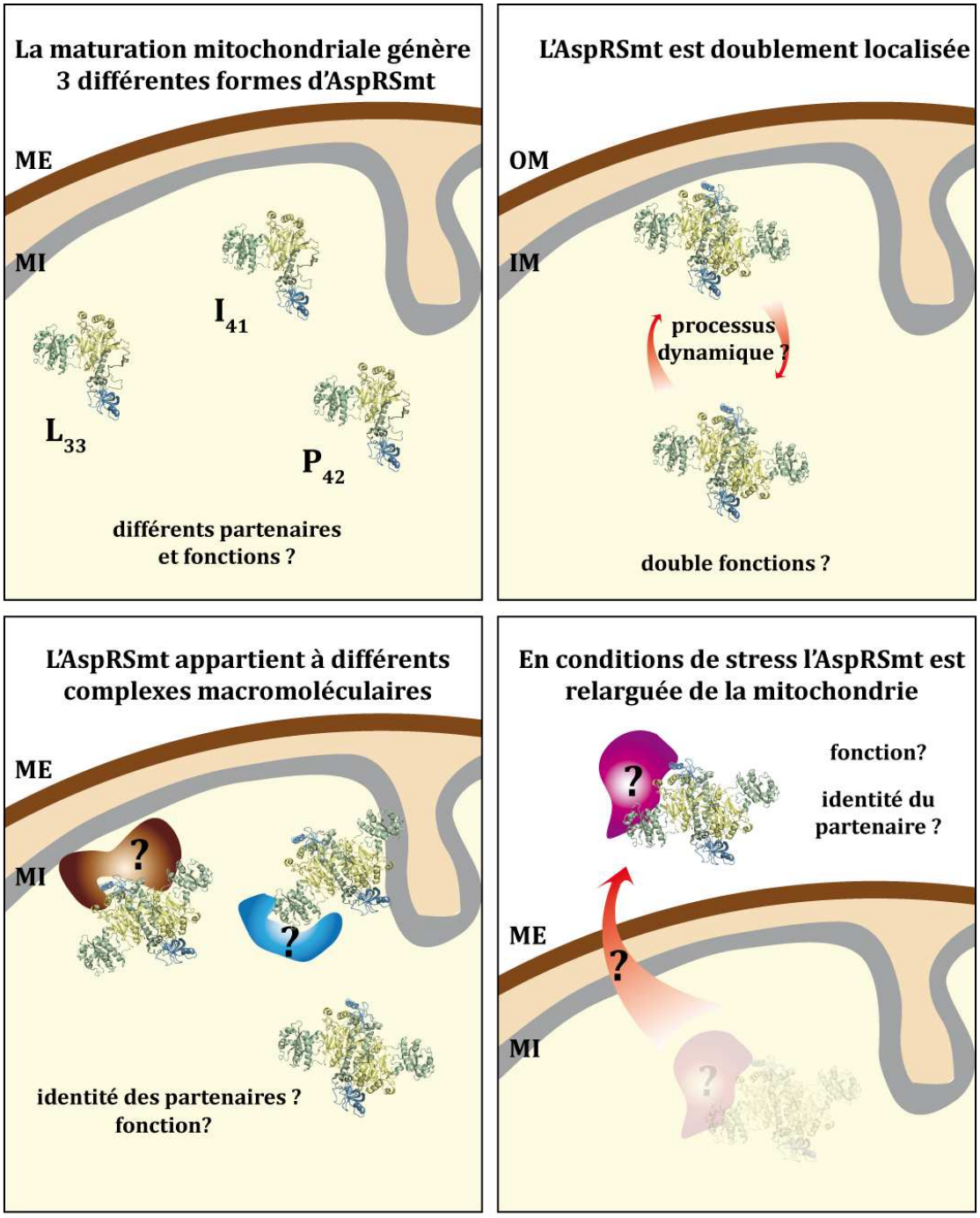

Figure : Résumé graphique des propriétés de l'AspRSmt, caractérisées au niveau cellulaire.

Concernant **l'analyse de l'impact de mutations liées au syndrome LBSL**, j'ai démontré que la solubilité est sévèrement affectée par l'une des mutations testées, et que les multiples localisations de l'AspRS mt ne le sont pas. L'étude des fibroblastes de patient devrait apporter plus de renseignements quant à situation physiopathologique de l'AspRS mt. Ma contribution a permis de renforcer l'idée selon laquelle chacune des mutations de l'AspRS mt impacte variablement la structure et/ou la fonction de l'enzyme. L'absence d'impact moléculaire commun soutien fortement l'hypothèse selon laquelle la pathologie est induite par un défaut de fonction alternative. LBSL étant une atteinte primaire du système nerveux central, cette autre fonction devra être aussi recherchée au niveau des cellules neuronales.

Mes travaux soulignent l'importance et la nécessité d'explorer les propriétés de l'AspRS mt dans son environnement cellulaire, en plus de sa caractérisation *in vitro*. L'intégration des différentes propriétés de l'AspRS mt permettra de décrypter davantage l'étiologie de la maladie du LBSL.

- Publications

Karim L, Schwenzer H, Gonzalez-Serrano LE, Rötig A, Munnich A and Sissler M. Multiple localizations of the human mitochondrial aspartyl-tRNA synthetase and impact of disease-associated mutations. (In preparation)

Carapito C, Kuhn L, **Karim L**, Rompais M, Rabilloud T, Schwenzer H and Sissler M. Two proteomic methodologies for defining N-termini of mature human mitochondrial aminoacyl-tRNA synthetases. (In preparation)

Sauter C, Lorber B, Gaudry A, **Karim L**, Schwenzer H, Wien F, Roblin P, Florentz C and Sissler M. Neurodegenerative disease-associated mutants of a human mitochondrial aminoacyl-tRNA synthetase present individual molecular signatures. Sci. Rep. 5, 17332; doi: 10.1038/srep17332 (2015).

Huot JL, Enkler L, Megel C, **Karim L**, Laporte D, Becker HD, Duchêne AM, Sissler M and Maréchal-Drouard L. Idiosyncrasies in decoding mitochondrial genomes. Biochimie, 100:95-106 (2014).

- Présentations par affiches

Karim L, Schwenzer H, Gonzalez-Serrano LE, Rötig A, Munnich A and Sissler M. Multiple localizations of the human mitochondrial aspartyl-tRNA synthetase and impact of disease-associated mutations. EMBO workshop "Molecular Biology of Mitochondrial Gene Expression" in Bro 23rd-26th May 2016, Bro, Sweden

Karim L, Schwenzer H, Florentz C, Maréchal-Drouard L and Sissler M. Impacts of LBSL-causing mutations on mitochondrial aspartyl-tRNA synthetase properties, in a cellular environment. 10th International Symposium on Aminoacyl-tRNA Synthetases, 18th-22nd October 2015, Barcelona, Spain

Karim L, Sauter C, Lorber B, Gaudry A, Florentz C and Sissler M. Characterization of human mitochondrial aspartyl-tRNA synthetase: a required step towards the deciphering of the impacts of LBSL causing mutations. 8th seminar of MeetOchondrie Network, 10th-13th May 2015, Guidel-Plages Morbihan, France

Karim L, Sauter C, Lorber B, Gaudry A, Florentz C and Sissler M. Characterization of human mitochondrial aspartyl-tRNA synthetase: a required step towards the deciphering of the impacts of LBSL causing mutations. Gordon Research Conferences: Translation in Health and Disease, 22nd-27th February 2015, Ventura CA, USA

Karim L, Schwenzer H, Florentz C and Sissler M. Impact of pathology-related mutations on cellular properties of human mitochondrial aspartyl-tRNA synthetase. Joint meeting LabEx MitoCross & NetRNA 20th & 22nd November 2014, Bischoffsheim, France

Karim L, Schwenzer H, Florentz C, Maréchal-Drouard L and Sissler M. Towards the deciphering of LBSL causing mutations impacts on mitochondrial Aspartyl-tRNA synthetase properties, in a cellular environment. FEBS-EMBO Conference, 30th August-04th September 2014, Paris, France

Loukmane KARIM

Organisation sous-mitochondriale de l'aspartyl-ARNt synthétase humaine et implication dans le syndrome LBSL

Résumé

Les travaux présentés dans cette thèse ont eu pour objectif de contribuer à la compréhension du lien entre l'aspartyl-ARNt synthétase mitochondriale (AspRSmt) humaine et le syndrome LBSL, en étudiant les propriétés de cette enzyme au niveau cellulaire. Les objectifs étaient : 1) d'explorer l'organisation de l'AspRSmt dans la mitochondrie (**Chapitre 1**), 2) d'identifier la forme mature de l'AspRSmt après son import, ainsi que la localisation sous-mitochondriale de cette enzyme (**Chapitre 2**), 3) d'évaluer l'impact de quelques mutations, impliquées dans le syndrome LBSL, sur les propriétés de l'AspRSmt (**Chapitre 3**). Nous avons démontré que l'AspRSmt existe sous différentes formes de produits de maturation, et qu'elle est retrouvée, au moins, dans deux complexes, suggérant potentiellement différents partenaires et/ou fonctions pour cette enzyme. Nous avons établi la localisation sous-mitochondriale de l'AspRSmt, et démontré que cette dernière est doublement localisée avec une fraction soluble et une fraction périphérique interagissant avec la membrane. Nous avons également découvert que, sous certaines conditions de stress, l'AspRSmt est relarguée de la mitochondrie et pourrait avoir un lien avec le processus d'apoptose. En outre, nous avons évalué l'impact de quelques mutations, impliquées dans le syndrome LBSL, et trouvé qu'elles n'ont pas d'effet significatif sur les propriétés de l'AspRSmt. L'ensemble des résultats souligne, d'une part, les lacunes restant à combler concernant les propriétés de l'AspRSmt dans la compréhension du lien mutations/pathologie (LBSL), et d'autre part, suggère fortement l'existence d'une éventuelle fonction non canonique (alternative) de l'AspRSmt.

Mots clés : traduction mitochondriale, aminoacyl-ARNt synthétase, fonction alternative, leukoencéphalopathie, organisation sous-mitochondriale, import/processing/maturation

Abstract

The aim of the PhD project was to contribute to the understanding of the link between mutations in the human mitochondrial aspartyl-tRNA synthetase (mt-AspRS) and LBSL disease, by studying the properties of this enzyme at the cellular level. Our objectives were: 1) to explore the organization of mt-AspRS in mitochondria (**Chapter 1**), 2) to identify the mature form of mt-AspRS after its import, and to characterize its submitochondrial localization (**Chapter 2**), 3) to assess, *in cellulo*, the impact of some LBSL-causing mutations on some properties of mt-AspRS (**Chapter 3**). We showed that mt-AspRS is processed into different mature forms, and that mt-AspRS belongs to two complexes likely suggesting different partners and/or functions. We demonstrated that mt-AspRS is dually localized with soluble and peripherally membrane-associated fractions. We also demonstrated that, under stress conditions, mt-AspRS is released outside mitochondria with a possible link to the apoptosis. Furthermore, we assessed the impact of some LBSL-causing mutation on some cellular properties of mt-AspRS, and showed that most mutations do not have a significant impact. This underscores the need for more studies about mt-AspRS properties, and strongly suggests a potential non-canonical (alternative) function of the enzyme.

Keywords: mitochondrial translation, aminoacyl-tRNA synthetase, alternative function, leukoencephalopathy, submitochondrial localization, import/processing/maturation